NANYANG TECHNOLOGICAL UNIVERSITY
SINGAPORE

UNRAVELLING GENE REGULATION IN THE EPIDERMIS DURING DIFFERENTIATION

ANISA BANU BTE ABDUL RAHIM
SCHOOL OF BIOLOGICAL SCIENCES

2018

DECLARATION

I hereby declare that this thesis is my original work and it has been written by me in its entirety. I have duly acknowledged all the sources of information which have been used in the thesis.

This thesis has also not been submitted for any degree in any university previously.

ANISA BANU BTE ABDUL RAHIM
28th January 2018

ACKNOWLEDGEMENTS

This thesis would not have been possible without the guidance and help of several individuals who in one way or another contributed and extended their valuable assistance in the preparation and completion of this study. First and foremost, I would like to earnestly thank my Ph.D. supervisor and mentor, **Dr. Leah Vardy** from the Institute of Medical Biology (IMB). Working under her guidance has been an enriching experience which I'll cherish for years to come. The intellectual scientific discussions about my project and the quality training that I have received under her leadership has only instilled more passion and helped me to grow as a better scientist. I can't thank her enough for being extremely patient with me and for motivating me during the lowest phases of my Ph.D. journey.

To the present and past members of the "*Epidermal Gene Regulation Lab" aka "LV Lab"*, it has been a joy sharing the lab space with you all. I am very grateful to **Dr. Lim Hui Kheng, Dr. Aishwarya Sridharan, Vonny Ivon Leo, Christina James, Shatarupa Das, Lee Li Ting, Nazreen Abdul Muthalif and Zhao Tian Yun** for providing an excellent, warm and conducive atmosphere to work in. The discussions about our projects over lunch and coffee have also contributed immensely to fine tune my project. Thank you for being good professional colleagues and great friends outside the lab.

I would like to sincerely thank **Associate Professor Tan Suet Mien**, my co-supervisor, from Nanyang Technological University (NTU) and the School of Biological Sciences (SBS), for undertaking me as his graduate student and his contribution to my thesis through great scientific discussions. I would also like to extend my thanks to **Dr. Prabha Sampath,** my co-supervisor, from IMB for her invaluable inputs and expertise in the field of skin biology as well as her words of encouragement and life advices.

I take this opportunity to thank my Thesis Advisory Committee comprising of **Associate Professor Maurice Van Steensel** and **Assistant Professor Lim Xin Hong,** from IMB as well as **Dr. Guo Huili**

from the Institute of Molecular and Cell Biology (IMCB) for their critical scientific discussions and useful suggestions for the improvement of my project.

I would like to extend my thanks to **Dr. Kim Robinson** from the Skin Cell Bank in IMB for sourcing out the human skin biopsies as well as **Dr. John Common** and **Declan Lunny** for some of the experimental reagents and sharing their vast knowledge with me on the field of skin biology. I thank **Dr. Rosanna Chua** for sharing her skills and optimisations with the 3-D organotypic skin cultures. I would like to extend my sincere thanks to **Professor Kazuei Igarashi** from Chiba University, Japan, for his collaboration on polyamine measurements and reagents. I thank **Dr. Radoslaw Mikolaj Sobota** for his collaboration on mass spectrometry sample preparation and analysis, **Professor Henry Yang** from National University of Singapore (NUS) and **Dr. Padmapriya Sathiyanathan** from IMB for their assistance on the analysis of microarray data.

I would also like to thank **IMB-Microscopy Unit (IMU)** for their excellent suite of microscopes and wonderful services. I sincerely thank **IMB** for funding my Ph.D. project.

Last but not least, I would like to dedicate this thesis to my family for believing in my dreams and leaving no stone unturned to help me accomplish this important milestone in my life.

TABLE OF CONTENTS

SUMMARY

My Ph.D. journey encompasses two projects that I have embarked on during the four years of research with the Agency for Science, Technology and Research (A*STAR), Institute of Medical Biology (IMB), Singapore. The first two years of my Ph.D. research was to uncover the role of a 'ribosomal code' in the epidermis during stress and this work was presented during my Ph.D. qualifying examination. I have enclosed this work of research under the **Appendix** section of my thesis. However, this project was proving to be challenging and hence I was advised to switch projects at the end of my second year of Ph.D. The bulk of my thesis comprises of the latest work of research which was performed during the third and fourth years of my Ph.D. and this project was to determine the role of a polyamine regulator, AMD1, during epidermal differentiation. Both work of research fall within the field of skin biology, while the former was to determine the translational regulation in the epidermis during wound healing and osmotic stress, the latter was to discover the gene regulatory networks that are regulated by polyamines during skin barrier formation. Both research work are summarised below in two parts:

Part 1: Unravelling the 'ribosomal code' in the epidermis, year 1-2

Control of mRNA translation is essential for the function and differentiation of many different cell types. This regulation is predominantly exerted by target specific microRNAs (miRNAs) and RNA binding proteins, which control the spatial and temporal expression of many proteins. Recently, the core of the ribosome itself has been shown to regulate the translation of specific mRNAs during embryonic development and this control is mediated by ribosomal proteins (RPs). The eukaryotic ribosome is composed of 4 RNA molecules and over 80 different RPs. There is considerable heterogeneity in RP composition of the ribosome in different cell types and under various environmental conditions. I am interested in understanding the role of RP heterogeneity in the skin during wound healing and osmotic stress. Polysome profiling of normal and osmotically stressed keratinocytes revealed that translation was repressed in keratinocytes subjected to osmotic stress while the polysome profiles of normal and wounded keratinocytes were comparable. iTRAQ™ labelling and subsequent mass spectrometry

analysis of pooled translational fractions from normal and stressed keratinocytes showed that the majority of RPs remain unchanged under stress. I did, however identify a number of RPs and non-RPs that were either up- or down-regulated upon keratinocyte stress. I have discussed these results, drawbacks as well as additional studies aimed at characterizing the role of the RPs/non-RPs in keratinocytes subjected to stress under the **Appendix** section of this thesis.

Part 2: Unravelling the role of AMD1 during epidermal differentiation, year 3-4

Polyamines are small polycationic molecules that are essential for many cellular processes including DNA replication, RNA modification and protein synthesis. The major polyamines in eukaryotic cells are putrescine (Put), spermidine (Spd) and spermine (Spm). Polyamine levels vary between tissues and are tightly regulated. They are differentially distributed throughout the epidermis and dermis of normal human skin with higher levels being found in the epidermis. The rate-limiting enzyme adenosyl methionine decarboxylase (AMD1) promotes the synthesis of Spd and Spm from Put and changes in AMD1 levels directly influence the ratio and levels of all three polyamines. I find that AMD1 is highly enriched in the suprabasal layers of the human epidermis and is translationally up-regulated during *in vitro* differentiation of immortalized and human primary keratinocytes. Polyamine measurements in undifferentiated and differentiated keratinocytes showed that Put levels were significantly reduced while Spm levels were elevated during differentiation. Knockdown or inhibition of AMD1 in cultured immortalized keratinocytes and 3-dimentional (3-D) organotypic skin equivalents reduced the expression of early and late differentiation markers and impeded keratinocyte stratification. The phenotype was rescued with extracellular addition of Spd and Spm suggesting that AMD1 plays a role during keratinocyte differentiation. The role of AMD1 during keratinocyte differentiation was determined by microarray analysis, to detect its potential downstream targets. I discovered that AMD1 is upstream of several key regulators of keratinocyte differentiation such as JUNB, KLF4, NOTCH1 and ZNF750. Additionally, I found CPEB4, an RNA binding protein to be downstream of AMD1 and is a novel marker of keratinocyte differentiation. While CPEB4 strongly stained the granular layer of the human epidermis, it also depicted a possible centrosomal staining in cells at the basal and suprabasal

layers by confocal microscopy. This study has paved ways to understand the critical role of polyamines in the epidermis and the complexity of the gene regulatory network that drives keratinocyte differentiation. This work of research is presented as the bulk of my thesis.

LIST OF FIGURES

LIST OF TABLES

LIST OF PUBLICATIONS

Rahim, A. B., Lim, H. K., Igarashi, K., Common, J., Vardy, A. (2018). **Polyamine regulator, AMD1, shifts the ratio of polyamines to drive keratinocyte differentiation.** *Journal of Investigative Dermatology. (Manuscript in preparation)*

Lim, H. K., **Rahim, A. B.,** Leo, V. I., Das, S., Lim, T. C., Uemura, T., Igarashi, K., Common, J., Vardy, A. (2018). **A polyamine shift regulates cell migration in epidermal wound healing.** *Journal of Investigative Dermatology. (Manuscript in Press)*

James, C., Zhao, T. Y**., Rahim, A. B.,** Muthalif, N. A., Tsuneyoshi, N., Ong, S., Dunn, R., Lim, C. Y., Igarashi, K. and Vardy, L. A. (2018). **MINDY1 is a downstream target of the polyamines and promotes embryonic stem cell self-renewal.** *Stem Cell Research,* pp.1-9

Carlevaro-Fita, J., **Rahim, A.,** Guigo, R., Vardy, L., and Johnson, R. (2015). **Widespread localization of long noncoding RNAs to ribosomes: Distinguishing features and evidence for regulatory roles.** *RNA,* 22(6):867-82

Rahim, A. B. and Vardy, L. A. (2015). **Analysis of mRNA Translation Rate in Mouse Embryonic Stem Cells,** *Methods in Molecular Biol.,* 1341:143-155

Kotoshiba, S., Gopinathan, L., Pfeiffenberger, E., **Rahim, A.,** Vardy, L. A., Nakayama, K., Nakayama, K. I. and Kaldis, P. (2013). **p27 is regulated independently of SPK2 in the absence of CDK2**, *Biochem. Biophys. Acta.,* 1843(2):436-445

LIST OF ABBREVIATIONS

293FT	Fast growing fibroblast line transformed with the SV40 large T-antigen
a.a	Amino acid
AD	Atopic Dermatitis
AdoDATAD	*S*-adenosyl-1,12-diamino-3-thio-9-azadodecane
AdoDATO	*S*-adenosyl-3-thio-1,8-diaminooctane
AdoMet	*S*-adenosylmethionine
AMD1	*S*-adenosylmethionine decarboxylase 1
And	Adenine
ANOVA	Analysis of variance
APAO	N^1-acetylated polyamine oxidase
AQP3	Aquaporin 3
ARCI	Autosomal recessive congenital ichthyosis
Arg1	Arginase 1
AZ	Antizyme
AZi	Antizyme inhibitor
BCA	Bicinochoninic Acid Protein
BCC	Basal cell carcinoma
BMP2	Bone morphogenetic protein 2
BPE	Bovine pituitary extract
$CaCl_2$	Calcium chloride
CALML5	Calmodulin-like protein 5
CDK	Cyclin dependent kinase
CE	Cornified envelope
CEBPz	CCAAT/enhancer binding protein zeta
CO_2	Carbon dioxide
CPEB4	Cytoplasmic polyadenylation binding protein 4
CT	Cycle threshold
D	Day(s)
DABCO	1,4-diazabicyclo[2.2.2]octane
DcAdoMet	Decarboxylated *S*-adenosylmethionine
DFMO	2-difluoromethylornithine
DHS	Deoxyhypusine synthase
DMBA	7,12-dimethylbenz[a]anthracene

DNMT	DNA methyltransferase
DOHH	Deoxyhypusine hydroxylase
DUOX1	Dual Oxidase 1
EBS	Epidermolysis bullosa simplex
ECM	Extracellular matrix
EDC	Epidermal differentiation complex
EGBG	Ethylglyoxal bis(guanylhydrazone)
EGF	Epidermal growth factor
EIF2S2	Eukaryotic translation initiation factor 2 subunit 2
EIF4EBP2	Eukaryotic translation initiation factor 4E-binding protein 2
eIF5A	Eukaryotic initiation factor 5A
ELL	Extracellular lipid lamellae
ESCs	Embryonic stem cells
Ezhz	Enhancer of zeste homolog 2
FBS	Fetal bovine serum
FLG	Filaggrin
GAPDH	Glyceraldehyde 3-phosphate dehydrogenase
h	Hour(s)
H&E	Haematoxylin & Eosin
H_2O_2	Hydrogen peroxide
HEKa	Human epidermal keratinocyte
HKGS	Human keratinocyte growth supplements
HOXA9	Homeobox A9
HRP	Horseradish peroxidase
HSE	Human skin equivalent
IL	Interleukin
IVL	Involucrin
JUNB	JUNB proto-oncogene
K	Keratin
Ki	Inhibitor constant
KLF4	Kruppel-like factor 4
KLK	Kallikrein related peptidase
K-SFM	Keratinocyte serum-free medium
L-Arg	L-arginine
LOR	Loricrin
MAPK3	Mitogen-activated protein kinase 3

MGBG	Methylglyoxal bis(guanylhydrazone) MGBG
min	Minute(s)
Ms	Mouse
MT	Microtubules
MTS	3-(4,5-dimethylthiazol-2-yl)-5-(3-carboxymethoxyphenyl)-2-(4-sulfophenyl)-2H-tetrazolium
MYC	Myc proto-oncogene protein
N/TERT-1	Telomerase reverse transcriptase (TERT)-immortalized human epidermal keratinocyte line
NB	Neuroblastoma
NHEK	Normal human epidermal keratinocyte
NMSC	Nonmelanoma skin cancer
NOTCH1	Neurogenic locus notch homolog protein 1
O/N	Overnight
ODC1	Ornithine decarboxylase 1
P/S	PenStrep
PBP	Polyamine binding protein
PBS	Phosphate buffered saline
PBT	Polyamine blocker therapy
PCA	Principal component analysis
PFA	Paraformaldehyde
PMSF	Phenylmethane sulfonyl fluoride
POLR2A	Polymerase II subunit A
Pro-FLG	Profilaggrin
PTI	polyamine transport inhibitor
PTS	Polyamine transport system
Put	Putrescine
PV	Psoriasis Vulgaris
qRT-PCR	Quantitative reverse transcription-polymerase chain reaction
RASL11B	Ras like family 11 member B
Rb	Rabbit
RBP	RNA Binding Protein
RIPA	Radioimmunoprecipitation assay
ROS	Reactive oxygen species
RPL13A	60S ribosomal protein L13a
RPL3L	60S ribosomal protein L3 like

RT	Room temperature
s	second(s)
S100A8/9	S100 calcium binding protein A8/9
SAM486A	4-amidinoidan-1-one-2'-amidinhydrazone
SAT1	Spermidine/Spermine N^1-acetyltransferase 1
SB	Stratum basale
SC	Stratum corneum
SCC	Squamous cell carcinoma
SD	Shine-Dalgarno
SDS-PAGE	Sodium dodecyl sulfate polyacrylamide gel electrophoresis
SFTP	S100 fused type proteins
SG	Stratum granulosum
shRNA	Short hairpin RNA
SIX4	SIX homeobox 4
SMAD5	SMAD family member 5
SMOx	Spermine oxidase
Spd	Spermidine
SPDS	Spermidine synthase
Spm	Spermine
SPMS	Spermine synthase
SPRR	Small proline rich proteins
SRS	Snyder-Robinson syndrome
SS	Stratum spinosum
T	Tween
T3	Liothyronine
TBP	TATA-box-binding protein
TBS-T	Tris-buffered saline-Tween 20
Tg	Transgenic
TGM	Transglutaminase
TINCR	Tissue differentiation-inducing non-protein coding RNA
TPA	12-*O*-tetradecanoylphorbol-13-acetate
TPRG1	Tumour protein p63 regulated gene 1
Tregs	Regulatory T cells
tRNA	Transfer RNA
Tsf	Transferrin
TWEL	Transepidermal water loss

uORF	Upstream open reading frame
Wnt11	Wnt family member 11
Wt	Wild-type
ZBTB7C	Zinc finger and BTB domain containing protein 7C
ZNF	Zinc finger protein

CHAPTER 1

INTRODUCTION

1.1 Structure of the skin

The human skin encompasses an estimated 16% of the body mass and is the largest organ of the body (Wickett and Visscher 2006). The integumentary system is made of three distinct layers: the hypodermis, dermis and epidermis (**Figure 1A**). The epidermis functions to provide a physical barrier between the skin and the external environment (Boer, Duchnik et al. 2016). Thus, the epidermal layer is dynamic and undergoes a continuous process of self-renewal and differentiation to regenerate the peripheral layers of the skin. This is indispensable to provide a barrier from harsh external insults as well as protect from harmful pathogenic infections (Eckhart, Lippens et al. 2013). The epidermis varies in thickness depending on the body site, where it is thinnest on the eyelids and thickest on the palms and soles of the feet. The epidermis rests on a basement membrane that separates it from the underlying dermis (**Figure 1A, B**) (Fuchs and Raghavan 2002). The dermis is made of collagen and is a layer filled with skin appendages, such as the sweat glands, sebaceous glands, hair follicles, nerve endings and blood vessels (**Figure 1A**). Beneath the dermis lies the hypodermis which is a layer of connective tissue or subcutaneous tissue that allows fat storage (**Figure 1A**).

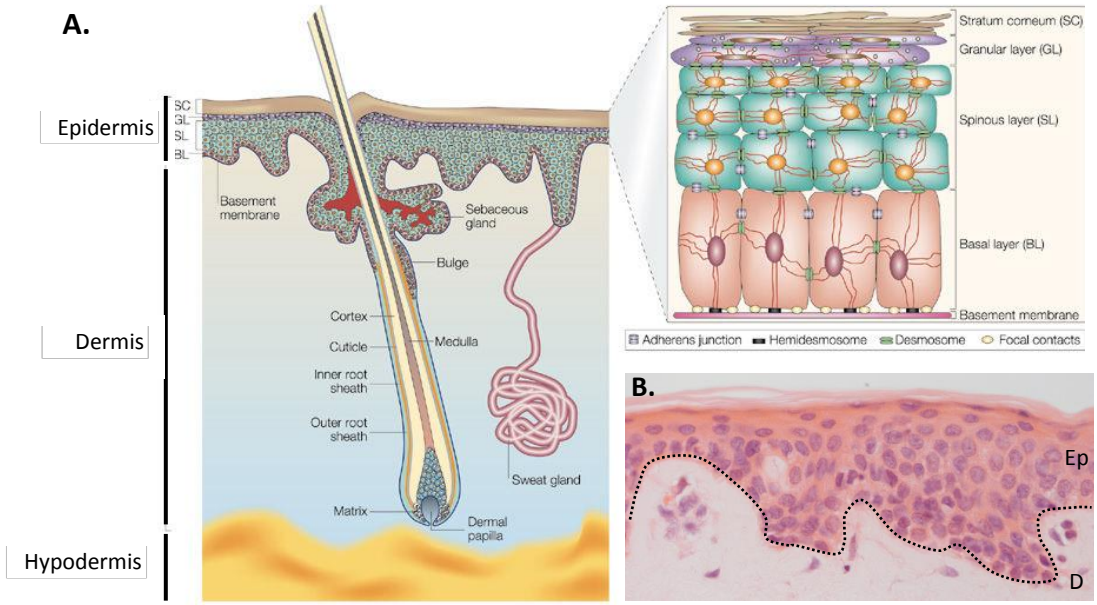

Figure 1: Anatomy of the human skin. A. Graphical dissection of the human skin portraying the hypodermis, dermis and the epidermis. Several skin appendages lie in the dermal layer of the epidermis, such as the hair follicles, sweat glands and sebaceous glands. **B.** Hematoxylin and Eosin (H&E) staining of a cross-section of human abdominal skin showing the epidermis (Ep) and the dermis (D). Dotted line represents the basement membrane. Adapted and modified from: (Fuchs and Raghavan 2002).

1.2 Layers of the Epidermis

The epidermis is a stratified squamous epithelium which consists of predominately keratinocytes and harbours additional cell populations such as Langerhans cells, Merkel cells and melanocytes (Baroni, Buommino et al. 2012). Langerhans cells are dendritic cells of the skin which provide an immune barrier function by activating resident memory T cells in response to an infection (Seneschal, Clark et al. 2012). Melanocytes of the skin are involved in the production of pigment called melanin that is responsible for the colour of eyes, hair and skin (Kondo and Hearing 2011, Baroni, Buommino et al. 2012).

The keratinocytes of the epidermis are stratified into four distinct sub-layers: the stratum basale (SB), stratum spinosum (SS) and stratum granulosum (SG) also interchangeably referred to as the basal, spinous and granular layers, followed by the outermost stratum corneum (SC) (**Figure 1A**). Keratins are the major structural component of keratinocytes providing tensile strength and support during epidermal differentiation and protecting the cells from physical trauma or injury. Keratins are subdivided into types I and II, and usually co-exist as specific heterodimers forming keratin

intermediate filaments (Eichner, Sun et al. 1986, Fuchs 1995). Mutations in keratin filaments affect their assembly and can cause skin blistering conditions such as epidermolysis bullosa simplex (EBS) (Moll, Divo et al. 2008).

The cytoskeletal network of keratin filaments is complex, and its expression is tightly regulated during epidermal differentiation (Alam, Sehgal et al. 2011). In the epidermis, the SB exists as a single layer of columnar-shaped keratinocytes attached to the underlying basement membrane via hemi-desmosomes (**Figure 2**) (Wikramanayake, Stojadinovic et al. 2014). Keratinocytes in this layer attach to one another through desmosomal junctions (Garrod and Chidgey 2008). These keratinocytes express keratin 14 (K14) together with its interacting partner, keratin 5 (K5) forming a K5/K14 intermediate filament complex (Alam, Sehgal et al. 2011). SB keratinocytes consists of either epidermal stem cells which are capable of self-renewal, transit amplifying cells or a small subset of early differentiation marker-expressing non-dividing cells (Fuchs and Raghavan 2002, Wikramanayake, Stojadinovic et al. 2014). Transit amplifying cells are mitotically active keratinocytes that have a restricted replicative potential and a tendency to "transit" from the cell cycle (Fuchs and Raghavan 2002). These cells detach from the basement membrane and commit to terminal differentiation. Cells that commit to differentiation move upwards to form approximately five to ten layers of large polyhedral keratinocytes of the SS (**Figure 2**). In the spinous layer, keratin filaments are bundled together and anchored to desmosomes of neighbouring keratinocytes. Keratinocytes in this layer express early differentiation-related keratins 1 and 10 (K1/10) (Fuchs and Raghavan 2002). Other keratins such as keratin 9 (K9) and keratin 2e (K2e) are expressed in thickened regions of the skin such as the soles and palms (Swensson and Eady 1996). Synthesis of involucrin (IVL), a precursor protein of the cornified epidermal layer and transglutaminase (TGM) enzymes that catalyse protein-protein cross-links occurs in the spinous layer (Banks-Schlegel and Green 1981, Eckert, Sturniolo et al. 2005). Caspase-14, which is important for keratinization is also synthesized in this layer (Nicotera and Melino 2007).

The SS is followed by the SG, which is an approximately three to four-cells thick layer of rhombic-shaped cells characterised by the presence of basophilic keratohyalin granules in the cytoplasm

(Wikramanayake, Stojadinovic et al. 2014). Keratin filaments, pro-filaggrin (pro-FLG) and loricrin (LOR) are found in granules in this layer (Wikramanayake, Stojadinovic et al. 2014). Pro-FLG is a precursor for filaggrin (FLG), which is a keratin filament aggregating protein (Sun and Green 1976). TGMs cross-link IVL to the cell membrane and keratin filaments in the SG. FLG bundles the keratin filaments tightly causing the cells to expel their nuclei, collapse and flatten to form the corneocytes of the SC (Sun and Green 1976). The SC consists of approximately 15-20 layers of corneocytes (Boer, Duchnik et al. 2016). During the process of desquamation, corneocytes shed from the surface of the epidermis and are constantly replaced by newly differentiated keratinocytes (**Figure 2**). Epidermal homeostasis is maintained by a precise balance between the proliferation rate of basal layer keratinocytes and the desquamation of the cornified envelope (Wikramanayake, Stojadinovic et al. 2014). A complete process of human keratinocyte differentiation starts with cell division in the SB and ends with a fully differentiated SC and takes approximately thirty days (Sun and Green 1976, Boer, Duchnik et al. 2016).

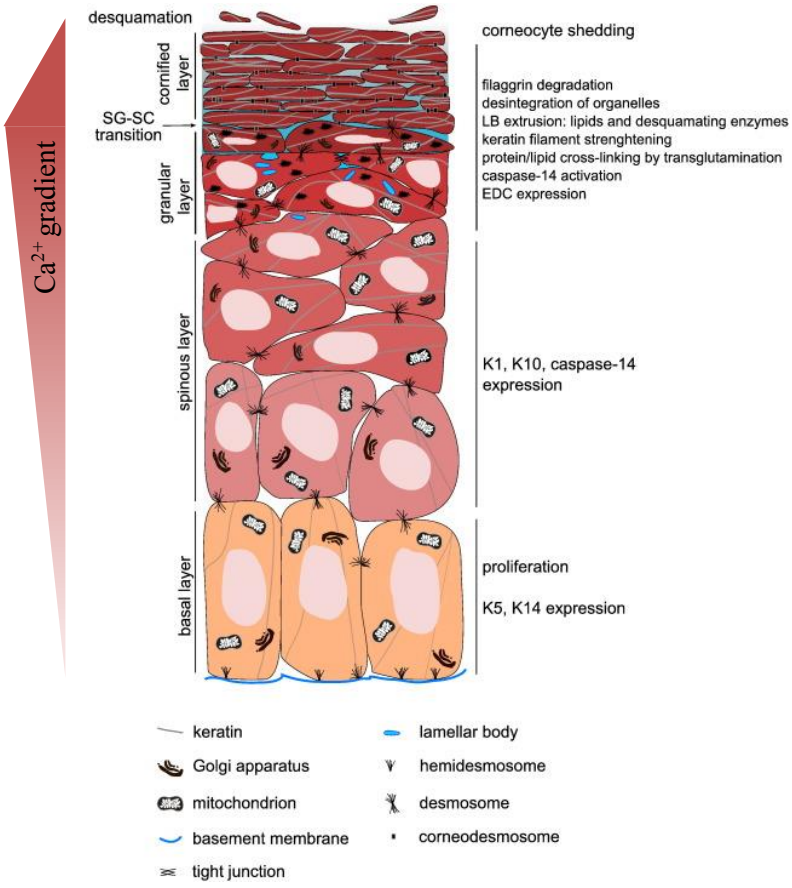

Figure 2: Cross section of the human epidermis, delineating the four major layers: stratum basale (SB), stratum spinosum (SS), stratum granulosum (SG) and stratum corneum (SC). Each layer of the epidermis is marked by distinct proliferative and differentiation makers. Proliferative basal layer keratinocytes express keratins 5 and 14 (K5/14). Spinous layer of the epidermis express early differentiation keratins such as keratin 1/10 (K1/10) as well as caspase-14. Granular layer of the epidermis has characteristic keratohyalin granules containing late differentiation markers involucrin (IVL), filaggrin (FLG) and loricrin (LOR). The SC is made of corneocytes completely devoid of nuclei. During desquamation, corneocytes shed off and are replaced by newly differentiated keratinocytes from beneath. Adapted from: (Eckhart, Lippens et al. 2013).

1.3 Epidermal Differentiation Complex (EDC)

The epidermal differentiation complex (EDC) is a region present on human chromosome 1q21 spanning approximately 2Mb in length (Kypriotou, Huber et al. 2012). Several proteins essential for epidermal differentiation are encoded by genes within this cluster (Kypriotou, Huber et al. 2012), most of which are involved in the formation of the cornified envelope such as small proline-rich proteins (SPRR), IVL and LOR. Others are classified as the (i) cornified envelope (CE) precursors, (ii) S100A family of calcium binding proteins and (iii) S100 fused type proteins (SFTP) family, such as FLG (Kypriotou, Huber et al. 2012). EDC proteins are regulated by transcription

factors, such as *Klf4*, *Grhl3* and *Arnt* in a tissue-specific manner. The deletion of these transcription factors is lethal in mice (Presland, Haydock et al. 1992). Deletion of *FLG*, a protein of the EDC, results in atopic dermatitis (AD) (Presland, Haydock et al. 1992). Mutations in TGM1 leads to the formation of a structurally defective cornified envelope which accounts for autosomal recessive congenital ichthyosis (ARCI) (Herman, Farasat et al. 2009).

1.4 Processing of filaggrin (FLG)

Pro-FLG is a precursor for FLG and is a large protein in mammals of approximately 400kDa in human (Kuechle, Thulin et al. 1999, Sandilands, Sutherland et al. 2009). It is an insoluble protein and is one of the major constituents of the keratohyalin granules. Pro-FLG protein is encoded by exon 3 of the *FLG* gene, which is found within the region of the EDC on chromosome 1q21 (Sandilands, Sutherland et al. 2009). Pro-FLG is a polyprotein that is made of 10-12 tandemly arranged repeats of FLG, flanked by partial FLG repeats on either side of the N- and C-terminal domains (Sandilands, Sutherland et al. 2009, Nishifuji and Yoon 2013). Each FLG repeat is 324 amino acids (a.a) in length and are separated from one another by a short linker (Sandilands, Sutherland et al. 2009). The N-terminal domain of Pro-FLG is 293 a.a long and consists of two Ca^{2+} binding motifs (**Figure 3**, pink and green), which regulate its processing during terminal differentiation. The C-terminal domain of Pro-FLG is 157 a.a in length (**Figure 3**, blue). Though the presence of the C-terminal domain is required for Pro-FLG processing, its precise function is not known (Presland, Boggess et al. 2000). Initial synthesis of Pro-FLG is marked by extensive phosphorylation to prevent its association with keratin filaments (Lonsdale-Eccles, Teller et al. 1982). Phosphorylated pro-FLG is rendered insoluble and inactive, and thus remains tightly packed into keratohyalin granules. An increase in Ca^{2+} concentration during keratinocyte differentiation causes keratohyalin granules to degranulate, allowing Pro-FLG to be dephosphorylated and proteolysed into FLG monomers by various proteases such as kallikreins (KLK) (Nishifuji and Yoon 2013). This occurs at an interface between the SG and SC. FLG monomers are free to bind to keratin intermediate filaments and aggregate them into tight bundles, thereby allowing them to

condense (Nishifuji and Yoon 2013). The collapse of the keratin cytoskeleton is followed by the cross-linking by TGMs and modification by deiminases to form a keratin matrix (Sandilands, Sutherland et al. 2009). This keratin matrix in combination with lipids and other cornified envelope proteins, form an insoluble SC. FLG monomers are further degraded into hygroscopic peptides such as urocanic acid and pyrrolidone carboxylic acid, by caspase-14 to serve as a natural moisturizing agent. This provides a hydrating skin barrier and protection from UV and other harmful external pathogens (**Figure 3**).

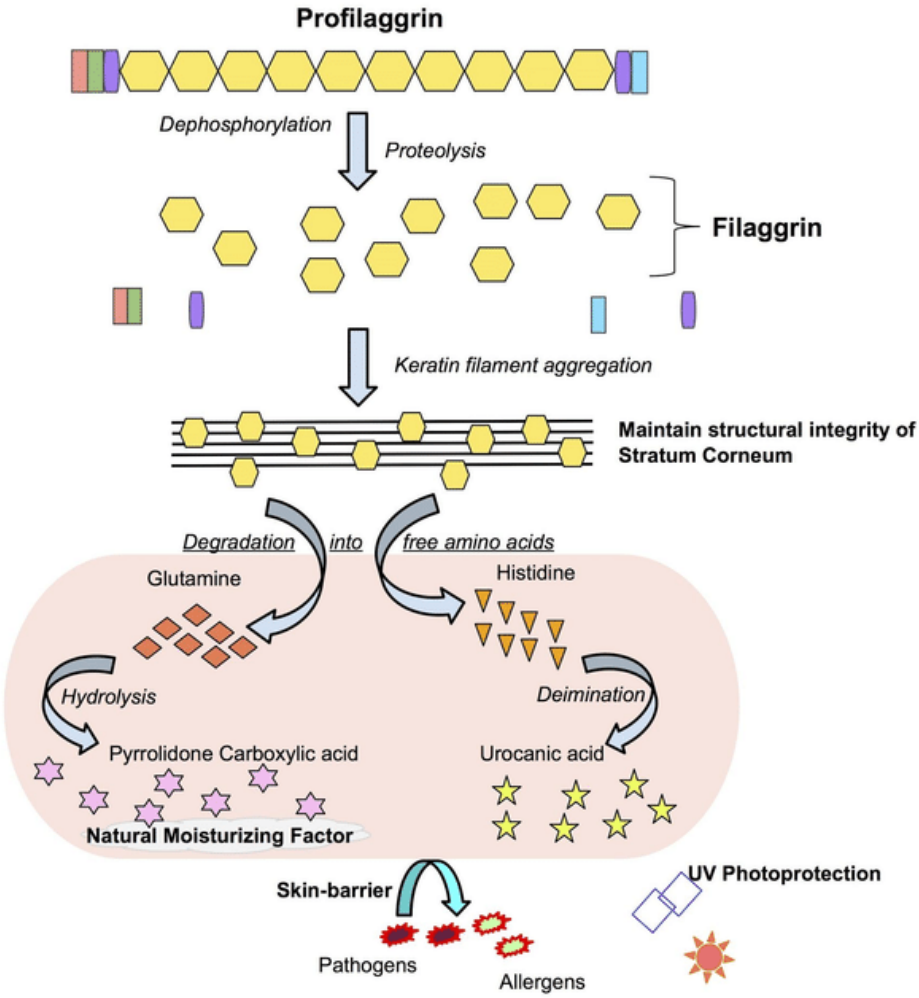

Figure 3: Expression of FLG in the epidermal skin barrier. Profilaggrin (Pro-FLG) exists in the keratohyalin granules as a tandemly arranged repeat of FLG monomers, flanked by two partial FLG on either side of the N- and C-terminal domains. With increasing Ca^{2+} concentration during keratinocyte differentiation, Pro-FLG forms FLG monomers by dephosphorylation and proteolysis. FLG monomers bind to and aggregate keratin filaments providing the structural integrity of the stratum corneum. FLG is further hydrolysed and deiminated to form a natural moisturizing factor for the skin. Adapted from: (Eaaswarkhanth, Xu et al. 2016).

1.5 Structural features and assembly of the epidermal cornified envelope

Terminal differentiation of the stratified epidermis ends with the formation of a cornified envelope beneath the plasma membrane (Kalinin, Marekov et al. 2001). It is comprised of a highly cross-linked network of insoluble proteins which form a layer approximately 10 nm in thickness (Kalinin, Marekov et al. 2001). On top of it lies a layer of ceramide lipids covalently bound to proteins and organized into a 5nm-thick orderly lamellae. The completely formed cornified envelope serves as an effective physical and water barrier to the skin. Assembly of the cornified cell envelope initiates at the spinous layer and follows through four primary phases (**Figure 4**). It begins with the expression of envoplakin (green), periplakin (pink) and IVL (light blue) as the Ca^{2+} concentration in the suprabasal cells increase during keratinocyte differentiation (Candi, Schmidt et al. 2005). Envoplakin and periplakin heterotetramers form, and together with IVL, are cross-linked by TGM1 and TGM5 onto the plasma membrane, thereby anchoring them to the desmosomes. During the phase of reinforcement that occurs in the granular layer, some lipids are covalently attached to the cornified envelope proteins by TGM1 while LOR (yellow) is cross-linked to SPRR (blue) by TGM3. This is followed by heavy cross-linking on the desmosomes where these proteins serve as substrates for TGMs (Candi, Schmidt et al. 2005, Eckhart, Lippens et al. 2013).

Following this, lipid-envelope formation occurs at the upper granular layer of the epidermis where keratinocytes accumulate lamellar bodies derived from the Golgi apparatus (Eckhart, Lippens et al. 2013). These lamellar bodies possess ω-hydroxy-ceramides with long fatty acid chains and are packaged together with other fatty acids, cholesterols and ceramides in a core (orange). During the interface between the SG and the SC, these lamellar bodies fuse with the apical side of the plasma membrane to extrude their contents to the extracellular membrane. TGM1 and TGM5 further reinforce the cornified envelope by cross-linking these lipids with the already cross-linked envoplakin-periplakin-IVL proteins (Kalinin, Marekov et al. 2001). The steps of reinforcement and lipid envelope formation take place concurrently. Finally, desquamation occurs at the cornified layer of the epidermis by a further cross-linking of LOR and other proteins to the protein scaffold

by TGM1. ω-OH-ceramides, fatty acids and cholesterol are extruded out of the plasma membrane (Eckhart, Lippens et al. 2013).

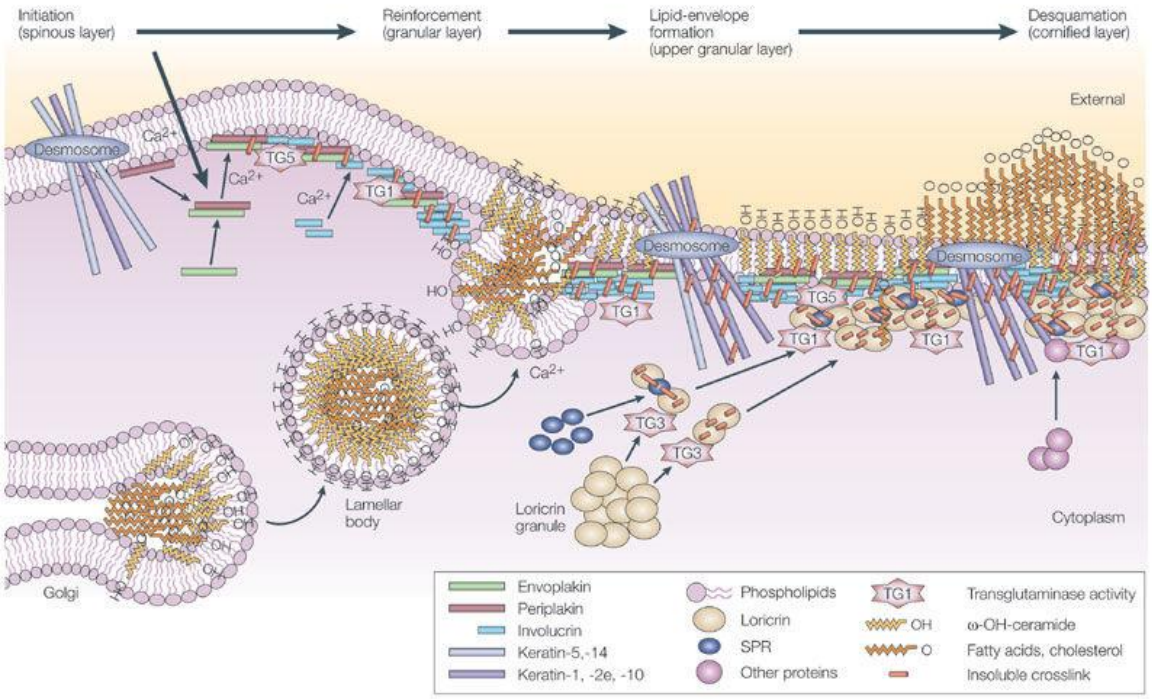

Figure 4: Formation of a cornified epidermal envelope. Assembly of the epidermal cornified envelope involves four stages from the (1) initiation phase in the spinous layer which involves the formation of a protein scaffold of envoplakin-periplakin-involucrin (IVL) on the apical surface of the plasma membrane. (2) This is followed by the synthesis and reinforcement of the cornified envelope with loricirn (LOR) and other SPRRs. (3) Lipid envelope formation takes place concurrently and the (4) final phase involves the extrusion of lamellar bodies containing long-chain ω-hydroxy ceramides and other constituents to the extracellular membrane. Adapted from: (Candi, Schmidt et al. 2005).

1.6 Epidermal cross-links by transglutaminases

In the presence of Ca^{2+}, TGMs catalyse the formation of covalent cross links between two proteins. These proteins are not keratins, but are proteins rich in glutamic acid or have high glutamine content with a few or no cysteine residues (Rothnagel and Rogers 1984). The covalent cross-link is a post-translational modification whereby an isopeptide bond is formed between the ɤ-carboxamide group of a glutamine residue of a protein acceptor and the amine group of the lysine reside of a protein donor (**Figure 5**) (Rothnagel and Rogers 1984). In the epidermis, these ε-(γ-glutamyl)lysine isopeptide cross-linked proteins are present in the cornified envelope (Abernethy, Hill et al. 1977). These enzyme generated cross-links act as a stabilizing force for the SC and proteins in this layer are highly resistant to proteolysis.

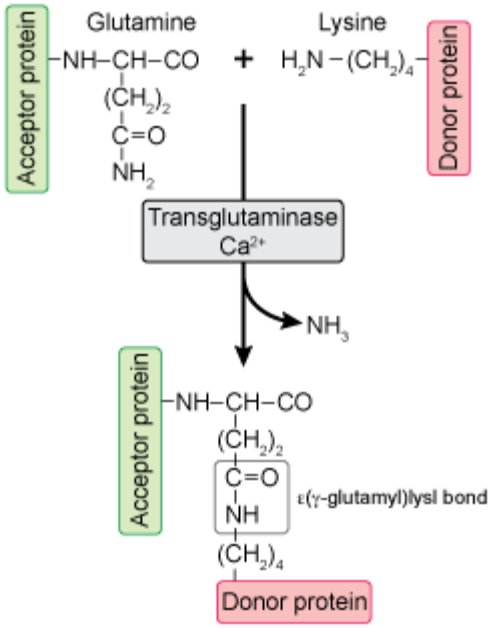

Figure 5: Cross-links formed by transglutaminases (TGMs). TGMs catalyse the formation of a covalent cross link between the glutamine residue of an acceptor protein with the lysine residue of a donor protein. These bonds are formed under high Ca^{2+} concentration and are referred to as the ε-(γ-glutamyl)lysine isopeptide bonds. Adapted from: https://mutagenetix.utsouthwestern.edu.

1.7 Monolayer keratinocyte differentiation

The mammalian epidermis exhibits a gradient of calcium, with the lowest levels in the SB while it increases progressively towards the outer SG then declines gradually at the SC (Elias, Ahn et al. 2002) (**Figure 2**). This calcium gradient is essential to drive the sequential differentiation of keratinocytes as they transverse through the different layers of the epidermis (Bikle, Xie et al. 2012). Keratinocytes at low calcium concentration of 0.3mM are proliferative and do not differentiate into a stratified epithelium (Bikle, Xie et al. 2012). In order to recapitulate keratinocyte differentiation in monolayer cultures, calcium concentration is often switched from a low concentration of 0.3mM to a high concentration of 1.2mM. Morphological changes of keratinocytes result as a consequence of Ca^{2+} signalling, which is involved in the formation of adherens junction, tight junctions and desmosomes that maintain cell-cell contacts. Ca^{2+} is also required to drive intracellular signalling events such as the activation of kinases and phospholipases to generate second messengers that are required for protein kinase C (PKC) activity to drive differentiation (Xie, Singleton et al. 2005, Bikle, Xie et al. 2012). Confluent normal human epidermal keratinocytes (NHEK) also express

higher levels of differentiation markers, K1, IVL, FLG and LOR compared to sub-confluent cultures, suggesting that high cell densities can induce keratinocyte differentiation (Lee, Yuspa et al. 1998). Attempts to culture human keratinocytes in suspension have also proven to be successful in expressing differentiation markers, and is mediated by calcium (Li, Tennenbaum et al. 1996). Here, we have cultured keratinocytes to confluence then switched to high calcium concentration to induce differentiation. Keratinocyte differentiation is best modelled *in vitro* using human primary keratinocytes but is un-sustainable due to their limited proliferative capacity. To overcome this, immortalized keratinocytes can be used for our studies, yet few human immortalized keratinocytes are available as substitutes for primary keratinocytes (Smits, Niehues et al. 2017). HaCaT cells have been a widely utilized immortalized keratinocyte cell line to perform monolayer keratinocyte differentiation (Deyrieux and Wilson 2007). While HaCaT keratinocytes respond well to differentiation stimuli such as high confluence and calcium concentration, these cells are aneuploid and differ in transcriptional gene profiles for differentiation markers, FLG, LOR, IVL and cornified envelope-associated proteins compared to normal human primary keratinocytes (Smits, Niehues et al. 2017). The N/TERT-1 human immortalized keratinocytes generated by Rheinwald's laboratory better recapitulates normal keratinocyte differentiation in monolayer cultures and organotypic skin equivalents, thus was predominately used for our experiments (Dickson, Hahn et al. 2000).

1.8 Organotypic three-dimensional (3-D) skin equivalents

To understand epidermal biology, two-dimensional tissue culture systems were initially exploited by seeding primary keratinocytes onto fibroblast feeder cells. However, such co-culture systems do not entirely recapitulate normal skin differentiation due to its limited replicative capacity and lack of ordered keratinocyte stratification and keratinization (Reijnders, van Lier et al. 2015, Smits, Niehues et al. 2017). As such, three-dimensional (3-D) organotypic culture systems were developed to culture keratinocytes at an air-liquid interface on various substrates representing a dermis (Vörsmann, Groeber et al. 2013). These substrates include, a devitalised dermis, porous cell-free membranes in the absence or presence of a collagen coated extracellular matrix (ECM) or with matrix-embedded dermal fibroblasts (**Figure 6**). Organotypic cultures exhibit a well-differentiated

and stratified epidermis that are beneficial in the study of exogenous compounds on skin barrier. However, the complexity of *in vivo* human skin is not entirely represented in such organotypic culture models due to its lack of dermal cellular heterogeneity and the absence of lymphatic system and blood vessels (Vörsmann, Groeber et al. 2013).

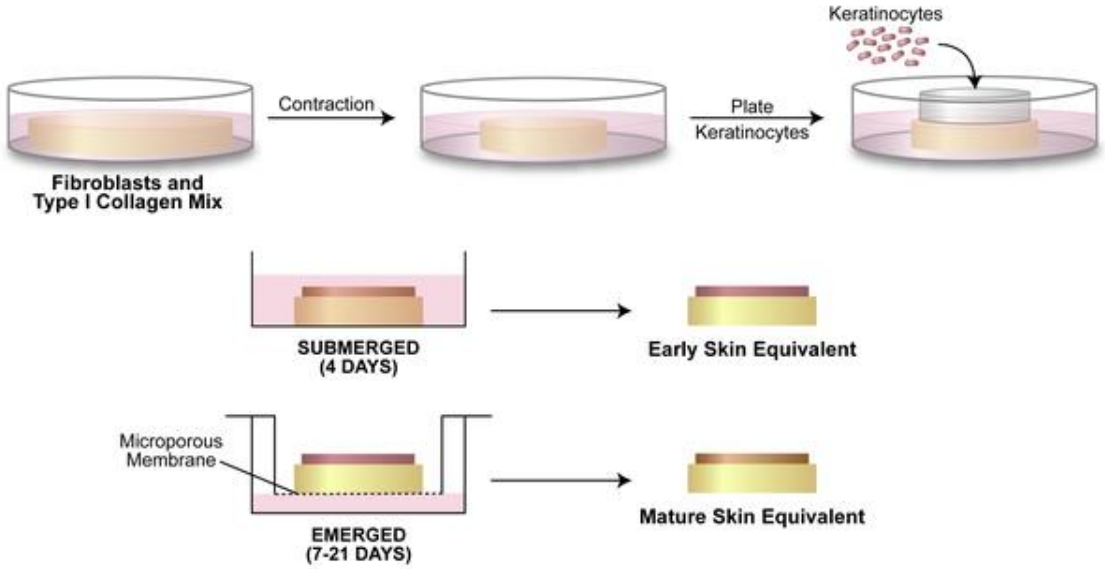

Figure 6: Three-dimensional (3-D) organotypic skin equivalents generated using collagen and dermal fibroblast matrix. Fibroblast cells are mixed with Type I collagen and plated onto a petri dish and allowed to contact for 7-14 days. Following that, keratinocytes are seeded onto this fibroblast/collagen matrix using a cloning ring. Keratinocytes are allowed to settle and attach to the contracted collagen matrix. Following 4 days of submerged culture, skin equivalents are raised to an air-liquid interface and harvested between 7-21 days. Adapted from: (Vaughan, Ramirez et al. 2009).

1.9 Skin diseases associated with aberrant skin differentiation

Several factors have been associated with perturbed skin differentiation and barrier function. Some of these factors include elevated pH, altered lipid content and disrupted calcium gradient in the epidermis (Lee, Jeong et al. 2006). Impaired skin barrier leads to several skin ichthyosis and chronic inflammatory skin diseases. Hereditary skin disorders as a result of genetic mutations of essential components of the epidermis are known as genodermatoses (Lee, Jeong et al. 2006). Atopic dermatitis (AD) and psoriasis are the most prevalent skin inflammatory disorders caused by genetic and/or environmental stimuli. These skin disorders are a huge economic burden on the healthcare sector and compromises the life of affected patients. As such, in order to treat such complex skin pathologies, understanding the molecular mechanism underlying normal skin differentiation is

indispensable. This could eventually pave ways to better elucidate therapies for restoring normal epidermal homeostasis in these patients.

1.9.1 Psoriasis

Psoriasis is a common chronic inflammatory skin disease which is genetically determined (Ota, Takekoshi et al. 2014). Though there are several types of psoriasis, the predominant form of psoriasis is called psoriasis vulgaris (PV) (Roberson and Bowcock 2010). In psoriasis, epidermal proliferation is more rapid than normal resulting in epidermal thickening, abnormal keratinization and the presence of increased inflammatory cell infiltrates (**Figure 7**) (Bhawan, Bansal et al. 2004). As a consequence, the epidermal barrier becomes defective and well-defined silvery flakes of lesions form on the skin (Roberson and Bowcock 2010). Several studies have demonstrated that psoriasis patients have lower levels of differentiation keratins, K1 and K10 in the suprabasal layers (Thewes, Stadler et al. 1991, Bernerd, Magnaldo et al. 1992, Stoler, Kopan et al. 1998) while the expression of proliferative markers K5 and K14 were altered in the basal layers of the epidermis (Holland, Wood et al. 1989). The dysregulated expression of keratins suggest that epidermal differentiation is abnormal in psoriatic skin. S100A7 proteins are present in the nucleus and cytoplasm of basal layer keratinocytes in the normal and psoriatic epidermis. However, in the spinous layer keratinocytes, these proteins are associated with the plasma membrane and are highly abundant in the psoriatic epidermis. S100A7 protein is also termed as psoriasin (Roberson and Bowcock 2010). The granular layer is normally absent in psoriasis lesions, thus the nuclei are retained within the cytoplasm of the corneocytes, a term referred to as parakeratosis (Roberson and Bowcock 2010). In psoriasis, connexin 26 (Cx26), a gap junction protein, is also highly abundant (Bowcock, Shannon et al. 2001). The lipid envelope is abnormal in psoriatic lesions, accounting for a defective skin barrier.

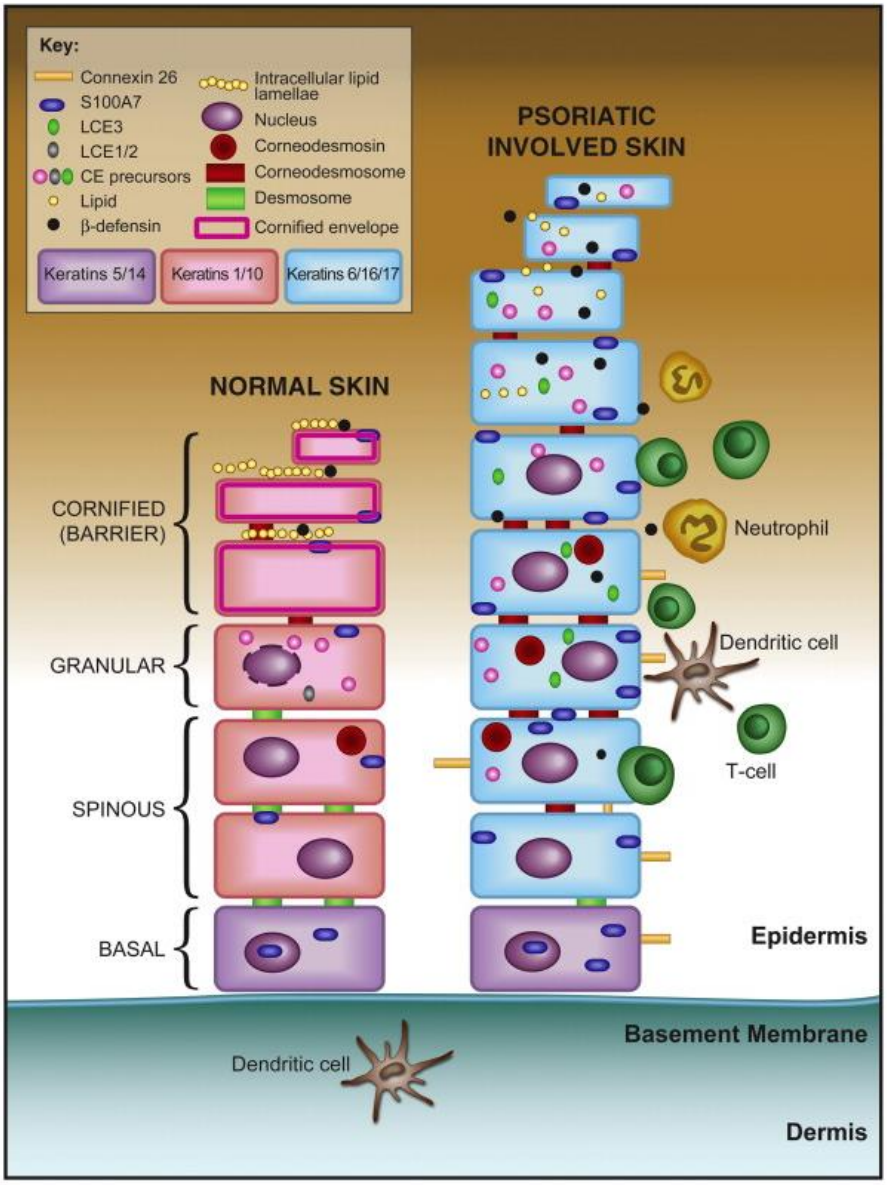

Figure 7: Pictorial representation of normal and involved psoriasis lesion (not represented to scale). The normal epidermis comprises of the basal, spinous, granular layers and the stratum corneum (SC). The SC is constantly replenished by cells in the basal layer. K5/14 and K1/10 are normally expressed during differentiation while K6/16 are largely present in response to a trauma. S100A7 protein is present in the basal and spinous layers of the normal epidermis but are highly abundant in the psoriasis epidermis. The granular layer is absent in psoriasis lesion and therefore the nuclei are retained in the corneocytes. Adapted from: (Roberson and Bowcock 2010).

1.9.2 Atopic dermatitis (AD)

Atopic dermatitis (AD) is a genetically associated skin disease that has the potential for chronic relapse (Rizzo, Oyelakin et al. 2016). It is an inflammatory skin disease prevalent worldwide, however it commonly affects the paediatric population. Immunological abnormalities and impaired

barrier function can lead to an onset of AD (Nishifuji and Yoon 2013). Reduced levels of ceramides are present in the SC of affected individuals, which eventually affects the overall organization of the extracellular lipid lamellae (ELL). This attributes to an increase in transepidermal water loss (TEWL), reduced water capacitance and dry flaky skin in AD patients. A few possible mechanisms underlying the prognosis of AD have been illustrated in the literature. A decrease in the activity of epidermal acid sphingomyelinase was reported by Jensen et al., to be correlative to reduced ceramide content in the SC of affected AD patients (Jensen, Fölster-Holst et al. 2004). Loss-of-function mutations (R501X and 2282del4) in *FLG* were first reported to be associated with the development of AD (Palmer, Irvine et al. 2006). Since then, more than 40 *FLG* mutations have been associated with AD with at least 20-25% of the AD patients having a mutation in *FLG* (Akiyama 2011, Kawasaki, Kubo et al. 2011). Mutations in the *KLK7* gene have been reported in AD patients (Vasilopoulos, Cork et al. 2004). Recent studies have revealed an important role for an isoform of p63, specifically ΔNp63, in the pathogenesis of AD. High levels of ΔNp63 were found in the skin lesions of patients with AD (**Figure 8**) (Rizzo, Oyelakin et al. 2016). IL-31 and IL-33 are both involved in pathways implicated with AD and were discovered to be downstream targets of ΔNp63 (Rizzo, Oyelakin et al. 2016).

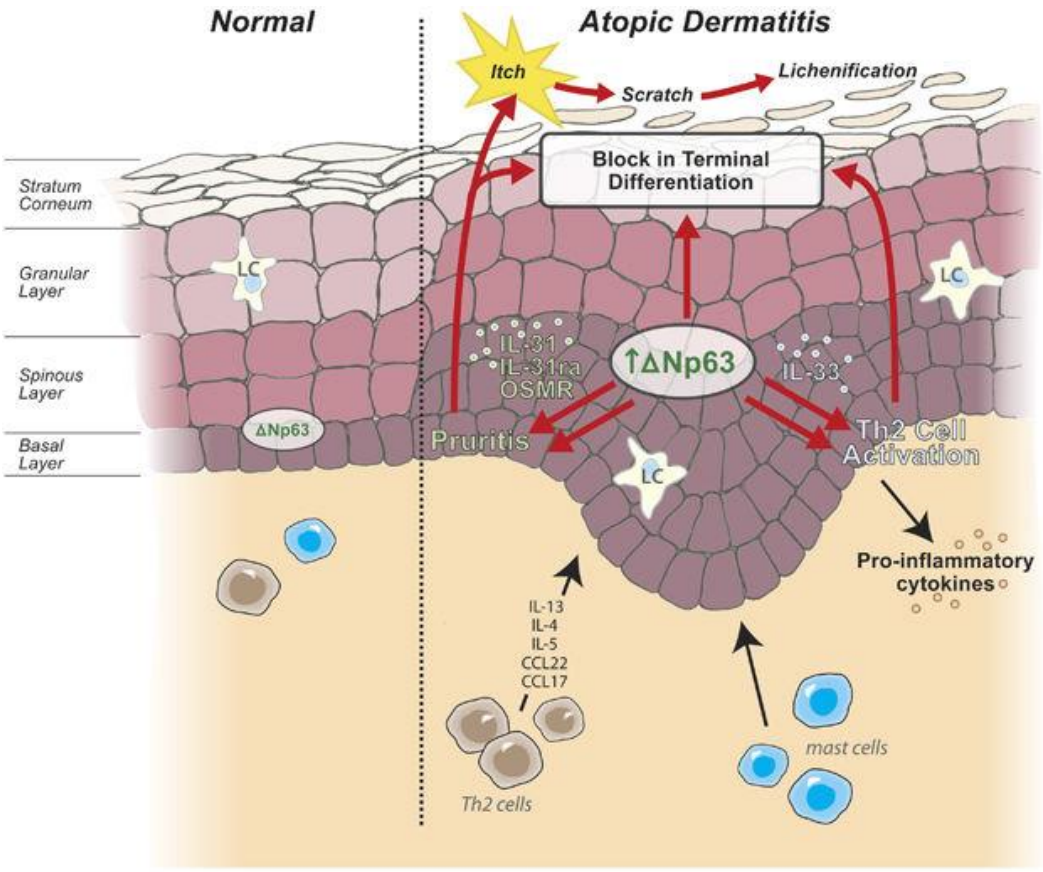

Figure 8: The role of ΔNp63 in the development of atopic dermatitis (AD). High levels of ΔNp63 in AD results in the activation of IL-33 signalling which subsequently stimulates Th2 cell activation that leads to the production of pro-inflammatory cytokines. ΔNp63 also induces pruritus or an itch response by increasing the levels of IL-31, IL-31ra and OSMR gene expression. Hence, the interplay between increased ΔNp63 expression, pruritus and Th2 cell activation accounts for an alteration in epidermal differentiation. Adapted from: (Rizzo, Oyelakin et al. 2016).

1.10 Non-centrosomal microtubule organization in differentiated keratinocytes

The centrosome is made of a centriole pair and pericentriolar material containing multi-protein complexes. These multi-protein complexes are involved in the nucleation and tethering of microtubules (MT) as the mitotic spindles form (Rieder, Faruki et al. 2001). In undifferentiated keratinocytes, the microtubules are organized in a radial fashion at the centrosome (**Figure 9A**) (Dyachuk, Bierkamp et al. 2016). Keratinocyte differentiation however, involves a dynamic reorganization of MT and centrosomal components to the cellular cortex. (**Figure 9B**) (Sanchez and Feldman 2016, Muroyama and Lechler 2017). Such an organization determines the shape and function of the keratinocytes. It has been evidenced that during keratinocyte differentiation, centrosomal protein such as Ninein dissociates from the pericentriolar material to the cell cortex, where it localizes with desmoplakin, a desmosomal protein (Lechler and Fuchs 2007). LIS1,

NDEL1 and CLIP170 are other known microtubule-organising proteins that associate with the cellular cortex (Sumigray, Chen et al. 2011, Sumigray, Foote et al. 2012). Knockout of desmoplakin, prevents the accumulation of microtubule organizing proteins, Ninein, LIS1 and NDELl at the cortical surface of cell (Sumigray, Chen et al. 2011). Whether Ninein is essential in microtubule anchoring or it simply relocalises due to microtubule network rearrangement remains unknown.

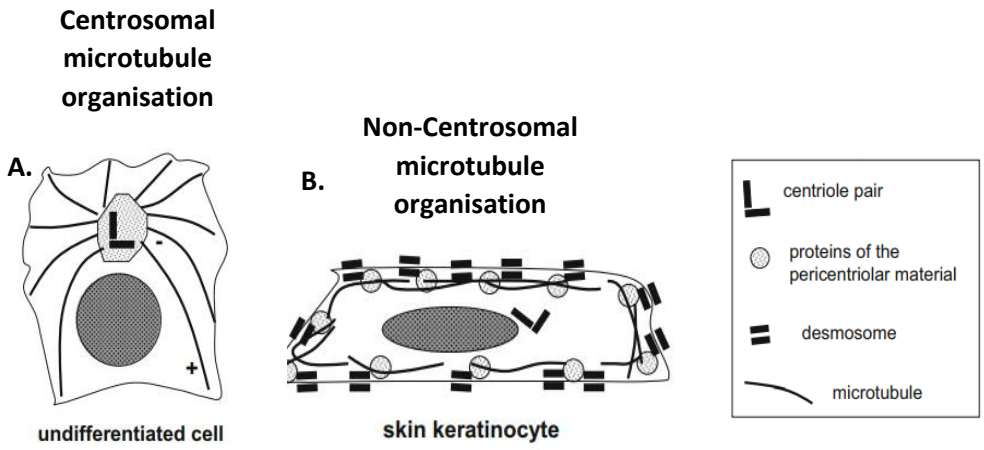

Figure 9: Microtubule organisation in undifferentiated and differentiated keratinocytes. A. In undifferentiated keratinocytes, microtubules are organized in a radial fashion, where the minus end of the microtubule is tethered to the pericentriolar material surrounding the centriole pair. **B.** In differentiated keratinocytes, microtubules are reorganized to the cortical region of the cells together with the redistribution of centrosomal proteins. In this example, Ninein, a centrosomal protein is relocated to the cellular cortex where it binds to desmosomes. Adapted from: (Dyachuk, Bierkamp et al. 2016).

1.11 Polyamines and Polyamine Metabolism

Polyamines are low molecular weight aliphatic metabolites that are highly positive charged and ubiquitously present in all living cells (Park and Igarashi 2013, Miller-Fleming and Olin-Sandoval 2015). The positive charge on polyamines allows their interaction with negatively charged nucleic acids, proteins and phospholipids, which is required for a wide array of essential functions within the cells, at the level of transcription, translation and post-translation (Bachrach 2005, Park and Igarashi 2013). The naturally occurring polyamines in eukaryotes are putrescine (Put), spermidine (Spd) and spermine (Spm) (**Figure 10**). Put is a diamine, while Spd and Spm are higher order polyamines containing three and four amine groups respectively (Pegg 2016). Spd and Spm were initially discovered in 1678 by Antonie van Leeuwenhoek to

be present in seminal fluids while Put derived its name due to its foul odour from putrefying flesh (Wallace 2009, Miller-Fleming and Olin-Sandoval 2015). The overall free and bound polyamines are present at millimolar concentrations within the cell (Stevens 1969, Lightfoot and Hall 2014). However, the amount of polyamines present in a cell is tissue and context specific (Tabor and Tabor 1976, Lightfoot and Hall 2014). While Put exists in either free or bound forms equally, Spd and Spm are usually bound to RNA and are able to influence protein synthesis (Frydman, Frydman et al. 1984, Igarashi and Kashiwagi 2010).

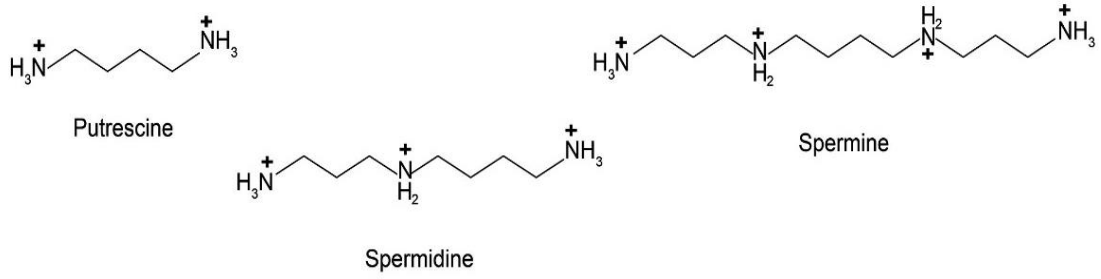

Figure 10: Polyamines present in eukaryotes. Putrescine (Put), spermidine (Spd) and spermine (Spm) are the three biologically relevant polyamines present in eukaryotes. Put contains two amine groups while Spd and Spm contain three and four amine groups, respectively. Polyamines are cations under normal physiological pH and that is essential for a broad spectrum of cellular functions. Adapted from: (Miller-Fleming and Olin-Sandoval 2015).

1.11.1 Polyamine Anabolism

Polyamine levels are tightly regulated within the cells through a combination of synthesis, catabolism and transport (**Figure 11**). Polyamine synthesis begins with ornithine, a by-product of the urea cycle that is decarboxylated by the first rate-limiting enzyme, ornithine decarboxylase 1 (ODC1) to generate Put (**Figure 11**) (Williams-Ashman and Canellakis 1979). Adenosyl methionine decarboxylase 1 (AMD1), a second rate limiting enzyme in the polyamine biosynthesis pathway, decarboxylates *S*-adenosylmethionine to decarboxylated *S*-adenosylmethionine (dcAdoMet), providing the aminopropyl donor groups for the formation of Spd and Spm (Grillo 1985). Addition of aminopropyl groups to Spd and Spm is mediated by spermidine synthase (SPDS) and spermine synthase (SPMS), respectively. Knockdown of

either ODC1 or AMD1 has been demonstrated to be lethal in mice, suggesting their crucial role in cellular function and embryonic development (Pendeville, Carpino et al. 2001, Nishimura, Nakatsu et al. 2002). However, a few mammalian cell lines with a lack of SPMS activity, were able to survive in cultures despite the absence of Spm. These were the 129/SvJ mouse embryonic stem cells (ESCs) and immortalized embryonic fibroblasts (Mackintosh and Pegg 2000, Korhonen, Niiranen et al. 2001). Gy mice with an absence of the *SpmS* gene still remained viable, but displayed neurological defects, with abnormal bone development, reduced body size and a shorter life span (Mackintosh and Pegg 2000, Pegg 2014). In human, mutations in the *SPMS* gene lead to a rare X-linked recessive disease referred to as Snyder-Robinson syndrome (SRS) (Cason, Ikeguchi et al. 2003). This mutation was attributed to an incorrect splicing, which leads to an insertion of a premature stop codon, resulting in the production of a truncated form of SPMS protein. Patients with SRS displayed mental retardation, speech abnormalities, reduced body size and skeletal abnormalities (Cason, Ikeguchi et al. 2003, Becerra-Solano, Butler et al. 2009). Cultured fibroblasts cells from patients with SRS showed a large reduction in SPMS activity, hence the levels of Spm were greatly reduced while Spd levels were significantly increased (Cason, Ikeguchi et al. 2003).

1.11.2 Polyamine Catabolism

Higher order polyamines can be catabolised to generate Spd or Put (**Figure 11**). Both Spd and Spm can be acetylated by a rate-limiting catabolic enzyme, spermidine/spermine N^1-acetyl transferase (SAT1) and then oxidised by acetyl polyamine oxidase (APAO) to regulate the levels of polyamines within the cells (Miller-Fleming and Olin-Sandoval 2015). H_2O_2 and acetaminopropanal are generated as by-products during this oxidation process. Formation of Put from Spd is absolutely dependent on SAT1. However, Spm can also be converted back to spermidine by spermine oxidase (SMOx). In contrast to APAO, SMOx favours Spm as a substrate instead of its acetylated derivative, N^1-acetylspermine (Miller-Fleming and Olin-Sandoval 2015).

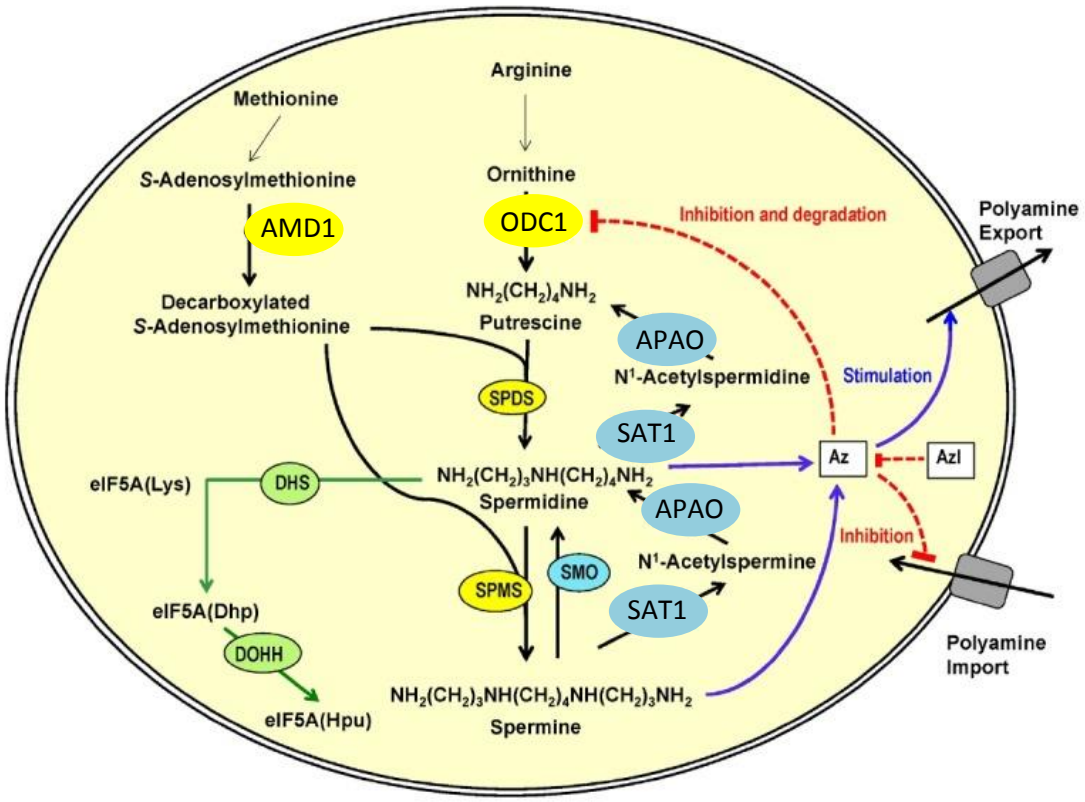

Figure 11: Polyamine synthesis, catabolism and transport in mammalian cells. Ornithine, a by-product from the urea cycle is converted to putrescine (Put) by ornithine decarboxylase 1 (ODC1). Adenosylmethionine decarboxylase 1 (AMD1) provides the aminopropyl donor groups for the formation of spermidine (Spd) and spermine (Spm) by spermidine synthase (SPDS) and spermine synthase (SPMS) respectively. Spm is catabolised to Spd by spermine oxidase (SMOx) or to Spd and Put by spermidine/spermine N^1-acetyltransferase (SAT1) and acetylpolyamine oxidase (APAO). Spd is used as a precursor for the formation of eIF5A(Hpu) by deoxyhypusine synthase (DHS) and deoxyhypusine hydroxylase (DOHH). Polyamines can be imported and exported by polyamine transporters. Anabolic enzymes are indicated in yellow, catabolic enzymes in blue and enzymes involved in hypusine modification in green. Adapted and modified from: (Park and Igarashi 2013).

1.11.3 Polyamine Transport

Besides polyamine metabolism, polyamine transport also plays a pivotal role in regulating the levels of polyamines within the cell (**Figure 11**). Polyamine uptake and export are less well understood in mammalian cells. However, polyamine transport has been well characterized in bacteria and plants. For instance in *E.coli*, two polyamine uptake systems have been identified, one displaying a preferential uptake of Spd, while the other Put. Two exporters, PotE and CadB have been identified in *E.coli* to excrete polyamines at an acidic pH (Tomitori, Kashiwagi et al. 2012). In *S. cerevisiae,* DUR3 and SAM3 proteins mediate polyamine uptake (Uemura, Kashiwagi et al. 2007). SLC3A2 and y^+LAT complexes were identified in colon epithelial cells,

responsible for exporting Put (Uemura, Yerushalmi et al. 2008). ATP13A3 and SLC12A8 are mammalian polyamines transporters that are not well characterized (**Figure 12B**) (Daigle, Carpentier et al. 2009, Madan, Patel et al. 2016). Though polyamine transporters regulate the import and export of polyamines, whether these transporters are selective for certain polyamines compared to others is not yet fully understood.

Polyamine uptake can also be mediated via caveolae-dependent endocytosis (Uemura and Gerner 2011). Caveolin-1 is a 22 kDa protein that forms the structural component of caveolae, which are invaginations of the plasma membrane (Tiwari, Copeland et al. 2016). Polyamine binding proteins (PBPs) are transiently present at the cell surface of mammalian cells (Uemura, Stringer et al. 2010) **(Figure 12A)**. These proteins contain mature heparin sulphate (HS) side chains that bind to polyamines by electrostatic interaction during endocytosis. Caveolin-1 negatively regulates caveolae-dependent endocytosis by stabilizing the caveolae structures in human colorectal carcinoma HCT116 cells (Roy, Rial et al. 2008, Uemura, Stringer et al. 2010). In the endosomes, nitric oxide (NO)-dependent cleavage of HS is mediated by nitric oxide synthase-2 (NOS2) and this is required for the release of polyamines. Phosphorylation on Tyrosine 14 (Y14) of caveolin-1 by Src, spatially loosens its association with caveolae thereby enhancing plasma membrane internalization and polyamine uptake (Gottlieb-Abraham, Shvartsman et al. 2013, Zimnicka, Husain et al. 2016).

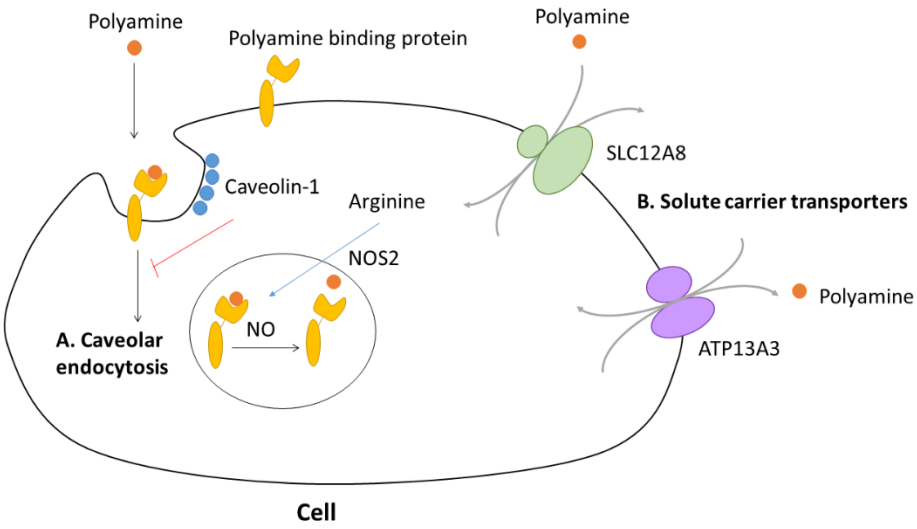

Figure 12: Caveolae-dependent endocytosis in mammalian cells. A. Polyamines bind to polyamine binding proteins (PBPs) and are internalized into the cell via caveolae-dependent endocytosis that is negatively regulated by caveolin-1. Nitric oxide (NO) produced by nitric oxide synthase-2 (NOS2) is required to release polyamines from the intracellular vesicles. **B.** Polyamines can be transported in and out of the cell by solute carrier transporters such as SLC12A8 and ATP13A3, though the affinity for specific polyamines for these transporters is not well understood. Adapted and simplified from: (Uemura, Stringer et al. 2010).

1.11.4 Other sources of polyamines

Cells salvage polyamines from the extracellular space through dietary intake and intestinal absorption of polyamines synthesized by the gut microbiota (Larqué, Sabater-Molina et al. 2007). Polyamine levels vary between individuals but the reason for these differences in blood polyamine concentrations between human remains elusive. However, one potential reason for the variability is due to the difference in food preferences between individuals and the ability of intestinal bacteria flora to synthesize polyamines. Altering the levels of polyamines through consumption and suppression of intestinal microbiota have been demonstrated to change the concentrations of polyamines in whole blood (Nishimura, Araki et al. 2001, Cipolla, Guilli et al. 2003, Soda 2009).

1.12 Hypusination of eIF5A and its isoform, eIF5A2

In addition to polyamine metabolism, a portion of cellular Spd is covalently incorporated onto eukaryotic initiation factor 5A (eIF5A) as a post-translational modification, to form an unusual amino acid hypusine (**Figure 11**) (Park and Nishimura 2009). This involves a two-step reaction which is briefly summarized in **Figure 13** (Mathews and Hershey 2015). In the initial step, deoxyhypusine synthase (DHS) catalyses the transfer of an aminobutyl moiety of Spd onto the ε-amino group of a specific lysine residue on eIF5A to form eIF5A(Dhp), a deoxyhypusine intermediate. The subsequent hydroxylation of eIF5A(Dhp) by deoxyhypusine hydroxylase (DOHH) results in the formation of biologically active eIF5A(Hpu) (Park and Igarashi 2013). Two isoforms of eIF5A exists, eIF5A and eIF5A2. While eIF5A is expressed abundantly in most cells, eIF5A2 is present in normal tissues to a lesser extent but highly enriched in many cancers (Clement, Johansson et al. 2006, Mathews and Hershey 2015). eIF5A and eIF5A2 are the only two known proteins bearing a hypusine modification identified to date (Clement, Johansson et al. 2006). This modification is absolutely crucial for its function in translational initiation and elongation. It was proposed that the increase in proliferation due to high levels of polyamines could be due to an increase in protein synthesis as a result of enhanced eIF5A activity (Nishimura, Murozumi et al. 2005).

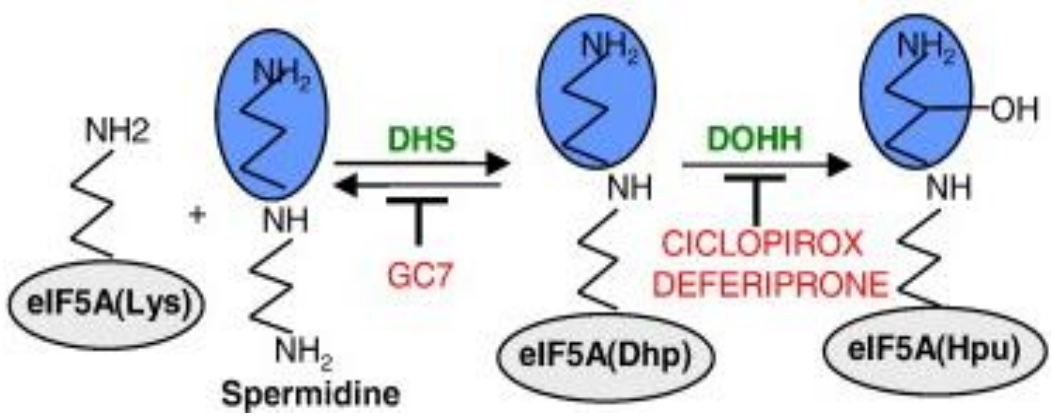

Figure 13: Hypusine synthesis pathway in eukaryotes. The formation of hypusinated-eIF5A involves a two-step process in which, the ε-amino-group on a specific lysine (Lys) residue of eIF5A is replaced by the aminobutyl moiety of spermidine (Spd) to form a deoxyhypusine-containing intermediate, eIF5A(Dhp) by deoxyhypusine synthase (DHS). eIF5A(Dhp) is hydroxylated to eIF5A(Hpu) by deoxyhypusine hydroxylase (DOHH). Adapted from: (Mathews and Hershey 2015).

1.13 Polyamine Regulators

Polyamine regulators are tightly controlled at the levels of transcription, translation and protein degradation by several feedback loop mechanisms. In this fashion, the cell maintains the polyamines within the physiological range that is relevant for normal cellular function. A hypothetical model demonstrating the tight regulation of polyamines is illustrated in **Figure 14**. Activation of polyamine biosynthesis in the presence of an additional stimulus such as an UV irradiation or chemical carcinogen is sufficient to drive tumorigenesis and hyper-proliferative disorders (Shantz, Guo et al. 2002, Nowotarski, Feith et al. 2015). On the contrary, extremely low levels of polyamines account for a cytostatic or cytotoxic effect. These are exemplified by several studies in the literature which demonstrate strong correlation between elevated polyamines and tumour formation in cancers such as the breast, colon, prostrate, neuroblastoma and skin carcinoma (Cipolla, Guille et al. 1993, Leveue, Foucher et al. 2000, Thomas and Thomas 2003, Gerner and Meyskens 2004, Casero and Marton 2007).

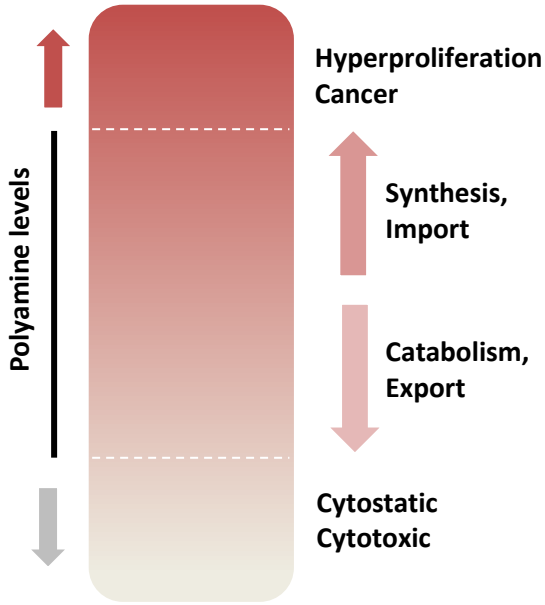

Figure 14: Polyamine levels are regulated within the cell. Hypothetical gradient showing the regulatory range of polyamines within the cell, tightly controlled by synthesis, import, catabolism and export. Polyamine levels above this regulatory range leads to hyper-proliferation and cancer while levels below this range leads to a cytostatic or cytotoxic effect.

1.13.1 Regulation of ODC1

ODC1 is a rate limiting enzyme for the production of Put, Spd and Spm. Thus, its expression is regulated at the levels of transcription, translation and post-translational modification. Several elements present within the promoter region of ODC1 respond differently to growth stimuli, hormones and tumour promoters to regulate ODC1 at the transcriptional level (Pegg 2006). The translation of ODC1 is highly dependent on polyamine concentrations. At high levels of cellular polyamines, the translational inhibition of ODC1 is mediated by an upstream open reading frame (uORF) (**Figure 15A**) (Shantz and Pegg 1999, Miller-Fleming and Olin-Sandoval 2015). The antizyme (AZ) protein also sequesters ODC1 monomers when polyamine levels are high, thereby preventing its dimerization (**Figure 15B**). Binding of AZ induces a conformation change in ODC1, exposing its unstructured C-terminus, that is recognised by the proteasome and targeted for degradation (Pegg 2009, Miller-Fleming and Olin-Sandoval 2015). ODC1 protein has a rapid turnover, with a half-life of between 10 to 30 minutes (Miller-Fleming and Olin-Sandoval 2015, Nowotarski, Feith et al. 2015). While most proteins are degraded by ubiquitin-dependent proteasomal degradation, the degradation of ODC1 is ubiquitin-independent and is mediated via the 26S proteasome (Murakami, Matsufuji et al. 1992, Wu, Chen et al. 2015). Nowotarski et al., have also reported that *Odc1* mRNA contains cis-regulatory elements at both its 3' and 5' UTR that directly influence its protein levels in mouse keratinocyte cell lines (Nowotarski and Shantz 2010, Nowotarski and Shantz 2017). In RAS12V rat intestinal epithelial cell lines, *Odc1* mRNA is stabilized by HuR protein in its 3' UTR, adding to its complexity of regulation (Origanti, Nowotarski et al. 2012).

1.13.2 Regulation of AZ

At low levels of polyamines, AZ is inactivated by an antizyme inhibitor (AZi) allowing ODC1 monomers to form active heterodimers, hence producing more Put (**Figure 15B**). AZ itself is translationally regulated by a ribosome frameshift (**Figure 15C**) (Ivanov and Atkins 2007, Miller-Fleming and Olin-Sandoval 2015). AZ is encoded by two ORF and in order to produce a functional AZ protein, a ribosomal frameshifting is essential. At low levels of polyamines, the synthesis of AZ is inhibited as the ribosome reads the stop codon of the first ORF (Palanimurugan, Scheel et al. 2004, Wu, Chen et al. 2015). When polyamine levels are high, ribosomes at the stop codon shift a nucleotide to continue reading the second ORF (Palanimurugan, Scheel et al. 2004, Kurian, Palanimurugan et al. 2011). The presence of an additional pseudoknot downstream of the frameshift site further promotes the +1 ribosomal frameshifting (Palanimurugan, Scheel et al. 2004, Wu, Chen et al. 2015). However, the mechanism of this frameshift and how it is induced is not entirely understood (Miller-Fleming and Olin-Sandoval 2015).

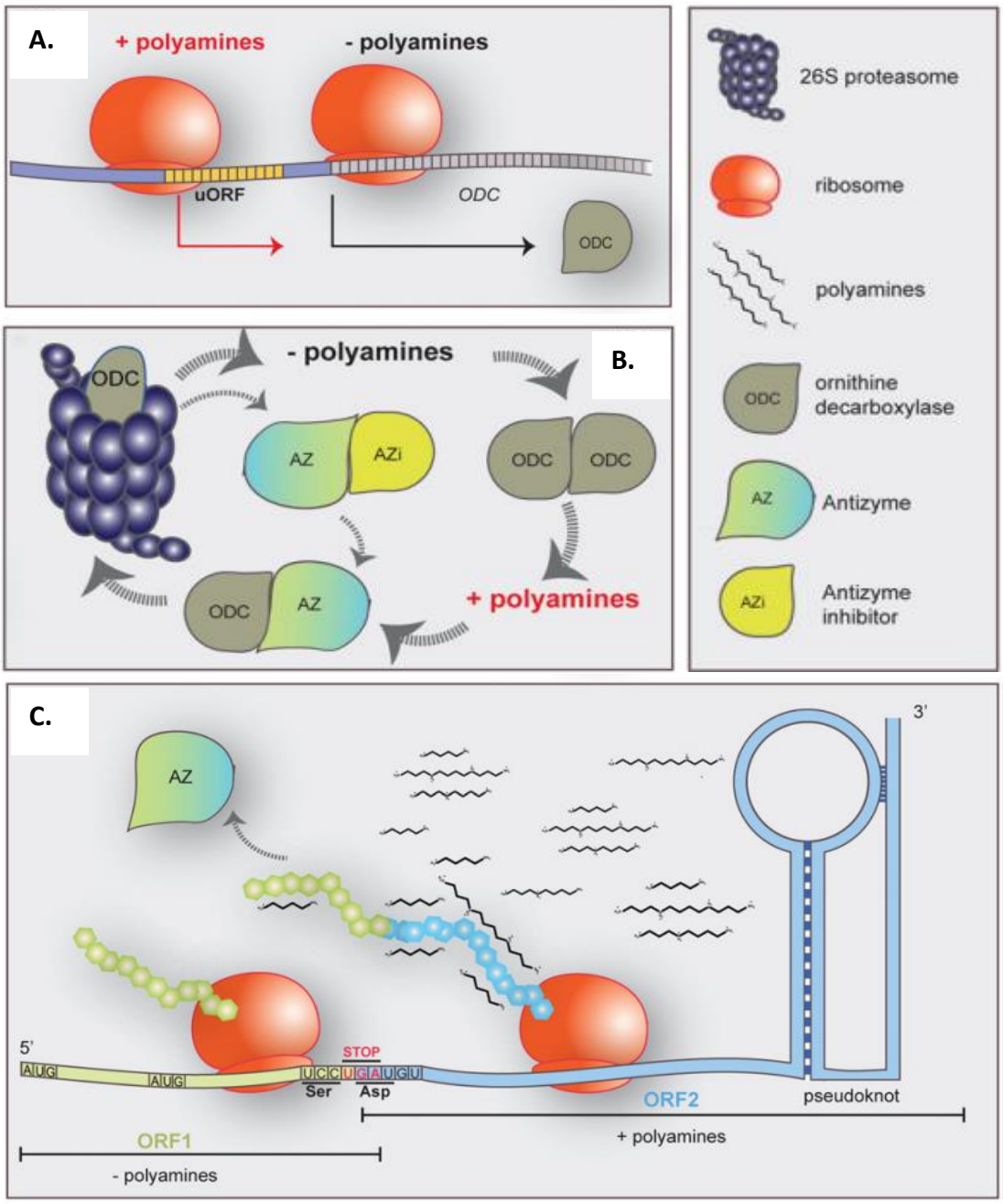

Figure 15: Mechanism of regulation of ornithine decarboxylase 1 (ODC1) and antizyme (AZ). A. When polyamine levels are high, the translation of ODC1 is repressed by an upstream open reading frame (uORF). **B.** ODC1 remains bound to antizyme (AZ) when polyamine levels are high, thus rendering it inactive. This promotes ODC1 degradation in an ubiquitin-independent manner. At low levels of polyamines, AZ in inactivated by an antizyme inhibitor (AZi), enabling ODC1 to form an active dimer to produce more Put. **C.** A hypothetical model for AZ regulation showing the possibility of AZ translation by two ORFs. Ribosomal frame shifting allows the translation of a functional AZ. A pseudoknot downstream of the second ORF promotes ribosome frameshift. Adapted and modified from: (Miller-Fleming and Olin-Sandoval 2015).

1.13.3 Regulation of AMD1

AdoMetDC (AMD1) is initially synthesized as an inactive proenzyme. At high levels of Put, it undergoes an internal serinolysis and cleavage reaction to form an α and β subunit **(Figure 16A)** (Bale, Lopez et al. 2008, Bale and Ealick 2010, Miller and Schoenberger 2015). In mammals, the α/β subunits of AMD1 form dimers and the binding of Put stimulates the processing of AMD1 (Lam, Zhang et al. 2005, Dayoub, Thasler et al. 2006, Pegg 2009). Mature AMD1 is required for the synthesis of Spd/Spm. In the presence of high levels of Spd/Spm, AMD1 undergoes a transamination reaction where it loses its function and is highly susceptible to polyubiquitination and proteasomal degradation **(Figure 16A)**. The half-life of AMD1 is also less than an hour, similar to ODC1 (Pegg 2009). Fluctuations in polyamine levels are known to regulate the expression of AMD1, and a few mechanisms of action have been detailed in the literature.

The regulation of AMD1 translation is known to be mediated by an upstream open reading frame (uORF), which is located 14 nucleotides downstream of its 5'cap. It encodes a hexapeptide, MAGDIS sequence (Hill and Morris 1993, Raney, Law et al. 2002) **(Figure 16B)**. During the synthesis of this peptide, the final tRNA for serine (S) encounters a ribosome and causes it to stall near the uORF termination site, making the AMD1 start codon inaccessible **(Figure 16B)**. This translational regulation of AMD1 is mediated by high levels of Spd/Spm to reduce the synthesis of AMD1.

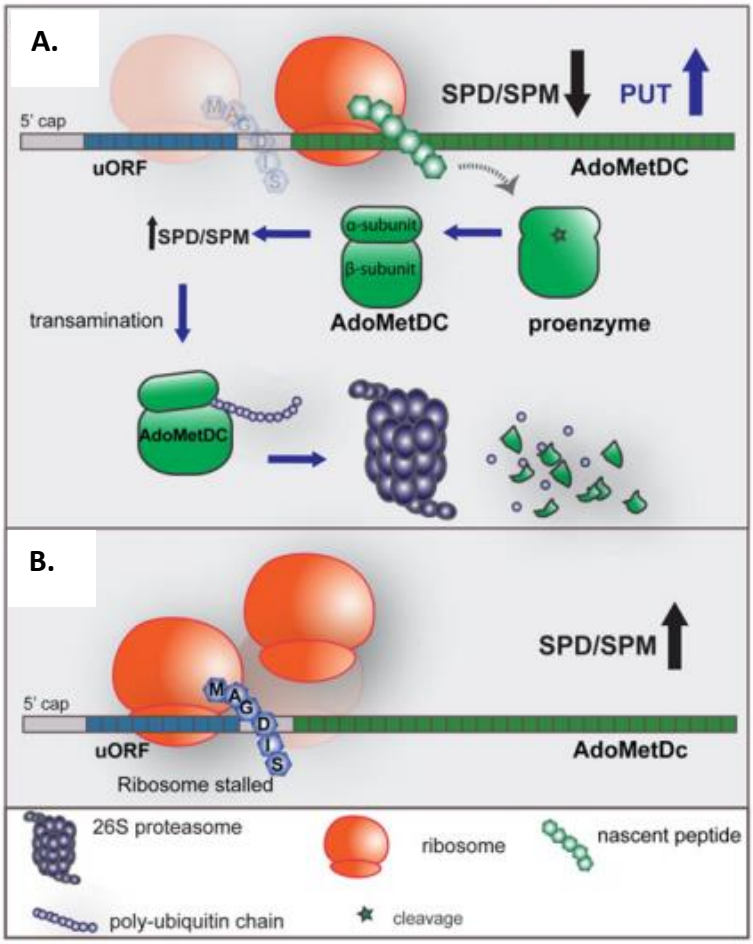

Figure 16: Mechanism of regulation of S-adenosylmethionine decarboxylase 1 (AMD1). A. High levels of Put triggers AMD1 processing from an inactive proenzyme to a mature form comprising of an α and β subunit. Active AMD1 increases Spd/Spm synthesis. High levels of Spd/Spm induces AMD1 transamination followed by ubiquitin-dependent proteosomal degradation. **B.** Additional regulation of AMD1 by an uORF, reduces the translation of AMD1 when Spd/Spm levels are high. Adapted from: (Miller-Fleming and Olin-Sandoval 2015).

Zhang et al. have also reported that *AMD1* is translationally repressed by miR-762 during the differentiation of embryonic stem cells (ESC) to neural precursor cells (NPC) (Zhang, Zhao et al. 2012, Zhao, Goh et al. 2012). Recently, Yordanova et al. described a novel mechanism in which the translation of *AMD1* mRNA could be inhibited when the AMD1 uORF-mediated repression is defective (Yordanova, Loughran et al. 2018). A small proportion of ribosomes translating the *AMD1* mRNA read through the main stop codon of the coding region and stall in the subsequent in-frame stop codon, resulting in a ribosome queue **(Figure 17)**. When the ribosome queue fills the spacer region between the two stop codons, it intervenes with the main *AMD1* coding region, thereby halting its translation **(Figure 17)**. This mechanism is adopted by mammalian cells to limit the number of AMD1 protein molecules that could be synthesized

from a single *AMD1* mRNA transcript and protects the cells from dysregulated *AMD1* translation attributed due to a transcriptional error or mRNA damage.

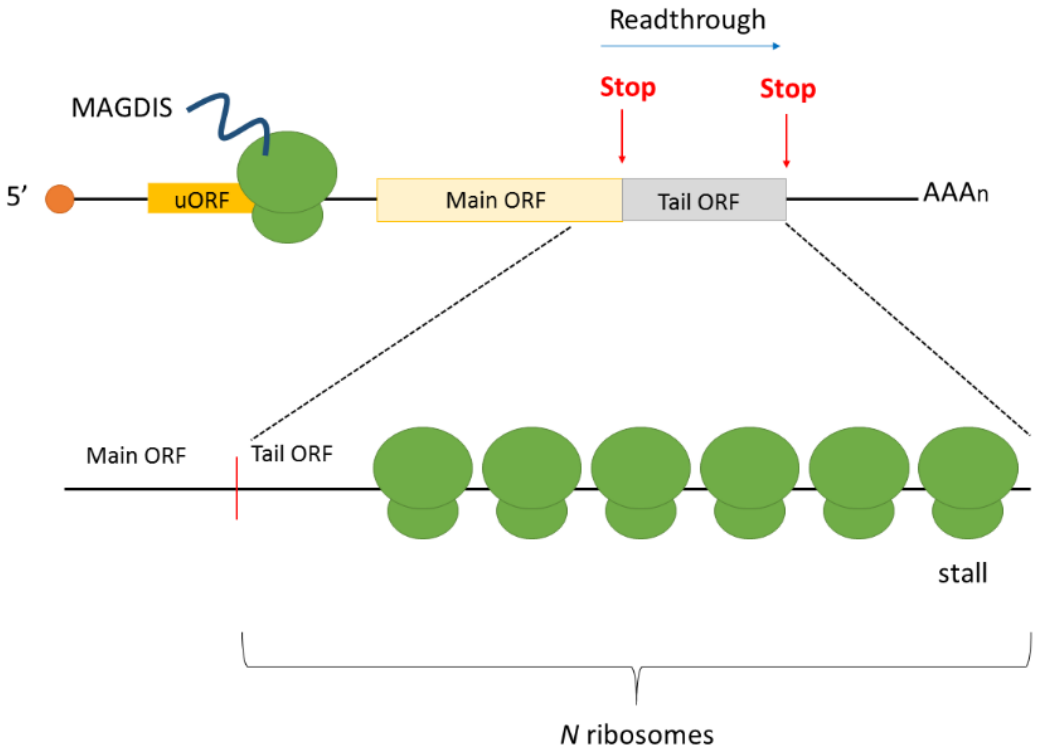

Figure 17: Translational regulation of AMD1. The translation of AMD1 is mediated by an upstream open reading frame (uORF) encoding a MAGDIS hexapeptide sequence. When Spd/Spm levels are high, MAGDIS peptide is synthesized and the ribosome is stalled at its termination site, making the start codon of AMD1 inaccessible. When the AMD1 uORF-mediated repression is defective, ribosomes translating the AMD1 mRNA read through the main stop codon and stall in the subsequent tail ORF stop codon, resulting in a ribosome queue. When the ribosome queue fills the spacer region between the two stop codons, it interferes with the main AMD1 ORF and stops its translation. Adapted and modified from: (Yordanova, Loughran et al. 2018).

Interestingly, AMD1 protein expression exhibits diurnal rhythmicity in accordance to clock gene *Per2* (Zwighaft, Aviram et al. 2015). It has been recently reported that AMD1, and its product Spd, levels oscillate throughout the day while peaking during the night at approximately zeitgeber time 16 (ZT16) in the mouse liver (Zwighaft, Aviram et al. 2015)

1.14 Regulation of RNA-related functions by polyamines

Polyamines, unlike other divalent cations such as Ca^{2+} or Mg^{2+}, have distinct regulatory roles in modulating the function of nucleic acids and proteins (Igarashi and Kashiwagi 2010, Lightfoot and Hall 2014). For instance, polyamines can bind to specific sequences on the DNA and facilitate the recruitment of other factors to enable transcription. The binding of polyamines to B-DNA allows a Z-DNA conformational change, thereby enhancing the affinity of mammalian estrogenic receptor to its response elements (ERE) (Thomas, Gallo et al. 1995). However, most of the polyamines are bound to RNA, suggesting a fundamental role in influencing RNA structure to promote protein translation. The interaction of Spd and Spm with transfer RNA (tRNA) for instance, provides structural stability (**Figure 18**) (Lightfoot and Hall 2014). Genes whose translation are enhanced by the binding of polyamines are referred to as 'polyamine modulons' (Igarashi and Kashiwagi 2010, Lightfoot and Hall 2014). Several polyamine modulons have been identified in yeast, *E.coli* and mammalian cells, but the exact mechanism underlying this stimulation is less well characterised (Igarashi and Kashiwagi 2006, Igarashi and Kashiwagi 2011).

Several hypotheses involving the modulation of RNA by polyamines have been described. For instance, polyamines can facilitate translation when the Shine-Dalgarno (SD) sequence is at an obscure position from the AUG start codon, as in the case of OppA, Fecl, Fis or RpoN (Igarashi and Kashiwagi 2010). The binding of polyamines at regions between the SD sequence and the AUG start codon induces a structural change, thereby allowing the formation of an initiation complex (**Figure 19A**) (Igarashi and Kashiwagi 2010, Lightfoot and Hall 2014). In other cases, the binding of polyamines to specific regions of the RNA can mediate the formation of secondary structures that allow the recruitment of other accessory proteins crucial for translational initiation (**Figure 19B**) (Igarashi and Kashiwagi 2010).

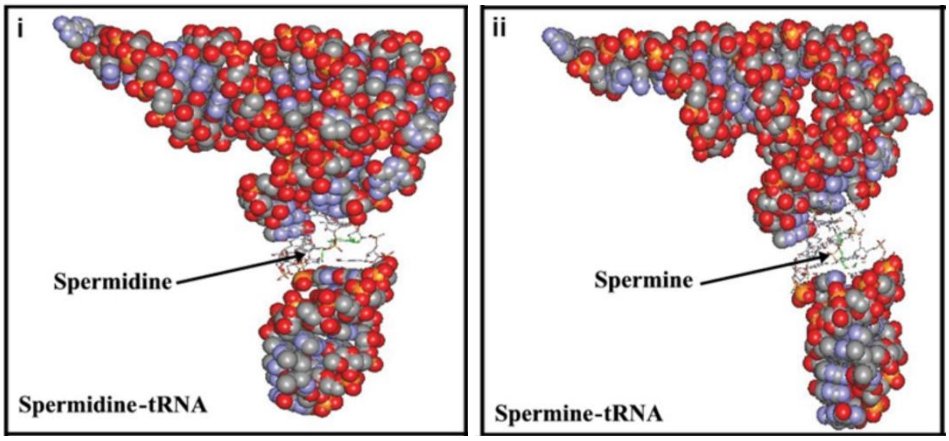

Figure 18: Sphere-filling model of tRNA-Spd/Spm interaction in yeast. Both Spd and Spm are docked to particular regions within the tRNA of yeast to stabilize its structure. Adapted and modified from: (Lightfoot and Hall 2014).

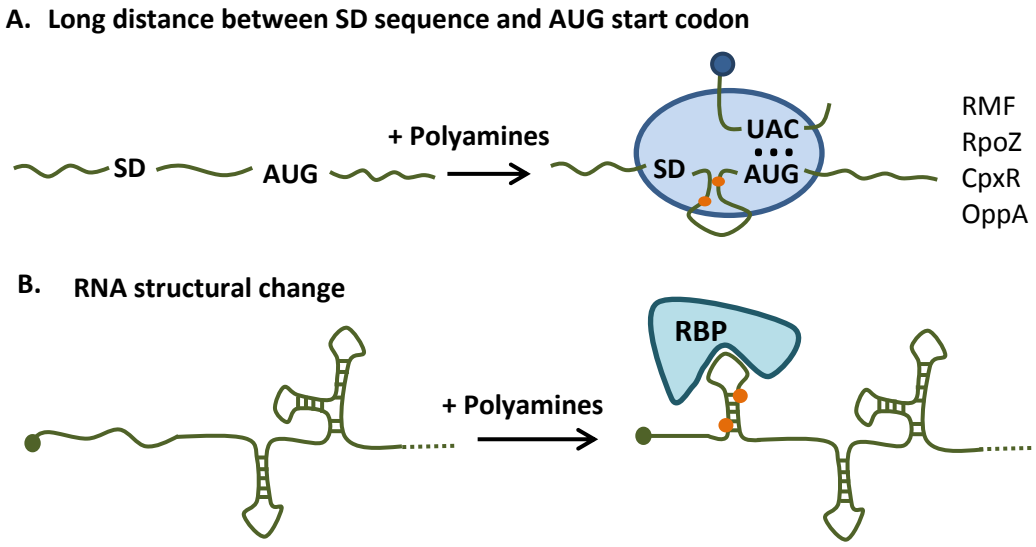

Figure 19: Postulated mechanisms regulated by polyamines in initiating translation. A. Polyamines (orange circles) can bind to regions near the Shine-Dalgarno (SD) sequence and the initiation codon AUG, allowing the formation of an initiation complex. **B.** Polyamines (orange circles) can bind to RNA and induce the formation of secondary structures thereby facilitating the recruitment of additional RNA binding proteins (RBP) necessary to initiate translation. Adapted and modified from: (Igarashi and Kashiwagi 2010).

1.15 Variation of polyamine levels in human

Polyamine levels show variable expression between individuals and different cell types and tissues. They exist at millimolar concentrations within the cells (Igarashi and Kashiwagi 2000). In the skin, polyamine levels were reported to be present at higher levels in the epidermis compared to the dermis. In particular, the levels of Spd and Spm were significantly elevated in

the human epidermis compared to the dermis, suggesting a potential role for these metabolites in normal skin homeostasis (**Figure 20**) (El, Milano et al. 1983). Variability in polyamine levels have also been observed during pregnancy, aging and cancers (Nishimura, Shiina et al. 2006, Minois, Carmona-Gutierrez et al. 2011).

Plasma levels of all polyamines reached their peak towards the end of pregnancy in humans, strongly correlating with increased levels of estradiol and progesterone (Hiramatsu, Eguchi et al. 1985). The ratios of Spd/Spm were significantly elevated in the mammary glands of lactating rats compared to unstimulated mammary glands, while the low levels of Put during lactation was postulated to be due to the rapid conversion of Put to Spd and Spm (Russell and McVicker 1972). Notably, the activities of ODC1 and AMD1 were also high at the initial stages of lactation before it declined (Russell and McVicker 1972). In psoriasis patients, the relative polyamine levels were doubled in lesional skin as opposed to non-lesional skin and the activities of both AMD1 and ODC1 were elevated, accounting for an increase in cell proliferation (**Figure 21A**) (McCullough, Weinstein et al. 1983, Broshtilova, Lozanov et al. 2012, Broshtilova, Lozanov et al. 2013). Polyamine levels were comparable between non-lesional skin of psoriasis patients and healthy individuals (**Figure 21A**). Similarly, basal cell carcinoma (BCC) patients had high levels of all polyamines compared to healthy individuals (**Figure 21B**) (Broshtilova, Lozanov et al. 2012).

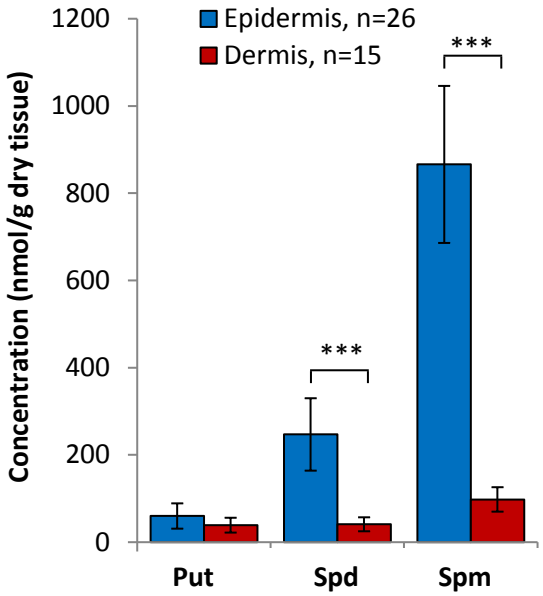

Figure 20: Polyamine concentration in the epidermis and dermis. The concentration of Spd and Spm per gram of dry tissue was significantly higher in the epidermis compared to the dermis. Put levels remained unchanged. Adapted from: (El, Milano et al. 1983).

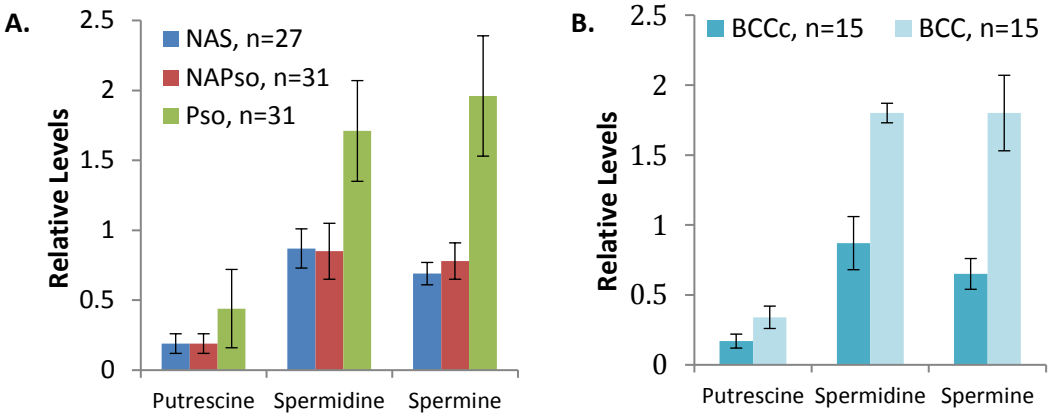

Figure 21: Relative polyamine levels in psoriasis and basal cell carcinoma patients. A. Higher levels of Spd and Spm were observed in psoriasis lesions compared to non-lesional skin in psoriasis patients and healthy controls. **B.** All three polyamines were elevated in basal cell carcinoma patients compared to healthy controls. NAS, Non Affected Skin from healthy patients; NAPso, Non Affected skin from psoriasis patients; Pso, Skin from psoriasis patients; BCCc, Basal Cell Carcinoma controls; BCC, Basal Cell Carcinoma. Adapted from: (Broshtilova, Lozanov et al. 2012).

1.16 Importance of polyamine regulators in epidermal differentiation

The importance of polyamine regulators in keratinocyte maturation was demonstrated in a recent study by Pietilä et al., using SAT1 overexpressing transgenic (Tg) mice. Overexpression of SAT1 will lead to an increase in polyamine catabolism and as a consequence, Put levels would rise. SAT1 overexpressed Tg mice epidermis displayed abundant K14 staining throughout all layers of the epidermis including the cornified layers but reduced expression of differentiation markers K1/10 and FLG as compared to wild-type (Wt) mice epidermis (**Figure 22A**) (Pietilä, Pirinen et al. 2005). By deriving organotypic skin equivalents using SAT1 overexpressed rat epidermal cells, this group further confirmed disturbed epidermal differentiation with an evidence of persistent K14 but diminished K1/10 and FLG expression in all layers of the organotypic epidermis compared to controls (**Figure 22B**) (Pietilä, Pirinen et al. 2005). Aside from a disrupted keratinocyte differentiation, these mice displayed a hairless phenotype with an absence of functional hair follicles as early as postnatal day 27 (Pietilä, Parkkinen et al. 2001, Pietilä, Pirinen et al. 2005). Instead, these mice developed dermal cysts and epidermal utriculi as a result of Put accumulation as confirmed by skin polyamine measurements (Pietilä, Parkkinen et al. 2001). This finding was further strengthened by severe skin changes and aberrant hair follicle development in double Tg mice overexpressing both SAT1 and ODC1 (Pietilä, Parkkinen et al. 2001) with extremely high level of Put concentrations. The skin and hair phenotypes were sufficiently rescued with an inhibition of Put biosynthesis. This suggests that proper regulation of Put levels by either polyamine biosynthesis or polyamine catabolism has a crucial role in epidermal neogenesis and cell proliferation.

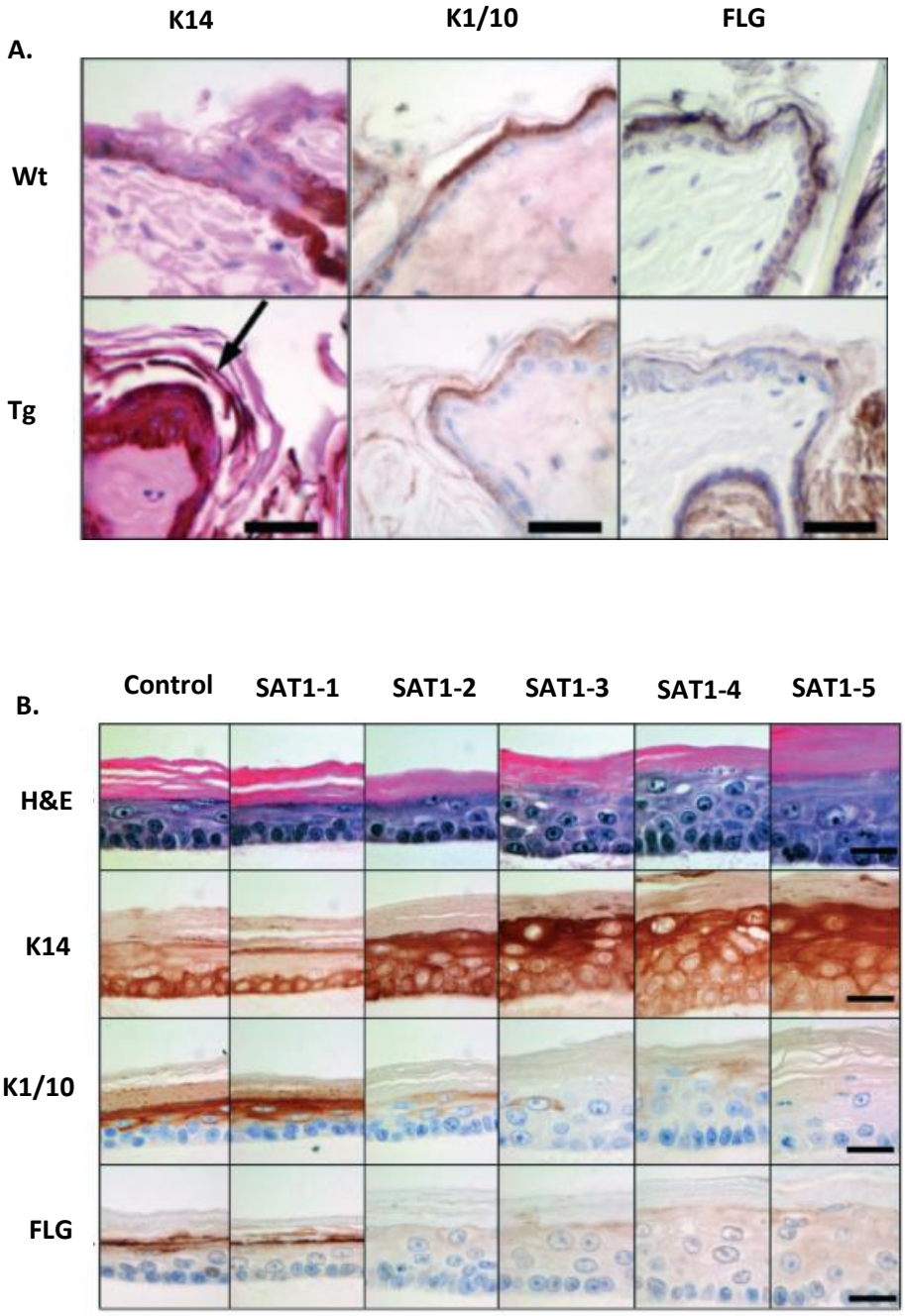

Figure 22: Expression of K14, K1/10 and FLG in mouse skin and organotypic skin equivalents with SAT1 overexpression. A. Abundant K14 staining but reduced K1/10 and FLG staining in SAT1 transgenic (Tg) mice epidermis compared to wild-type (Wt) controls. **B.** Persistent K14 staining was detected in all layers of SAT1 overexpressed organotypic skin equivalents compared to control organotypic skin equivalents. Reduced expression of K1/10 and FLG was detected in organotypic skin equivalents derived from SAT1-2-5 cell lines; scale bar=25μm. Adapted and simplified from: (Pietilä, Pirinen et al. 2005)**.**

1.17 Polyamine levels during aging

Polyamine levels have been shown to decline with age in several model organisms. A study by Nishimura et al. showed that polyamine levels varied in 14 different tissues isolated from female mice aged 3, 10 and 26 weeks- old (Nishimura, Shiina et al. 2006). While Spd levels were found to be reduced in 11 of the 14 tissues with age, the decrease in the levels of Spd was restricted to the muscles, heart and the skin. A study by Vivo et al. showed a decrease in Spd and Spm content with aging in human basal ganglia cells of the brain (Vivo, de Vera et al. 2001). Following this, Gupta et al., reported that Put and Spm levels were found to decline in aging fruit flies in correlation with decreasing memory (Gupta, Scheunemann et al. 2013). The polyamine levels were restored to the levels present in juvenile fruit flies by feeding them with a Spd-rich diet (Davis 2013, Gupta, Scheunemann et al. 2013). The impaired memory was suppressed as a consequence. These Spd-fed fruit flies displayed enhanced autophagy, which could be a potential mechanism of regulation by which Spd function to restore memory (Gupta, Scheunemann et al. 2013). Similar report of decreased Spd levels was observed in yeast with age (Minois, Carmona-Gutierrez et al. 2011).

Exogenous supplementation of polyamines was used as a means to modulate intracellular polyamine levels to increase longevity. Serafini-Fracassini et al., classified Spm and to a lesser extent Spd and Put, as a "juvenility" factor delaying senescence in *Nicotiana tabacum* flowers (Serafini-Fracassini, Del Duca et al. 2002). Soda et al. manipulated the levels of polyamine uptake in mice by feeding male mice with low, medium or high polyamine chow, and the lifespan of these mice was assessed (Soda, Kano et al. 2013). Mice fed with a high polyamine diet displayed a lower mortality compared to mice that consumed a low or medium polyamine diet. However, the mice were sacrificed by 88 weeks, hence impeding further mortality data collection (Soda, Kano et al. 2013). The authors further reported that aged mice fed with a high polyamine diet had a lower risk of developing age-related kidney atrophy (Soda, Kano et al. 2013).

Normally, cells utilise autophagy as a mechanism to degrade intracellular macromolecules and organelles damaged during aging, diseases or in the process of developmental remodelling (Madeo, Zimmermann et al. 2015). Autophagy was deduced as the mechanism of action of Spd to reduce aging and increase life-span. Upon Spd addition in yeast, histone acetyltransferases, Iki3p and Sas3p were inhibited, thus histone H3 is hypoacetylated (**Figure 23**). Epigenetic reprogramming of the cellular transcriptome as a consequence, increases the expression of the autophagy protein network, which is essential for inhibiting cellular necrosis and promoting longevity (Madeo, Eisenberg et al. 2010).

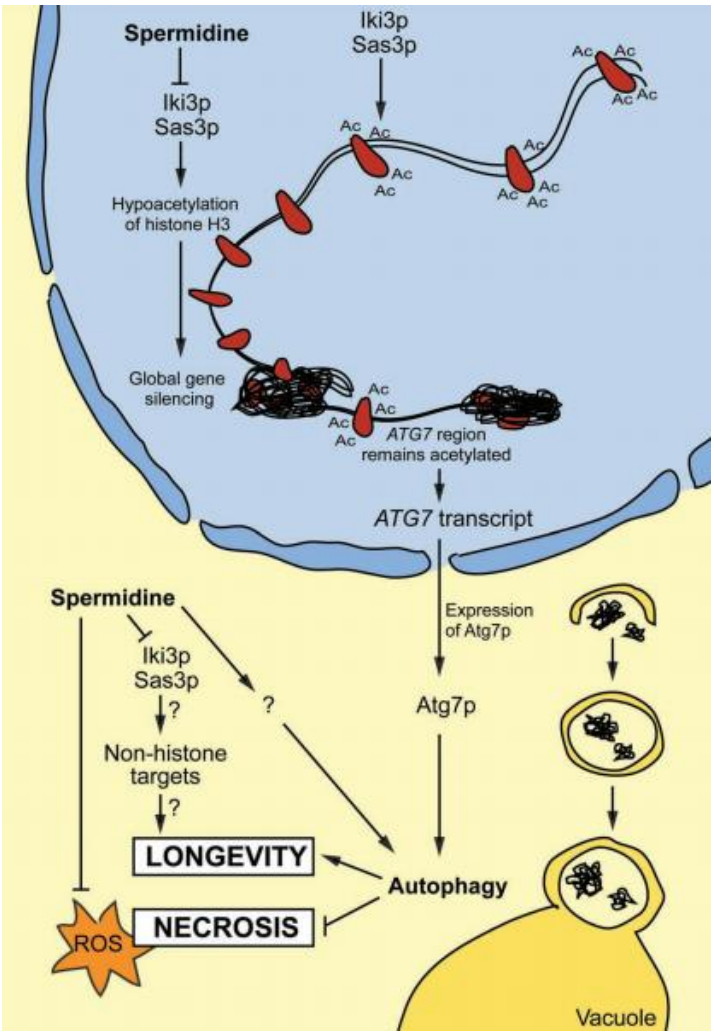

Figure 23: Mechanism of action of spermdine (Spd) in promoting longevity in yeast. Inhibition of histone acetyltransferases (Iki3p and Sas3p) by Spd prevents histone H3 acetylation. This epigenetic reprogramming attributes to changes in the yeast transcriptomics leading to increased expression of genes related to autophagy. Increased autophagy confers longevity and prolongs life-span. Spd may be involved in several yet unknown mechanisms that promotes autophagy thereby increasing longevity. Adapted from: (Madeo, Eisenberg et al. 2010).

Mice fed with Spd have also shown reduction in oxidative damage associated with age (Eisenberg T. 2009, Minois 2014). Spd stimulates the production of anti-inflammatory cytokines and could potentially act through other pathways to reduce chronic inflammation associated with aging (Bjelaković, Stojanović et al. 2010, Minois 2014). Lipid metabolism has an emerging role in increasing lifespan and its dysfunction is linked to aging (Minois 2014). Spd was proven to promote the maturation of adipocytes when 3T3-L1 cells were completely blocked from adipogenesis with a polyamine inhibitor, DFMO (Vuohelainen, Pirinen et al. 2010, Hyvönen, Koponen et al. 2013, Minois 2014). While polyamines decline with age, centenarians were found to have significantly higher levels of Spd and Spm in their whole blood compared to adults aged between 31 to 80 (Pucciarelli, Moreschini et al. 2012). Although a correlation between polyamines and longevity has been established, further work is still needed to fully understand the role of polyamines in increasing lifespan.

1.18 Role of polyamines in non-melanoma skin cancers (NMSC)

Polyamines have known functions in increasing cell proliferation, promoting tumour growth and are present at high abundance in neoplastic tissues (Tabor and Tabor 1984, Pegg 1988, Gilmour 2007, Nowotarski, Feith et al. 2015). Understanding the function of polyamines in regulating skin cancers is important as the polyamine pathway serves as a potential target for chemotherapy and chemoprevention (Pegg 1988). The initial discovery of a role for ODC1 in skin tumorigenesis was demonstrated by O'Brien et al. When Tg mice were constitutively overexpressed with ODC1 under a K5 promoter (K5-ODC1) targeted at the basal layer keratinocytes, Put levels were dramatically increased (O'Brien, Megosh et al. 1997, Peralta Soler, Gilliard et al. 1998). With this targeted overexpression of ODC1 in the skin, these mice were highly vulnerable to the development of tumours when exposed to an additional chemical carcinogen, 7,12-dimethylbenz[a]anthracene (DMBA) or UV irradiation compared to control littermates (O'Brien, Megosh et al. 1997, Peralta Soler, Gilliard et al. 1998).

Similarly, in Tg mice that were constitutively overexpressing ODC1 regulated by a K6 promoter (K6-ODC1) targeting the hair follicles, severe hair loss and the formation of dermal cysts in the hair follicles was observed. These mice developed more dermal papillomas when exposed to UV irradiation compared to Wt mice (Megosh, Gilmour et al. 1995, O'Brien, Megosh et al. 1997). The use of DFMO, an irreversible inhibitor of ODC1 was sufficient to prevent skin tumour growth at the initial stages in carcinogen-treated mice while mice with a heterozygous deletion of ODC1 gene were less susceptible to DMBA/12-*O*-tetradecanoylphorbol-13-acetate (TPA) carcinogenesis (Takigawa, Verma et al. 1982, Tang, Kim et al. 2004, Feith, Origanti et al. 2006). In double Tg mice with a targeted ODC1 overexpression in the hair follicles in addition to an activated Ras protein (K6-ODC/Ras mice), skin carcinomas developed spontaneously without additional chemical carcinogen treatment (Smith, Trempus et al. 1998, Lan, Trempus et al. 2000). This suggests that increased ODC1 activity in combination with Ras activation was sufficient for development of tumours in mice skin. Likewise, constitutively active mutation of MEK in the basal layer keratinocytes (K14-MEK mice) induces ODC1 activity leading to the formation of tumours (Feith, Bol et al. 2005, Feith, Origanti et al. 2006). DFMO treatment in both K6-ODC1/Ras mice and K14-MEK mice showed tumour regression. Though no change in proliferation index was observed, an increase in apoptosis was evident in both cases (Lan, Trempus et al. 2000). Another ODC1 inducible Tg mouse (ODCER) was generated under an *IVL* promoter targeting the suprabasal keratinocytes (Lan, Hayes et al. 2005). This ODCER mice displayed proliferation in both the basal and suprabasal layers of the epidermis, while proliferation was only restricted in the basal layer of the epidermis in WT mice (Lan, Hayes et al. 2005). The disruption in skin homeostasis in ODCER mice, was attributed to the high levels of Put in both the basal and suprabasal layers of the epidermis thereby disrupting keratinocyte differentiation. Taken together, these results suggest that increase in ODC1 activity and as a consequence elevated levels of cellular Put is essential to drive tumour formation making DFMO a promising chemopreventive agent.

AZ1 is a crucial regulator of ODC1 and also functions by limiting the uptake of polyamines. Tg mice with an AZ overexpression driven by either K5/K6 promoter (K5-AZ1 and K6-AZ1) displayed a delayed onset of tumorigenesis when treated with DMBA/TPA chemical carcinogens (Feith, Origanti et al. 2006, Feith, Shantz et al. 2007). Unlike DFMO treatment which induced apoptosis, AZ1 Tg mice reduced the proliferation of tumour cells (Feith, Origanti et al. 2006).

Mice with an overexpression of SAT1 (K6-SAT1) in the epidermis, developed multiple large tumours in comparison to WT mice when treated with DMBA/TPA and were highly susceptible to squamous cell carcinoma (SCC) (Coleman, Pegg et al. 2002). This was attributed to an increase in both Put levels and elevated oxidative damage as a consequence of polyamine catabolism. It was reported that a family with a rare X-linked syndrome called keratosis follicularis spinulosa decalvans had an X-chromosome duplication in the region containing SAT1 (Gimelli, Giglio et al. 2002). These patients developed follicular hyperkeratosis and this was in consistent with a perturbed differentiation phenotype observed in SAT1 overexpressed Tg mice (Pietilä, Pirinen et al. 2005).

In another study, a tetracycline-inducible AMD1 Tg mice (Tet-OAMD1) was crossed with K5-tTA mice containing a tetracycline-regulated transcriptional activator in the basal layer keratinocytes of the skin (Shi, Cooper et al. 2012). With a targeted overexpression of AMD1 in the basal layer keratinocytes expressing K5, Put levels were decreased while increasing Spm:Spd ratios in the basal layer of the epidermis (Shi, Cooper et al. 2012). Though high polyamine levels are associated with neoplastic growth, TAMD1/K5-tTA mice developed less tumours compared to WT mice, when both were treated with a chemical carcinogen, DMBA/TPA (Shi, Cooper et al. 2012). This substantiates the complexity of polyamine metabolism and points towards a crucial role for Put in tumour formation. The role for Put as a tumour promoting agent was further illustrated by a widespread overexpression of SPMS in CAG-SpmS mice which displayed low levels of Spd, but higher Spm and significantly higher

ratios of Spm:Spd. These mice with higher SPMS activity, were not susceptible to tumour development even when treated with DMBA/TPA skin chemical carcinogen nor when a spontaneous intestinal carcinogenesis was induced by a loss of *APC* tumour suppressor gene in CAG-SpmS/Min mice (Welsh, Sass-Kuhn et al. 2012).

1.19 Inhibition of polyamine biosynthesis as an anti-cancer therapy

Since polyamines are involved in cell proliferation and polyamine metabolism is dysregulated in many cancers, targeting the polyamine biosynthesis pathway serves as a potential means to inhibit unwanted cell proliferation that arises during tumorigenesis and other hyper-proliferative skin disorders. Several drugs have been developed over the years, targeting each step of the polyamine biosynthesis pathway. Here, the commonly used drugs in polyamine anabolism will be described.

1.19.1 Inhibition of ODC1

2-difluoromethylornithine (DFMO) is the most successful and extensively used inhibitor targeting polyamine biosynthesis. It is an irreversible enzyme-activated inhibitor of ODC1 (Metcalf, Bey et al. 1978). DFMO competes with ornithine for the active site of ODC1. DFMO initially binds to a cofactor pyridoxal phosphate then gets decarboxylated, which makes it susceptible for covalent bond formation with ODC1, thereby rendering it inactive (Murray-Stewart, Woster et al. 2016). Inhibition of ODC1 with DFMO results in a nearly complete depletion of Put and Spd while the levels of Spm are affected variably (Casero and Marton 2007, Murray-Stewart, Woster et al. 2016). Most studies have demonstrated that DFMO-induced polyamine depletion in cells and tissues is cytostatic but not cytotoxic (Porter and Bergeron 1983, Seidenfeld 1985). Interest in DFMO as an anti-cancer drug started when it was demonstrated that promyelocytic leukemias and lung carcinoma cells responded in a cytotoxic manner without affecting the normal cells (Luk, Civin et al. 1982, Luk, Goodwin et al. 1982).

These results lead to the use of DFMO in clinical trials as a single agent for chemotherapy. Though it was well tolerated by patients, the early clinical trials did not produce any significant clinical improvement (Abeloff, Slavik et al. 1984, Abeloff, Slavik et al. 1986, Meyskens, Kingsley et al. 1986, Horn, Schechter et al. 1987). Recently, DFMO has been used in the treatment of neuroblastoma (NB) (Bassiri, Benavides et al. 2015). Here, DFMO induced cell cycle arrest by suppressing MYC oncogenesis as well as dephosphorylating p27Kip1 and Rb in NB (**Figure 24**) (Wallick, Gamper et al. 2005, Hogarty, Norris et al. 2008, Koomoa, Yco et al. 2008). The oncogenic factor, MYC, is highly up-regulated in the majority of cancers (Maris, Guo et al. 2001). MYC is a transcription factor that dimerizes with its binding partner MAX (Casero and Marton 2007). This complex then binds to an E-box sequence, CACGTG to regulate the transcription of target genes. Since, ODC1 has two E-box sequences, MYC regulates ODC1 expression. Thus, inhibiting ODC1 using DFMO, is an important mechanism of chemoprevention for NB.

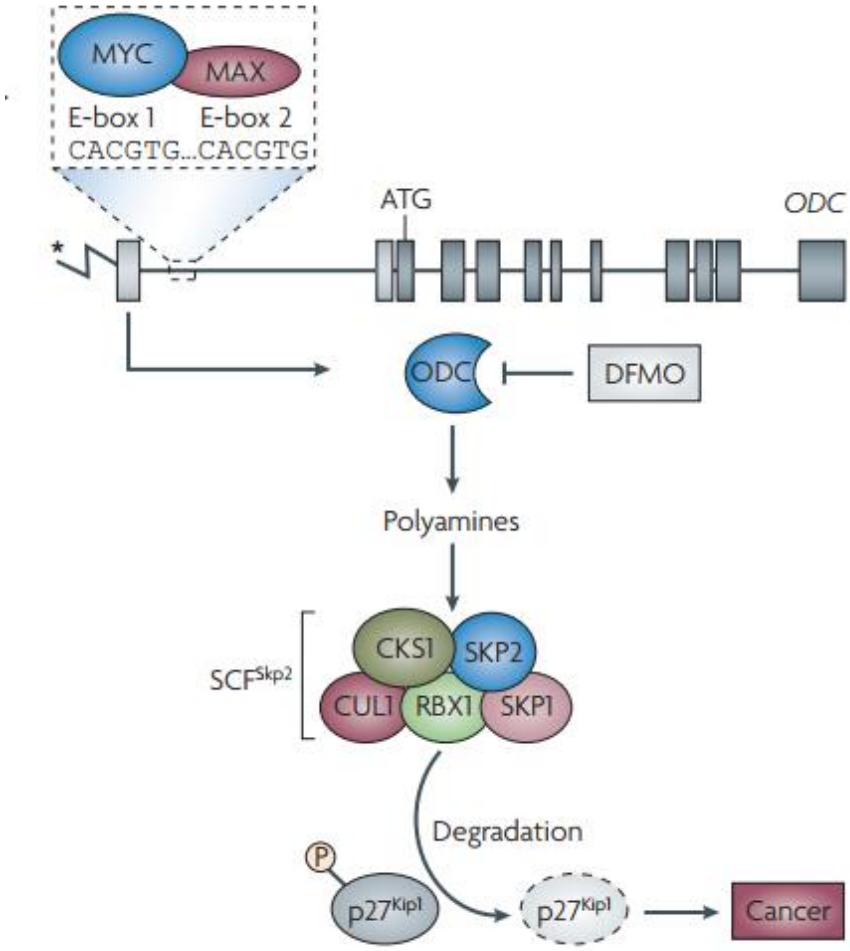

Figure 24: Regulation of ODC1 by MYC in tumour oncogenesis. MYC is a transcription factor that dimerizes with its binding partner MAX. This complex then binds to an E-box sequence, CACGTG to regulate the transcription of target genes. Since ODC1 has two conserved E-box sequences in its intron 1, MYC is able to bind and activate the transcription of ODC1. ODC1 produces Put, which is in turn converted to Spd and Spm, thus accounting for high polyamine levels in MYC-overexpressing cell. MYC promotes carcinogenesis by down-regulating cyclin dependent kinase inhibitor (CDKi), $p27^{Kip1}$. Under normal circumstances, $p27^{Kip1}$ binds and inactivates cyclin E/CDK2 and cyclinA/CDK2 complexes allowing cell cycle progression into S phase. MYC induces the expression of CKS1 and SKP2 thereby targeting $p27^{Kip1}$ degradation by SCF^{Skp2} E3 ubiquitin ligase complex. The effects of MYC on CKS1 and SKP2 expression is dependent on ODC1, which is abolished by its inhibitor, DFMO. Adapted from: (Casero and Marton 2007).

1.19.2 Inhibition of AMD1

AMD1 was first inhibited with an anti-proliferative agent, methylglyoxal bis(guanylhydrazone) (MGBG) (**Figure 25**). The structure of MGBG is similar to Spd. It acts as a competitive inhibitor for AMD1 to reduce the levels of both Spd and Spm.(Williams-Ashman and Schenone 1972). While MGBG decreased the polyamine pools and reduced cell proliferation, its effects

were exerted as a consequence of a considerable amount of mitochondrial toxicity (Pleshkewych, Kramer et al. 1980, Gamble, Hogarty et al. 2012). As such, MGBG was too toxic for clinical trials and hence other derivatives of MGBG were developed and assessed for their ability to decrease Spd and Spm levels without producing any off-target effects. Ethylglyoxal bis(guanylhydrazone) (EGBG) is a close derivative of MGBG. EGBG inhibits AMD1 and causes a depletion in the levels of Spd and Spm fully comparable to MGBG in L1210 leukemia cells at micromolar concentrations (**Figure 25**) (Seppanen, Ruohola et al. 1984). Additionally, no profound mitochondrial toxicity was observed with EGBG suggesting that this compound was suitable as an alternative AMD1 inhibitor (Helariutta, Elomaa et al. 1993). One other derivative that was structurally similar to MGBG was 4-amidinoidan-1-one-2'-amidinhydrazone (SAM486A) (**Figure 25**) (Regenass, Caravatti et al. 1992, Regenass, Mett et al. 1994). SAM486A has been used as a drug to treat non-Hodgkin's lymphoma and was under clinical trials (Siu, Rowinsky et al. 2002, Pless, Belhadj et al. 2004). However, unsuccessful clinical trials were attributed to the compensatory mechanisms that may be activated such as, an increased import of extracellular polyamines, induction of other anabolic enzymes or reduced polyamine catabolism following SAM486A treatment alone.

1.19.3 Inhibition of SPDS and SPMS

Other compounds targeting higher polyamine synthases have been synthesized. These are S-adenosyl-3-thio-1,8-diaminooctane (AdoDATO) and S-adenosyl-1,12-diamino-3-thio-9-azadodecane (AdoDATAD) which specifically inhibit SPDS and SPMS respectively (**Figure 25**) (Casero and Marton 2007, Murray-Stewart, Woster et al. 2016). However, since both compounds bear primary amine groups, they are recognised as substrates by SAT1 and amine oxidases, hence are rapidly catabolised. Thus, these drugs were not suitable for any clinical trials (Murray-Stewart, Woster et al. 2016).

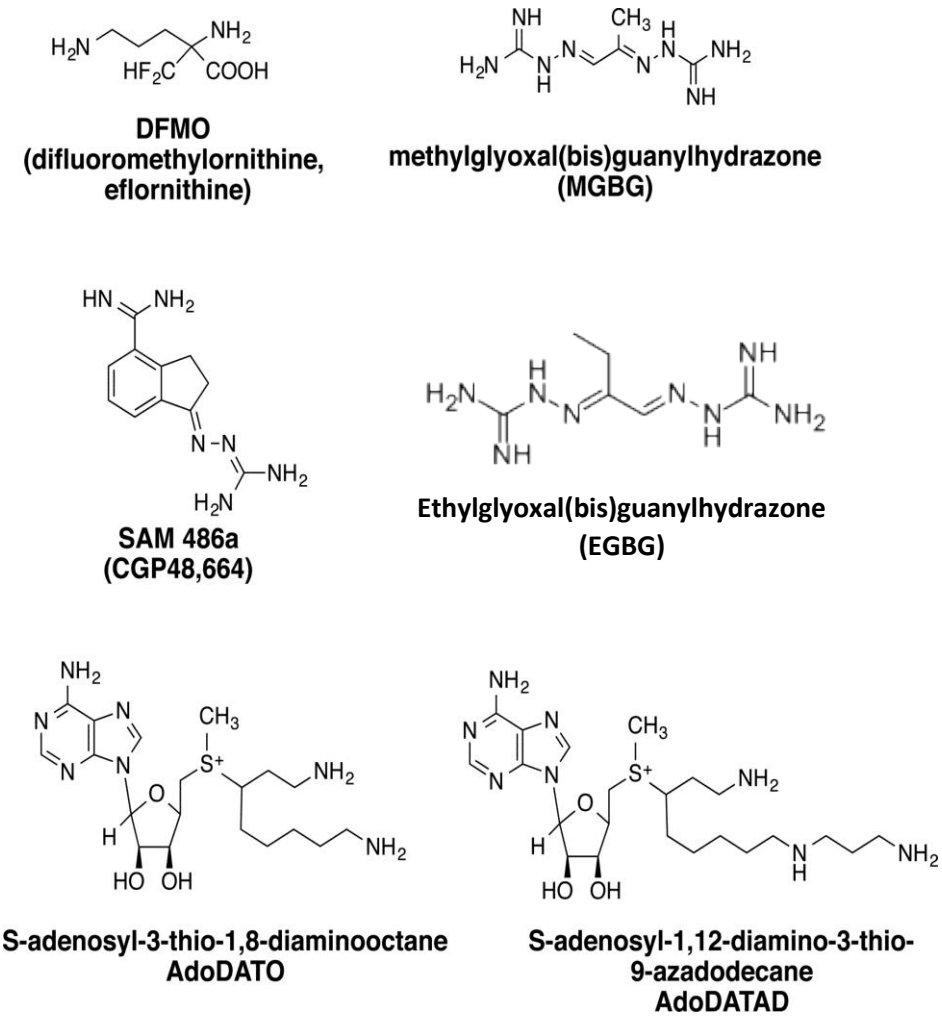

Figure 25: Polyamine biosynthesis inhibitors. DFMO is an irreversible inhibitor of ODC1. MGBG is a potent competitive inhibitor of AMD1, which causes mitochondrial toxicity. EGBG and SAM486A are derivatives of MGBG that do not exhibit mitochondrial toxicity. EGBG however, is structurally similar to MGBG. AdoDATO and AdoDATAD are inhibitors of SPDS and SPMS respectively. Adapted and modified from: (Murray-Stewart, Woster et al. 2016).

1.19.4 Use of DFMO drug in combination therapy

While DFMO is well tolerated by many cells, its major drawback as a single agent in cancer therapy is attributed to the cells innate response in driving polyamine transport when its biosynthesis is blocked. As such, combination therapies involving DFMO and polyamine transport inhibitors (PTI) are currently being investigated. AMXT 1501 is a promising PTI and has demonstrated to produce synergistic effects with DFMO in the treatment of breast, prostate and melanoma cell lines (Burns, Graminski et al. 2009). While the treatment of NB with DFMO

showed positive results previously, a combination treatment with AMXT 1501 showed far greater inhibition of cellular growth by inducing Rb hypophosphorylation and increasing apoptosis as evidenced by the high expression of cleaved PARP and caspase 3 (Samal, Zhao et al. 2013). Recently, Chen et al. reported that a combination therapy using DMFO and PTI, MQT 1426 was more efficacious in treating a mouse model for SCC compared to a single treatment with either of the compounds alone (Chen, Weeks et al. 2006).

1.19.5 Use of DFMO and EGBG in the treatment of psoriasis

Topical treatment of psoriasis patients with MGBG, a competitive AMD1 inhibitor, proved to be partially therapeutic but was discontinued due to its substantial cytotoxicity (McCullough, Weinstein et al. 1983). However, a "priming" effect of DFMO on MGBG to prevent the accumulation of polyamines in the mouse skin was demonstrated (Kapyaho, Lauharanta et al. 1982, Kapyaho, Linnamma et al. 1982). Intradermal administration of either DFMO or EGBG resulted in a decrease in polyamine levels in psoriasis (Kousa, Kapyaho et al. 1982). Thus, further research on psoriasis treatment was directed at a combination therapy using DFMO and EGBG.

1.20 Novel polyamine strategy in promoting anti-tumour immunity

In a tumour microenvironment, malignant cells supress innate immune responses by complex survival mechanism which accounts for the unsuccessful attempts at anti-cancer immunotherapy (Pardoll 2012). Tumour cells surpass the host immune response by altering the expression of their cell surface antigens, modulating the production of pro- and anti-inflammatory cytokines, such as T_H1 and T_H2, and recruiting immunosuppressive regulatory T cells (Tregs) (Hayes, Burns et al. 2014). Since polyamines are known modulators of immune response, they could be used as a means to overcome tumour-elicited immunosuppression (Nowotarski, Woster et al. 2013).

Tumour cells can satisfy their requirement for polyamines to promote growth through polyamine uptake from diet and gut flora, in the circumstance when polyamine levels are depleted using DFMO as a single-drug therapy for cancers. Thus, a novel polyamine blocker therapy (PBT) was adopted by coupling DFMO treatments with AMXT 1501 (Hayes, Burns et al. 2014, Hayes, Shicora et al. 2014). PBT blocked tumour growth and enhanced anti-cancer immune response. The mechanism of action by PBT is illustrated in **Figure 26**.

In a tumour microenvironment, high levels of T_H2 cytokines, interleukin-4 (IL-4) and interleukin 10 (IL-10) are present (Hayes, Shicora et al. 2014). These cytokines up-regulate arginase 1 (Arg1), which converts L-arginine (L-Arg) to ornithine and urea in tumour-infiltrating myeloid cells thereby resulting in Treg cell dysfunction. High levels of Arg1 concomitantly enhances tumour cell survival and progression by depleting L-Arg and promoting polyamine synthesis (Hayes, Burns et al. 2014, Hayes, Shicora et al. 2014). Arg1 depletion using DFMO favours tumour-associated immunosuppression. Additionally, the inhibition of ODC1 with DFMO and polyamine transport system (PTS) by AMXT 1501 serves as a novel anti-cancer therapy.

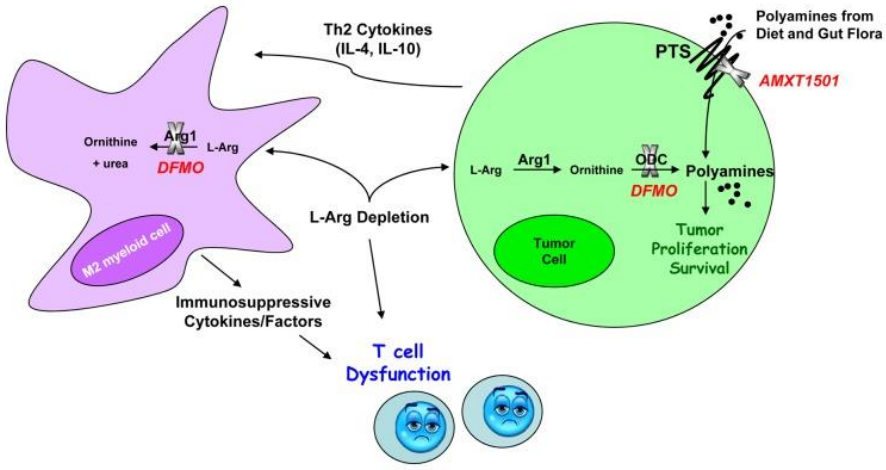

Figure 26: The interplay between polyamine and arginine biosynthesis pathway and its role in T-cell dysfunction in a tumour microenvironment. T_H2 cytokines such as interleukin (IL)-4 and IL-10 are secreted in a tumour microenvironment which activates arginase 1 (Arg 1) in tumour-infiltrating myeloid cells. This allows the progression of myeloid cells to a M2 phenotype thereby releasing immunosuppressive cytokines and causing T cell dysfunction. Arg1 is involved in the conversion of L-arginine (L-Arg) to L-ornithine which is a substrate for ODC1. Polyamine levels are increased with enhanced ODC1 activity, thus promoting tumour growth. Arg1 is depleted with DFMO to limit the immune dysfunction. With ODC1 inhibition using DFMO and polyamine uptake with PTI, AMXT 1501, tumour progression could be suppressed. Adapted from: (Hayes, Burns et al. 2014).

1.21 Hypothesis

We hypothesize that polyamine regulators play a fundamental role in human epidermal differentiation by regulating their expression and concurrently driving a shift in the ratios of polyamines to mediate keratinocyte differentiation.

To address this hypothesis, I would attempt to delineate the role of polyamines and their regulators during epidermal differentiation, with a prime focus on polyamine anabolic enzyme, AMD1.

1.22 Aims

The aims of my project is dissected as follows:

1. To determine the RNA and protein expression of polyamine regulator, AMD1 during keratinocyte differentiation using human primary keratinocytes and immortalized keratinocyte cell line, N/TERT-1.
2. To determine the RNA and protein expression of AMD1 in human skin sections.
3. Perform functional assays to determine the role of AMD1 during keratinocyte differentiation, such as knockdown and inhibition studies using N/TERT-1 keratinocytes and organotypic skin equivalents.
4. Perform rescue studies to determine the necessity of AMD1 during keratinocyte differentiation using N/TERT-1 keratinocytes and organotypic skin equivalents.
5. Determine downstream targets of AMD1 during keratinocyte differentiation using microarray analysis.
6. Characterization of downstream targets of AMD1.

CHAPTER 2

MATERIALS & METHODS

2.1 Cell Culture

The human telomerase reverse transcriptase (hTERT) immortalized keratinocyte cell line (N/TERT-1) obtained from Rheinwald's laboratory (Dickson, Hahn et al. 2000) were maintained in keratinocyte serum-free medium (K-SFM; Gibco®, Life Technologies, CA, USA) supplemented with 25µg/mL of bovine pituitary extract (BPE; Life Technologies, CA, USA), 0.2ng/mL of epidermal growth factor (EGF; Gibco®, Life Technologies, CA, USA), 100U/mL PenStrep (P/S) and 0.3mM $CaCl_2$ (Alfa Aesar, MA, USA) at 37°C, 5% CO_2 incubator. Cells were maintained within passages 50-90 and at approximately 50-60% confluency to prevent differentiation. Fresh media was replenished every other day.

Human Epidermal Keratinocytes (HEKa; Gibco®, Life Technologies, CA, USA) were cultured in EpiLife Medium (Gibco®, Life Technologies, CA, USA) containing Human Keratinocyte Growth Supplement (HKGS; cat. no. S-001-5, Gibco®, Life Technologies, CA, USA) for up to 4 passages. Cells were maintained at 37°C, 5% CO_2 incubator and media was replenished every 3-4 days.

2.2 Lentiviral transduction

Lentiviral particles were produced by co-transfection of the scrambled shRNA (shScrambled) or AMD1 shRNA (shAMD1) pGIPZ vector with packaging plasmids A3 tTA, A5 Rev/Tat, A10 VprRTIN, A19 VSVG and A23 GagPro (GE Dharmacon, Co, USA) into ~50-60% confluent 293FT cells with Lipofectamine 2000 reagent (Invitrogen, CA, USA; **Figure 27**). Lentiviral supernatant was harvested 72h post-transfection, filtered through a 0.45µm filter and pelleted by ultracentrifugation at 70, 000 xg for 2.5h at 4°C in Beckman ultracentrifuge using a SW28 rotor (Beckman Coulter, CA, USA). Virus pellet was re-suspended in 300µl of K-SFM and incubated for

1h at 4°C. N/TERT-1 keratinocytes were transduced with viral medium and incubated for 24h at 37°C, 5% CO_2. Selection was performed in the presence of 2µg/mL of puromycin (Sigma-Aldrich, MO, USA). Cells were checked for GFP expression using the EVOS Digital Microscope (Thermo Fisher Scientific, MA, USA). pGIPZ short hairpin RNA (shRNA) sequences are summarised in **Table 1**.

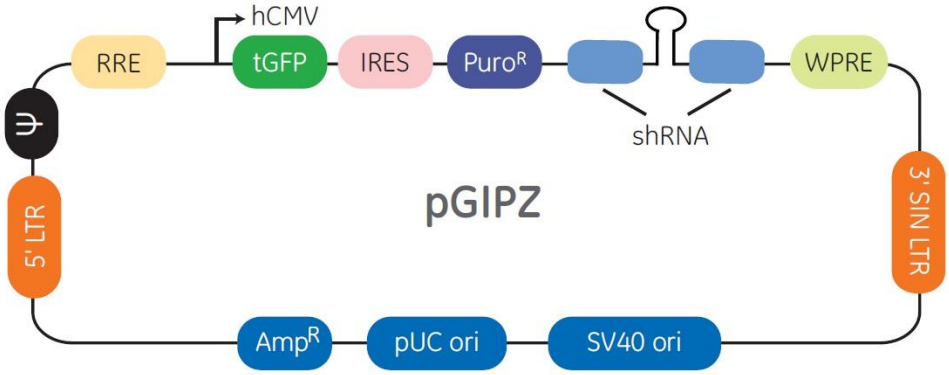

Figure 27: Components in the pGIPZ lentiviral plasmid. hCMV: human cytomegalovirus promoter which drives strong shRNA expression. tGFP: TurboGFP reporter which enables visual tracking of transduction and expression. Puro^R: Puromycin resistance allows antibiotic-selective pressure and proliferation of shRNA-transduced cell. IRES: internal ribosome entry site which allows expression of TurboGFP and puromycin resistance genes in a single transcript. 5' LTR: 5' long terminal repeat, 3' SIN LTR: 3' self-activating long terminal repeat for enhanced lentivirus safety. Ψ: Psi packaging sequence which allows viral genome packaging using lentiviral packaging systems. RRE: Rev response element which improves titre by increasing packaging efficiency of full-length viral genomes. WPRE: Woodchuck hepatitis post-transcriptional regulatory element which enhances transgene expression in the target cells. Diagram and captions were excerpted from GE Dharmacon manual.

Table 1. shScrambled and shAMD1 shRNA sequences.

shRNA	shRNA sense sequence
shScrambled	5'-ATCTCGCTTGGGCGAGAGTAAG-3'
shAMD1-3	5'-AGACTTCTACAACTTTCCT-3'
shAMD1-4	5'-TTAATAGAACAGTCCTAGA-3'

2.3 MTS Cell Proliferation Assay

Cell viability at various concentrations of Put (cat no. P7505; Sigma-Aldrich, MO, USA), Spd (cat no. S2626 Sigma-Aldrich, MO, USA) and Spm (cat. no. S3256; Sigma-Aldrich, MO, USA) was

determined using CellTiter 96® AQueous One Solution Cell Proliferation Assay (MTS; Promega, WI, USA). N/TERT-1 keratinocytes were seeded at a density of 3000 cells/ well in 96- well plates in K-SFM. After 24h, fresh media was changed and supplemented with either Put, Spd, Spm or Spd/Spm at concentrations ranging from 0.1-20mM every day for 72h. 20µl of MTS reagent was added to each well containing 100µl of fresh K-SFM and incubated at 37°C, 5% CO_2 for 1-2h. Absorbance was read at 490 nm with a microplate reader (Tecan, Switzerland) to determine cell viability. The principles of MTS assay is summarised in **Figure 38A.** Cell viability was determined similarly with AMD1 inhibitor, EGBG (received from Igarashi, K., Japan), at concentrations ranging from 1-200µM for 48h.

2.4 Monolayer keratinocyte differentiation

2.4.1 N/TERT-1 keratinocytes

For differentiation experiments using N/TERT-1 keratinocytes, cells were seeded at a density of 0.1 million cells/ well in 6-well plates and cultured to 100% confluence for four days in supplemented K-SFM. Confluent keratinocytes were harvested as day 0 (D0) undifferentiated samples for RNA and protein. To induce differentiation, cells were switched to high calcium media prepared by adding 1.2mM of $CaCl_2$ in a 1:1 mixture of supplemented-KSFM and DF-K media (contains 1:1 (vol/vol) Dulbecco's Modified Eagle Medium/High Glucose (Hyclone ™, GE Healthcare Life Sciences, IL, USA) and Ham's F-12 (Gibco®, Life Technologies, CA, USA) supplemented with 25µg/mL BPE, 0.2ng/mL EGF, 100U/mL P/S and 100U/mL L-glutamine (Gibco®, Life Technologies, CA, USA)). Differentiated keratinocytes were harvested for RNA and protein at D2, D4 and D6 respectively with fresh media change every other day, as depicted in **Figure 29A.**

For AMD1 inhibition differentiation experiments, EGBG was added at a concentration of either 5µM, 25µM or 50µM at the start (D0) or at D3 of differentiation as described in figure legends. AMD1 inhibition was rescued by the addition of 1mM Spd/Spm in combination. Fresh media and

drugs were replenished every other day till harvest. D0 undifferentiated and D6 differentiated keratinocytes were harvested for RNA and protein.

For differentiation experiments using shAMD1 knockdown keratinocytes, lentiviral transduced shScrambled N/TERT-1 keratinocytes were seeded at a density of 0.1 million cells/well while shAMD1-3 knockdown keratinocytes were seeded at a density of 0.125 million cells/well and shAMD1-4 knockdown keratinocytes were seeded at 0.115 million cells/well in 6-well plates to compensate for the marginally reduced proliferation efficiency after AMD1 knockdown. Differentiation was performed as previously described. shAMD1 knockdown keratinocytes were rescued with the addition of 1mM Spd/Spm in combination from the start of differentiation at D0. Fresh drugs were supplemented with media every other day till D6 of differentiation.

2.4.2 HEKa

For differentiation experiments using HEKa, cells were seeded at a density of 0.1 million cells/ well in 6-well plates and cultured to 100% confluence for up to 10 days in supplemented-EpiLife medium. Confluent keratinocytes were harvested at D0 as undifferentiated keratinocytes for RNA and protein. Differentiation was induced similarly as N/TERT-1 keratinocytes, as previously described.

2.5 Human skin biopsies

In collaboration with the skin cell bank of IMB, human skin biopsies were sourced from the National University Hospital (NUH) and Singapore General Hospital (SGH). Patients' written consent were obtained in all cases. All studies were performed in accordance with the declaration of Helsinki and was approved by a local scientific ethics review board. Freshly obtained skin were dissected into approximately 6-mm cubes and cultured at an air-liquid interface in RM^+ media (**Table 2**) for 24 hours (h). *Ex vivo* skin was further dissected into two, with one half snap-frozen in Tissue-Tek® Optimal Cutting Temperature formulation (OCT; Sakura® Finetek, USA Inc.) and the other fixed in 10% neutral buffered formalin (NBF; Sigma-Aldrich, MO, USA) and embedded

in Surgipath® Paraplast paraffin wax (Leica Biosystems, Wetzlar, Garmany) prior to histological analysis.

Table 2. Components of RM+ media

Components	Volume
Dulbecco's High Glucose Modified Eagles Medium (HyClone™, GE Healthcare Life Science, IL, USA)	300mL
Ham's F-12 (Gibco®, Life Technologies, CA, USA)	110mL
Fetal Bovine Serum (FBS) (Gibco®, Life Technologies, CA, USA)	50mL
P/S (Gibco®, Life Technologies, CA, USA)	5mL
Transferrin (Tsf) (5mg/mL) (Sigma-Aldrich, MO, USA)	0.5mL
Adenine (And) (9.72mg/mL) (Sigma-Aldrich, MO, USA)	1.25mL
Liothyronine (T3) (2 X 10^{-6}M) (Sigma-Aldrich, MO, USA)	0.5mL
Insulin (5mg/mL) (Sigma-Aldrich, MO, USA)	0.5mL
Hydrocortisone (200µg/mL) (Sigma-Aldrich, MO, USA)	1mL
EGF (10µg/mL) (Sigma-Aldrich, St. Louis, MO, USA)	0.5mL

2.6 Generation of organotypic skin equivalents

shScrambled N/TERT-1 keratinocytes were seeded at a density of 0.3 million cells/ polycarbonate 24-well plate cell culture inserts (Nunc™, Waltham, MA USA) while shAMD1-3 N/TERT-1 keratinocytes were seeded at a density of 0.325 million cells/ insert of 0.4μm in CnT-Prime epidermal culture media (CellnTech Advanced Cell Systems AG, Bern, Switzerland) and allowed to grow to full confluence for 2 days. One of the inserts was fixed with 100% methanol for 30 mins, washed with 1X PBS and then stained with 10% Gimesa stain (Merck, Singapore) for 30 mins. The stain was washed under running tap water and the confluency of the cells was determined visually by the purple stain. If a confluent monolayer was formed, cells were then switched to CnT-PR-3D media (CellnTech Advanced Cell Systems AG, Bern, Switzerland) inside and outside of the insert

for 16h. Airlift was performed by removing media from the inside of the inserts and replacing 3mL of fresh CnT-PR-3D media on the outside of the inserts. Media was replenished every other day for 7 days. shAMD1-3 knockdown keratinocytes were rescued by addition of 100μM of Spd/Spm in combination at D3 and D5 of airlift. At D7, all media were removed and the insets were fixed with 4% paraformaldehyde (PFA; Sigma-Aldrich, MO, USA) overnight at 4°C, then switch to 70% ethanol for 24h. Schematic flow of organotypic skin cultures is illustrated in **Figure 42.1.** Organotypic skin equivalents were cut into halves and sandwiched between two sponges (Thermo Fisher Scientific, Waltham, MA USA) soaked in 70% ethanol in a cassette (Thermo Fisher Scientific, Waltham, MA USA). Rehydration was performed by switching the cassettes from 70% to 80%, 90%, 100% and 100% ethanol followed by twice in 100% xylene for 1h each. Cassettes were soaked in warm paraffin wax (Leica Biosystems, Wetzlar, Germany) overnight at 65°C. The following day, fresh warm wax was changed and cassettes were soaked for an additional 1h. Organotypic skin equivalents were removed from cassettes and embedded into paraffin blocks and kept at 4°C overnight prior to sectioning. All organotypic skin equivalents were sectioned at 7μm thickness using a microtome (Leica Biosystems, Wetzlar, Germany) onto microscopic glass slides (Leica Biosystems, Wetzlar, Garmany). All slides were dried on a heat block at 50°C overnight (O/N) and baked at 60°C to melt the paraffin wax 30 mins prior to dewaxing.

2.7 Immunohistochemistry on organotypic skin equivalents

Organotypic skin equivalents were dewaxed in xylene for three times at 3 mins each followed by three times in 100% ethanol, then through descending percentages of ethanol from 90%, 80%, and 70% and to water for 3 min each. Slides were heat exposed in 1X DAKO Target retrieval solution, citrate pH 6.0 (Agilent, CA, USA) diluted in deionised water for 20 mins at 120°C in a pressure cooker. Slides were cooled and rinsed three times for 5 mins each in 1X PBS containing 0.05% Tween-20 (PBS-T). Endogenous peroxidase was quenched from the de-waxed skin sections for 30 mins in 1% hydrogen peroxide (H_2O_2) (Merck Millipore, MA, USA) in PBS. Slides were rinsed under running tap water for 5 mins then another 5 mins in PBS-T on shaking. DAKO pen (Agilent, CA, USA) was used to mark a circumference around each skin section. Skin sections were blocked

using 10% DAKO goat serum (Agilent, CA, USA) in PBS for 30 mins in a humidified chamber. Blocking serum was soaked off and primary antibody was diluted in 10% DAKO goat serum (Agilent, CA, USA) in PBS and added at a concentration of 1:10,000 for rabbit (Rb) anti-LOR (cat. no. ab176322, Abcam, UK) and 1:1000 for mouse (Ms) anti-FLG (cat. no. ab17808, Abcam, UK) antibodies for 2h. For negative control, slides were left on with 10% blocking serum instead of a primary antibody. Skin sections were washed under running tap water for 10 mins then in PBS-T for 5 mins on shaking. Undiluted DAKO Real™ EnVision™+ System-HRP Labelled Polymer anti-Ms or anti-Rb secondary antibody (Agilent, CA, USA) was added accordingly for 30 mins. Skin sections were washed under running tap water for 10 mins then in PBS-T for 5 mins on shaking. Skin samples were developed using 1 drop of Dako REAL™ DAB+ Chromogen diluted in 1mL of Dako REAL™ Substrate Buffer (Agilent, CA, USA) for 30sec. Skin sections were washed under running tap water for 10 mins to stop the DAB reaction then counterstained with haematoxylin (Sigma-Aldrich, MO, USA) for 12 mins followed by acid alcohol (1% HCL, 70% ethanol in 1L water) for 30s and Scott's tap water (2g $NaHCO_3$, 20g $MgSO_4$ in 1L water) for 30s. Slides were rinsed in water for 10s between each stain. Slides were rehydrated from water to ascending percentages of ethanol from 70%, 80%, 90% and three times in 100% ethanol followed by three times in xylene for 3 mins each. Slides were left to dry and mounted using Cytoseal™ Mounting medium (Richard-Allen Scientific Co., CA, USA). For H&E staining of organotypic skin equivalents, skin sections were immersed in eosin (Sigma-Aldrich, St. Louis, MO, USA) for 3mins prior to rehydration steps. Fiji ImageJ software was used for post-processing of images.

2.8 Immunofluorescence (IF) on human skin biopsies

OCT embedded frozen skin sections from -80°C were thawed at room temperature (RT) for 30 mins. DAKO pen (Agilent, CA, USA) was used to draw a circle around each skin section. Skin sections were blocked with 10% DAKO goat serum (Agilent, CA, USA) in PBS for 30 mins in a humidified chamber. Blocking serum was soaked off and primary antibodies diluted in 10% DAKO goat serum (Agilent, CA, USA) in PBS were added at an appropriate concentrations as stated in **Table 3** for 1h. For negative control, blocking serum was left on instead of a primary antibody.

Skin sections were washed in running tap water for 10 mins then rinsed in PBS-T for 5 mins on shaking. Anti-Ms or anti-Rb fluorophore-conjugated secondary antibody was added at a dilution of 1:500 in 10% goat serum in PBS accordingly as stated in **Table 3**, for 30 mins in the dark. Skin sections were washed in running tap water for 10 mins then rinsed in PBS-T for 5 mins on shaking. Skin sections were counterstained with either Hoechst dye or 4',6-diamidino-2-phenylindole (DAPI) for 10 mins at 1:2000 dilution in PBS. Slides were rinsed under running tap water for 10 mins and mounted in aqueous non-fluorescing hydromount (NHG Diagnostics, Singapore) containing 2.5% DABCO (Sigma-Aldrich, MO, USA). Slides were stored in 4°C in dark and fluorescence images were captured using Zeiss Axioimager GU or Olympus FV1000 Upright microscopes. Fiji ImageJ software was used for post-processing of images.

Table 3. List of primary antibodies used for immunofluorescence (IF).

Antibody	Type	Brand (Country)	Cat. no.	Dilution
anti-AMD1	Ms monoclonal	Santa Cruz Biotechnology (TX, USA)	sc-390073	1:300
anti-CPEB4	Rb polyclonal	Abcam (UK)	ab83009	1:100
anti-FLG	Rb polyclonal	Abcam (UK)	ab81468	1:500
anti-IVL	Rb polyclonal	Abcam (UK)	ab53112	1:100
anti-K10	Rb monoclonal	Abcam (UK)	ab76318	1:100
anti-K14	Ms monoclonal	Abcam (UK)	ab9220	1:500
anti-SPD	Rb polyclonal	Abcam (UK)	ab7318	1:100
anti-SPM	Rb polyclonal	Abcam (UK)	ab26975	1:100

2.9 RNAscope® In Situ Hybridization

Microtome was prepped by spraying with RNase*Zap*™ RNase decontamination solution (Thermo Fisher Scientific, MA, USA) prior to sectioning formalin-fixed, paraffin-embedded skin biopsies at 7μm onto Superfrost® Plus microscopic slides (Thermo Fisher Scientific, MA, USA). Slides were

baked for 1h at 60°C then deparaffinised by submerging in xylene twice for 5 mins each followed by 100% ethanol twice for 1 min each, then air-dried. Deparaffinised slides were incubated with ~5-8 drops of RNAscope® hydrogen peroxide solution (Thermo Fisher Scientific, MA, USA) for 10 mins at RT then soaked off and washed with fresh distilled water. Slides were acclimatized in distilled water at 95°C for 10s then steamed in RNAscope® 1X Target Retrieval Reagent (Thermo Fisher Scientific, MA, USA) for 15 mins. Slides were subsequently rinsed in distilled water for 15s then transferred to 100% ethanol for 3mins and air-dried at RT. A hydrophobic barrier was drawn around each skin section using an Immedge™ hydrophobic barrier pen (Vector Laboratories Inc., CA, USA). Skin sections were entirely covered with ~5 drops of RNAscope® Protease Plus (Thermo Fisher Scientific, MA, USA) solution and placed in a HybEZ™ Humidity Control Tray (Advanced Cell Diagnostics, CA, USA) in the HybEZ™ Oven (Advanced Cell Diagnostics, CA, USA) for 30 mins at 40°C. Slides were removed from the oven and rinsed in distilled water for 3-5 mins by agitation. Approximately 4 drops of AMD1 RNA probe was added to cover the skin section and incubated in the oven for 2h at 40°C. As a positive control, polymerase II subunit A (POLR2A) RNA probe was used. Slides were removed from the oven and washed with 1X RNAscope® Wash Buffer (Thermo Fisher Scientific, MA, USA) twice for 2 mins each at RT with occasional agitation. This was followed by six hybridization steps using ~ 4 drops of RNAscope® Hybridize AMP1-6 (Thermo Fisher Scientific, MA, USA), alternating between 30 min and 15 mins incubation at 40°C in the oven. After each hybridization step, reagent was soaked off and rinsed twice in 1X RNAscope® Wash Buffer for 2 mins each by occasional agitation. After the final wash step, slides were flicked off from excess liquid and skin sections were completely covered with ~4 drops of RNAscope® RED Working solution (Thermo Fisher Scientific, MA, USA) and incubated for 10 mins at RT. Solution was soaked off and rinsed under fresh tap water. Slides were counterstained with 50% Haematoxylin staining solution (Sigma-Aldrich, MO, USA) diluted in water for 2 mins at RT. Slides were washed in distilled water for 3-5 times on agitation then submerged in 0.02% Ammonia water (Sigma-Aldrich, MO, USA) followed by distilled water for 2 mins at RT. Slides are dried in a 60°C oven for 15 mins, mounted with EcoMount (Advanced Cell

Diagnostics, CA, USA) and visualized at 40X magnification using a Zeiss AxioImager GU bright-field microscope. Fiji ImageJ software was used for post-processing of images.

2.10 RNA extraction

Total RNA was harvested by adding 1mL of TRIzol reagent (Life Technologies, CA, USA) directly onto cultured keratinocytes. Samples were immediately snap-frozen in liquid nitrogen and stored at -80°C till further processing. To extract RNA, TRIzol samples were thawed to RT. 200uL of chloroform (Merck, NJ, USA) was added, vortexed and spun at 16, 100 xg for 15 mins at 4°C. 600µl of aqueous phase was transferred to a new eppendorf tube containing 600µl of 70% ethanol. Samples were mixed and subsequent RNA extraction steps were performed on-column with DNAse-I digestion using the RNeasy kit (Qiagen, Germany) as per manufacturers' protocol. RNA was eluted in ultra-pure water (Biological Industries, CT, USA) and the concentration and purity of the RNA was measured using Nanodrop ND-1000 spectrophotometer (Thermo Fisher Scientific, MA, USA).

2.11 cDNA synthesis and Quantitative Real-Time PCR (qRT-PCR)

1µg of RNA was used from cDNA synthesis using the RevertAid H Minus First Strand cDNA synthesis kit (Thermo Fisher Scientific, MA, USA). Components and cycling conditions for cDNA synthesis are started in **Tables 4 and 5** respectively. 6µl of cDNA was diluted in 194µl of RNAse-free water and loaded onto 384-well plates (Applied Biosystem, UK) as specified in **Table 6**. qRT-PCR was performed using 7900HT Fast Real-Time PCR system (Thermo Fisher Scientific, MA, USA) with thermal profile as stated in **Table 7**. Primer sequences used are summarized in **Table 8**. Target genes were normalized to housekeeping gene, ribosomal protein large 13A (RPL13A).

Table 4. Components for cDNA synthesis

Part	Components	per reaction
A	RNA	1µg
	100µM oligo $(dT)_{18}$	0.5µl
	100µM random hexamers	0.5µl
	RNase-free water	(x – 11 µl)
B	5X Reaction buffer	4µl
	RiboLock RNase inhibitor, 20U/µl	1ul
	10mM dNTP mix	2µl
	RevertAid M-MuLV Reverse Transcriptase, 200U/µl	1µl
	Total	20µl

Table 5. cDNA synthesis cycling conditions.

Temperature (°C)	Duration (min)
65	5
25	5[a]
42	60
70	5
4	∞

[a] Following this step, samples were placed on ice for at least 1 min before adding the reagents from part B of **Table 4**.

Table 6. qRT-PCR reaction mixture

Components	per reaction (µl)
2X POWER SYBR Green Master Mix (Applied Biosystem, UK)	5
Forward + Reverse gene specific primer mix, 2.5µM (IDT, Singapore)	1
Diluted cDNA	4
Total	10

Table 7. qRT-PCR thermal profile

Step	Temperature (°C)	Duration	Cycle(s)
1	90	2 min	1
2	95	10 min	1
3	95 60 72	30 s 30 s 1 min	40
4	95 60 95	15 s 15 s 15 s	1

Table 8. Sequence of forward and reverse primers used for qRT-PCR.

Gene	Primer Sequence
AMD1	F 5'-CTG GGG ATC TTC GCA CTA TC- 3' R 5'-CCC TAG CAA GCT TCA ACA GG- 3'
AQP3	F 5'-ATC TAC ACC CTG GCA CAG AC- 3' R 5'-GCT GTG CCT ATG AAC TGG TC- 3'
BMP2	F 5'-GAT TCG TGG TGG AAG TGG-3' R 5'-GTG TCT CTT ACA GCT GGA C- 3'
CALML5	F 5'-GGA AAC GGC ACC ATC AAT GC- 3' R 5'-GTT TCC TTA GCT GGG CCT CC- 3'
CPEB4	F 5'-CCA CTG GGC TAG GTA CTT C- 3'

	R 5’-CAA AGC CAG GGC TGA CAT G- 3’
CPEBz	F 5’-CAG TAG AAG ATC CGG ACG AG- 3’ R 5’-CAC CTT GCT GAA GGT CAT CG- 3’
Dap	F 5' -CCC ACA GTG ATG ATG TCG AG- 3' R 5' -GCT GCT TCA GCT GCT TCT TC- 3'
DUOX1	F 5’-CAG GAC AAG GAG GAA CTG AC- 3’ R 5’-CAT ATC CTG GCT GAT GTA GG- 3’
EGF	F 5’-CAG CAC TGG AGC TGT CCT- 3’ R 5’-TCA CTG AGA CAC CAG CAT CC- 3’
EIF2S2	F 5’-GGG CTC TGA CTG AGA AAC TG- 3’ R 5’-GAC TTG GCG GTG AGG TAG TA- 3’
EIF4EBP2	F 5’-CAT GAC TAT TGC ACC ACG CC- 3’ R 5’-CAG GGC TAG TGA CTC CTG- 3’
FLG	F 5’-GGT ATT CAA GTT GGC TCA AG- 3’ R 5’-GCT CTT GGA TCT TCC CTT AT- 3’
GAPDH	F 5' - TGC ACC ACC AAC TGC TTA GC- 3' R 5' -GGC ATG GAC TGT GGT CAT GAG- 3'
HOXA9	F 5’-GAC CGA GCA AAA GAC GAG-3’ R 5’-GTG GCC TGA GGT TTA GAG- 3’
IVL	F 5’-AGG AGG AAC AGT CTT GAG GA- 3’ R 5’-TCT GCC TCA GCC TTA CTG T- 3’
JUNB	F 5’-CGA CTC ATA CAC AGC TAC GG- 3’ R 5’-GAG CCC TGA CCA GAA AAG TAG- 3’
K10	F 5’-CGA CCT TCT GTT TCT GCC AA- 3’ R 5’-TGA GAC GTA ATG TAC AAG CTC TG- 3’
K14	F 5’-TCT CCT CCA GGC TGT TCT- 3’ R 5’-GTG CAG AGC GGC AAG AG- 3’
KLF4	F 5’-CAA CGA TCT CCT GGA CCT G- 3’ R 5’-GAT AGG TGA AGC TGC AGG TG- 3’
KLK9	F 5’-GCA GTC TAC ACC AGC GTA TG- 3’ R 5’-GCG GAG TCT TAG TGT CCA GA- 3’
LOR	F 5’-GGA GTT GGA GGT GTT TTC CA- 3’ R 5’-ACT GGG GTT GGG AGG TAG TT- 3’
MAPK3	F 5’-CTT CCT GAC GGA GTA TGT GG- 3’ R 5’-GAG CTG ATC CAG GTA GTG CT- 3’
NOTCH1	F 5’-GTG ACT GCT CCC TCA ACT TC- 3’

	R 5’-GTC CTT GCA GTA CTG GTC GT- 3’
ODC1	F 5’-CTG CCA AGG ACA TTC TGG AC- 3’ R 5’-GGT AGC AGC AAG GGT CTT CA- 3’
RASL11B	F 5’-GGC CAA CAA AGC TGA CCT G- 3’ R 5’-GGT TCT TCG CTT CTC GGG- 3’
RPL13A	F 5’-GCC TTC ACA GCG TAC GA- 3’ R 5’-CGA AGA TGG CGG AGG TG- 3’
RPL3L	F 5’-TGC TTT TTC CCG TCT GTG TC- 3' R 5’-ATC TTT GCA GAA CAC CTC AGT- 3'
S100A8	F 5’-CCG TCT ACA GGG ATG ACC T- 3’ R 5’-GCC ACG CCC ATC TTT ATC AC- 3’
S100A9	F 5’-GAG GAC CTG GAC ACA AAT GC- 3’ R 5’-GTC ACC CTC GTG CAT CTT C- 3’
SIX4	F 5’-CAA CCT CAG CCT TTC CAG TC- 3’ R 5’-CTC CAC TGG GTC CCT GAA TA- 3’
SMAD5	F 5’-GTT GGT GGA GAG GTG TAT GC- 3’ R 5’-GAG CCA GAA GCT GAG CAA AC- 3’
TBP	F 5' -CGC CGA ATA TAA TCC CAA GC- 3' R 5' -TCC TGT GCA CAC CAT TTT CC- 3'
Thr	F 5' - CTC GCT CAA GCT GTC ATG TAC- 3' R 5' - CGG TGA TTT CTC ACA GAT GG- 3
TINCR	F 5’-AGA TGA CAG TGG CTG GAG TTG TCA- 3’ R 5’-TGT GGC CCA AAC TCA GGG ATA CAT- 3’
TPRG1	F 5’-GAT GAC CAA CCC TCT GAG AC- 3’ R 5’-CTC AGC TAC GTG ACC TTT CAA G- 3’
WNT11	F 5’-CGT GTG CTA TGG CAT CAA GTG- 3’ R 5’-GCT CAA TGG AGG AGC AGT TC- 3’
ZNF256	F 5’-GTG AGA TAT GTG GCC CAG TC- 3’ R 5’-GTG AAG GGC TTC CCA GAT AC- 3’
ZNF750	F 5’-AGC TCG CCT GAG TGT GAC- 3’ R 5’-TGC AGA CTC TGG CCT GTA- 3’

2.12 Protein Quantification and Immunoblotting

Protein was harvested by scrapping cells in appropriate volumes of radioimmune precipitation assay (RIPA) buffer containing supplements as listed in **Table 9**. Cell lysates were immediately snap-frozen in liquid nitrogen and stored at -80°C prior to protein quantification. Cell lysates were centrifuged at 4°C for 30 mins at 16, 100 xg and supernatant was collected in a new centrifuge tube. Protein concentration was determined using Pierce Bicinchoninic Acid Protein Assay kit (BCA; Thermo Fisher Scientific, MA, USA) as per manufacturers' instructions. Protein samples were mixed with Lamelli buffer (Bio-rad, CA, USA) and heat-denatured at 95°C for 5 mins, separated using either 10%, 12% or 4-20% sodium dodecyl sulfate-polyacrylamide gels by electrophoresis at 90V and then transferred onto nitrocellulose membrane using Trans-blot Turbo Transfer System (Bio-Rad, CA, USA) for 7 mins. Membrane was then blocked in 5% milk in TBS-T, components as stated in **Table 10**, for 1h at RT on shaking. Membrane was incubated with primary antibodies diluted in 5% milk in TBS-T O/N at 4°C with constant rotation. Antibody dilution used is as stated in **Table 11**. The following day, membrane was washed thrice with 1X TBS-T for 15 mins each and incubated with goat anti-Ms (sc-2007; Santa Cruz Biotechnology, TX, USA) or donkey anti-Rb (sc-2055; Santa Cruz Biotechnology, TX, USA) horse radish peroxidase (HRP)-conjugated IgG secondary antibody at 1:5000 dilution in 5% milk in TBS-T for 1h. For chemiluminescence detection, SuperSignal Western Blot Enhancer substrates (Thermo Fisher Scientific, MA, USA) were used and blots were developed at several exposures.

Table 9. Components of RPIA buffer with supplements.

Components	
NaCl (Sigma-Aldrich, MO, USA)	150mM
Triton X-100 (Sigma-Aldrich, MO, USA)	1%
Sodium deoxycholate (Sigma-Aldrich, MO, USA)	0.5%
SDS (Invitrogen, CA, USA)	0.1%
Tris-HCl, pH 8.0 (1st BASE, Singapore)	50mM
NP-40 (GE Healthcare Life Sciences, IL, USA)	1%
Diluted in PBS	
Supplements	
Halt Protease Inhibitor Cocktail (100X; Thermo Fisher Scientific, MA, USA)	1X
0.5M EDTA (Thermo Fisher Scientific, MA, USA)	5μM
Phenylmethylsulfonyl fluoride (PMSF) Protease Inhibitor (100X; Life Technologies, CA, USA)	1X

Table 10. Components of TBS-T

Components	
NaCl (Sigma-Aldrich, MO, USA)	87.65g
Tris base (Trizma®, Sigma-Aldrich, MO, USA)	62.55g
Adjust pH using HCl (MERCK, NJ, USA)	pH 7.5
10X TBS, pH 7.5	1 L
10X TBS, pH 7.5	100mL
Ultra-pure water	900mL
Tween-20, molecular biology grade (Promega, WI, USA)	1mL
1X TBS-T	1L

Table 11. List of primary antibodies used in western blotting.

Antibody	Type	Brand (Country)	Cat. number	Dilution
anti-AMD1	Ms monoclonal	Santa Cruz Biotechnology (TX, USA)	sc-390073	1:500
anti-AQP3	Rb polyclonal	Biorybt (Cambs, UK)	orb47955	1:1000
anti-ATP13A3	Rb polyclonal	Sigma-Aldrich (MO, USA)	HPA029471	1:500
anti-Caspase 14	Rb polyclonal	Abcam (UK)	ab45415	1:1000
anti-Caveolin-1	Rb polyclonal	Sigma-Aldrich (MO, USA)	C4490	1:500
anti-CPEB4	Rb polyclonal	Abcam (UK)	ab83009	1:1000
anti-eIF5A	Rb monoclonal	Abcam (UK)	ab32443	1:5000
anti-eIF5A2	Rb monoclonal	Abcam (UK)	ab150439	1:1000
anti-FLG	Ms monoclonal	Abcam (UK)	ab17808	1:500
anti-FLG	Rb polyclonal	Abcam (UK)	ab81468	1:500
anti-GAPDH	Ms monoclonal	Abcam (UK)	ab9484	1:1000
anti-GAPDH	Rb polyclonal	Sigma-Aldrich (MO, USA)	G9545	1:1000
anti-Hypusine	Rb polyclonal	Merck Millipore (MA, US)	ABS1064	1:1000
anti-IVL	Rb polyclonal	Abcam (UK)	ab53112	1:1000
anti-K10	Rb monoclonal	Abcam (UK)	ab76318	1:10000
anti-KLF4	Rb monoclonal	Abcam (UK)	ab215036	1:1000
anti-KLK7	Ms monoclonal	Santa Cruz Biotechnology (TX, USA)	sc-514447	1:1000
anti-LOR	Rb monoclonal	Abcam (UK)	ab176322	1:10000
anti-NOTCH1	Ms monoclonal	Santa Cruz Biotechnology (TX, USA)	sc-373891	1:1000
anti-ODC1	Rb monoclonal	Abcam (UK)	ab126590	1:500

anti-p53	Ms monoclonal	Abcam (UK)	ab28	1:5000
anti-S100A8/9	Ms monoclonal	Merck Millipore (MA, US)	MABF291	1:1000
anti-SLC12A8	Rb polyclonal	Sigma-Aldrich (MO, USA)	HPA031123	1:250
anti-Spd	Rb polyclonal	Abcam (UK)	ab7318	1:1000
anti-Spm	Rb polyclonal	Abcam (UK)	ab26975	1:1000
anti-β-actin	Ms monoclonal	Sigma-Aldrich (MO, USA)	a5441	1:1000

2.13 Polysome Profiling

Polysome profiling was performed using ~10 million N/TERT-1 D0 and D6 keratinocytes incubated in 100µg/mL of cycloheximide (Chx; cat. no. C4859, Sigma-Aldrich, MO, USA) for 10 mins. Cells were harvested, pelleted, washed with PBS and re-suspended in 200µl of RSB buffer containing 20mM Tris-HCl, pH 7.4, 20mM NaCl, 30mM $MgCl_2$ and 200µg/mL Chx, 1000units/mL RNasin then lysed in an equal volume of lysis buffer containing 1X RSB, 1% Triton-X 100, 2% Tween-20 and 1% sodium deoxycholate. Cells were incubated on ice for 10 mins, and subsequently the extracts were centrifuged at 13, 200 rpm for 3 mins to remove nuclei. The cell supernatant was spun at 13, 200 rpm for an additional 10 mins at 4°C. The OD units for D0 and D6 cell lysates were measured and equal OD units were loaded onto 10-50% linear sucrose gradients (prepared in 10mM Tris-HCl pH 7.4, 75mM KCl and 1.5mM $MgCl_2$) and centrifuged at 36,000 rpm for 1.5h at 8°C in a SW41 rotor (Beckman Coulter, CA, USA). Absorbance was measured at 254 nm using a UV-M II monitor (Bio-rad, CA, USA) while twelve fractions were collected from the top of the gradient using a piston gradient fractionator (BioComp Instruments, Canada). Fractions were stored at -80°C till further use. 110µl of 10% sodium dodecyl sulphate (SDS; Life Technologies, CA, USA) and 12µl of 10mg/mL proteinase K (Thermo Fisher Scientific, CA, USA) was added to 1mL of each fraction and incubated at 42°C on a heat block for 30mins on shaking. Fractions 1-4, 5-7 and 8-11 were pooled corresponding to non-, low- and high- translational fractions respectively. These fractions were purified using phenol:chloroform:isoamyl (Ambion®, Thermo Fisher Scientific, MA, USA) extraction and the purity of the RNA was measured using a Nanodrop ND-1000

spectrophotometer (Thermo Fisher Scientific, MA, USA). For qRT-PCR analysis, equal volumes of RNA was used to synthesize cDNA using the Superscript III Reverse Transcriptase (Invitrogen, CA, USA) according to manufacturers' protocol. 10µl of bacterial spike-in RNAs, *Dap* and *Thr* were added to equal volumes of pooled polysomal RNA, prior to RNA extraction. Gene specific primers for *AMD1, ODC1, GAPDH, TBP, Dap* and *Thr* (**Table 8**) were used with POWER SYBR Green Master Mix (Applied Biosystem, UK) for qRT-PCR on an ABI PRISM 7900 Sequence Detection System, as previously described. Candidate CT values were normalized to spike-in controls *Dap* and *Thr* that were present at equal concentrations per pool. Relative RNA levels are presented as a percentage of the RNA present in each pool with 100% RNA calculated as the sum of non-, low- and high-translated pools.

2.14 Measurement of polyamine levels

Polyamines were extracted from D0 undifferentiated and D6 differentiated keratinocytes using 5% trichloroacetic acid (TCA; Sigma-Aldrich, MO, USA) diluted in deionized water then centrifuged at 27,000 xg for 15min at 4°C. The polyamines in 10µl of TCA were separated on a high-performance liquid chromatography system (HPLC; Toyo Soda Manufacturing Co., Japan) on which a TSK gel IEX215 column (4 by 80 mm) heated to 50°C was mounted, as previously described (Igarashi, Kashiwagi et al. 1986). The flow rate of the polyamines was measured by fluorescence intensity at an excitation wavelength of 388 nm and an emission wavelength of 410 nm.

2.15 Microarray and gene expression analysis

Total RNA was extracted from 4 biological replicates of each sample as shown in **Figure 28,** using an RNeasy kit (Qiagen, Germany) according to manufacturers' instructions. The concentration and the purity of the extracted RNA was obtained using Nanodrop ND-1000 spectrophotometer (Thermo Fisher Scientific, MA, USA) and the integrity of RNA was confirmed using Bioanalyzer (Agilent Technologies, USA). 500ng of extracted RNA was reverse transcribed into cDNA using ArrayScript™ Reverse Transcriptase (Illumina CA, USA) with T7oligo(dT) primer for 2h at 42°C.

This was followed by an *in vitro* transcription of cDNA to biotin-labelled cRNA by T7 RNA polymerase in the presence of biotinylated ribonucleotides (Enzo Diagnostics, USA) at 37°C for 4h using the Illumina TotalPrep RNA Amplification kit (Applied Biosystems, CA, USA). 750ng of each cRNA sample was hybridized to HumanHT-12 v4 Expression BeadChip (Illumina CA, USA) for 16h at 58°C. After the incubation period, the arrays were washed and stained with Streptavidin-Cy3 (GE Healthcare, CSP, UK), followed by scanning the arrays using Illumina Bead Array Reader (Illumina, CA, USA) at 25 scan factor 1. The signal values of cRNA bound to each probe was further translated into gene expression values using GeneSpring GX 11 software (Agilent Technologies Inc., CA, US). Background subtraction was applied on raw intensity values and subsequent data was subjected to quantile normalization on the GenomeStudio Data Analysis platform (Illumina, CA, USA) with a normalized expression value cut-off at 100. Principal component analysis (PCA) was performed before analysis of gene expression to ensure quality control. Two-way Analysis of variance (ANOVA) followed by Benjamini-Hochberg (BH) post-hoc was conducted on the complete data set and a list of differentially expressed genes were obtained with $p < 0.05$. Unsupervised two-dimensional average-linkage hierarchical clustering of the genes differentially expressed, was performed for all cell types by using Spearman's correlation as similarity matrix. Genes with at least 2-fold change or more for all conditions were selected and considered for further analysis. Biological significance of the differentially expressed gene list was better realised by classifying the genes based on their biological pathways and molecular functions using DAVID 69 (**D**atabase for **A**nnotation, **V**isualization and **I**ntegrated **D**iscovery v6.7) (Huang da, Sherman et al. 2009, Huang da, Sherman et al. 2009) and PANTHER gene analysis tools.

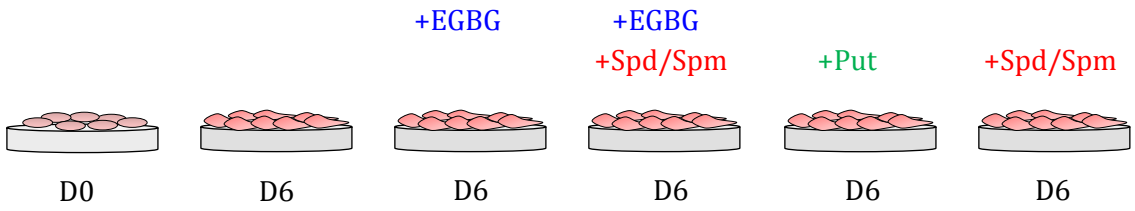

Figure 28: Sample preparation for microarray analysis. Samples used for microarray analysis were (i) D0, undifferentiated keratinocytes, (ii) D6 differentiated keratinocytes, (iii) D6 differentiated keratinocytes treated with 50µM of EGBG, (iv) D6 differentiated keratinocytes treated with 50µM of EGBG and rescued with 1mM of Spd/Spm in combination, (v) D6 differentiated keratinocytes treated with 1mM of Put and (vi) D6 differentiated keratinocytes treated with 1mM of Spd/Spm.

2.16 Statistical Analysis

All values were represented as ±S.E.M of at least 3 biological replicates unless otherwise stated in the figure legends. Significant differences between the control and experimental groups were evaluated by two-tailed, paired Student's *t*-test (Microsoft Excel Software). Statistical comparison for microarray analysis was performed using two-way ANOVA test between multiple groups, followed by Benjamini-Hochberg's post-hoc test. * $p < 0.05$; ** $p < 0.01$ and *** $p < 0.001$ were considered to be statistically significant.

CHAPTER 3

RESULTS

3.1 Calcium-induced keratinocyte differentiation using human primary epidermal keratinocytes and N/TERT-1 immortalized keratinocytes.

A calcium gradient exists within the epidermis, with the highest levels being present in the stratum granulosum (Elias, Ahn et al. 2002). Calcium is a key driver for the sequential progression of keratinocyte differentiation. While suspension cultures and cell confluence are known inducers of keratinocyte differentiation, modulating extracellular calcium concentration best recapitulates keratinocyte differentiation and stratification *in vitro* (Li, Tennenbaum et al. 1996, Lee, Yuspa et al. 1998). In order to induce keratinocyte differentiation in *vitro*, commercially available human epidermal keratinocytes (HEKa) or N/TERT-1 immortalized keratinocytes obtained from J. Rheinwald's laboratory were grown to ~100% confluence in K-SFM containing 0.3mM calcium chloride. Differentiation was induced by the addition of 1.2mM calcium chloride at confluence **(Figure 29A)**. RNA and protein lysates of D0 undifferentiated and D2, D4 and D6 differentiated keratinocytes were harvested. Phase contrast images captured at the time of harvest depict morphological changes as the cells transitioned from single monolayer keratinocytes at D0 to flattened and tightly packed squame-shaped cells by D6 of differentiation (**Figure 29B**). Efficient calcium-induced keratinocyte differentiation was determined by a significant increase in mRNA and protein expression of early differentiation marker, K10 and late differentiation markers IVL and FLG by D6 of differentiation (**Figure 30A, B and Figure 31A, B**).

Pro-FLG is a precursor of FLG and is present in undifferentiated keratinocytes. During keratinocyte differentiation, Pro-FLG is cleaved, which results in FLG monomers. FLG monomers are instantaneously modified and processed to form FLG dimers, trimers and tetramers etc., which results in a smear by immunoblotting. HEKa cells differentiate less efficiently compared to N/TERT-1 keratinocytes, hence the protein expression of FLG was not detected. In human

abdominal skin sections, different layers of the epidermis could be distinguished by the expression of K14 in the proliferative basal layer, K10 expression marking the suprabasal layers while IVL and FLG, are late differentiation markers delineating the stratum granulosum (**Figure 32**).

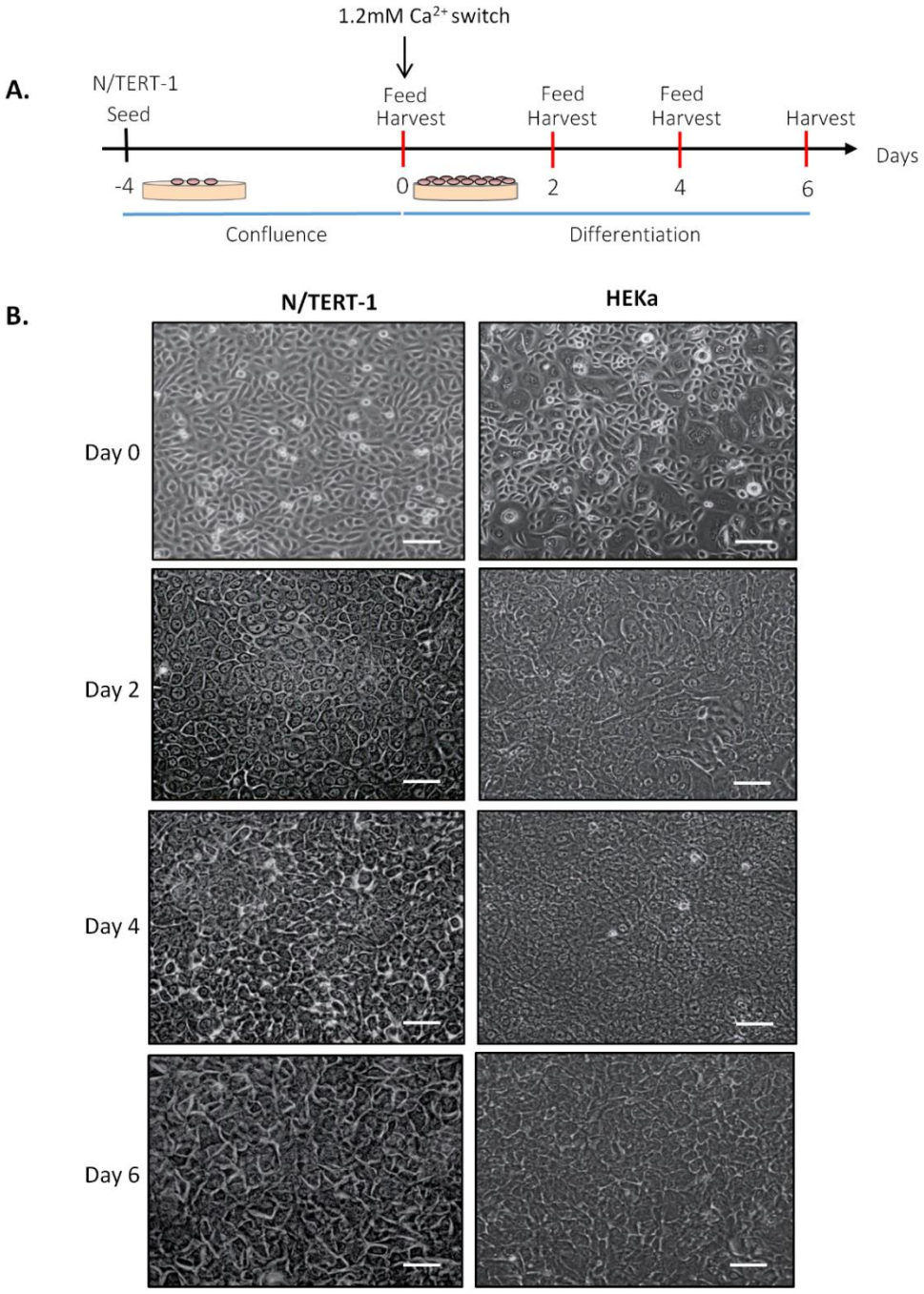

Figure 29: Calcium-induced keratinocyte differentiation. A. Schematic representation of confluent monolayer calcium-induced keratinocyte differentiation. RNA and protein were harvested at day0 (D0), day 2 (D2), day 4 (D4) and day (D6) of differentiation. **B.** Phase contrast images of N/TERT-1 and HEKa cells at D0, D2, D4 and D6 of calcium-induced keratinocyte differentiation. Images were captured at 40X magnification; scale bar = 20μm.

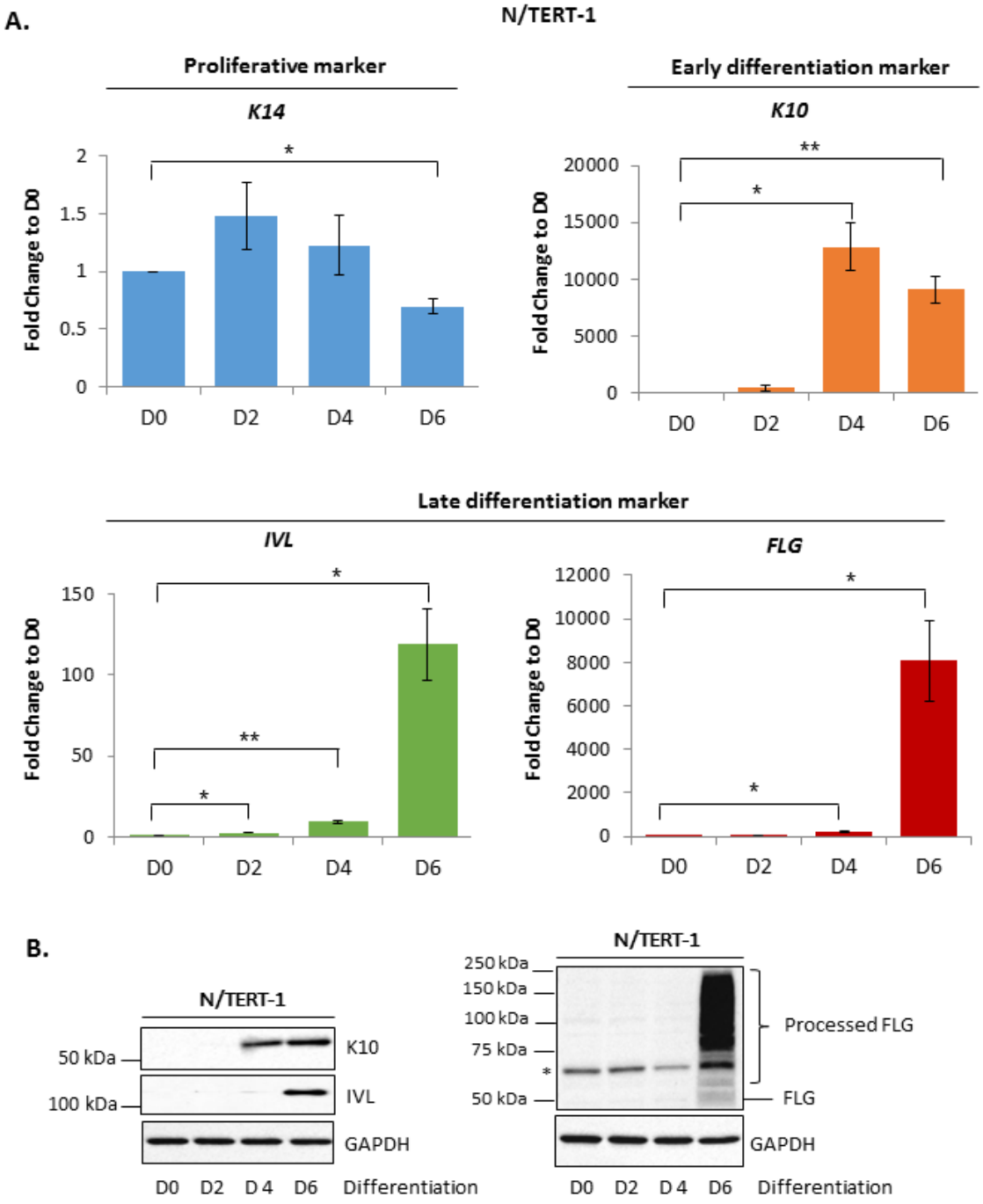

Figure 30: Expression of proliferative and differentiation markers during calcium-induced N/TERT-1 keratinocyte differentiation. A. mRNA expression of proliferative marker, keratin 14 (K14), showing significant down-regulation while mRNA expression of early and late differentiation markers, keratin 10 (K10), involucrin (IVL) and filaggrin (FLG) showing significant up-regulation by day 6 of N/TERT-1 keratinocyte differentiation. Genes were normalized to house-keeping gene, *RPL13A* and results were represented as ±S.E.M. of three independent biological replicates; p values of <0.05 *, <0.01 ** and <0.001 *** were considered as statistically significant. **B.** K10, IVL and FLG protein are up-regulated upon N/TERT-1 keratinocyte differentiation. GAPDH was used as a loading control. *Asterisk denotes a non-specific band.

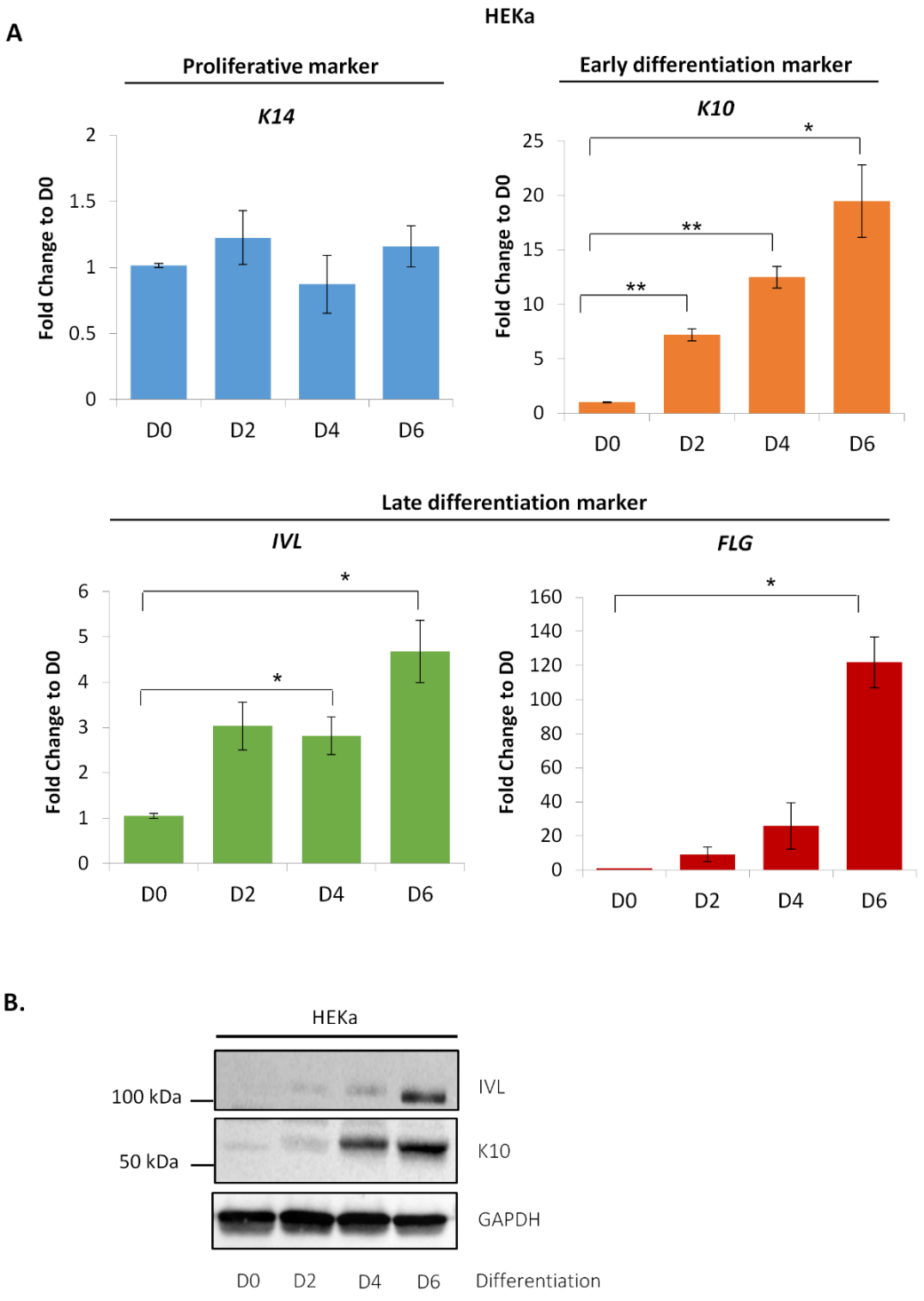

Figure 31: Expression of proliferative and differentiation markers during calcium-induced HEKa differentiation. A. mRNA expression of proliferative marker, keratin 14 (K14) remains unchanged while mRNA expression of early and late differentiation markers, keratin 10 (K10), involucrin (IVL) and filaggrin (FLG) show a significant up-regulation by D6 of HEKa differentiation. Genes were normalized to house-keeping gene, *RPL13A* and results were represented as ±S.E.M. of three independent biological replicates; p values of <0.05 *, <0.01 ** and <0.001 *** were considered as statistically significant. **B.** K10 and IVL protein are up-regulated upon HEKa differentiation. GAPDH was used as a loading control.

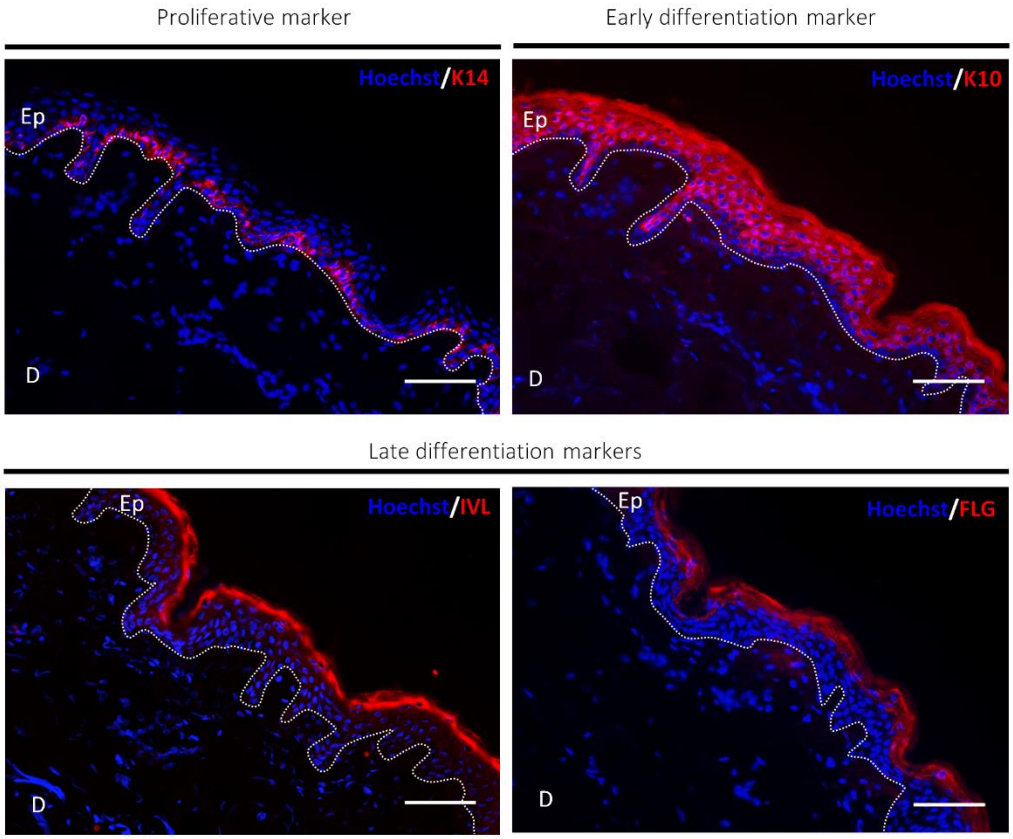

Figure 32: Expression of proliferative and differentiation markers in the human epidermis. Keratin 14 (K14), is a proliferative marker which is expressed in the basal layer of the human epidermis. Early differentiation maker keratin 10 (K10) is expressed in all suprabasal layers of the human epidermis, starting from the stratum spinosum to the stratum corneum. Late differentiation markers, involucrin (IVL) and filaggrin (FLG) are highly expressed in the stratum granulosum. Hoechst dye is used to stain the nuclei. Ep=Epidermis, D=Dermis, dotted lines represent the basement membrane; Scale bar = 50μm. Skin biopsy was obtained from the abdomen of a Chinese, female aged, 54.

3.2 Polyamine regulators, AMD1 and ODC1 are differentially expressed during keratinocyte differentiation.

After confirming the efficiency of the 2-D keratinocyte differentiation, I then determined the mRNA and protein expression levels of polyamine regulators, AMD1 and ODC1 during keratinocyte differentiation. AMD1 and ODC1 are rate-limiting enzymes of the polyamine biosynthesis pathway, where ODC1 is responsible for the conversion of ornithine, a by-product of the urea cycle to Put while AMD1 decarboxylates adenosyl methionine to decarboxylated adenosyl methionine, providing the amino propyl donor groups for the synthesis of Spd and Spm from Put (Pegg 2016). qRT-PCR showed that *AMD1* mRNA levels remained unchanged throughout the course of keratinocyte differentiation (**Figure 33A**). *ODC1* mRNA expression however, was significantly decreased by approximately 80% at D2, D4 and D6 of differentiation (**Figure 33A**). In the case of HEKa cells, a mild but significant increase in *AMD1* mRNA expression was observed at D2 and D6 of differentiation (**Figure 33B**). A significant reduction in *ODC1* mRNA levels was observed at all days of HEKa differentiation, similar to N/TERT-1 keratinocytes (**Figure 33B**).

Immunoblotting revealed a strong AMD1 protein up-regulation, peaking at D4 of N/TERT-1 keratinocyte differentiation (**Figure 33C**). No change in ODC1 protein expression was observed during N/TERT-1 keratinocyte differentiation **(Figure 33C**). As for HEKa cells, AMD1 protein expression peaked at D6 of keratinocyte differentiation while the ODC1 protein expression remained unchanged throughout the course of differentiation **(Figure 33D)**. Subsequent experiments were performed using N/TERT-1 keratinocytes for the ease of cell expansion.

Keratinocytes are well differentiated at D6 as evidenced by the high expression of early and late differentiation markers, K10, IVL, FLG and LOR compared to D4 of differentiation. Though AMD1 peaks at D4 in N/TERT-1 keratinocytes, the relatively high expression of both AMD1 and differentiation markers at D6 makes it a suitable time point to investigate the role of AMD1 during keratinocyte differentiation. HEKa cells differentiate slower than immortalized N/TERT-1

keratinocytes. Hence, the expression of both AMD1 and differentiation markers start to peak at D6. Since the expression of both AMD1 and differentiation markers are high in N/TERT-1 keratinocytes and HEKa cells at D6 of differentiation, D6 was chosen as a suitable time point for subsequent experiments.

In summary, I have found that AMD1 and not ODC1 protein is up-regulated on keratinocyte differentiation. Interestingly, the mRNA and protein expression levels of AMD1 and ODC1 did not correlate on differentiation, suggesting they may be post-transcriptionally regulated.

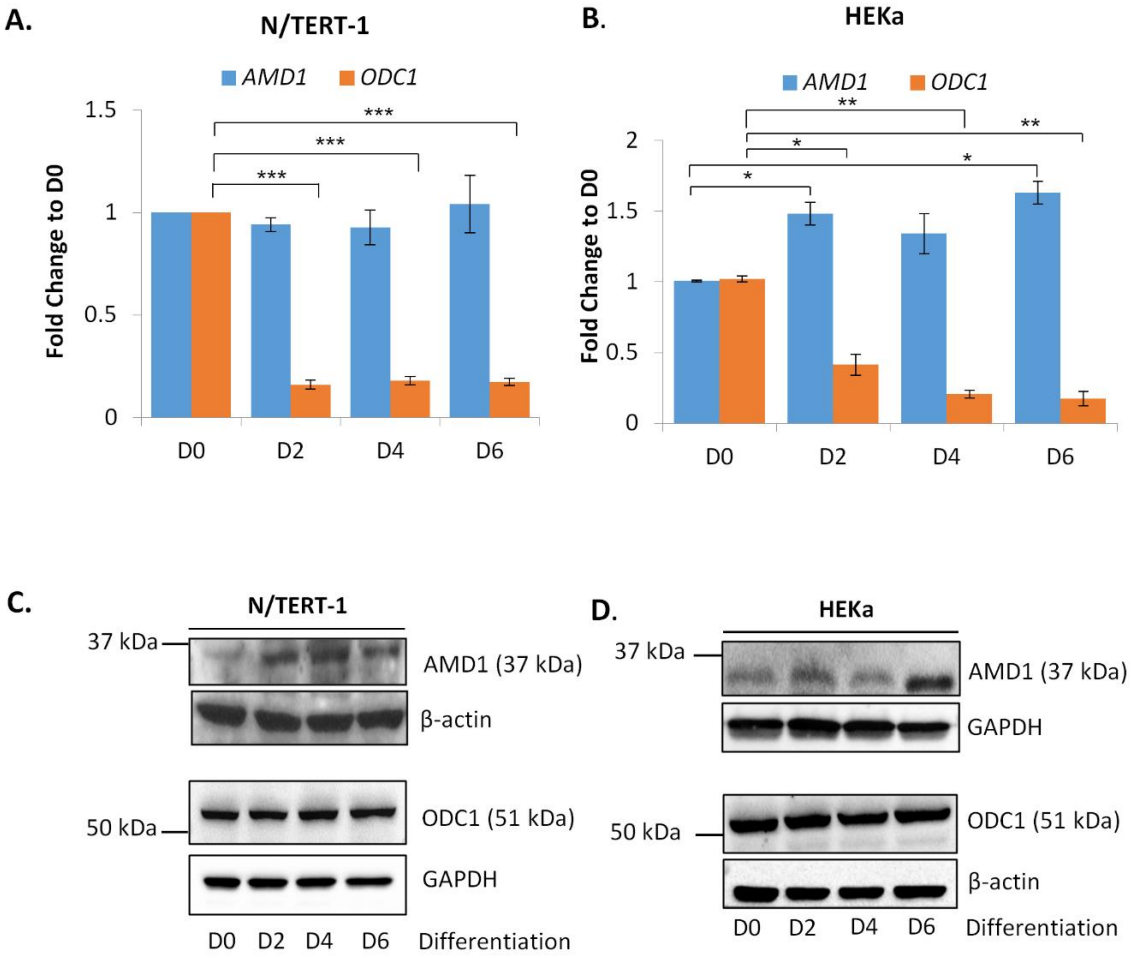

Figure 33: Differential mRNA and protein expression of polyamine regulators during calcium-induced differentiation in N/TERT-1 and human primary keratinocytes. A. mRNA expression of *ODC1* is significantly down-regulated while mRNA expression of *AMD1* remains unchanged in N/TERT-1 keratinocytes and **B.** in HEKa during calcium-induced keratinocyte differentiation. Expression was normalized to house-keeping gene, *RPL13A* and results were represented as ±S.E.M. of three independent biological replicates; p values of <0.05 *, <0.01 ** and <0.001 *** were considered as statistically significant. **C.** ODC1 protein remains unchanged while AMD1 protein is up-regulated during N/TERT-1 and **D.** HEKa differentiation. Either GAPDH or β-actin was used as a loading control. *#AMD1 immunoblot for N/TERT-1 keratinocytes was produced by Lim Hui Kheng.*

3.3 AMD1 is translationally up-regulated during keratinocyte differentiation

Since, *AMD1* mRNA expression is unchanged, the increase in AMD1 protein expression could be attributed to either a translational up-regulation of *AMD1* or an increase in AMD1 protein stability (Jansen, de Moor et al. 1995). To determine whether *AMD1* is translationally up-regulated during keratinocyte differentiation, polysome profiling was performed. This method involves the high velocity centrifugation of linear translational complexes in 10-50% sucrose gradients. Centrifugation allows the sedimentation of free mRNA transcripts at the top of the gradient, free ribosomal subunits and mRNA transcripts with few bound-ribosomes at the middle of the gradient and mRNA transcripts with several ribosomes bound at the bottom of the gradient (**Figure 34A**) (Chassé, Boulben et al. 2017). Polysome profiles representing global translation of D0 undifferentiated (blue) and D6 differentiated (orange) keratinocytes were obtained by measuring absorbance at 254nm (**Figure 34B**). Fractions 1-4 were categorised as non-translated, fractions 5-7 as low translation and fractions 8-11 as high translation ribosomal fractions respectively (**Figure 34B**). Phenol-chloroform RNA extraction was performed using equal volumes of each fraction and an equal volume of *Dap* and *Thr* bacterial mRNAs were spiked-in as internal controls. qRT-PCR was performed to determine the percentage mRNA abundance of *AMD1* and *ODC1* across these fractions by normalization to *Dap* and *Thr*. The percentage mRNA abundance of *GAPDH* and *TBP* were used as positive controls.

Prior to keratinocyte differentiation (blue), the *AMD1* mRNA was predominantly present in the low translational fractions (F5, 6) (**Figure 34C**). At D6 of calcium-induced keratinocyte differentiation (orange), *AMD1* mRNA abundance was shifted from low to high translational fractions (F7, 8), suggesting that more ribosomes were recruited onto the *AMD1* mRNA transcript during differentiation (**Figure 34C**). On the contrary, *ODC1* mRNA remained enriched in the low translational fractions (F5) when keratinocytes were in the undifferentiated and differentiated state (**Figure 34C**). This suggests that the same number of ribosomes remained bound on the *ODC1* mRNA transcript during keratinocyte differentiation. The percentage mRNA shift for *GAPDH* was

inverse, from F9 to F8, likely due to a decrease in global translation during keratinocyte differentiation (**Figure 34C**). However, *TBP* mRNA remained high in the low translational fractions (F7) at the undifferentiated and differentiated states as expected (**Figure 34C**). These data show that on keratinocyte differentiation *AMD1* mRNA is translationally up-regulated, while *ODC1* mRNA translation rate remains unchanged.

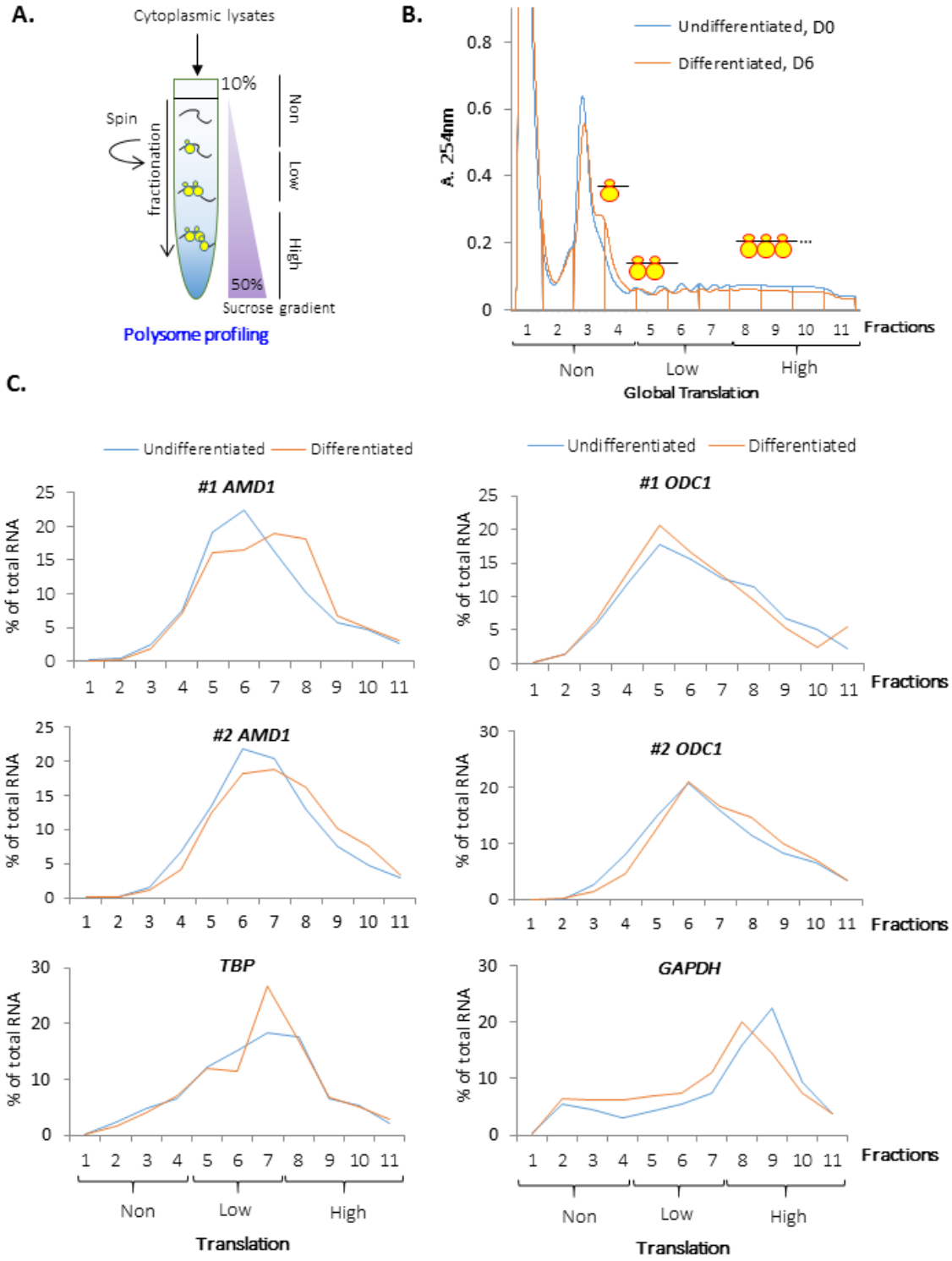

Figure 34: *AMD1* is translationally up-regulated during N/TERT-1 keratinocyte differentiation. A. Pictorial representation of polysome profiling showing the separation of cytoplasmic lysates on 10-50% sucrose gradient subjected to high speed centrifugation. **B.** Polysome profiles of D0, undifferentiated (blue) and D6, differentiated (orange) N/TERT-1 keratinocytes. Fractions 1-4 are non-translated, fractions 5-7 are low translation and fractions 8-11 are high translation fractions. **C.** Percentage mRNA abundance of *AMD1* and *ODC1* in non-, low- and high translational fractions. *GAPDH* and *TBP* were used as positive controls. Three independent biological replicates were performed, of which two representative replicates (#1 & #2) are represented for *AMD1* and *ODC1* mRNA.

3.4 AMD1 is enriched in the suprabasal layers of the human epidermis

To determine the localization and expression pattern of AMD1 in the human epidermis, immunofluorescence (IF) was performed for AMD1 in human abdominal skin sections. AMD1 (red) was highly expressed in the suprabasal layers of the human epidermis and co-localized with late differentiation marker IVL (**Figure 35A**), confirming its high expression observed during N/TERT-1 keratinocyte differentiation. RNAscope® in situ hybridization (ISH) assay was performed to further confirm that *AMD1* RNA expression was not changing throughout all layers of the human abdominal epidermis, while AMD1 protein expression was particularly enriched in the stratum granulosum (**Figure 35B**). This is in line with our previous observation that AMD1 is translationally up-regulated during keratinocyte differentiation.

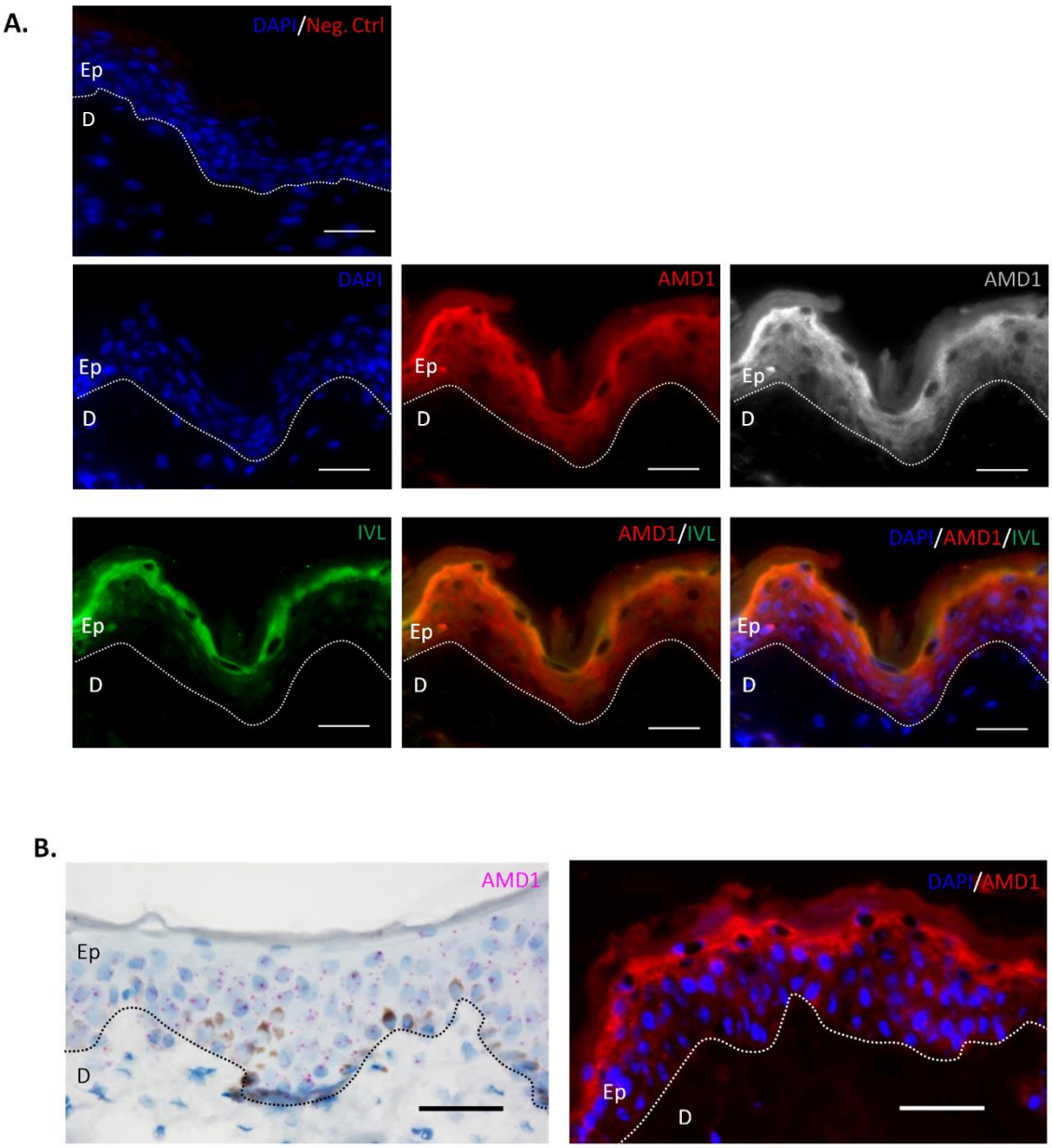

Figure 35: AMD1 expression in the suprabasal layers of the human epidermis. A. AMD1 (red) is expressed in the suprabasal layers of the epidermis, particularly enriched in the stratum granulosum. Involucrin, IVL (green) was used to stain the stratum granulosum and DAPI (blue) stains the nuclei, Ep=Epidermis, D=Dermis; Scale bar = 50μm. **B.** RNAscope® in situ hybridization showing *AMD1* (pink) mRNA expression throughout all layers of the human epidermis while AMD1 protein expression is high in the suprabasal layers of the epidermis particularly restricted to the stratum granulosum; dotted lines represent the basement membrane; Ep=Epidermis, D=Dermis, Scale bar = 50μm. Skin biopsy was obtained from the abdomen of a Chinese, female aged, 54. *#RNAscope® in situ hybridization (ISH) assay was performed by Vonny Ivon Leo.*

3.5 Spd/Spm is highly expressed in the suprabasal layers of the human epidermis.

An increase in AMD1 protein expression during keratinocyte differentiation would result in the conversion of Put to Spd/Spm. In the absence of increased ODC1, this would result in a decrease in Put and an increase in Spd/Spm. In order to determine the expression pattern of Spd/Spm in the human epidermis, immunofluorescence staining was performed using commercially available Spd and Spm antibodies respectively. Both antibodies were raised in rabbit independently but cross-react with each other, hence individual staining of Spd or Spm could not be distinguished. Importantly, neither antibody binds to Put. Spd and/or Spm staining was highly abundant in the suprabasal layers of the epidermis, but completely devoid in basal layer keratinocytes (**Figure 36**). This observation was consistent with the high AMD1 protein expression in the differentiated layers of the human epidermis.

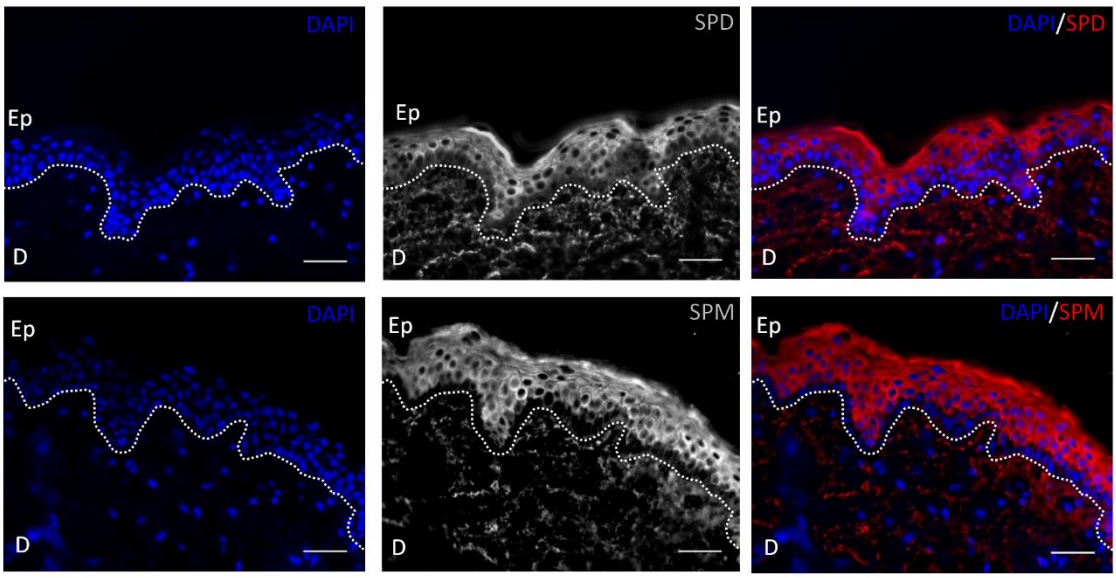

Figure 36: Spd/Spm is highly expressed in the suprabasal layers of the human epidermis. Immunofluorescence staining depicting high Spd (red) and Spm (red) expression in the suprabasal layers but completely absent in the basal layer of the human abdominal skin sections. DAPI (blue) was used to stain the nuclei and dotted lines represent the basement membrane. Skin biopsy was obtained from the abdomen of a Chinese, female aged, 56; Scale bar = 50μm.

3.6 A Shift in polyamine levels was observed during keratinocyte differentiation.

An increase in AMD1 protein during keratinocyte differentiation would drive a shift in polyamine levels resulting in a decrease in Put and an increase in Spd and Spm. To measure the polyamine levels during keratinocyte differentiation, an equal number of D0 undifferentiated and D6 differentiated keratinocytes were harvested and re-suspended in 5% trichloroacetic acid (TCA), then subjected to high performance liquid chromatography (HPLC). Polyamine levels are presented as nmol/mg protein under each condition. Put levels were significantly decreased to almost half its level while Spm levels were doubled by D6 of keratinocyte differentiation (**Figure 37A and 37C**). This correlates well with an increase in AMD1 protein level in differentiated keratinocytes. Interestingly, Spd levels were significantly reduced during keratinocyte differentiation likely due to its conversion to Spm (**Figure 37B**). An increase in Put levels was observed in D6 differentiated keratinocytes that were treated with an AMD1 inhibitor, EGBG, compared to D6 untreated keratinocytes; though this was not significant (**Figure 37A**). However, a significant decrease in the levels of Spm was observed in D6 differentiated keratinocytes with AMD1 inhibition compared to D6 untreated keratinocytes (**Figure 37C**). The levels of Spm in AMD1 inhibited keratinocytes at D6 of differentiation were similar to the levels of Spm in D0 undifferentiated keratinocytes (**Figure 37C**). There was a significant decrease in Spd levels in AMD1 inhibited keratinocytes at D6 compared to D0 undifferentiated keratinocytes. This decrease was similar to D6 untreated keratinocytes (**Figure 37B**).

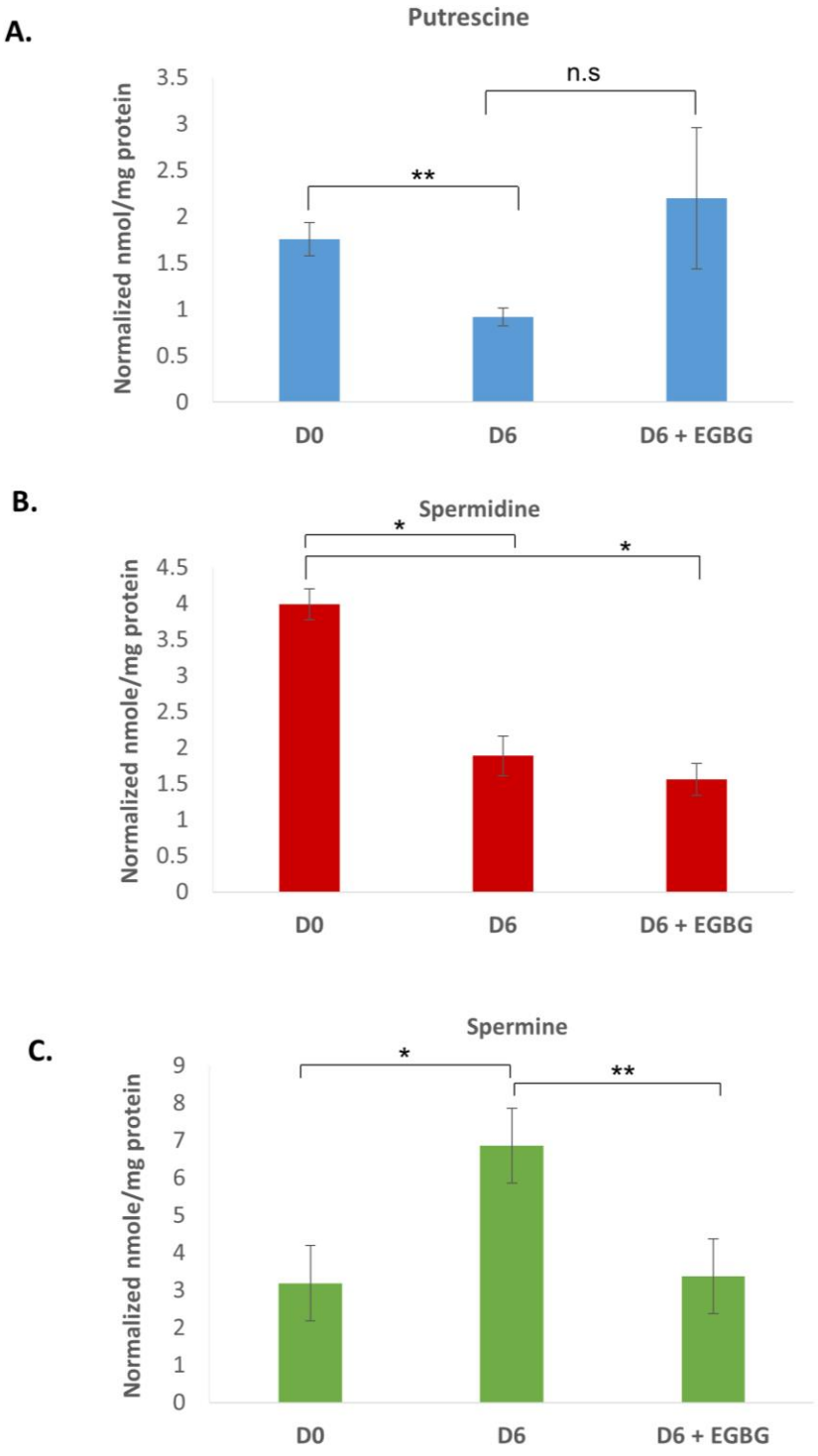

Figure 37: Polyamine ratios shift during N/TERT-1 keratinocyte differentiation. A. Putrescine levels were significantly down-regulated during D6 keratinocyte differentiation compared to D0 undifferentiated keratinocytes. AMD1 inhibition using EGBG increased the levels of putrescine comparable to D0 undifferentiated keratinocytes but was not significant. **B.** Spermidine levels were significantly down-regulated during keratinocyte differentiation in the absence and presence of AMD1 inhibitor, EGBG. **C.** Spermine levels were significantly up-regulated during D6 keratinocyte differentiation and significantly down-regulated in the presence of EGBG. Results were represented as ±S.E.M. of four independent biological replicates and p values of <0.05 *, <0.01 ** and <0.001 *** were considered as statistically significant.

3.7 Exogenous addition of Spd/Spm promotes keratinocyte differentiation.

To further determine whether extracellular addition of polyamines could promote keratinocyte differentiation, we first performed a MTS cytotoxicity assay to determine a concentration of Spd and Spm at which N/TERT-1 keratinocytes remained viable. MTS is a colorimetric assay to determine the number of viable cells based on the ability of NAD(P)H-dependent dehydrogenase enzymes present in metabolically active cells to reduce yellow MTS tetrazolium compound to form a brown formazan product (**Figure 38A**). The formazan dye is soluble in cell culture media and is quantified by measuring its absorbance at 490nm (Wang, Henning et al. 2010). N/TERT-1 keratinocytes were viable in up to 1mM of Spd and Spm when added alone or in combination and cell viability started to decrease at higher concentrations (**Figure 38B**). I performed calcium-induced keratinocyte differentiation using N/TERT-1 cells, and supplemented 1mM of Spd/Spm in combination to fresh media on alternate days. RNA and protein were harvested at the start and end of 6 days of differentiation. mRNA levels of early differentiation marker, *KRT10* was significantly increased by approximately 1.4-folds and late differentiation markers *LOR* and *FLG* were significantly increased by approximately 1.7-folds and 2-folds respectively at D6 of keratinocyte differentiation with Spd/Spm addition as compared to untreated D6 keratinocytes (**Figure 39A**). There was no significant difference in mRNA expression of *IVL* when Spd/Spm was added (**Figure 39A**). While the protein expression of K10 was mildly increased, the expression of FLG and LOR were strongly up-regulated with the addition of Spd/Spm compared to D6 differentiated keratinocytes without polyamine addition (**Figure 39B**). IVL protein expression remained unchanged in the absence and presence of Spd/Spm treatment (**Figure 39B**). My data shows that exogenous addition of Spd/Spm promotes keratinocyte differentiation.

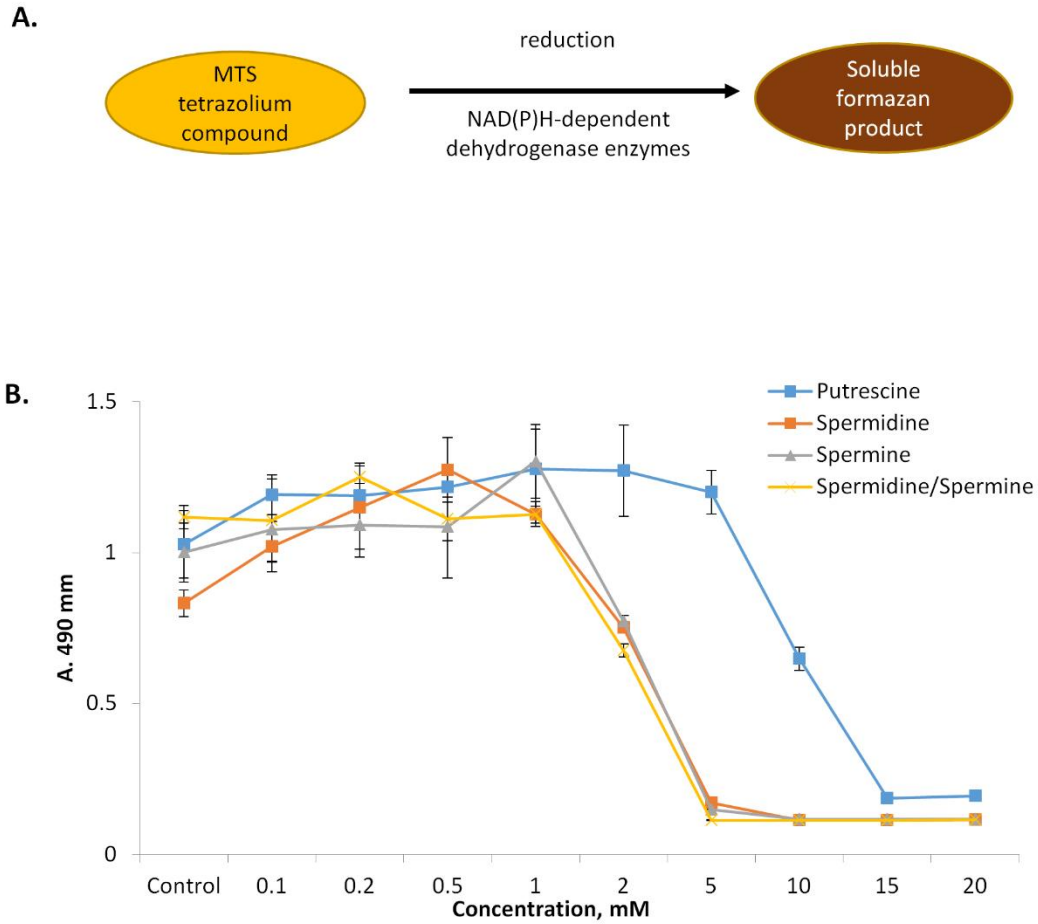

Figure 38: Extracellular addition of polyamines and cell toxicity assay. A. MTS tetrazolium compound (yellow) is reduced by NAD(P)H-dependent dehydrogenase enzymes which are present in metabolically active cells to generate formazan product (brown). The amount of formazan product generated by viable cells is determined by measuring the absorbance at 490nm. Brown color indicates high cell viability while yellow represents low cell viability. **B.** Graph depicting the cell viability at increasing concentrations of the three polyamines. N/TERT-1 keratinocytes were viable up to 1mM for spermidine, spermine and spermidine/spermine in combination and up to 5mM for putrescine following 72h treatment. Results were represented as ±S.D. of two independent biological replicates with six technical replicates each.

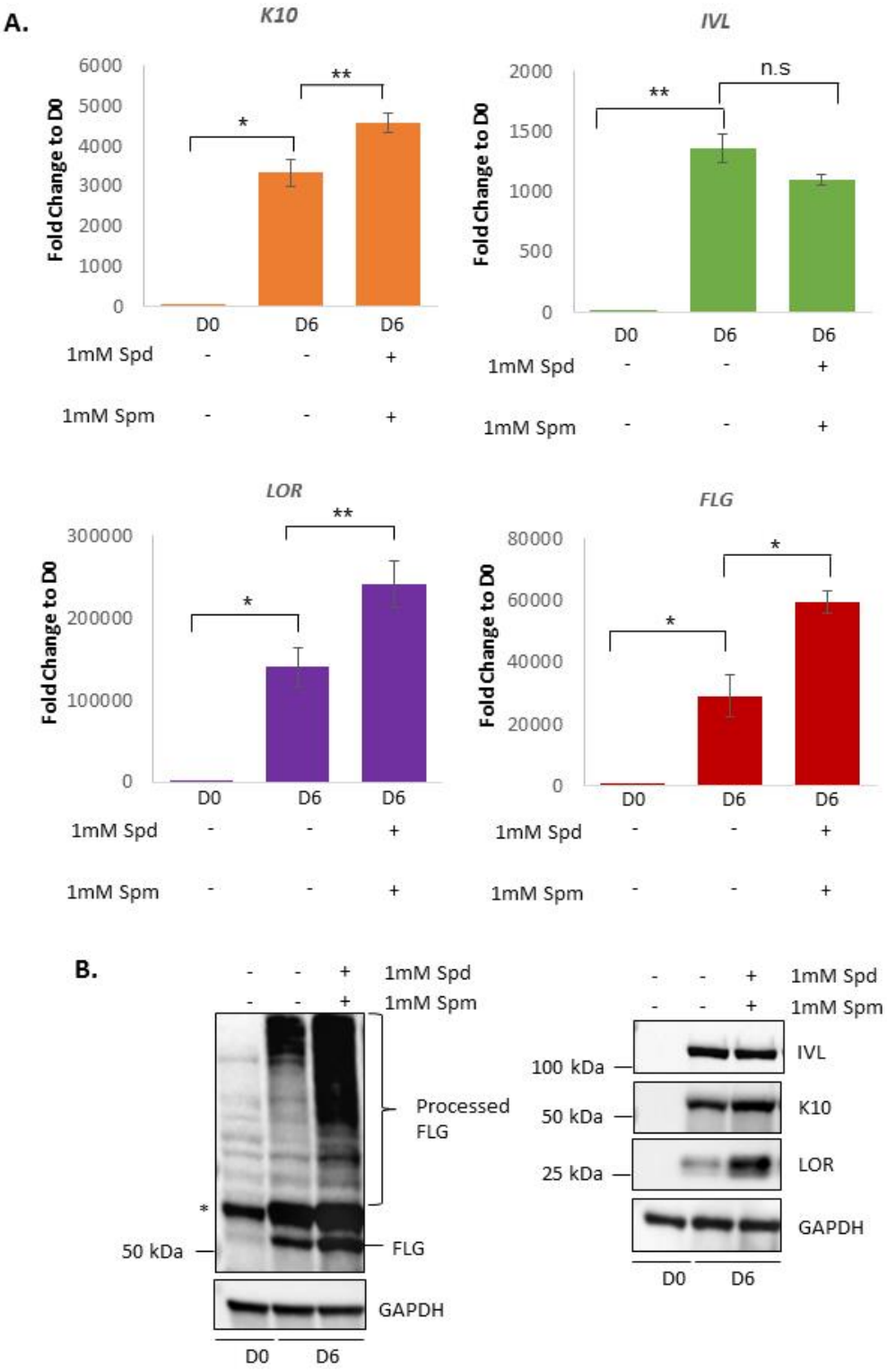

Figure 39: Exogenous addition of Spd/Spm increases N/TERT-1 keratinocyte differentiation. A. mRNA expression of *K10, LOR* and *FLG* significantly increased with the extracellular supplementation of 1mM Spd/Spm to N/TERT-1 keratinocytes at the start of differentiation**.** The increase in *IVL* mRNA with 1mM Spd/Spm addition was not significant. Results were represented as ±S.E.M. of three independent biological replicates and p values of <0.05 *, <0.01 ** and <0.001 *** were considered as statistically significant. **B.** Immunoblot showing an increase in protein expression of K10, FLG and LOR when 1mM of Spd/Spm was supplemented during keratinocyte differentiation compared to without treatment. GAPDH was used as a loading control. *Asterisk indicates a non-specific band.

3.8 AMD1 knockdown using lentiviral transduction

In order to determine the function of AMD1 during keratinocyte differentiation, shAMD1 GIPZ lentiviral transduction was performed using N/TERT-1 keratinocytes to establish two independent AMD1 knockdown stable cell lines, shAMD1-3 and shAMD1-4, in parallel with a non-silencing shScrambled control. GFP expression was captured under EVOS FL cell imaging system to confirm lentiviral transduction and efficient expression of shRNA (**Figure 40A**). Approximately 85-90% knockdown of AMD1 was achieved with shAMD1-3 and shAMD1-4 at the mRNA and protein level as compared to scrambled controls (**Figure 40B**). Since AMD1 protein is important for cell proliferation, we checked the effect of knockdown on the proliferation rate of the cells. By D3 of cell seeding, there was no significant change in cell proliferation but a marginal decrease in cell number was observed in shAMD1-3 and shAMD1-4 knockdown keratinocytes by D5 (**Figure 40C**). To account for the decreased cell proliferation, 25% more shAMD1-3 and 15% more shAMD1-4 keratinocytes were compensated at the time of seeding for each differentiation experiment as compared to shScrambled controls, to ensure that the differentiation phenotype we observe is not a consequence of decreased cell proliferation. Cell count at D0, D3 and D6 of differentiation were invariable after cell compensation (**Figure 40D**).

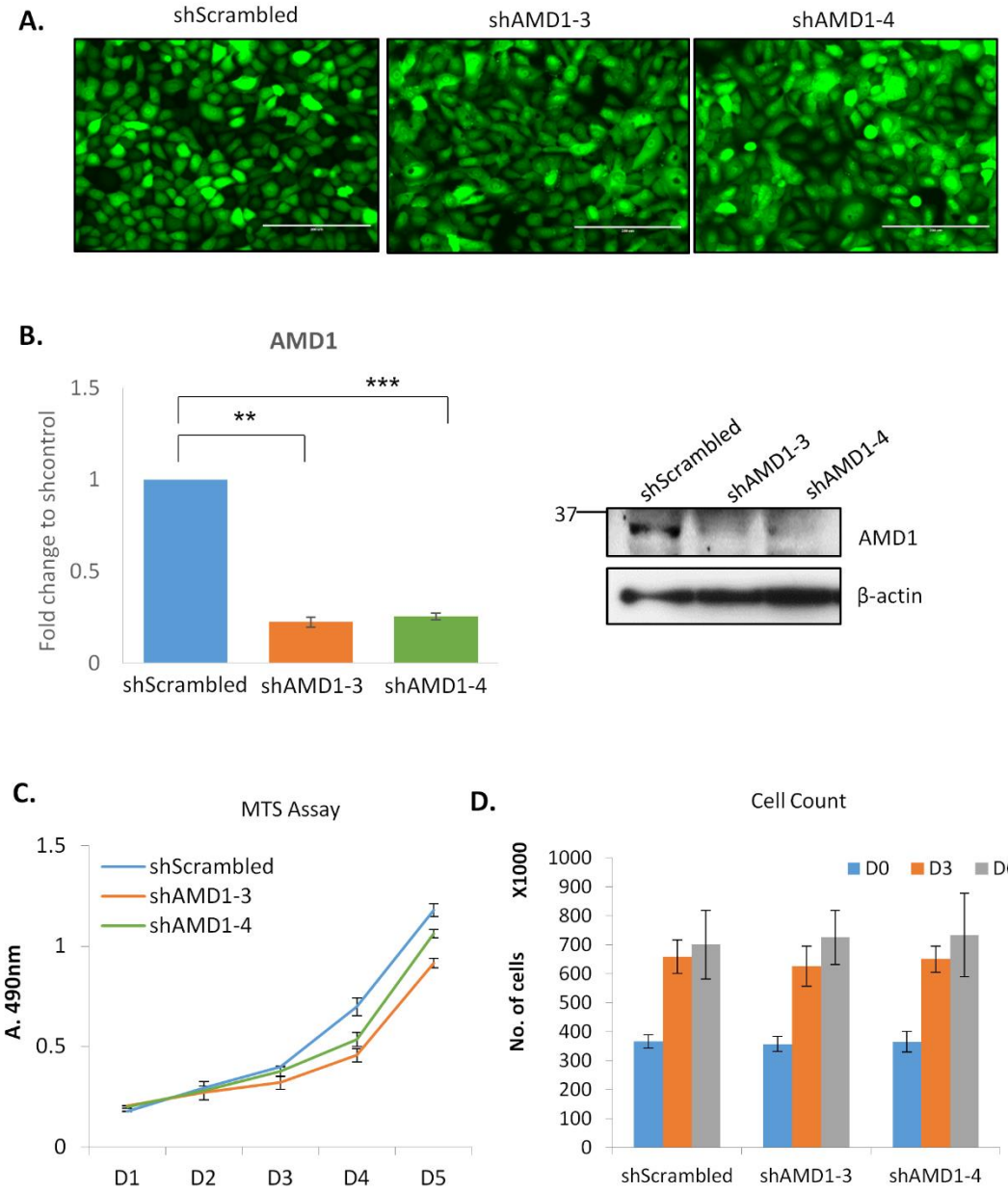

Figure 40: Successful AMD1 knockdown in N/TERT-1 keratinocytes using a GIPZ lentiviral transduction system. A. GFP positive keratinocytes successfully transduced with either shScrambled, shAMD1-3 or shAMD1-4 GIPZ lentiviral shRNAs; scale bar=200μm. **B.** mRNA expression of *AMD1* showing a significant 85-90% knockdown with two independent shRNAs, shAMD1-3 and shAMD1-4. Results were represented as ±S.E.M. of three independent biological replicates and p values of <0.05 *, <0.01 ** and <0.001 *** were considered as statistically significant. Immunoblot showing a strong reduction in AMD1 protein with shAMD1-3 and shAMD1-4 knockdown keratinocytes compared to shScrambled controls. β-actin was used as a house-keeping control. **C.** Knockdown of AMD1 showed a marginal reduction in keratinocyte cell proliferation by D5 of seeding. Results were represented as ±S.D. of two independent biological replicates. **D.** No significant difference in cell density was observed at D3 and D6 of monolayer keratinocyte differentiation using shScrambled and shAMD1 knockdown cells after cell compensation. Results were represented as ±S.E.M. of three independent biological replicates.

3.9 AMD1 is required for keratinocyte differentiation.

I performed differentiation experiments as mentioned above using shAMD1-3 keratinocytes in parallel with shScrambled control keratinocytes. A significant 80-90% reduction in AMD1 was maintained at day 6 of keratinocyte differentiation at the RNA and protein level (**Figure 41.1A and B**). Compared to shScrambled keratinocytes, shAMD1-3 keratinocytes displayed a significant 3.2-fold reduction in the expression *K10*, 6.2-fold reduction in *FLG* and a 28.1-fold reduction in *LOR* mRNA at D6 of differentiation (**Figure 41.1A**). A similar reduction in K10, FLG and LOR protein was observed with AMD1 knockdown while the reduction in IVL protein was mild (**Figure 41.1C**). Addition of 1mM Spd/Spm was able to significantly rescue the expression of K10, IVL, FLG and LOR in shAMD1-3 knockdown keratinocytes (**Figure 41.1A and C**).

The supplementation of Spd/Spm alone was sufficient to promote keratinocyte differentiation. This was observed with an increase in *K10, FLG* and *LOR* mRNA expression when shScrambled keratinocytes were treated with Spd/Spm. With the supplementation of Spd/Spm to shAMD1-3 knockdown keratinocytes, I would expect a rescue in the mRNA levels of FLG similar to that of untreated shScrambled keratinocytes, which is what I observe in Figure 40.1A. The mRNA expression of FLG also correlates with its protein expression, whereby the FLG protein expression in shAMD1-3 knockdown keratinocytes rescued with Spd/Spm is similar to untreated D6 shScrambled keratinocytes.

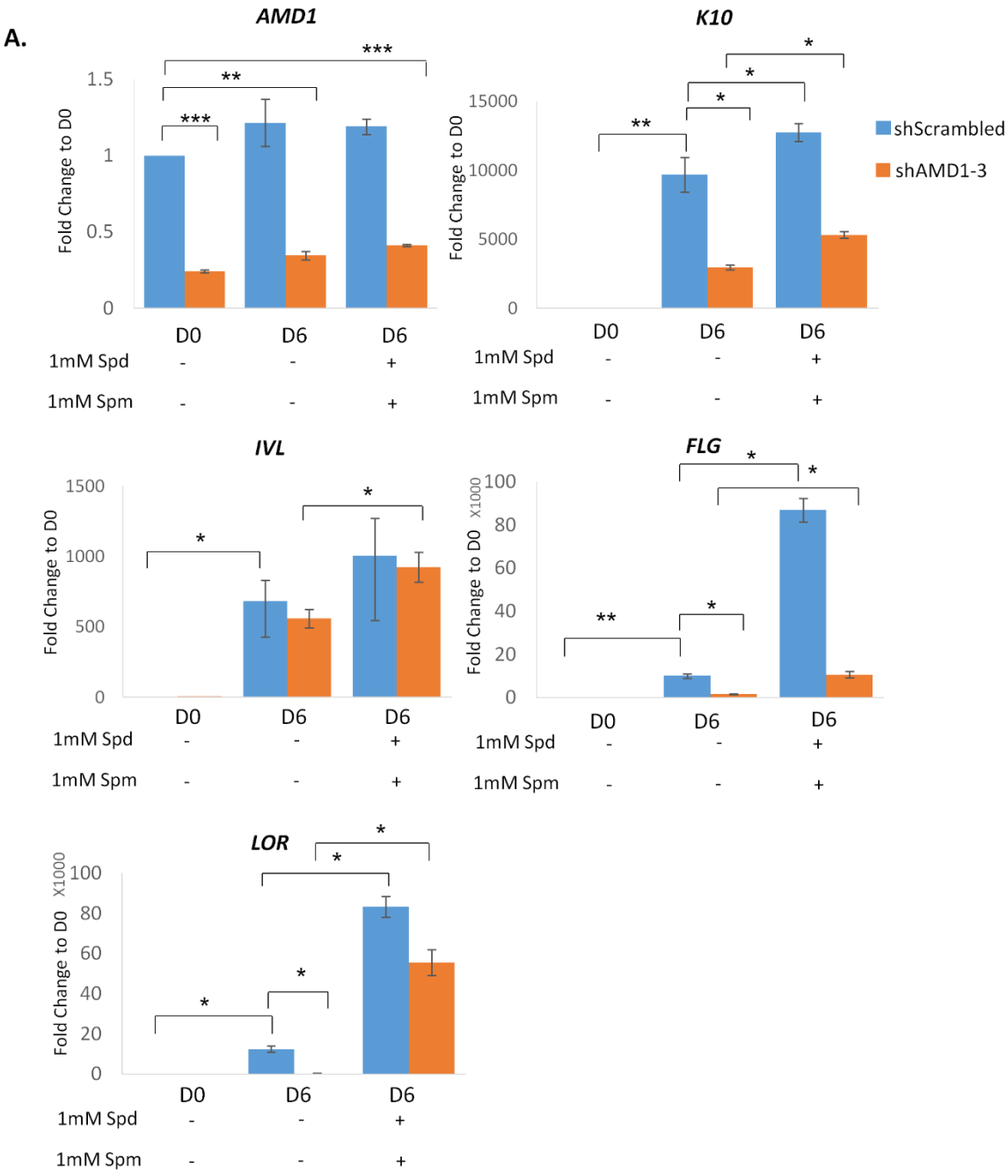

Figure 41.1: AMD1 is required for keratinocyte differentiation. A. mRNA levels of *AMD1* in shAMD1-3 keratinocytes had a significant 80% knockdown at D0 and D6 of keratinocyte differentiation. A significant decrease in mRNA levels of *K10, FLG* and *LOR* was observed with shAMD1-3 knockdown keratinocytes during differentiation compared to shScrambled keratinocytes. Differentiation markers were significantly rescued with the addition of 1mM Spd/Spm. Results were represented as ±S.E.M. of three independent biological replicates and p values of <0.05 *, <0.01 ** and <0.001 *** were considered as statistically significant.

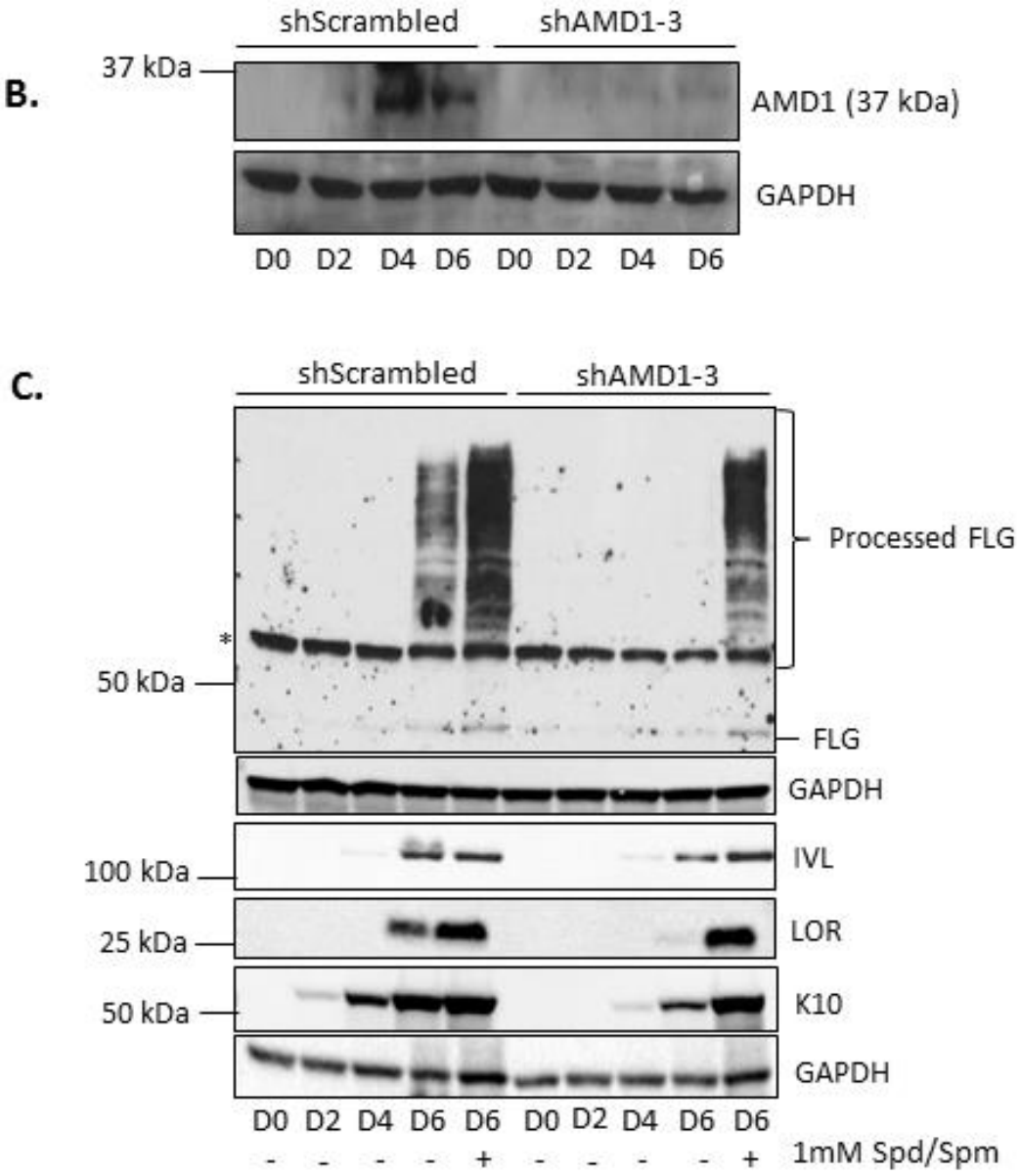

Figure 41.1: AMD1 is required for keratinocyte differentiation. B. Immunoblots showing strong AMD1 knockdown at D6 of keratinocyte differentiation. GAPDH was used as a loading control. **C.** Immunoblots showing a strong decrease in K10, FLG and LOR protein expression in shAMD1-3 knockdown cells following differentiation. Protein expression of differentiation markers were rescued with the addition of 1mM Spd/Spm. GAPDH was used as a loading control. *Asterisk indicates a non-specific band.

To confirm that the phenotype was not due to an off-target effect of the shRNA, I performed differentiation experiments using shAMD1-4 keratinocytes. A similar 80-90% knockdown in *AMD1* mRNA and protein was observed (**Figure 41.2A and B**). A similar decrease in *K10, IVL* and *LOR* mRNA was observed in shAMD1-4 keratinocytes compared to shScrambled controls, and the decrease in *FLG* mRNA was significant during keratinocyte differentiation. shAMD1-4 keratinocytes showed reduced K10 and IVL protein expression compared to shScrambled controls as early as D2, and LOR protein expression at D6 of keratinocyte differentiation (**Figure 41.2C)**. IVL, FLG and LOR mRNA and protein expression were rescued by the addition of 1mM Spd/Spm (**Figure 41.2A and C**). Overall, AMD1 knockdown affected early and late differentiation markers to somewhat a similar extent and my data suggests that AMD1 up-regulation is essential for keratinocyte differentiation. My subsequent experiments were performed using shAMD1-3 keratinocytes.

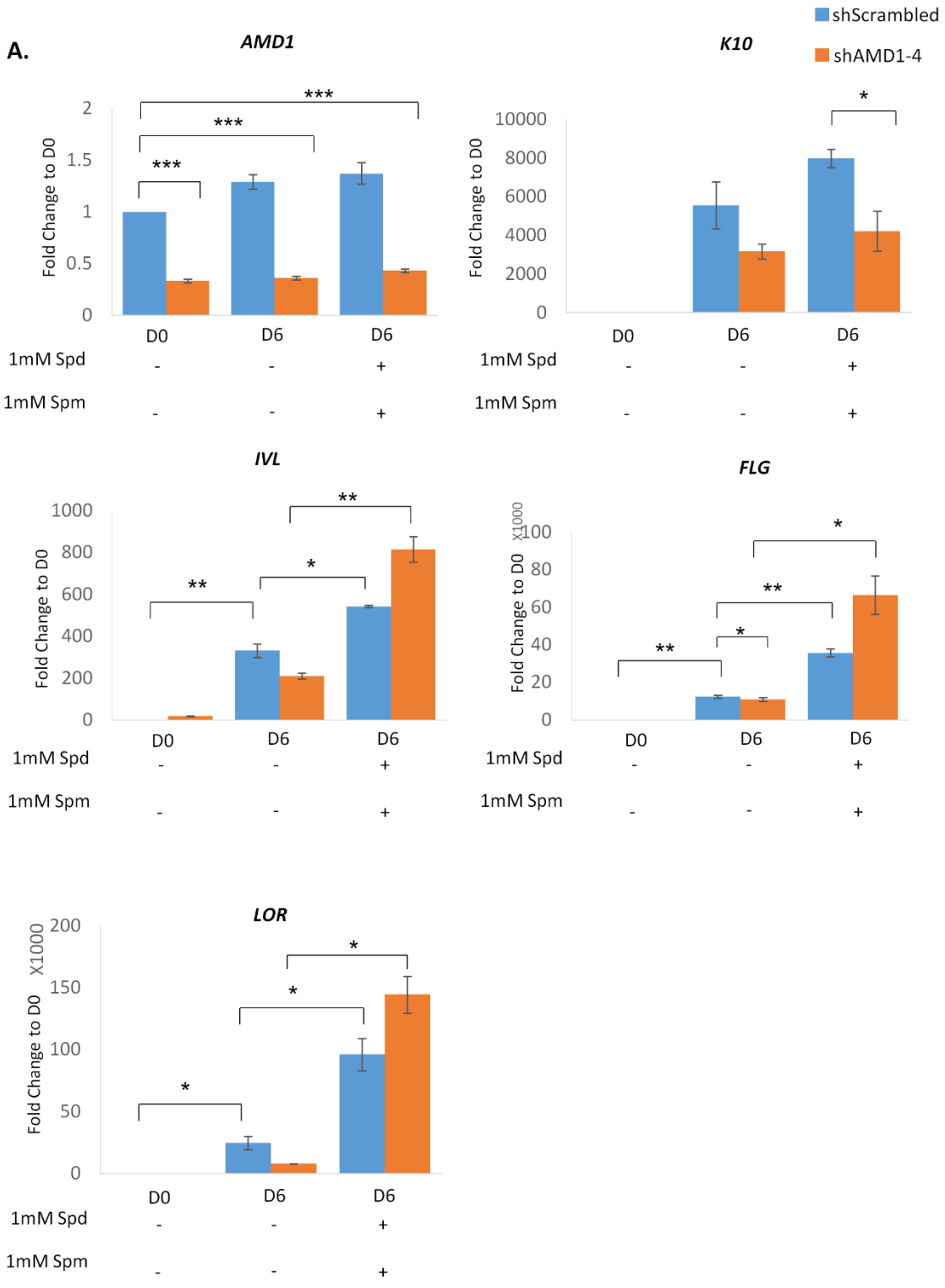

Figure 41.2: AMD1 is required for keratinocyte differentiation. A. mRNA levels of *AMD1* in shAMD1-4 keratinocytes had a significant 80% knockdown at D0 and D6 of keratinocyte differentiation. A significant decrease in *FLG* mRNA was observed with shAMD1-4 knockdown keratinocytes during differentiation compared to shScrambled keratinocytes. The decrease in late differentiation markers, *K10, IVL* and *LOR* were mild but not significant. All differentiation genes were rescued with the addition of 1mM Spd/Spm. Results were represented as ±S.E.M. of three independent biological replicates and p values of <0.05 *, <0.01 ** and <0.001 *** were considered as statistically significant.

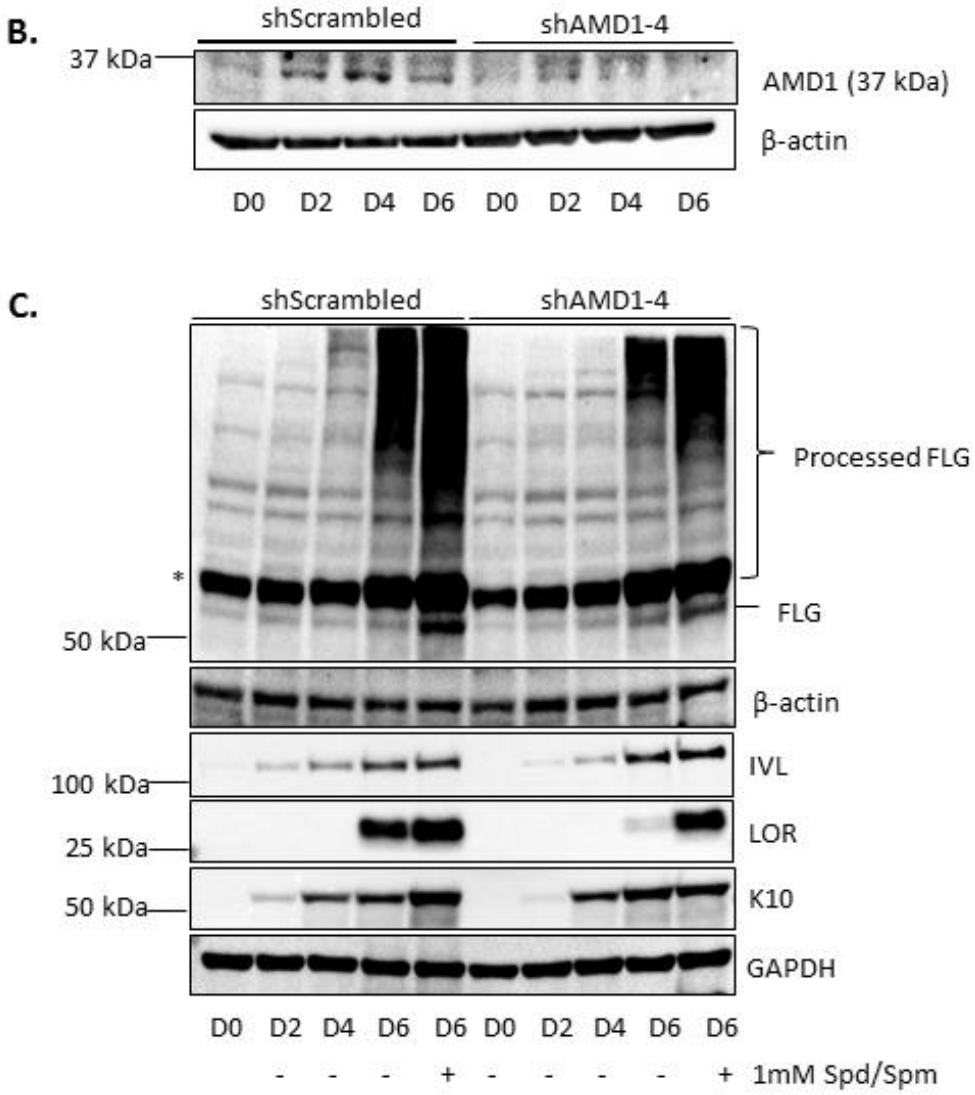

Figure 41.2: AMD1 is required for keratinocyte differentiation. B. Immunoblots showing strong AMD1 knockdown in shAMD1-4 knockdown keratinocytes at D6 of keratinocyte differentiation. β-actin was used as a loading control. **C.** Immunoblots showing a strong decrease in LOR and a mild decrease in FLG at D6 but a mild decrease in K10 and IVL protein expression by D2 of keratinocyte differentiation. Protein expression of FLG and LOR were rescued with the addition of 1mM Spd/Spm. Either GAPDH or β-actin was used as a loading control. *Asterisk indicates a non-specific band.

3.10 shAMD1-3 knockdown organotypics showed reduced stratification and expression of late differentiation markers FLG and LOR.

To better recapitulate the human epidermis, I performed 3-D organotypic skin equivalents by seeding shScrambled and shAMD1-3 keratinocytes onto CellnTEC cell culture inserts in epithelial cell culture media, allowing them to grow to full confluence for 2 days. Cells were lifted to the air-liquid interface and supplied with 3-D barrier media deprived of any growth factors to promote vertical stratification of keratinocytes (Gangatirkar, Paquet-Fifield et al. 2007) (**Figure 42.1**). 100μM of Spd/Spm was added to the media at D3 and D5 of airlift for rescue organotypics using shAMD1-3 keratinocytes. All organotypic skin equivalents were harvested 7 days post airlift, fixed with 4% PFA and processed for immunohistological analysis.

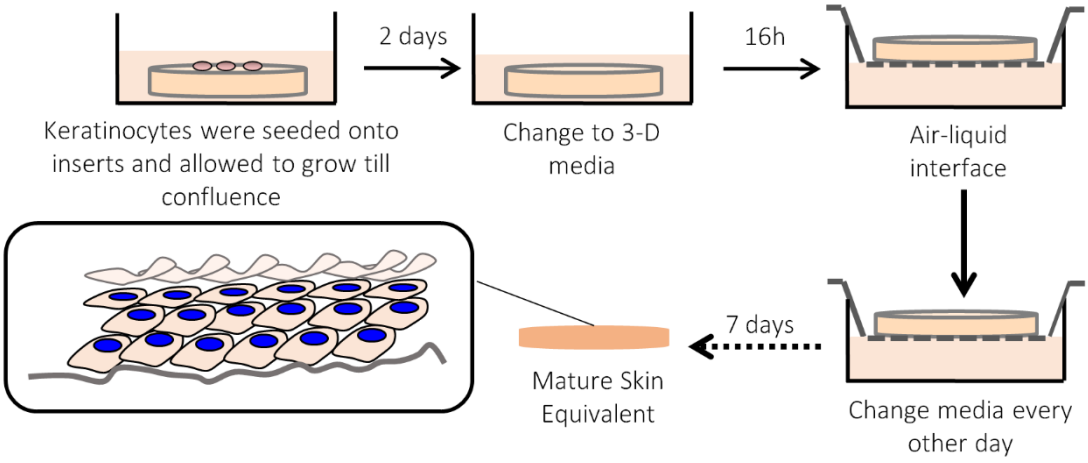

Figure 42.1: Establishment of 3-D organotypic skin equivalents using shScrambled and shAMD1-3 knockdown N/TERT-1 keratinocytes. Schematic representation of organotypic skin cultures performed by growing N/TERT-1 keratinocytes to confluence followed by lifting inserts to an air-liquid interface for 7 days for stratification of keratinocytes.

H&E staining of organotypic skin equivalents derived from shScrambled keratinocytes showed all four layers of the epidermis: SB, SS, SG and SC (**Figure 42.2A**). Two representative biological replicates of skin equivalents were included (**Figure 42.2A**). While all layers of the epidermis were formed using shScrambled keratinocytes, the organotypics derived from shAMD1-3 knockdown keratinocytes displayed perturbed differentiation, showing fewer keratohyalin granules in the SG and the presence of parakeratotic nuclei in the SS and SC as indicated by white arrowheads in **Figure 42.2A**. All layers of the epidermis were formed when shAMD1-3 knockdown organotypics were rescued by the addition of 100μM of Spd/Spm (**Figure 42.2A**). While shScrambled-derived organotypics showed high expression of late differentiation markers FLG and LOR, the expression of these markers were reduced in shAMD1-3 derived organotypics and were rescued in 100μM of Spd/Spm-treated shAMD1-3 organotypics (**Figure 42.2B**).

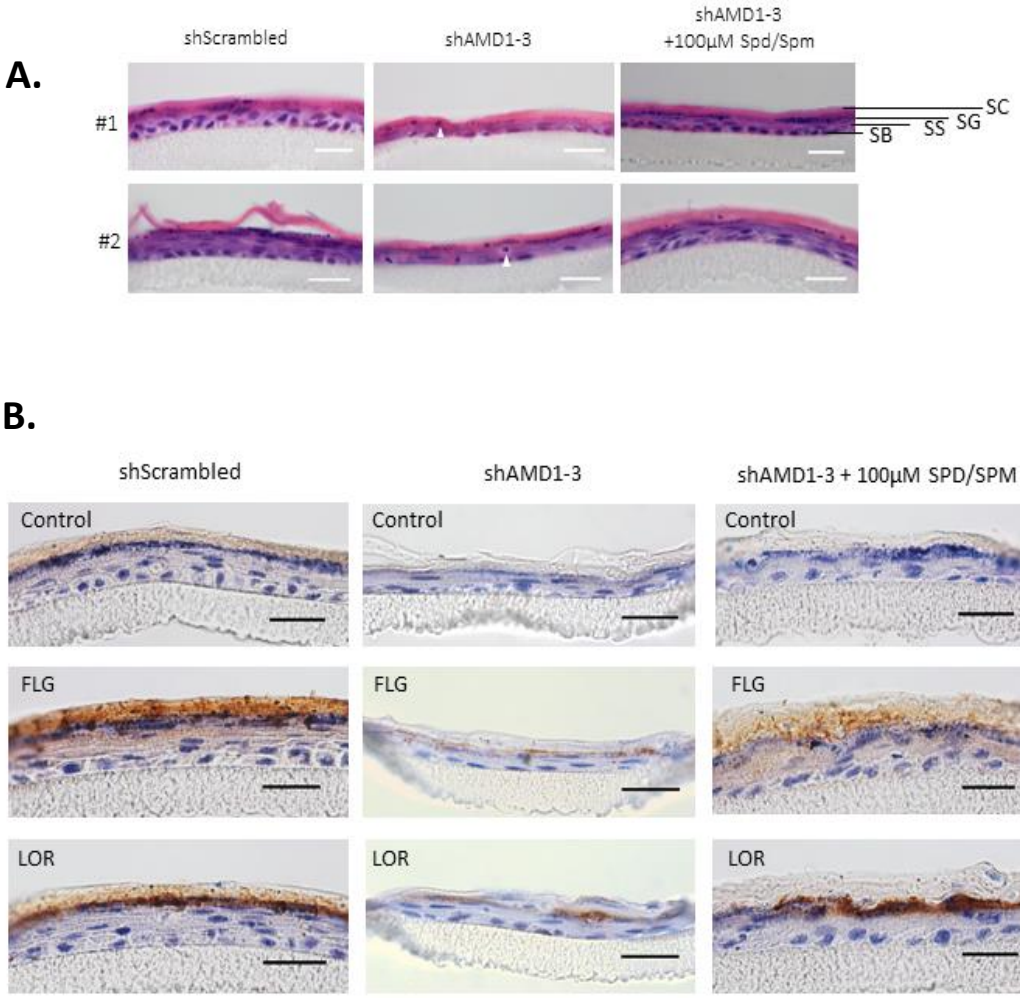

Figure 42.2: Establishment of 3-D organotypic skin equivalents using shScrambled and shAMD1-3 knockdown N/TERT-1 keratinocytes. A. Hematoxylin and Eosin (H&E) staining showing fully stratified organotypic skin equivalents derived from shScrambled keratinocytes but aberrant stratification with shAMD1-3 knockdown keratinocytes. Stratification was reversed when shAMD1-3 keratinocytes were supplemented with 100μM of Spd/Spm. Arrowheads represent parakeratotic nuclei. SB=Stratum Basale, SS=Stratum Spinosum, SG=Stratum Granulosum and SC=Stratum Corneum, Three biological replicates were performed and two replicates are represented **B.** High expression of FLG and LOR observed in shScrambled and shAMD1-3 derived organotypics treated with 100μM of Spd/Spm but not in shAMD1-3 derived organotypics. Three independent biological replicates were performed; Scale bar=50μm.

3.11 Shift in polyamine levels were observed during AMD1 knockdown keratinocyte differentiation.

As I observe a shift in polyamine levels from Put to Spm during keratinocyte differentiation, I wanted to determine whether this shift was dependent on AMD1. To do this, D0 and D6 shScrambled and shAMD1-3 keratinocytes were prepared for HPLC as described above. There was a significant 2-fold reduction in Put, 1.6-fold decrease in Spd and 2.3-fold increase in Spm in D6 shScrambled keratinocytes compared to D0 shScrambled keratinocytes (**Figure 43**). This polyamine shift was similar to my differentiation using non-transduced N/TERT-1 keratinocytes (**Figure 37**). I observed a 3.9-fold increase in Put levels in D0 shAMD1-3 keratinocytes and 1.6-fold decrease in Spm levels compared to D0 shScrambled keratinocytes, as expected (**Figure 43**). A significant 1.5-fold decrease in Spm levels was observed in D6 shAMD1-3 keratinocytes compared to D6 shScrambled keratinocytes (**Figure 43**). These data suggest that a shift in polyamine ratios from Put to Spm may enhance keratinocyte differentiation.

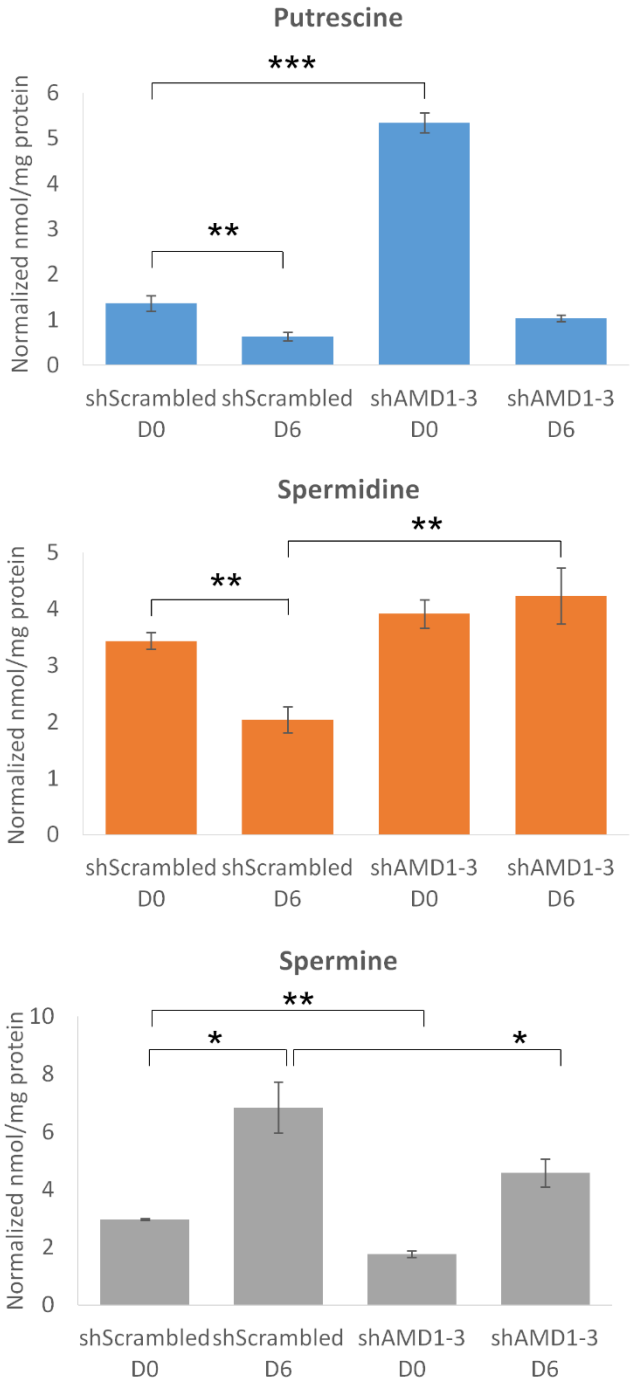

Figure 43: Polyamine shift during keratinocyte differentiation is impaired in shAMD1-3 knockdown keratinocytes. shAMD1-3 knockdown significantly increased putrescine levels but decreased the levels of spermine in D0 undifferentiated keratinocytes compared to shScrambled keratinocytes. A significant decrease in spermine levels was observed in shAMD1-3 knockdown keratinocytes during D6 of differentiation. Results were represented as ±S.E.M. of four independent biological replicates and p values of <0.05 *, <0.01 ** and <0.001 *** were considered as statistically significant.

3.12 AMD1 inhibition perturbs keratinocyte differentiation and is rescued by the addition of Spd/Spm

To confirm the AMD1 knockdown phenotype, I used EGBG, an irreversible AMD1 inhibitor to block AMD1 activity. An MTS assay was performed to determine a non-toxic concentration of EGBG after 48h of treatment in N/TERT-1 keratinocytes. Keratinocytes were tolerant of up to 200μM of EGBG, beyond which the cell viability was compromised (**Figure 44A**). Hence, EGBG concentrations of either 5, 25 or 50μM were used to inhibit AMD1 in subsequent differentiation experiments. While the percentage inhibition of AMD1 was not determined, an increase in Put levels with 50μM of EGBG treatment compared to untreated D6 differentiated keratinocytes suggest that AMD1 was inhibited (**Figure 37**).

Initial experiments were performed with the addition of either 5 or 50μM of EGBG alone or in combination with 1mM of Spd/Spm at the start of differentiation. Drugs were replenished every alternate day with fresh media. There was a dose-dependent decrease in the expression of differentiation markers K10, IVL and FLG with the addition of 5 and 50μM of EGBG respectively, and all markers were rescued by the addition of 1mM Spd/Spm (**Figure 44B and C**). Since approximately one population doubling was observed by D3 of keratinocyte differentiation, I decided to add 25 and 50μM of EGBG at D3 instead of D0 of keratinocyte differentiation to prevent the interference of EGBG on cell proliferation (**Figure 40D**). Similarly, I observed a significant decrease in mRNA expression of *IVL* and *LOR* with 25μM and 50μM of EGBG at D6 of keratinocyte differentiation (**Figure 45A**). mRNA expression of *IVL* and *LOR* were significantly rescued by the addition of 1mM of Spd/Spm. Likewise, 25 and 50μM of EGBG reduced the protein expression of K10, IVL, LOR and caspase-14, another marker of keratinocyte differentiation (**Figure 45B**). The protein expression of all four differentiation markers were rescued when EGBG was added in combination with 1mM of Spd/Spm (**Figure 45B**). Though the increase in Put levels with AMD1 inhibition was not statistically significant in comparison to D6 differentiated keratinocytes, the decrease in Spm levels were consistent with the polyamine measurement in

AMD1 knockdown keratinocytes (**Figure 37**). My data confirms that AMD1 is necessary for efficient keratinocyte differentiation.

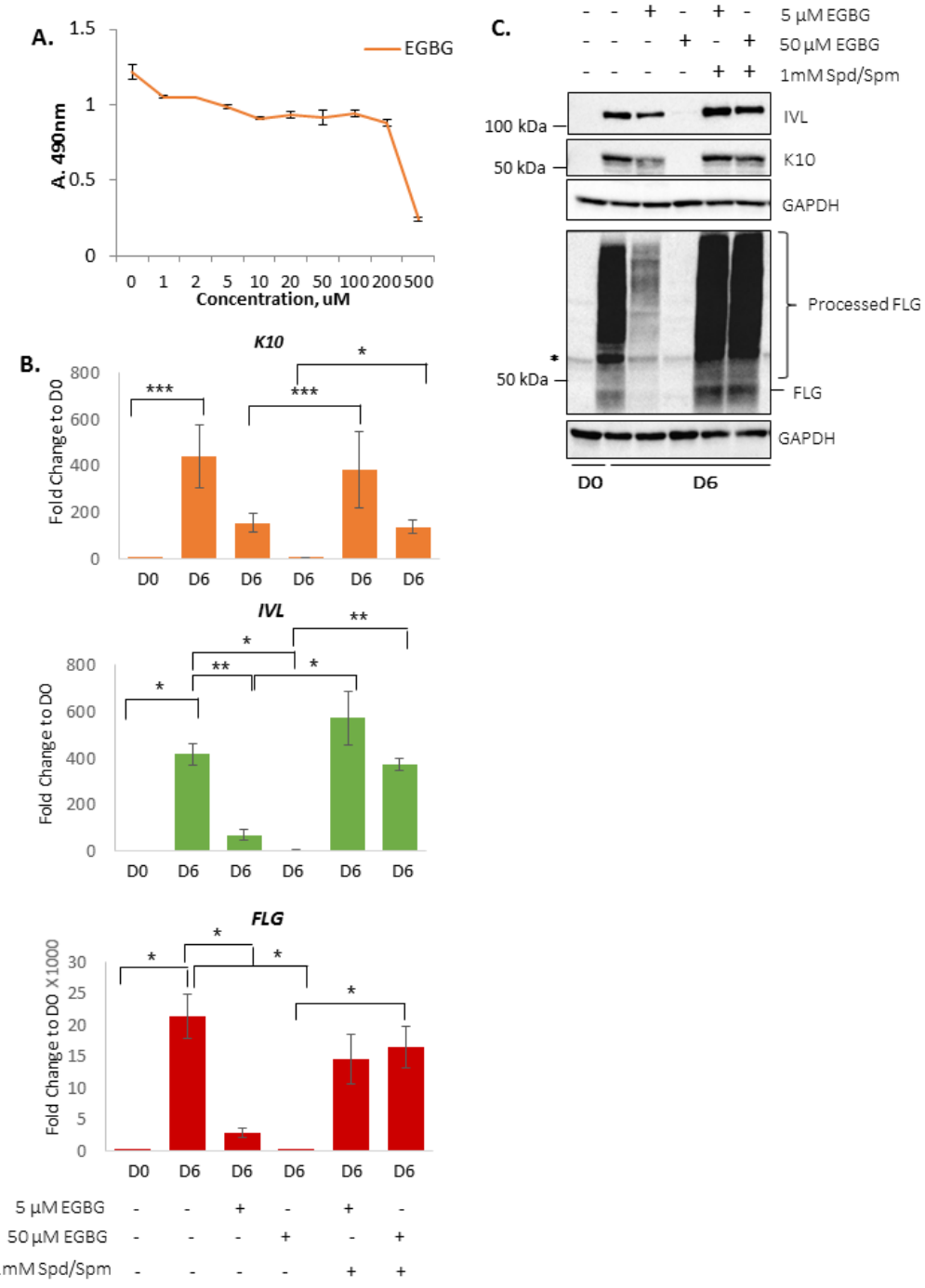

Figure 44: AMD1 inhibition from D0 post-confluence perturbs keratinocyte differentiation and is rescued by the addition of 1mM Spd/Spm. A. Graph depicting the cell viability of N/TERT-1 keratinocytes cultured at increasing concentrations of AMD1 inhibitor, EGBG for 48h. **B.** Significant down-regulation of *K10, IVL* and *FLG* mRNA levels were observed with a dose-dependent increase of EGBG at D6 of keratinocyte differentiation. mRNA levels were rescued by the addition of 1mM Spd/Spm. mRNA levels were normalized to house-keeping gene, *RPL13A*. Results were represented as ±S.E.M. of three independent biological replicates and p values of <0.05 *, <0.01 ** and <0.001 *** were considered as statistically significant. **C.** Immunoblots showing a dose-dependent down-regulation of K10, IVL and FLG protein, with increasing EGBG concentrations. Protein levels were completely rescued by the addition of 1mM Spd/Spm. GAPDH was used as a loading control. *Asterisk indicates a non-specific band.

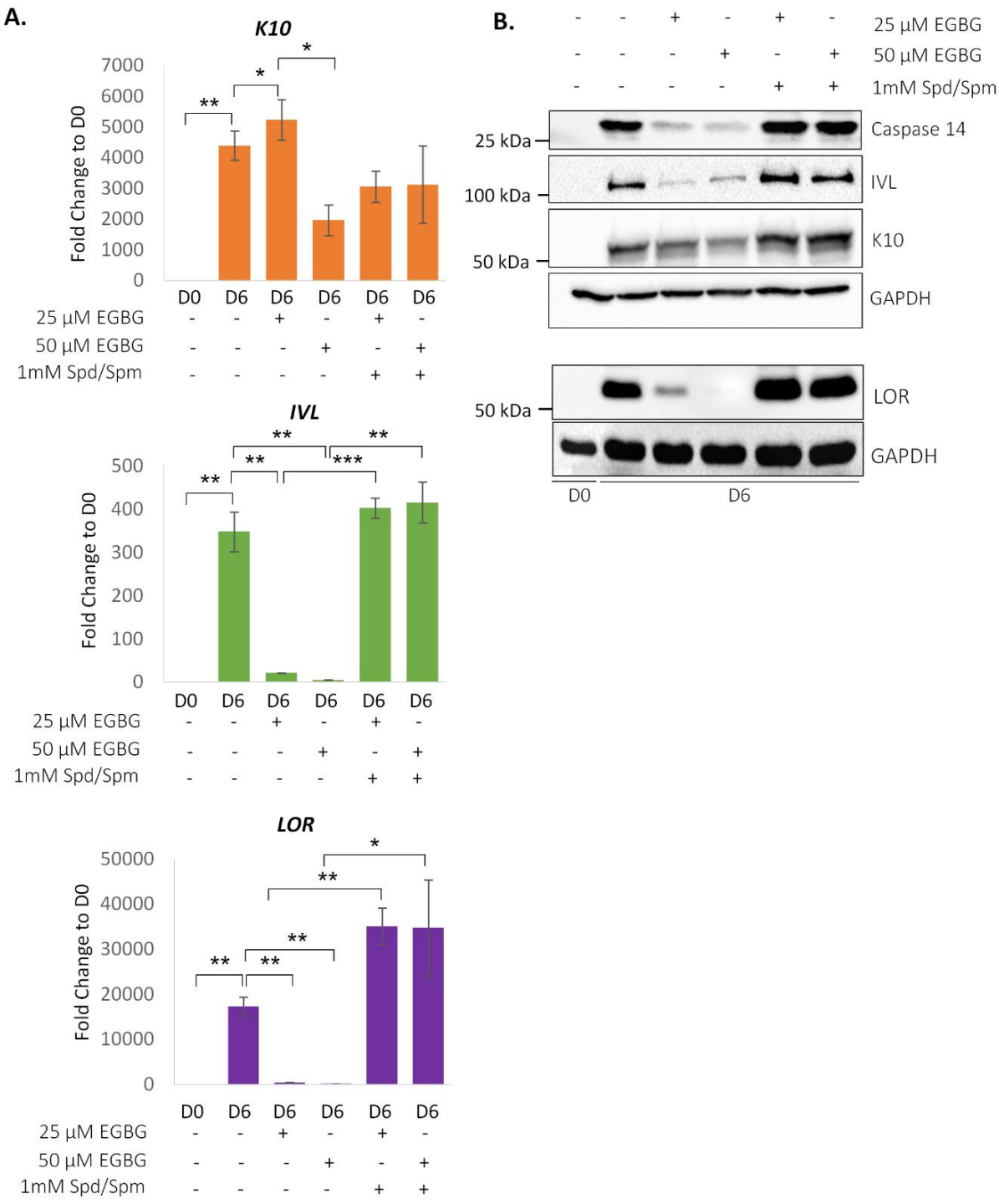

Figure 45: AMD1 inhibition from D3 post-confluence impedes keratinocyte differentiation. A. A significant down-regulation of *IVL* and *LOR* mRNA levels was observed with a dose-dependent increase of EGBG added from D3 of keratinocyte differentiation. mRNA levels were rescued by the addition of 1mM Spd/Spm. mRNA levels were normalized to house-keeping gene, *RPL13A*. Results were represented as ±S.E.M. of three independent biological replicates and p values of <0.05 *, <0.01 ** and <0.001 *** were considered as statistically significant. **B.** Immunoblots showing dose-dependent down-regulation of K10, IVL, LOR and caspase-14 protein, with increasing EGBG concentrations added from D3 of keratinocyte differentiation. Protein levels were completely rescued by the addition of 1mM Spd/Spm. GAPDH was used as a loading control.

3.13 Identification of downstream targets of AMD1

Next, I performed a microarray analysis to determine downstream targets of AMD1 during keratinocyte differentiation. Samples included for microarray analysis were D0 undifferentiated keratinocytes and D6 differentiated keratinocytes with no treatment or treated with 50μM EGBG, 50μM EGBG in combination with 1mM Spd/Spm, 1mM Put alone or 1mM Spd/Spm. Hierarchical clustering of these samples demonstrated proximal clustering of D0 undifferentiated keratinocytes with D6 differentiated keratinocytes treated with EGBG (**Figure 46A**). D6 differentiated keratinocytes were clustered close together with those treated with EGBG and rescued with 1mM Spd/Spm, treated with 1mM Put alone or treated with 1mM Spd/Spm (**Figure 46A**). Since I wanted to identify downstream targets of AMD1, D6 keratinocytes treated with 1mM Put and 1mM Spd/Spm were excluded for subsequent gene analysis.

D0 undifferentiated keratinocytes were compared to D6 differentiated keratinocytes to determine genes that were differentially expressed during keratinocyte differentiation. Among these genes, I selected genes that were affected by 50μM of EGBG treatment and rescued by the addition of 1mM of Spd/Spm (**Figure 46B**). Differentially expressed genes that displayed 2-fold or more changes were selected for further analysis (**Figure 46B**).

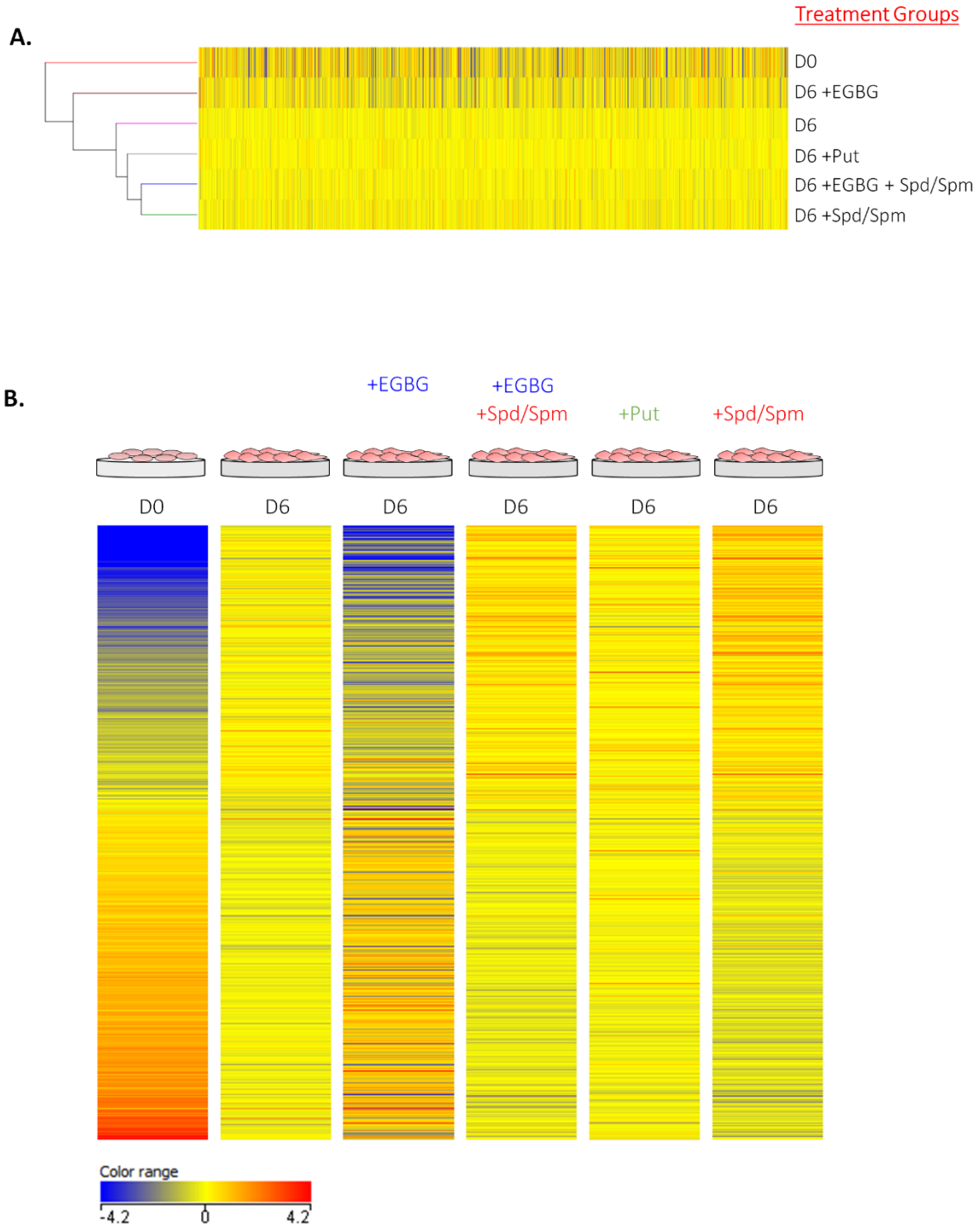

Figure 46: Gene expression changes observed during AMD1 inhibition and with 1mM of Spd/Spm rescue during monolayer N/TERT-1 keratinocyte differentiation. A. Heat map showing the proximal clustering of D0 undifferentiated and D6 differentiated keratinocytes treated with EGBG but distally clustered from D6 differentiated keratinocytes that were un-treated or treated with either putrescine (Put) alone, spermidine/spermine (Spd/Spm) or EGBG with Spd/Spm rescue. **B.** Heat map showing all 2-fold change or more differentially expressed genes. Four independent biological replicates were used; color bar of blue represents down-regulated and red represents up-regulated genes.

mRNAs that were two-fold or more up-regulated (**Figure 47A**) or down-regulated on differentiation **(Figure 47B**) were represented as heat-maps. Among 1927 genes that displayed 2-fold or more changes during keratinocyte differentiation, 1515 genes were affected by AMD1 inhibition (**Figure 48A**). Among these genes, 1507 genes were rescued by the addition of 1mM Spd/Spm, suggesting that 78.2% of mRNAs that are differentially expressed on keratinocyte differentiation are AMD1-sensitive **(Figure 48B**). I performed a gene ontology analysis on AMD1-sensitive genes, and observed that AMD1-sensitive up-regulated genes were primarily involved in epidermal development, keratinocyte differentiation, peptide cross-linking and cytoskeletal organization (**Figure 49A**). AMD1-sensitive down-regulated genes were enriched for structural constituents of the ribosome and were involved in mitochondrial translational elongation and termination (**Figure 49B**). A significant number of the AMD1-sensitive up-regulated genes were a subset of the epidermal differentiation complex (EDC) (**Figure 50**), as highlighted in red.

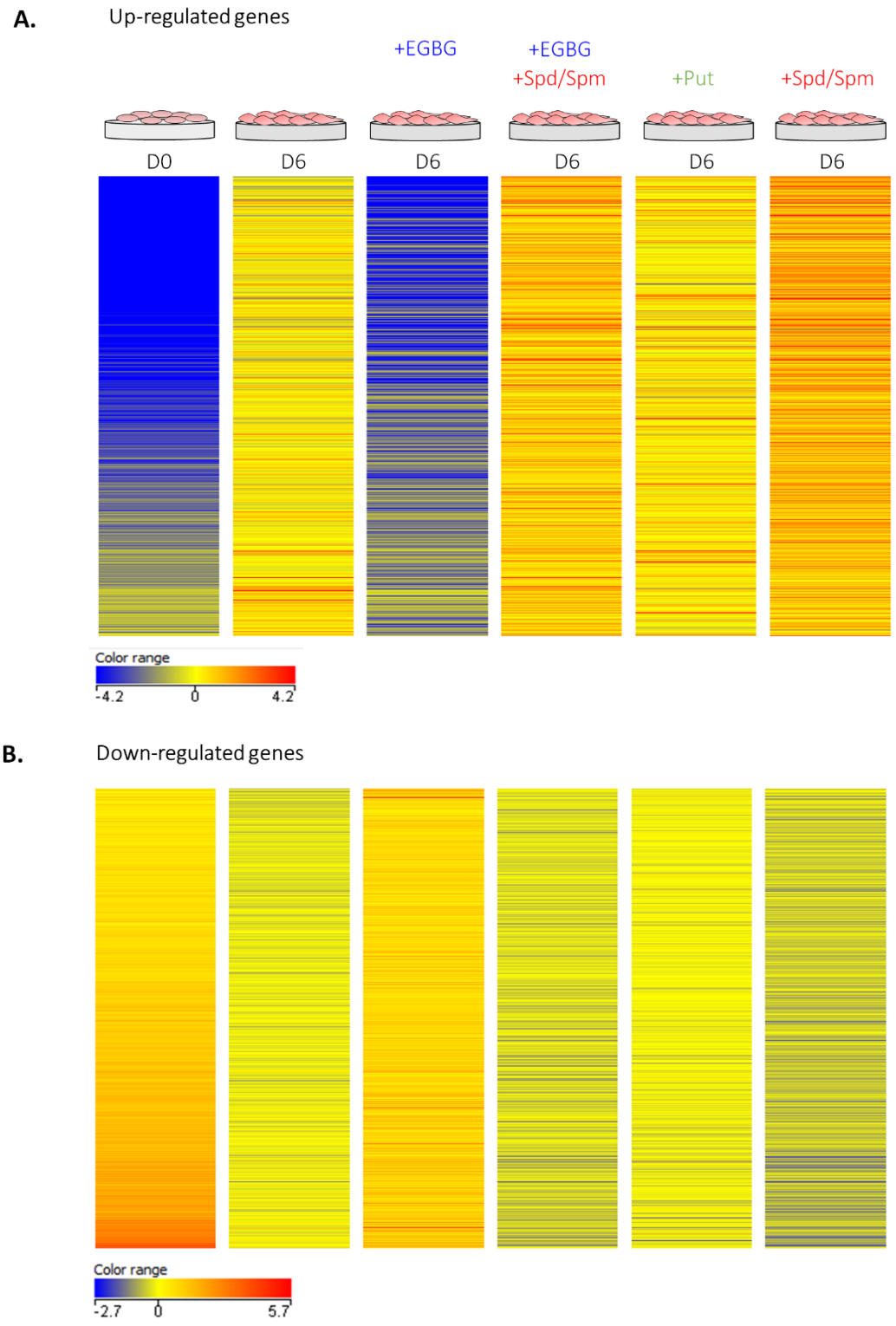

Figure 47: 2-fold change or more differentially expressed genes during AMD1 inhibition and 1mM Spd/Spm rescue during monolayer N/TERT-1 keratinocyte differentiation. A. Heat map showing 2-fold change or more up-regulated genes during keratinocyte differentiation. **B.** Heat map showing 2-fold change or more down-regulated genes during keratinocyte differentiation. Genes represented had a p value of at least <0.05; color bar of blue represents down-regulated and red represents up-regulated genes.

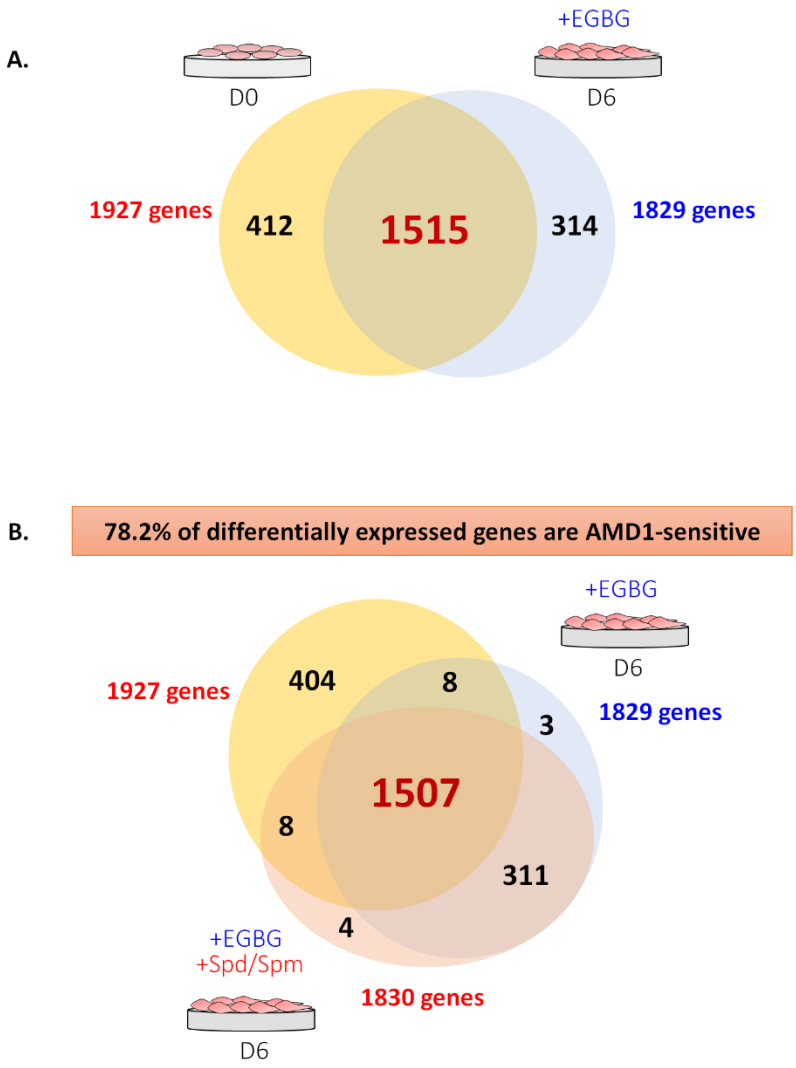

Figure 48: Venn diagram of 2-fold change or more differentially expressed genes during keratinocyte differentiation. A. 1515 genes that are regulated during keratinocyte differentiation showed differential changes with AMD1 inhibition. **B.** Out of the 1515 genes, 1507 genes were AMD1-sensitive. Genes represented had a p value of at least <0.05.

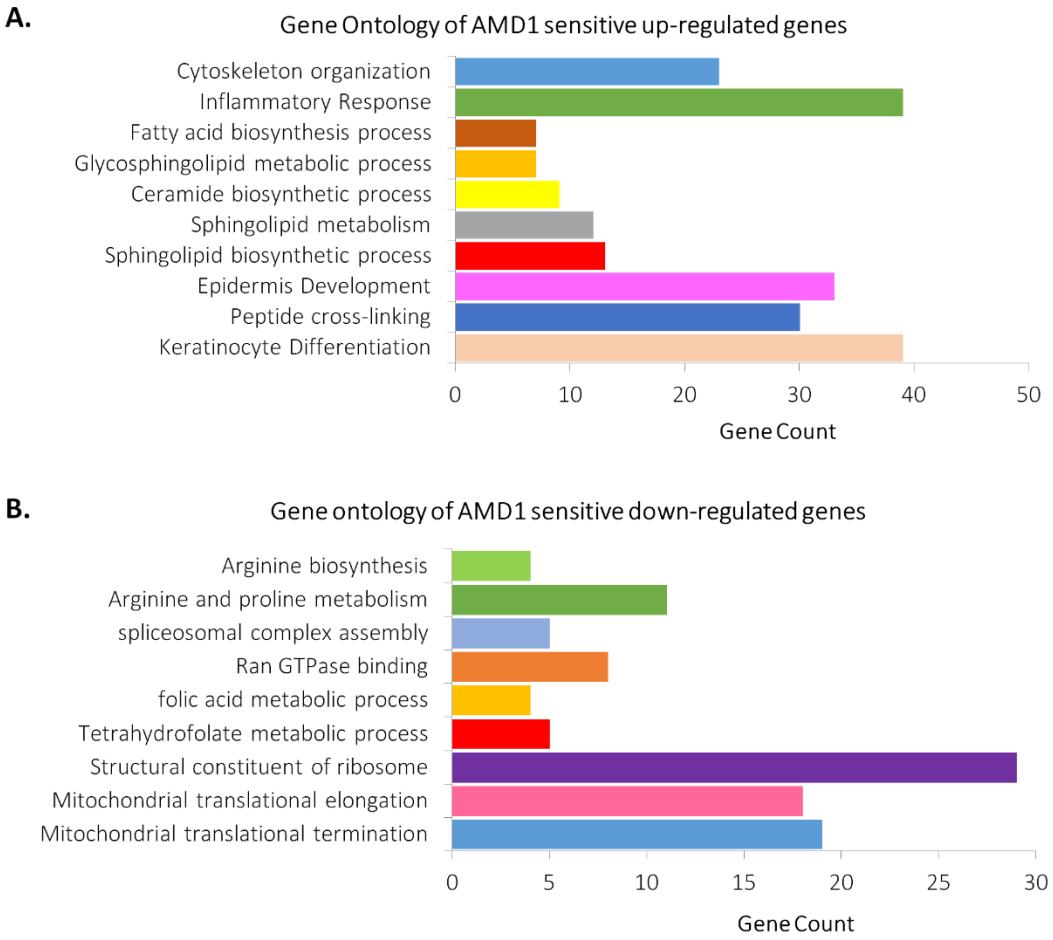

Figure 49: Molecular function of AMD1-sensitive genes during keratinocyte differentiation. A. Gene ontology analysis showing the predominant involvement of AMD1-sensitive up-regulated genes in keratinocyte differentiation, peptide cross-linking, epidermal development and inflammatory response. **B.** Gene ontology analysis showing the predominant involvement of AMD1-sensitive down-regulated genes in mitochondrial translational elongation/termination and structural components of the ribosome.

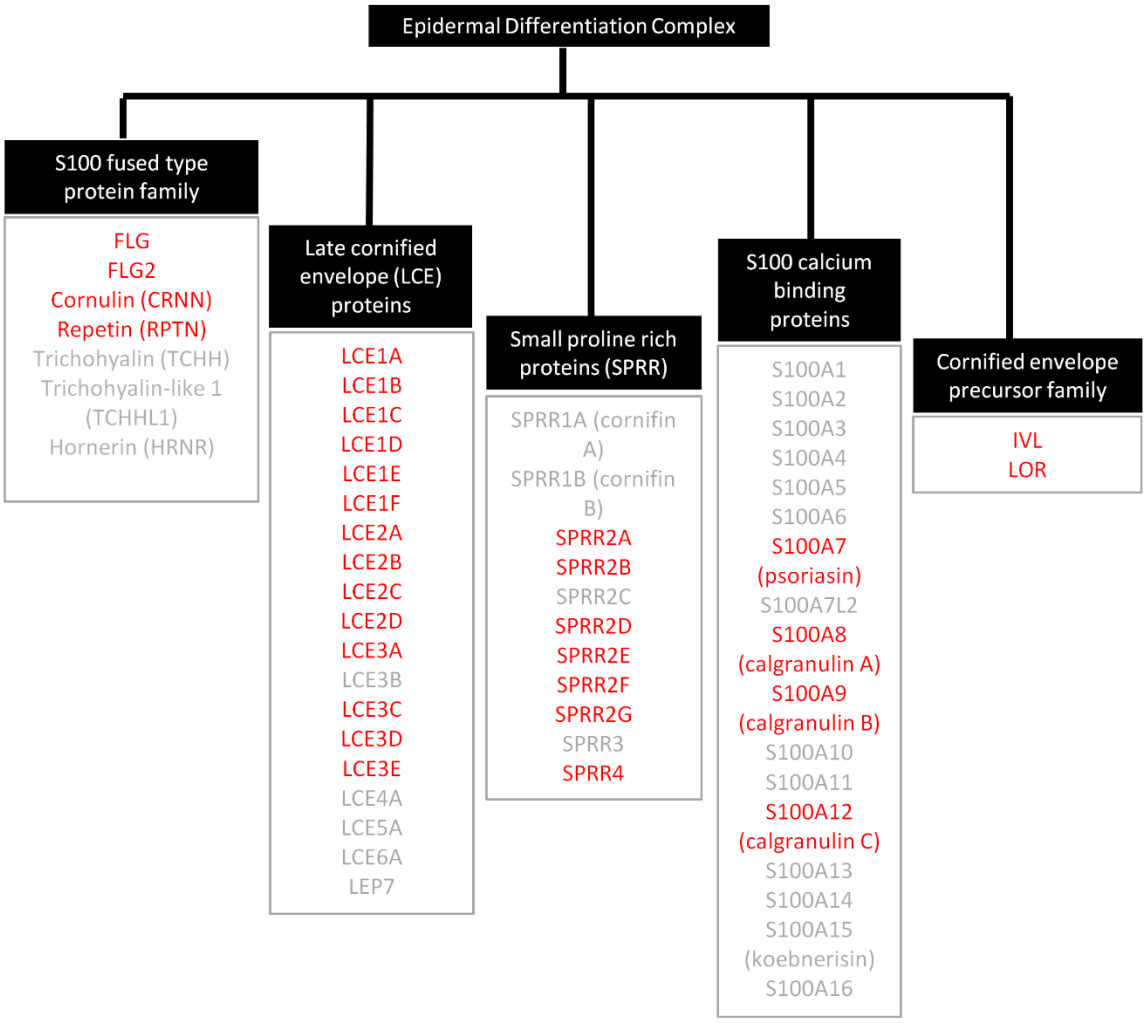

Figure 50: AMD1-sensitive genes in the epidermal differentiation complex (EDC). AMD1-sensitive genes in red are part of the network of epidermal differentiation complex (EDC). Genes represented had a p value of at least <0.05.

3.14 AMD1 is an upstream regulator of key transcription factors, RNA binding proteins and signaling molecules that drive keratinocyte differentiation.

Using DAVID, a gene list analysis tool, I screened for AMD1-sensitive genes that are either transcription factors, RNA binding proteins or signaling molecules (**Table 12**). From these gene lists, I selected genes that displayed strong regulation by AMD1 based on their fold changes. I then validated a panel of these genes by qRT-PCR. Transcription factors known to regulate keratinocyte differentiation such as JUNB, KLF4, NOTCH1 and ZNF750 were all AMD1-sensitive (**Figure**

51.1). Other transcription factors that showed either up/down regulation at D6 of keratinocyte differentiation, down/up regulation upon AMD1 inhibition and up/down regulation by the addition of 1mM Spd/Spm were tumour protein p63 regulated 1 (TPRG1), mitogen-activated protein kinase 3 (MAPK3), zinc finger protein 416 (ZNF416), zinc finger and BTB domain containing protein 7C (ZBTB7C), CCAAT/enhancer binding protein zeta ($CEBP_Z$), SMAD family member 5 (SMAD5), homeobox A9 (HOXA9), eukaryotic translation initiation factor 4E-binding protein 2 (EIF4EBP2), SIX homeobox 4 (SIX4) and zinc finger protein 256 (ZNF256) (**Figure 51.1 and 51.2**). Some of the signalling molecules I identified were kallikrein related peptidase 9 (KLK9), epidermal growth factor (EGF), S100 calcium binding protein A8/9 (S100A8/9), bone morphogenetic protein 2 (BMP2) and Wnt family member 11 (Wnt11), that were AMD1-sensitive (**Figure 51.3**). RNA binding proteins such as eukaryotic translation initiation factor 2 subunit 2 (EIF2S2), Ras-like family 11 member B (RASL11B) and ribosomal protein L3 like (RPL3L) were validated from the microarray dataset to be dependent on AMD1 (**Figure 51.4**). Other targets known to be important for keratinocyte differentiation such as calmodulin-like protein 5 (CALML5), tissue differentiation-inducing non-protein coding RNA (TINCR), aquaporin-3(AQP3) and dual oxidase 1 (DUOX1) were also proven to be downstream of AMD1 (**Figure 51.5**). I then validated some on these candidates by immunoblotting based on the readily available in-house antibodies (**Figure 52**). At the protein level, AQP3, KLK7, KLF4 and S100A8/9 were all up-regulated upon differentiation, down-regulated with AMD1 inhibition and rescued by 1mM Spd/Spm treatment (**Figure 52**). On the contrary, NOTCH1 was down-regulated upon differentiation, up-regulated with AMD1 inhibition and down-regulated with 1mM Spd/Spm rescue (**Figure 52**). My microarray dataset validated well by qRT-PCR and immunoblotting, thereby increasing the confidence of the dataset.

Table 12. List of 3-FC or more AMD1-sensitive genes with p value of at least <0.05 classified as transcriptions factors, signaling molecules and RNA binding proteins.

Transcription factors	
Up-regulated genes	
ZNF750	Zinc finger protein 750
GRHL1	Grainyhead-like
ZNF416	Zinc finger protein 416
NPAS1	Neuronal PAS domain protein 1
JUNB	Jun B proto-oncogene
KLF4	Kruppel Like Factor 4
TPRG1	Tumour protein p63 regulated 1
MAPK3	Mitogen-activated protein kinase 3
ZBTB7C	Zinc finger and BTB domain containing protein 7C
EIF4EBP2	Eukaryotic translation initiation factor 4E binding protein 2
Down-regulated genes	
HOXA5	Homeobox A5
HOXA9	Homeobox A9
ZNF256	Zinc finger protein 256
NOTCH1	Neurogenic locus notch homolog protein 1
SIX4	SIX homeobox 4
CEBPz	CCAAT/enhancer binding protein zeta (CEBPZ)
SMAD5	SMAD family member 5
Signaling molecules	
Up-regulated genes	
S100A8	S100 calcium binding protein A8 (Calgranulin A)
S100A7	S100 calcium binding protein A7
IL1F10	Interleukin 1 family, member 10 (theta)
S100A9	S100 calcium binding protein A9 (Calgranulin B)
KLK9	Kallikrein-related peptidase 9
ELF5	E74-like factor 5 (ets domain transcription factor)
WNT11	Wingless-type MMTV integration site family, member 11
IL1RN	Interleukin 1 receptor antagonist
BMP2	Bone morphogenetic protein 2
EGF	Epidermal growth factor
Down-regulated genes	
PRPH	Peripherin
UCN	Urocortin
RNA Binding Proteins	
Up-regulated genes	
CPEB4	Cytoplasmic polyadenylation element binding protein 4
RPL3L	Ribosomal protein large 3-like
HFM1	HFM1, ATP-dependent DNA helicase homolog
Down-regulated genes	
RSL11B	Ras like family 11 member B
WDR21A	WD repeat domain 21A
EIF2S2	Eukaryotic translation initiation factor 2, subunit 2
RBM12B	RNA binding motif protein 12B
WDR36	WD repeat domain 36

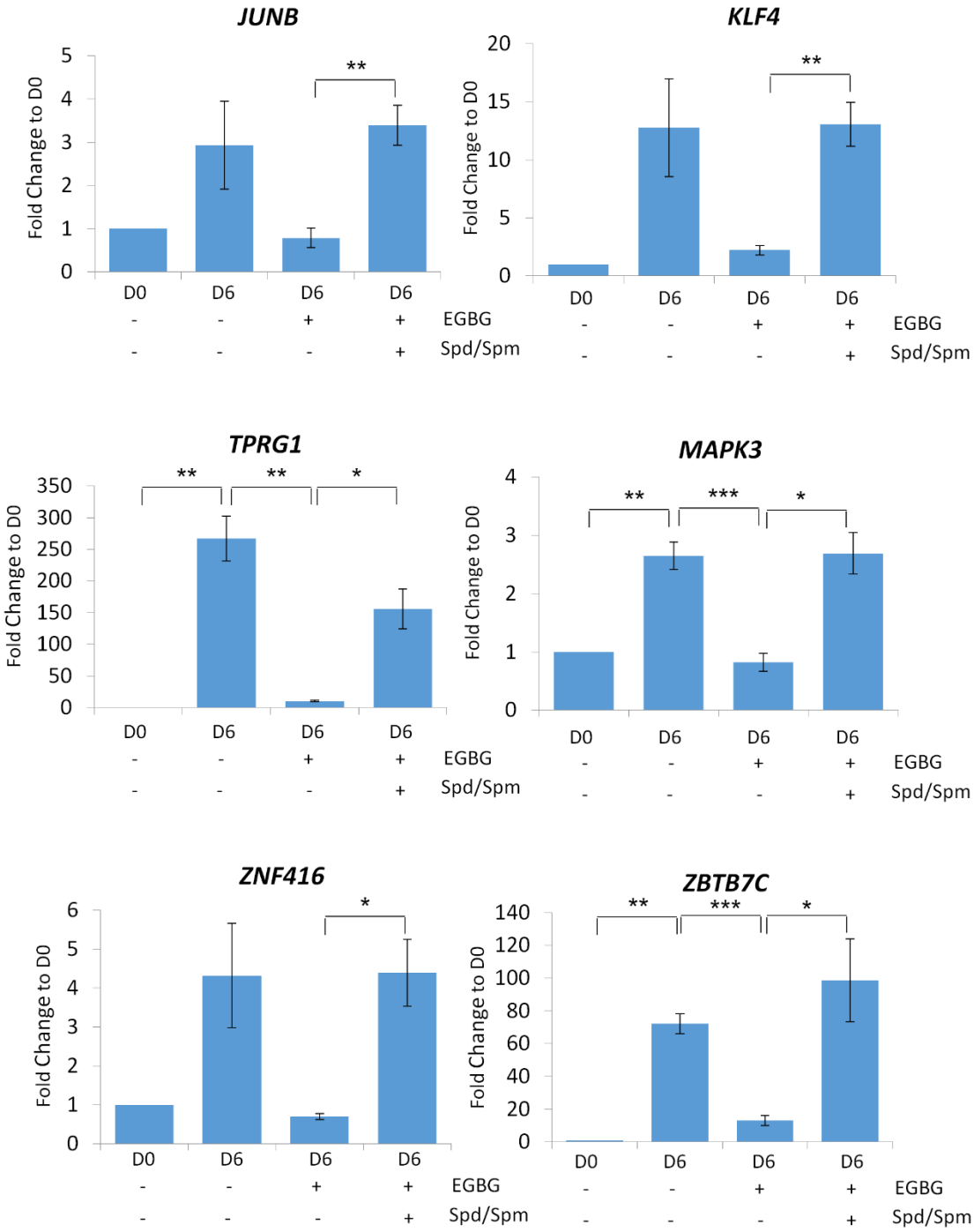

Figure 51.1: Microarray validation of differentially expressed AMD1-sensitive genes. qRT-PCR validation of selected transcription factors that are up-regulated during keratinocyte differentiation, down-regulated upon AMD1 inhibition and rescued by the addition of 1mM Spd/Spm. Genes were normalized to house-keeping gene, *RPL13A*. Results were represented as ±S.E.M. of four independent biological replicates and p values of <0.05 *, <0.01 ** and <0.001 *** were considered as statistically significant.

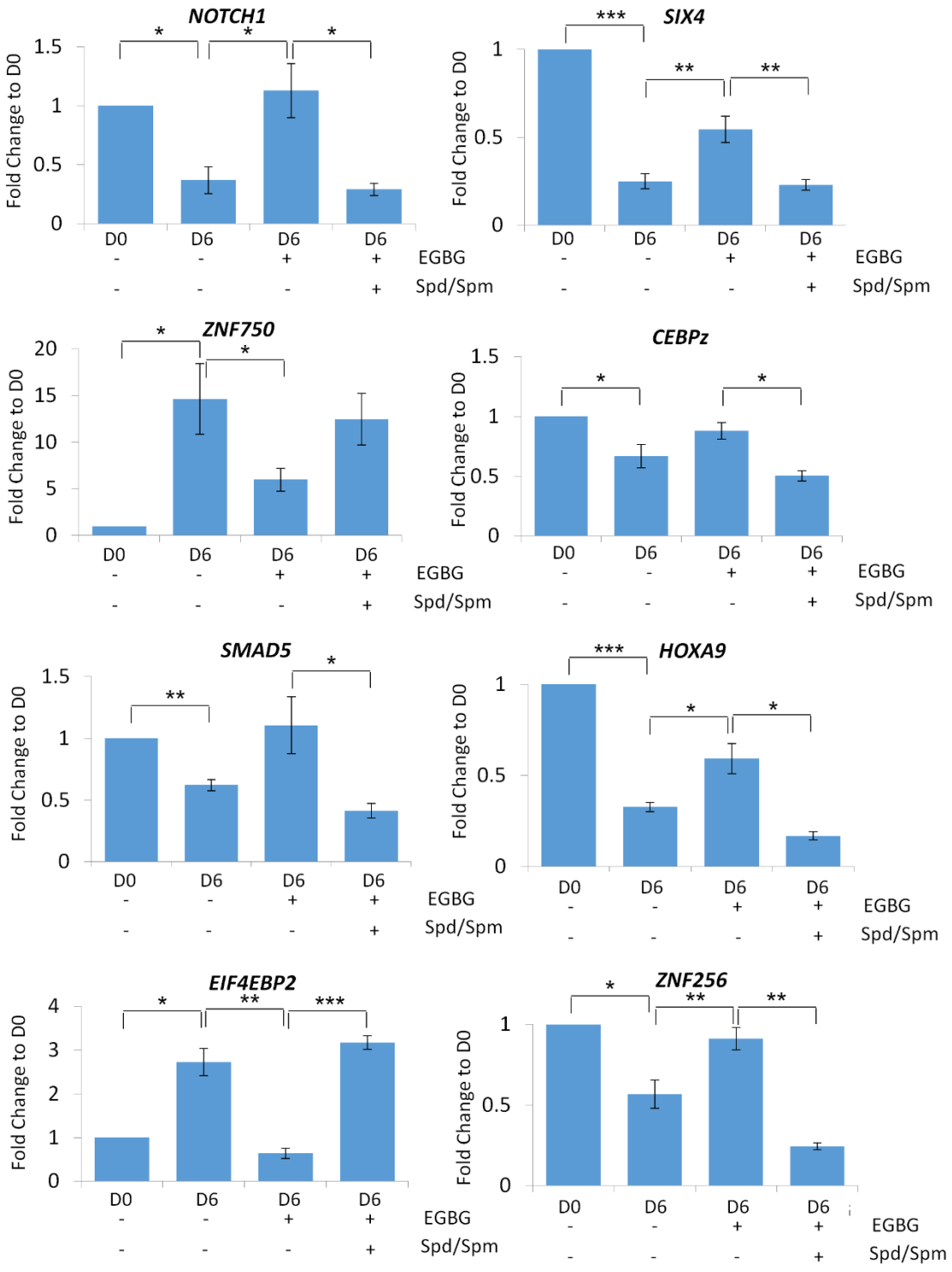

Figure 51.2: Microarray validation of differentially expressed AMD1-sensitive genes. qRT-PCR validation of selected transcription factors that are up/down-regulated during keratinocyte differentiation, down/up-regulated upon AMD1 inhibition and rescued by the addition of 1mM Spd/Spm. Genes were normalized to house-keeping gene, *RPL13A*. Results were represented as ±S.E.M. of four independent biological replicates and p values of <0.05 *, <0.01 ** and <0.001 *** were considered as statistically significant.

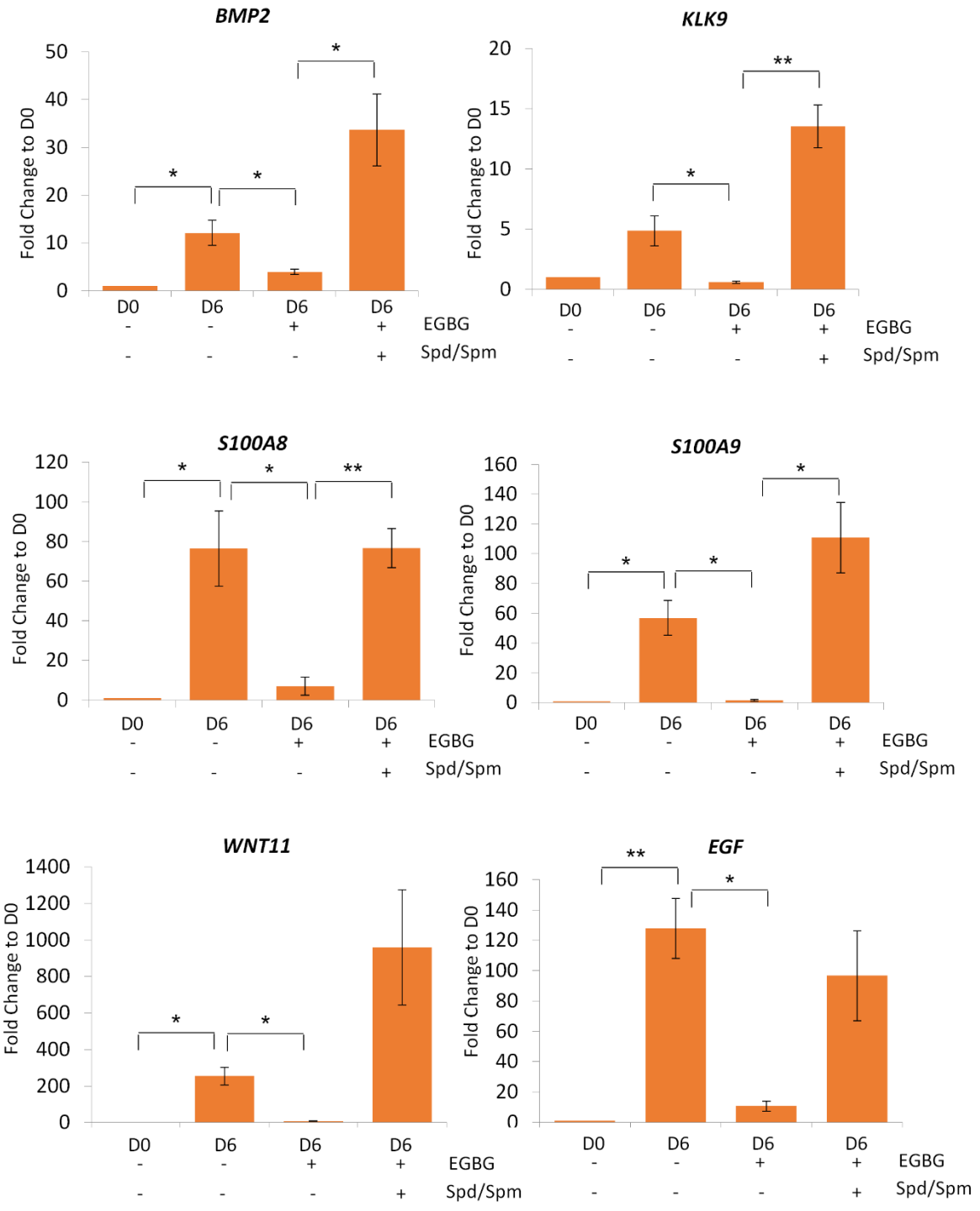

Figure 51.3: Microarray validation of differentially expressed AMD1-sensitive genes. qRT-PCR validation of selected signaling molecules that are up-regulated during keratinocyte differentiation, down-regulated upon AMD1 inhibition and rescued by the addition of 1mM Spd/Spm. Genes were normalized to house-keeping gene, *RPL13A*. Results were represented as ±S.E.M. of four independent biological replicates and p values of <0.05 *, <0.01 ** and <0.001 *** were considered as statistically significant.

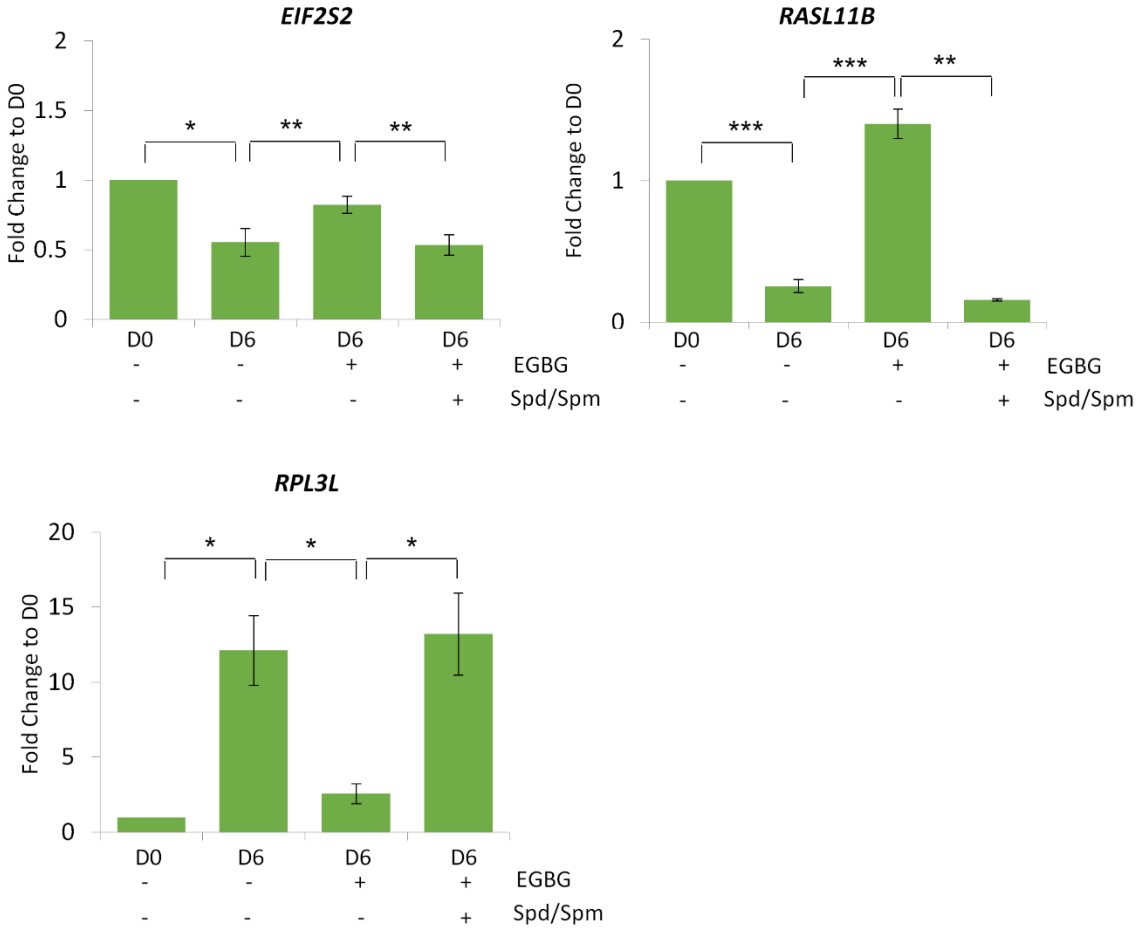

Figure 51.4: Microarray validation of differentially expressed AMD1-sensitive genes. qRT-PCR validation of selected RNA-binding proteins that are up/down-regulated during keratinocyte differentiation, down/up-regulated upon AMD1 inhibition and rescued by the addition of 1mM Spd/Spm. Genes were normalized to house-keeping gene, *RPL13A*. Results were represented as ±S.E.M. of four independent biological replicates and p values of <0.05 *, <0.01 ** and <0.001 *** were considered as statistically significant.

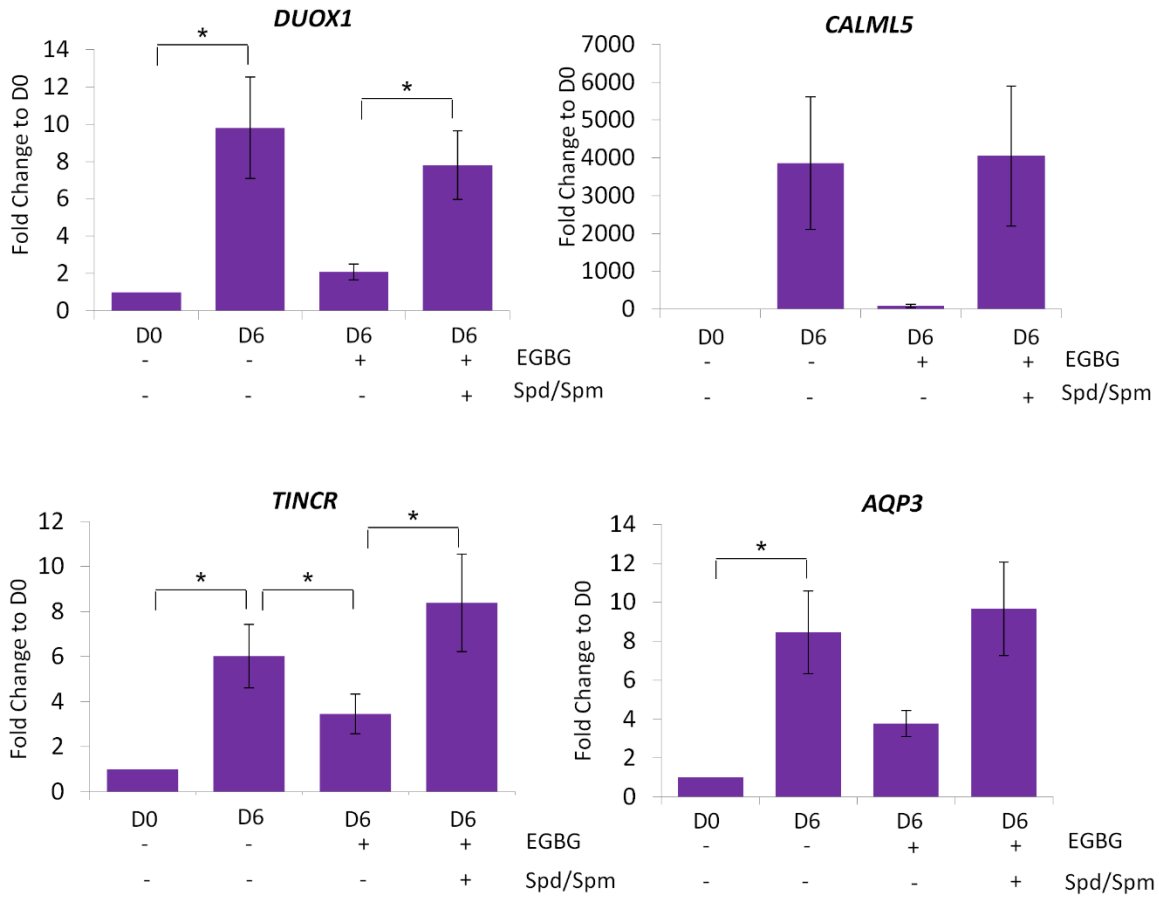

Figure 51.5: Microarray validation of differentially expressed AMD1-sensitive genes. qRT-PCR validation of AMD1 sensitive genes that are known targets of keratinocyte differentiation. Genes were normalized to house-keeping gene, *RPL13A*. Results were represented as ±S.E.M. of four independent biological replicates and p values of <0.05 *, <0.01 ** and <0.001 *** were considered as statistically significant.

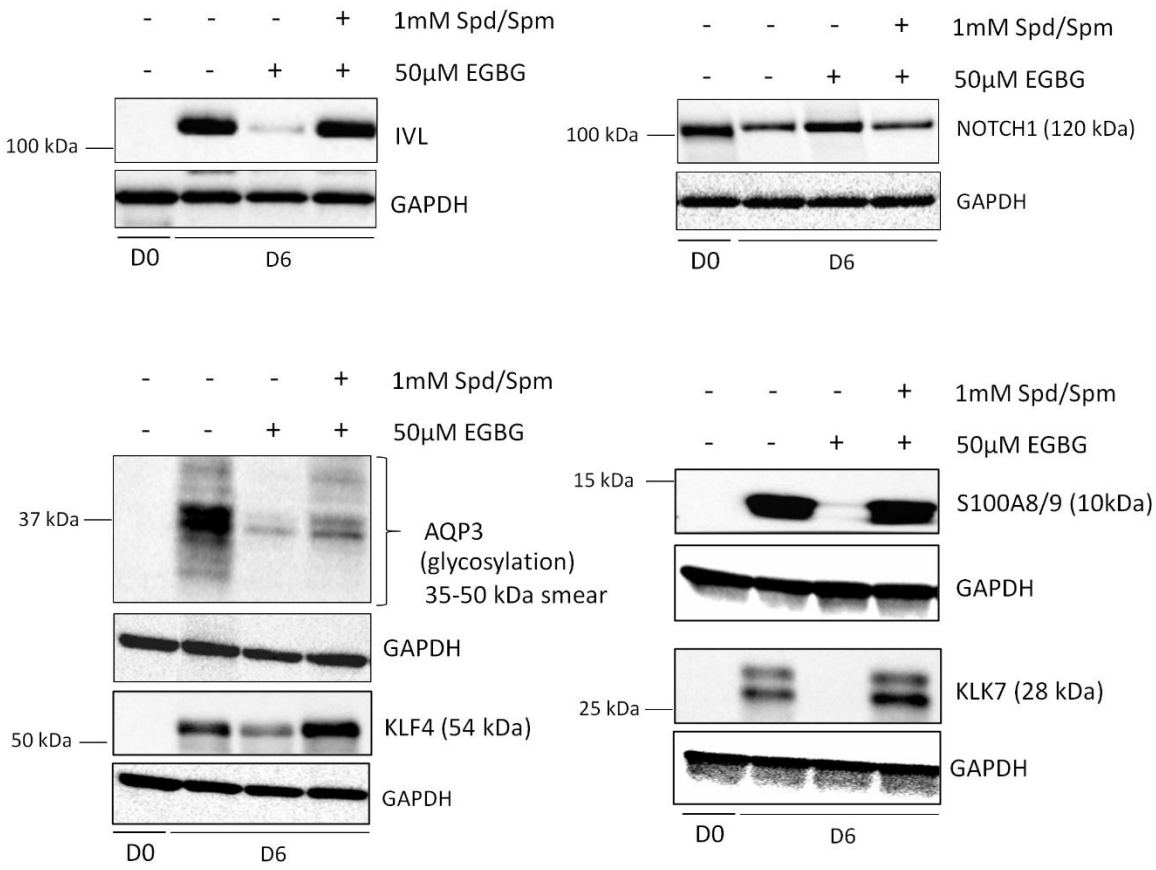

Figure 52: Microarray validation of differentially expressed AMD1-sensitive genes by immunoblotting. Immunoblot validation of NOTCH1, AQP3, KLF4, S100A8/9 and KLK7 that are known targets of keratinocyte differentiation. IVL protein expression was used to determine efficient keratinocyte differentiation. GAPDH was used as a loading control.

3.15 CPEB4 is a target of AMD1 and is a novel marker of keratinocyte differentiation.

Among the potential RNA-binding proteins that displayed at least 3-fold changes in response to AMD1 inhibition and rescue by the addition of Spd/Spm, I identified cytoplasmic polyadenylation element binding protein 4 (CPEB4), an RNA-binding protein which showed a significant 18-fold up-regulation at D6 of keratinocyte differentiation compared to D0 undifferentiated keratinocytes (**Figure 53A**). *CPEB4* mRNA levels significantly decreased by 9-fold upon AMD1 inhibition and increased by 13.5-fold in response to Spd/Spm rescue as compared to D0 undifferentiated keratinocytes (**Figure 53A**). CPEB4 protein expression validated the changes in mRNA observed by qRT-PCR (**Figure 53B**). I then performed immunofluorescence to determine the localization of CPEB4 in human abdominal skin sections. CPEB4 (green) displayed a distinct stratum granulosum localization under a 40X microscopic magnification (**Figure 54A**). A further 100X magnification obtained using confocal imaging revealed CPEB4 staining as a single foci at the periphery of the nuclei, suggesting a potential centrosomal localization of CPEB4 in basal and suprabasal keratinocytes (**Figure 54B**). My data suggests that CPEB4 is a downstream target of AMD1 and it switches its localization potentially from the centrosome to the granular layer of the epidermis during keratinocyte differentiation.

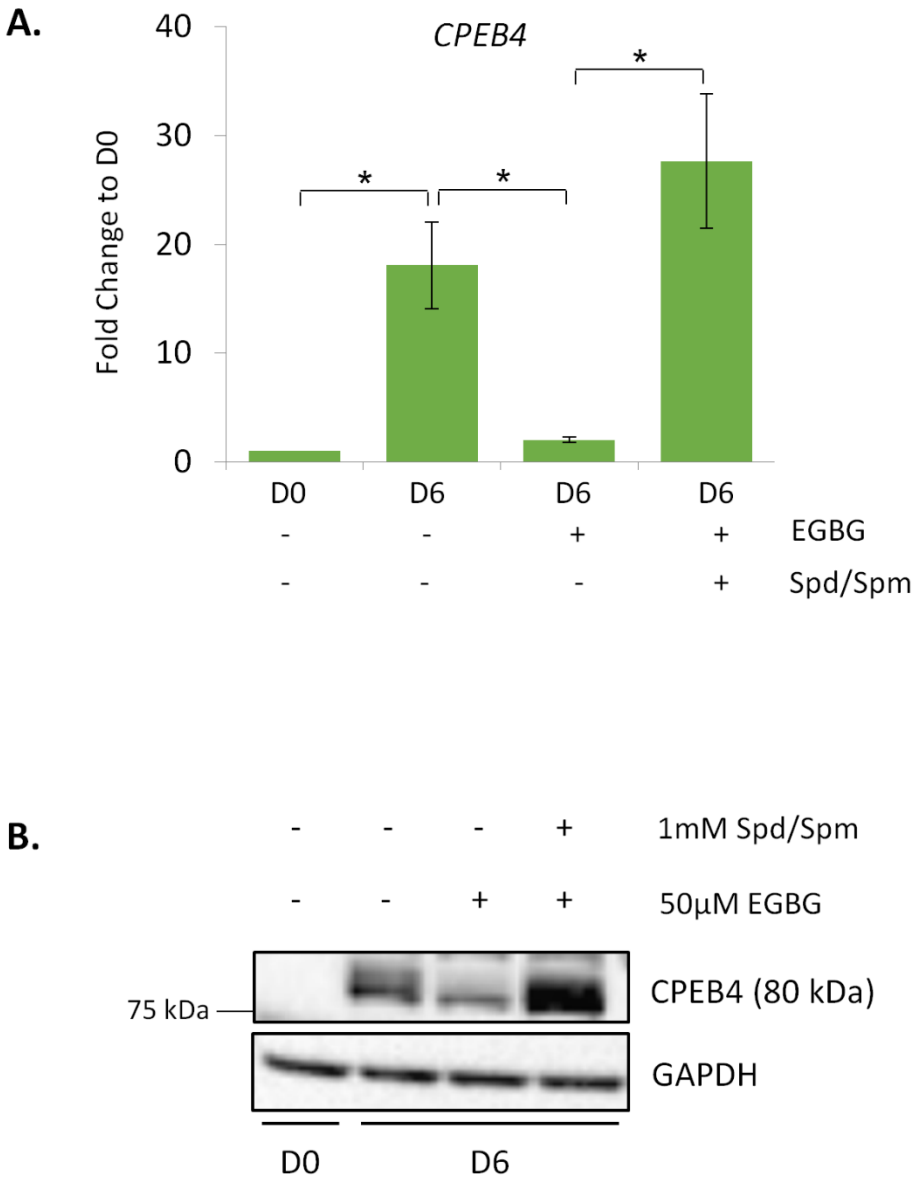

Figure 53: CPEB4 is downstream of AMD1. A. *CPEB4* mRNA expression is up-regulated during keratinocyte differentiation, down-regulated with AMD1 inhibition and is rescued by the addition of 1mM Spd/Spm in combination. Gene was normalized to house-keeping gene, *RPL13A*. Results were represented as ±S.E.M. of four independent biological replicates and p values of <0.05 *, <0.01 ** and <0.001 *** were considered as statistically significant. **B.** CPEB4 protein expression is up-regulated during keratinocyte differentiation, down-regulated with AMD1 inhibition and is rescued by the addition of 1mM Spd/Spm in combination. GAPDH was used as a loading control.

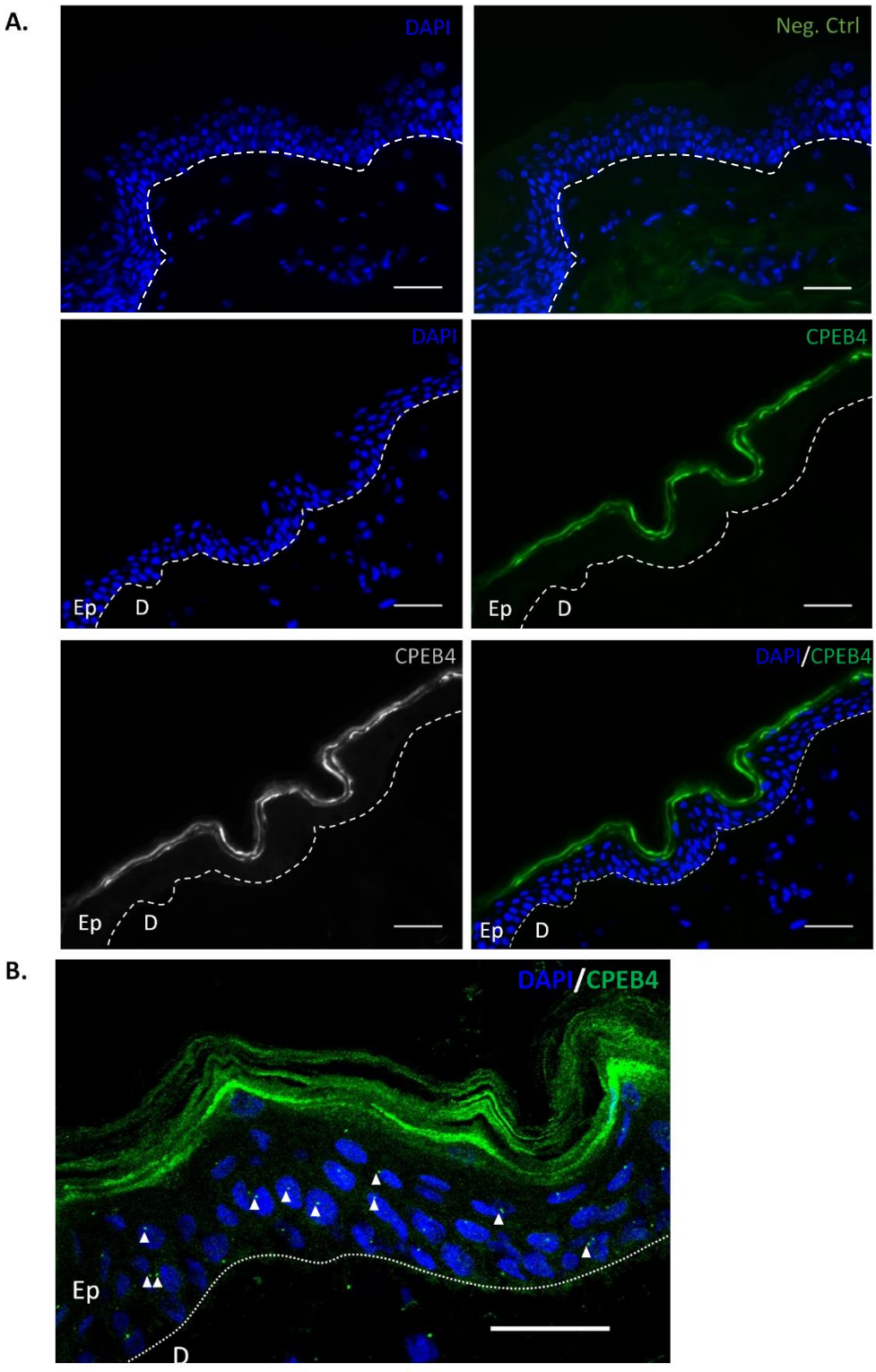

Figure 54: CPEB4 is expressed in the human skin. A. CPEB4 (green) is expressed in the stratum granulosum of the epidermis. DAPI is used to stain the nuclei. Dotted line represents the basement membrane; Ep=Epidermis; D=Dermis, scale bar=50μm **B.** Confocal image showing centrosomal-like expression of CPEB4 as indicated with white arrowheads; DAPI is used to stain the nuclei. Dotted line represents the basement membrane; Ep=Epidermis; D=Dermis, scale bar=20μm. Skin biopsy was obtained from the abdomen of a Chinese, female aged, 64.

3.16 AMD1 protein expression is higher in adult compared to juvenile skin sections.

Polyamines promote longevity in several model organisms and are known to decrease continuously with age, with the exception of high levels of polyamines reported in centenarians (Pucciarelli, Moreschini et al. 2012). Hence, we wanted to compare the AMD1 protein expression between juvenile and adult skin. Immunofluorescence was performed using three foreskin sections obtained from juvenile patients ranging between 6-12 years of age and three abdominal skin sections from adult patients between 40-60 years of age. The integrity of the epidermis was determined by K10 expression in green (**Figure 55.1 and 55.2**).

In the adult abdominal skin sections, AMD1 was highly expressed in the suprabasal layers of the epidermis (**Figure 55.1**), similar to our previous observations (**Figure 35A and B**). However, in comparison to the adult skin, AMD1 protein expression was low to negligible in the differentiated layers of the epidermis in the majority of the juvenile foreskins (**Figure 55.2**). This data suggests that there are differences in AMD1 expression between young and adult skin, though differences in gender, ethnicity and body site many have an influence on AMD1 expression.

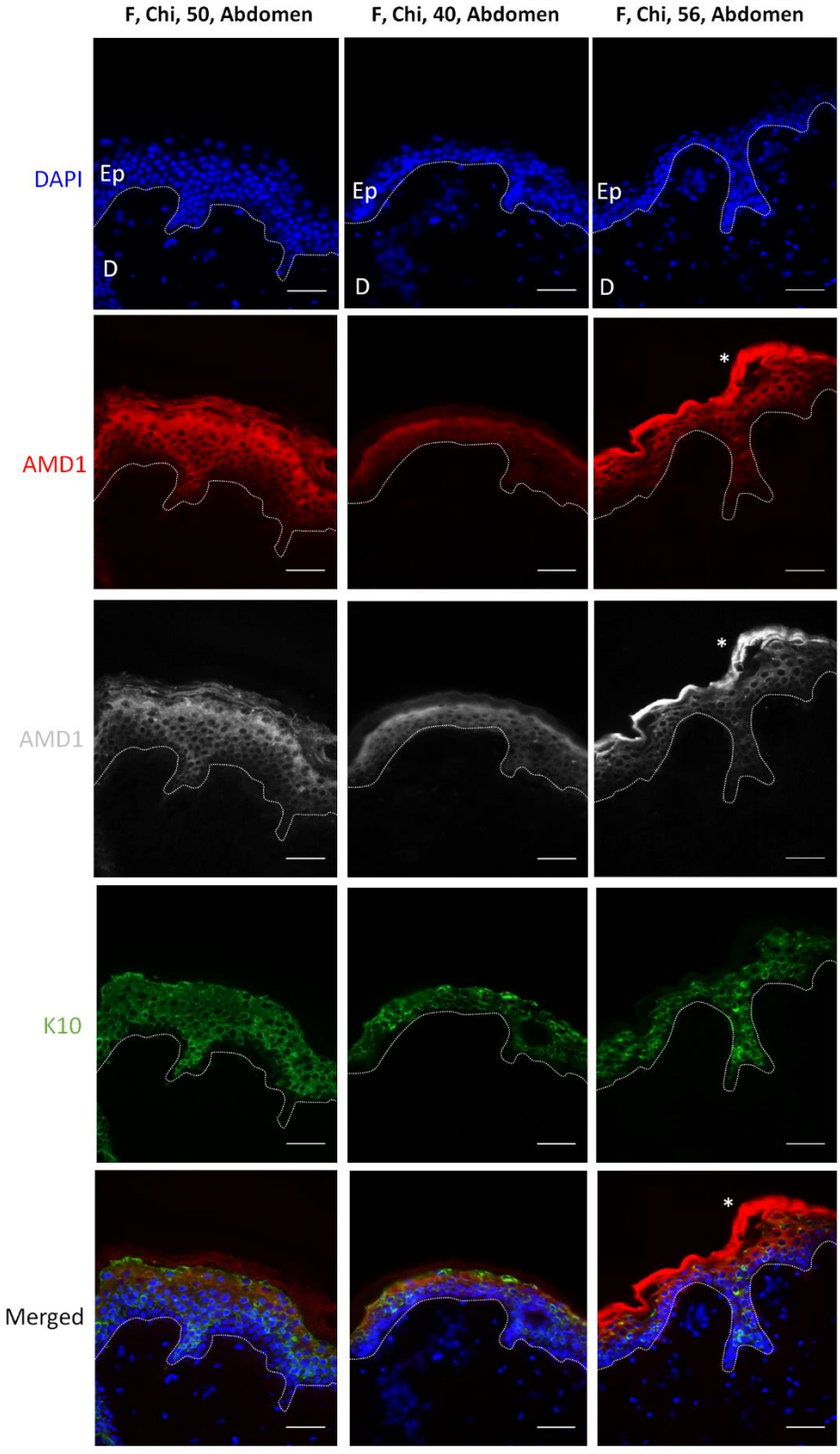

Figure 55.1: Comparison of AMD1 expression in adult and juvenile skin sections. AMD1 (red) shows high expression in the suprabasal layers of the human epidermis of adult abdominal skin between 40-60 years of age. In some cases, AMD1 was particularly enriched in the stratum granulosum. K10 is used to determine the integrity of the epidermis. DAPI is used to stain the nuclei. *Asterisk represents non-specific stratum corneum staining. Ep=Epidermis; D=Dermis; F=Female; Chi=Chinese. Dotted lines represent the basement membrane, scale bar=50μm.

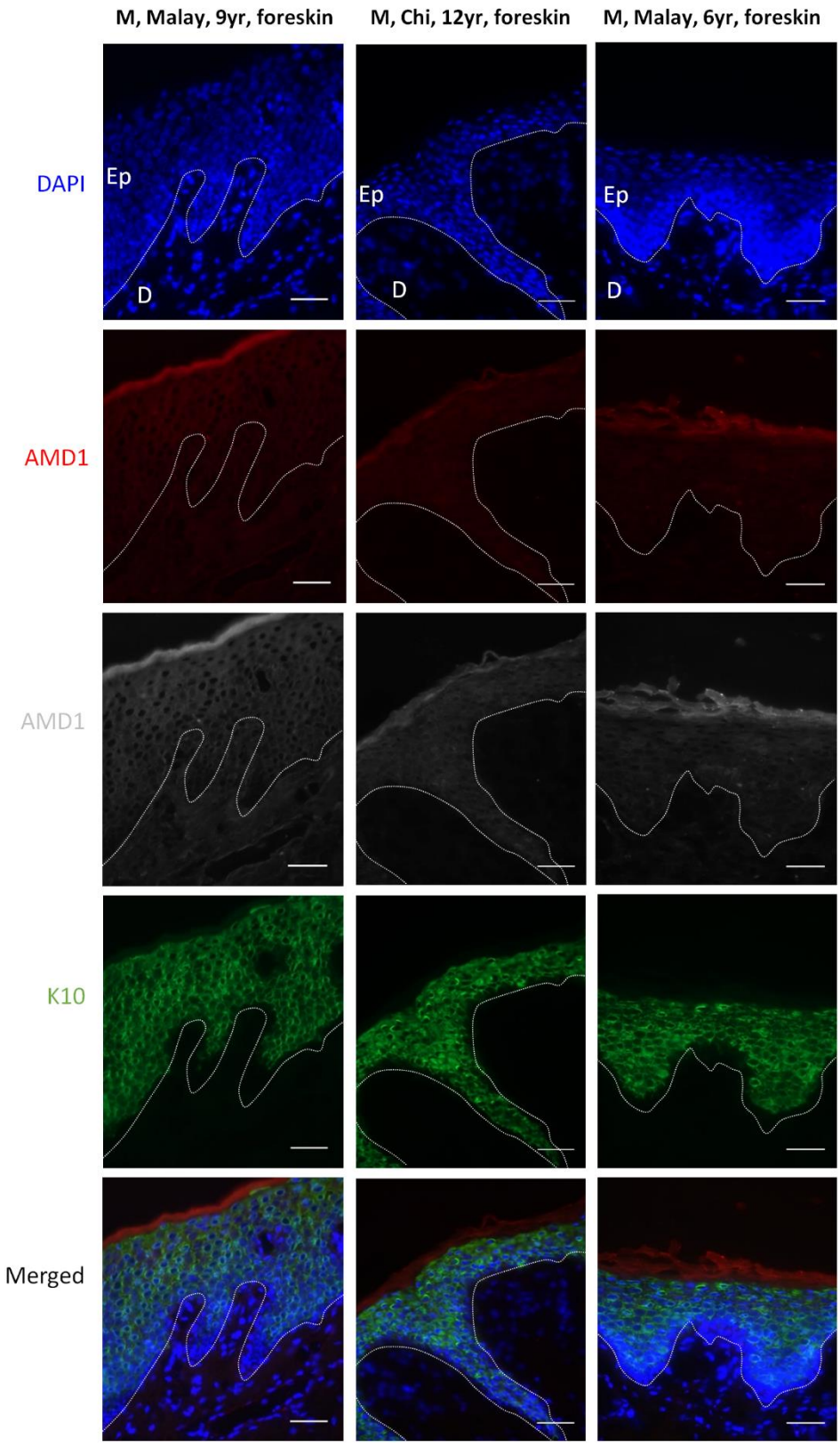

Figure 55.2: Comparison of AMD1 expression in adult and juvenile skin sections. AMD1 (red) shows low to negligible expression in the suprabasal layers of the human epidermis of juvenile foreskin between 6-12 years of age. K10 is used to determine the integrity of the epidermis. DAPI is used to stain the nuclei. Ep=Epidermis; D=Dermis; M=Male; Chi=Chinese. Dotted lines represent the basement membrane, scale bar=50μm.

3.17 Polyamine transporters are differentially expressed during keratinocyte differentiation.

While polyamine levels are tightly regulated through anabolic and catabolic enzymes, polyamine transporters also play a crucial role in maintaining the physiological levels of polyamines within the cell (Miller-Fleming and Olin-Sandoval 2015). I determined the protein expression of three polyamine transporters SLC12A8, caveolin-1 and ATP13A3 during keratinocyte differentiation. SLC12A8 is a solute carrier which is expressed ubiquitously at low levels in the human skin (Hewett, Samuelsson et al. 2002). A significant and gradual down-regulation of SLC12A8 was observed during keratinocyte differentiation (**Figure 56A, B**). In N/TERT-1 keratinocytes, the expression of caveolin-1 remained unchanged upon keratinocyte differentiation (**Figure 56, B**).

ATP13A3 is a cation transporter that is known to export polyamines out of the cell (Madan, Patel et al. 2016). The protein expression of ATP13A3 increases during calcium-induced keratinocyte differentiation, while it peaks at D2, its expression gradually decreases at D4 and D6 of differentiation (**Figure 56A**). The increase in ATP13A3 protein expression at D2 and the decrease in D6 was significant (**Figure 56B**). The change in protein expression of polyamine transporters suggests that they may have a role in regulating polyamine levels during keratinocyte differentiation.

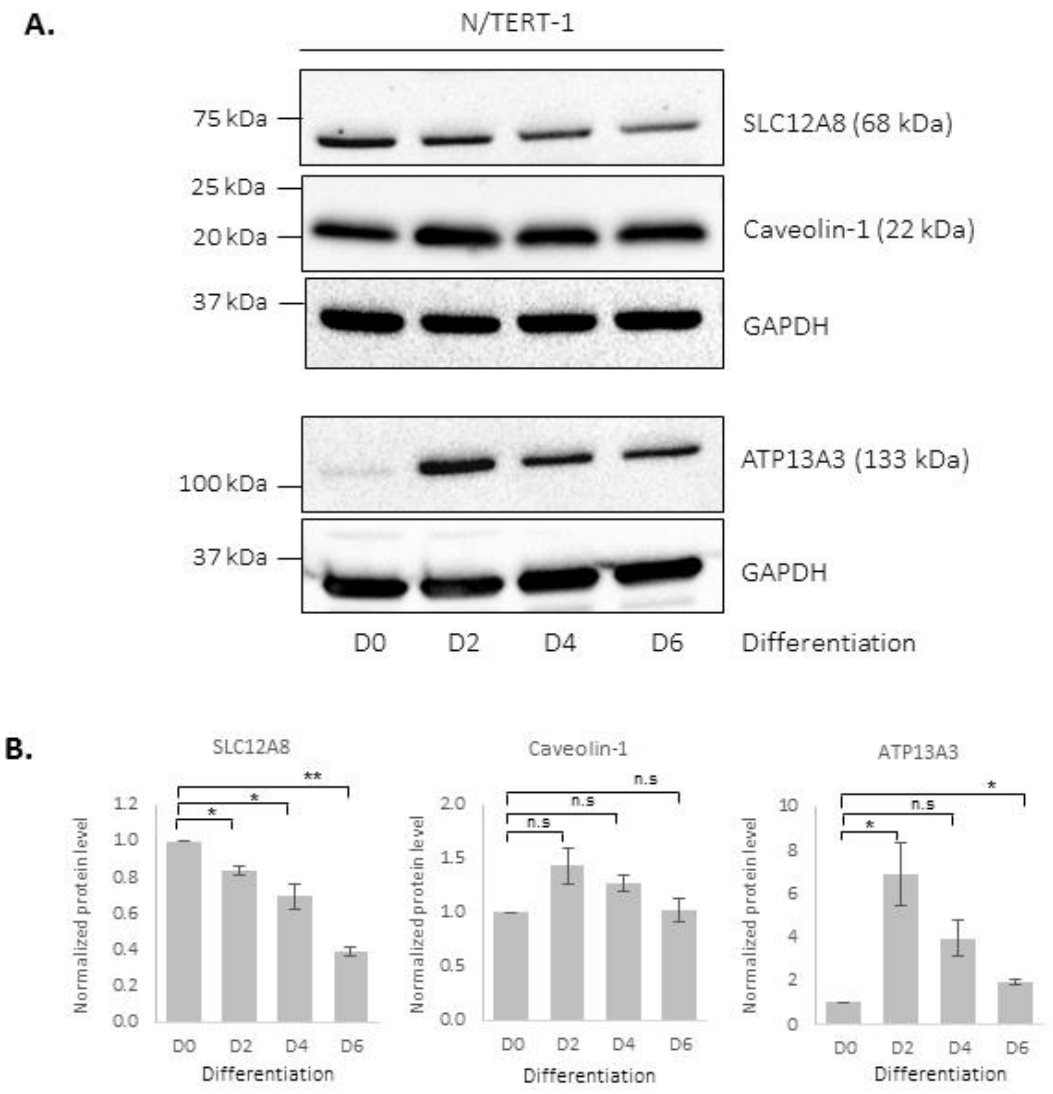

Figure 56: Polyamine transporters are differentially expressed during keratinocyte differentiation. A. Protein expression of transporter, SLC12A8 is down-regulated upon keratinocyte differentiation. Caveolin-1 protein expression remains unchanged during keratinocyte differentiation. ATP13A3 protein expression increases and peaks at D2 but decreases at D4 and D6 of keratinocyte differentiation. GAPDH was used as a loading control. **B.** Normalized protein levels are represented for SLC12A8, Caveolin-1 and ATP13A3 respectively. Results were represented as ±S.E.M. of three independent biological replicates and p values of <0.05 *, <0.01 ** and <0.001 *** were considered as statistically significant while n.s. represents a non-significant p value.

3.18 Identification of SPD/SPM-conjugated protein

Polyamines present in mammalian tissues can be cross-linked to proteins as a post-translational protein modification (Piacentini, Farrace et al. 1990). To identify polyamine conjugated proteins, I performed immunoblotting on D0 undifferentiated and D6 differentiated keratinocytes without or with EGBG and EGBG+Spd/Spm treatment, then probed these membranes independently with anti-SPD and anti-SPM antibody. I detected a predominant 15-kDa band that was up-regulated upon keratinocyte differentiation but down-regulated upon AMD1 inhibition using EGBG and rescued by the addition of 1mM Spd/Spm in combination (**Figure 57A**).

An extensively studied post-translational modification involving polyamines, is the formation of an unusual amino acid hypusine from Spd. To date, eukaryotic translation initiation factor 5A (eIF5A) is the only cellular protein that contains a hypusine modification which is essential for the translation of mRNAs containing poly-proline rich sequences (Park and Nishimura 2009). The polyamine Spd present on a specific lysine residue on eIF5A is cleaved by a two-step enzymatic reaction to generate hypusine-conjugated mature eIF5A (Clement, Johansson et al. 2006).

In order to determine whether this unidentified band is hypusinated-eIF5A, I probed D0 undifferentiated and D6 differentiated keratinocytes with an anti-hypusine antibody. No change in hypusine-conjugated eIF5A was observed upon keratinocyte differentiation (**Figure 57B**). There was no change in eIF5A hypusination, upon AMD1 inhibition with EGBG or when inhibition was rescued with the addition of 1mM Spd/Spm (**Figure 57B**), suggesting that the unidentified Spd/Spm-conjugated protein is not hypusinated-eIF5A. Total eIF5A remained unchanged in D0 undifferentiated and D6 differentiated keratinocytes (**Figure 57B**). The protein band for total-eIF5A and hypusinated-eIF5A runs slightly higher than the unidentified ~15kDa protein. eIF5A2 is an isoform of the eIF5A family and has been reported to promote tumour growth and cancer progression (Clement, Johansson et al. 2006). eIF5A2 protein expression was high in D0 undifferentiated keratinocytes and decreased upon keratinocyte differentiation (**Figure 57C**).

eIF5A2 protein expression remained low when AMD1 was inhibited and its expression was rescued by the addition of Spd/Spm. Given this, the banding pattern of eIF5A2 was unlikely the unidentified ~15-kDa SPD/SPM-conjugated protein.

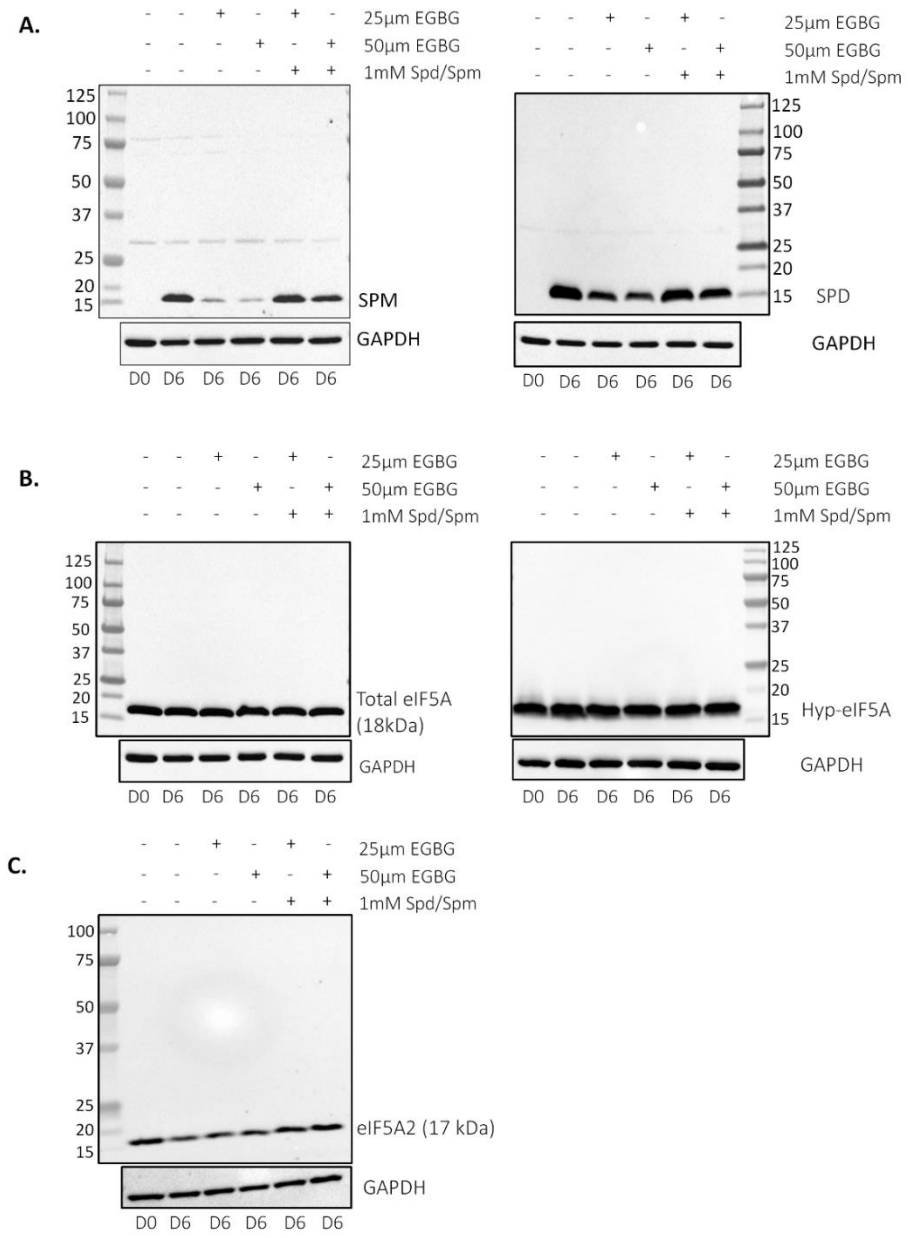

Figure 57: Identification of a Spd/Spm conjugated protein at approximately 15 kDa. A. Immunoblot showing a predominant 15 kDa protein band that is expressed during keratinocyte differentiation, down-regulated with AMD1 inhibition and rescued by the addition of Spd/Spm when probed with either anti-SPM or anti-SPD antibody. **B.** The unidentified 15 kDa protein band does not resemble total eIF5A or hypusinated-eIF5A (Hyp-eIF5A) which remain unchanged during keratinocyte differentiation or when AMD1 was inhibited. **C.** The unidentified 15 kDa protein band is not eIF5A2 which is highly expressed in D0 undifferentiated keratinocytes and down-regulated upon differentiation showing no effects with AMD1 inhibition. GAPDH was used as a loading control.

CHAPTER 4

DISCUSSION

An effective skin barrier is formed by the sustained presence of progenitor keratinocytes in the stratum basale and the ability of a portion of keratinocytes to asymmetrically divide, giving rise to a differentiated stratified epidermis. The commitment to terminal differentiation involves the precise expression of genes as the non-mitotic keratinocytes transition through each stratified layer of the epidermis. Several mechanisms are instrumental in fine-tuning the balance between keratinocyte proliferation and differentiation, and that includes epigenetic gene regulation, transcriptional regulation, cell signalling cues and cell-to-cell interaction (Lechler and Fuchs 2005, Blanpain and Fuchs 2009). Mis-expression of genes in these regulatory networks dysregulate this balance, leading to the pathogenesis of skin disorders and diseases. Polyamines are ubiquitous polycations involved in a wide array of cellular function, that incudes cellular growth, proliferation and differentiation (Wallace 2009, Miller-Fleming and Olin-Sandoval 2015, Pegg 2016). While their tight regulation is mandatory to drive essential cellular functions, high levels of polyamines and a dysregulation of polyamine regulators have been reported in skin cancers and neoplastic growth (Gilmour 2007). Genetic manipulation of polyamine regulators has been commonly used in mouse models to determine their role in tumour promotion (Nowotarski, Feith et al. 2015). This has paved ways for the development of pharmacological inhibitors targeting polyamine metabolism, as a promising cancer therapy for individuals with non-melanoma skin cancers (NMSC) (Nowotarski, Woster et al. 2013). Extensive research has been done on modulating polyamine regulators during cancer. The role of polyamine regulators under normal homeostasis was illustrated by a SAT1 overexpression in Tg mice which resulted in perturbed epidermal differentiation (Pietilä, Pirinen et al. 2005). With these evidence illustrating the importance of the tight regulation of polyamines and their regulators, it stimulated our interest to uncover the role of polyamines and its anabolic regulators under normal skin homeostasis and determine the pathways regulated by polyamines during epidermal differentiation.

My dissertation is focused on the function of polyamine anabolic enzyme, AMD1 and its role in regulating polyamine levels to drive keratinocyte differentiation. Here, I have shown that, AMD1 protein is expressed in the suprabasal layers of the human epidermis and is up-regulated during keratinocyte differentiation *in vitro*. Lentiviral knockdown of AMD1 or AMD1 inhibition using a specific inhibitor, EGBG, reduced the expression of differentiation-related genes in monolayer keratinocyte cultures and organotypic skin equivalents. Impaired keratinocyte differentiation was rescued by the supplementation of Spd and Spm, suggesting that AMD1 is necessary for keratinocyte differentiation. By measuring polyamine levels in D0 undifferentiated and D6 differentiated keratinocytes, I have shown that there is a shift in polyamine ratios such that there is low levels of Put but high levels of Spm and possibly Spd during differentiation. My data suggests that Put levels are high and Spd/Spm levels are low in the basal layer of the epidermis (**Figure 58**). This inverse polyamine gradient is indispensable for efficient keratinocyte differentiation and either knockdown or inhibition of AMD1 activity disrupts this polyamine shift resulting in aberrant keratinocyte differentiation (**Figure 58**).

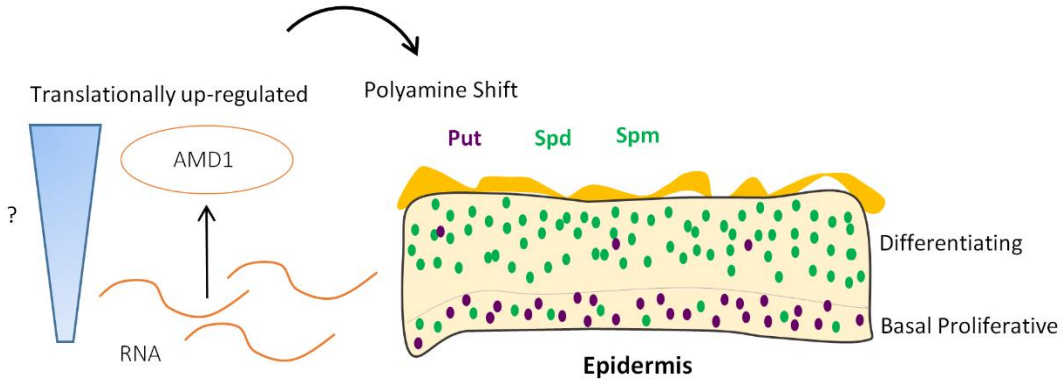

Figure 58: AMD1 regulation in the human epidermis. AMD1 is translationally up-regulated in the epidermis and this drives the shift in polyamines such that there is low levels of Put and high levels of Spd/Spm in the suprabasal layers of the epidermis.

Following this, I dissected the gene regulatory networks that were controlled by AMD1 and found key transcription factors, including JUNB, KLF4, ZNF750, and NOTCH1 that have been previously described to drive keratinocyte differentiation (**Figure 59**) (Mehic, Bakiri et al. 2005, Cohen, Birnbaum et al. 2012, Sen, Boxer et al. 2012). Additionally, I discovered CPEB4, an RNA

binding protein, as a novel marker of keratinocyte differentiation that was downstream of AMD1 (**Figure 59**). While AMD1 was highly expressed in the differentiated layers of epidermis in adults, its expression was markedly reduced in juvenile foreskin shedding light into the role of polyamines and its regulators during aging.

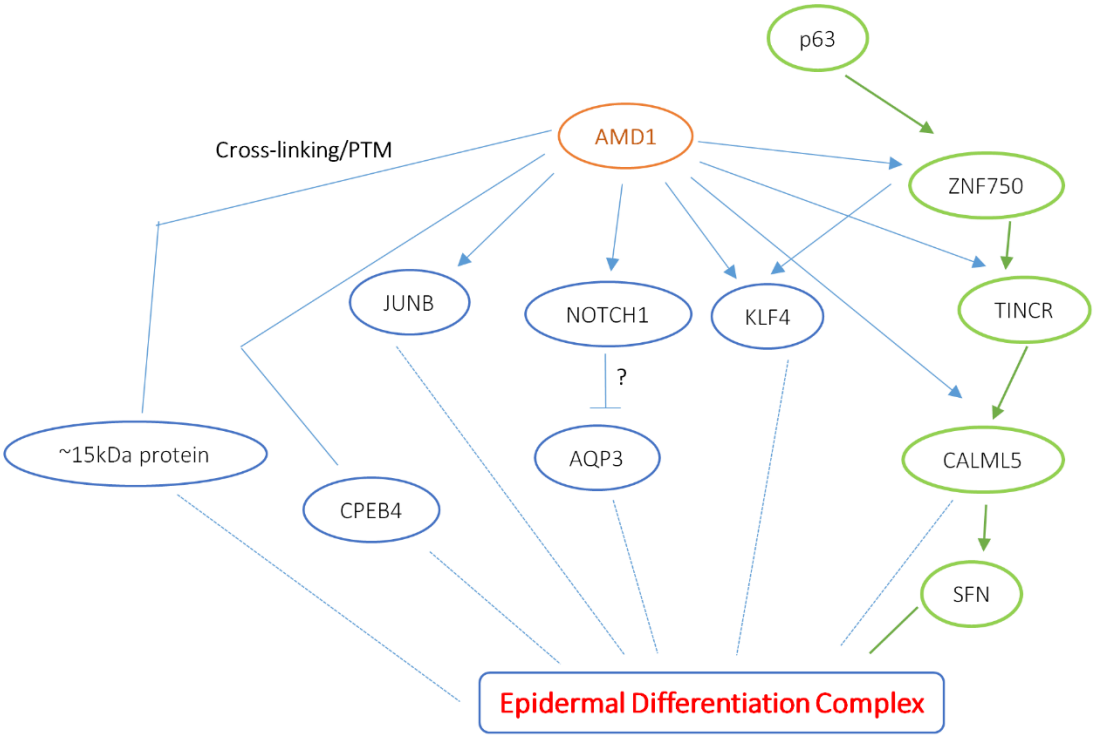

Figure 59: AMD1 as an upstream regulator of keratinocyte differentiation. Hypothetical pathway showing AMD1 as an upstream regulator of key transcription factors that are known to drive keratinocyte differentiation. Pathway in green represents the gene regulatory network established by (Sun, Boxer et al. 2015). AMD1 is also involved in Spd/Spm crossing linking or post-translational modification (PTM).

4.1 Expression of anabolic enzyme, AMD1 in the human epidermis

AMD1 was highly expressed in the suprabasal layers of the adult epidermis similar to the expression of Spd/Spm. A comparative study between pure dermis and epidermis revealed significantly higher levels of Spd and Spm in the epidermis compared to the dermis. However, the differences in the levels may not be necessarily reflective of the intracellular levels of polyamines present in the two layers (El, Milano et al. 1983). This is because, the dermis comprises of primarily connective tissue, collagen and fibroblast cells while the majority of the epidermis consists of

keratinocytes (Blanpain and Fuchs 2009). Hence, there are relatively more abundant cells present per gram of dry epidermis compared to the dermis, which could account for the elevated levels of Spd and Spm in the epidermis. However, I have now confirmed that AMD1 is highly expressed in the suprabasal layers of the human epidermis in line with a high expression of Spd/Spm in the suprabasal layers. AMD1 staining in adult abdominal skin sections displayed variations, either gradually increasing in protein expression throughout the suprabasal layers of the epidermis or being particularly enriched in the granular layers of the epidermis. These variations in AMD1 protein expression could be influenced by variations among individuals in terms of ethnicity, age and the levels of polyamine uptake through consumption or intestinal absorption of polyamines (Larqué, Sabater-Molina et al. 2007, Wallace 2009, Pegg 2016). Despite these differences, there was a clear increase in expression on differentiation.

The increase in AMD1 protein expression during keratinocyte differentiation was also validated using HEKa cells and human immortalized N/TERT-1 keratinocytes. The mature form of AMD1 runs just below 37 kDa while the AMD1 proenzyme has been shown to run below 45 kDa (Zabala-Letona, Arruabarrena-Aristorena et al. 2017). While I observe the mature form of AMD1 and confirmed it by shRNA knockdown, the AMD1 proenzyme band was not detected. Mammalian AMD1 is usually synthesized as an inactive proenzyme which is subsequently cleaved into its two subunits very rapidly during maturation (Bale and Ealick 2010). Hence, it is possible that only the mature form of AMD1 is detected during keratinocyte differentiation.

4.2 Expression of polyamines in the human epidermis

I have shown that Spd/Spm expression was highly abundant in the suprabasal layers of the adult human epidermis as determined by commercially available antibodies. I used antibodies raised against Spd or Spm and while neither antibody reacts with Put, they both react with Spd and Spm so I cannot distinguish between them. No well-characterized antibody was available to detect Put expression in the human epidermis. Based on my polyamine measurements, I have shown that Put levels are higher in D0 undifferentiated keratinocytes compared to D6 differentiated keratinocytes.

Piacentini et al. have also reported that mouse epidermal cells treated with retinoic acid (RA), inhibits differentiation and promotes proliferation resulting in free Put levels to rise (Piacentini, Martinet et al. 1988). There are also evidence in the literature suggesting that polyamines especially Put promotes tumour growth. Treatment with DFMO, an ODC1 inhibitor blocks its activity, resulting in lesser Put and a reduction in skin tumours (Takigawa, Inoue et al. 1977, Smith, Trempus et al. 1998, Chen, Megosh et al. 2000, Lan, Hayes et al. 2005). Thus, I would expect Put to be high in keratinocytes predominantly at the SB that closely resemble D0 undifferentiated keratinocytes and gradually decrease in keratinocytes of the suprabasal layers.

While HPLC involves the extraction of polyamines from cells, desorption electrospray ionization-time of flight (DESI-TOF) enables the detection of polyamines in intact tissue sections. This method could be performed to confirm the spatial distribution of polyamines within a tissue (Kubo, Kajimura et al. 2012, Eberlin 2014).

4.3 Post-transcriptional control of AMD1 and ODC1 in the human epidermis

I have shown that AMD1 is translationally up-regulated during keratinocyte differentiation. However, it was not unusual that AMD1 and ODC1 mRNA and protein expression were not correlated during keratinocyte differentiation, as they are tightly regulated under normal physiological conditions to allow for quick adjustments when polyamine levels fluctuate. For instance, it is known that AMD1 is translationally regulated at the 5' UTR by a small uORF in human cells (Law, Raney et al. 2001, Raney, Law et al. 2002, Miller-Fleming and Olin-Sandoval 2015). The uORF encodes a peptide MAGDIS, that stalls the ribosome at its stop codon and prevents its access to the downstream ORF encoding AMD1, thereby reducing the synthesis of AMD1 protein when Spd/Spm levels are high (**Figure 16**) (Law, Raney et al. 2001, Raney, Law et al. 2002, Miller-Fleming and Olin-Sandoval 2015). Recently, a novel mechanism has been reported to limit the number of AMD1 proteins synthesized from a single AMD1 mRNA transcript. As a subset of ribosomes read through the first stop codon of the ORF, they stall at the next in-frame stop codon. Successive stalling of ribosomes results in a ribosomal queue as it extends until

the initial stop codon, hence as a consequence halts *AMD1* mRNA translation (**Figure 17**) (Yordanova, Loughran et al. 2018). While the former translational control occurs to maintain cellular polyamine levels, the latter mechanism was suggested to protect the cells from a dysregulated *AMD1* translation when a transcriptional error or mRNA damage occurs.

Since *AMD1* mRNA levels are unchanged while AMD1 protein expression is increased during keratinocyte differentiation, I propose that AMD1 is translationally regulated during keratinocyte differentiation. An alternative translational regulation mechanism for AMD1 is possible because our group has previously demonstrated that AMD1 protein expression is high in ESCs and it is translationally down-regulated during NPC differentiation by miR-762 (Zhang, Zhao et al. 2012). It is possible that additional *cis*-acting elements are present either at the 3' or 5' UTR of *AMD1* mRNA to increase the production of AMD1 protein in order to drive keratinocyte differentiation. To determine this, we would clone the 3' and 5' UTR of AMD1 individually and in combination into the PsiCheck2 vector under the control of a Renilla luciferase reporter gene. Normalization of Renilla luciferase to a control reporter gene, Firefly luciferase, and measuring overall changes in Renilla luciferase activity would give a read out of post-transcriptional control. If AMD1 is translationally up-regulated on differentiation, this would be seen by a relative increase in Renilla luciferase activity in differentiated cells. The *cis*-acting element within the 3' or 5' UTR of AMD1 responsible for the translational control would then be mapped by a series of UTR deletions.

In addition to a translational up-regulation, it is also possible that AMD1 protein is stabilized during D6 of keratinocyte differentiation. Similarly, it is also important to address the role of ODC1 during keratinocyte differentiation. Since ODC1 does not show a shift in ribosomal load on keratinocyte differentiation, it suggests that translation may not be regulated. It is possible that ODC1 protein is stabilized during differentiation. In order to determine whether AMD1 and ODC1 are stabilized during keratinocyte differentiation, D0 undifferentiated and D6 differentiated keratinocytes would be subjected to a time-course cycloheximide (chx) treatment, a drug that stall ribosomes on the

mRNA transcript and inhibit further translation. AMD1 or ODC1 protein expression would be compared between untreated and chx-treated keratinocytes at D0 and D6 of differentiation. If AMD1 or ODC1 protein is stabilized at D6, we would expect AMD1 or ODC1 protein expression to decrease rapidly with progressive chx treatment at D0 but remain unchanged at D6 of keratinocyte differentiation. The reason for a complex control over ODC1 protein levels is currently not clear but could be a consequence of the shifting regulation that accompanies differentiation and a shift from a proliferative to a post mitotic state.

4.4 Organotypic skin equivalents derived from shAMD1 knockdown keratinocytes

I have demonstrated that the stratification of organotypic skin equivalents was impaired when using AMD1 knockdown N/TERT-1 keratinocytes but was rescued by the supplementation of Spd/Spm in the media. Human primary keratinocytes are usually preferred over immortalized cell lines to generate organotypic skin equivalents as they more closely resemble cells in the native human skin (Reijnders, van Lier et al. 2015, Smits, Niehues et al. 2017). However, they are limited by their replicative potential and are proven to be challenging to perform transient gene knockdown studies with (Smits, Niehues et al. 2017). Thus, I generated in *vitro* organotypic skin models using stable shScrambled and shAMD1 knockdown N/TERT-1 keratinocytes to study the effect of AMD1 knockdown on keratinocyte stratification. While it was challenging to achieve highly reproducible organotypic skin equivalents using the commercially available CellnTEC kit, I managed to establish all four layers of the epidermis. It is relatively easy to achieve fully differentiated human skin equivalents (HSE) from only immortalized N/TERT-1 keratinocytes, using the CellnTEC organotypic cell culture system. This model however, does not completely recapitulate the human epidermis. The HSEs consisting of a dermal equivalent, reconstituted with collagen and fibroblasts underlying the epidermis would have been a better representation; however would take a longer time to completely stratify (Gangatirkar, Paquet-Fifield et al. 2007). I still need to validate the phenotype with HSEs that has a dermal component.

HSEs lacking dermal fibroblasts would exhibit a thinner epidermal equivalent possessing approximately 3-4 layers of keratinocytes (Sriram, Bigliardi et al. 2015). Reinstating a dermal fibroblast compartment would induce a thicker epidermis with approximately 5–8 layers, more closely resembling the human epidermis (Sriram, Bigliardi et al. 2015). Hence, the different epidermal layers would be more apparent. The presence of dermal fibroblasts would allow cross-talk between the fibroblast and keratinocytes, which is essential for the generation of a well-defined basement membrane (Miner and Yurchenco 2004, Mokkapati, Baranowsky et al. 2008, Breitkreutz, Koxholt et al. 2013). However, this would be less of a concern, since I am investigating the role of AMD1 in keratinocyte stratification. Besides staining the organotypic skin equivalents for differentiation markers, differentiation dynamics could be further assessed by determining the percentage of transepidermal water loss (TEWL) between shScrambled and shAMD1 knockdown keratinocytes, as a greater percentage of TEWL would be expected when the barrier function of the skin is impaired.

4.5 Shift in polyamine levels during keratinocyte differentiation

Polyamines can exist as either free, bound or conjugated forms within the cells **(Figure 60)** (Igarashi and Kashiwagi 2010, Igarashi and Kashiwagi 2015). While most polyamines form complexes with RNA, polyamines can also bind to DNA or remain unbound within the cell (Lightfoot and Hall 2014). Evidence of polyamine conjugation present in the cornified epidermal envelope has also been detailed in earlier studies but this field of research has been less explored (Piacentini, Martinet et al. 1988, Martinet, Beninati et al. 1990).

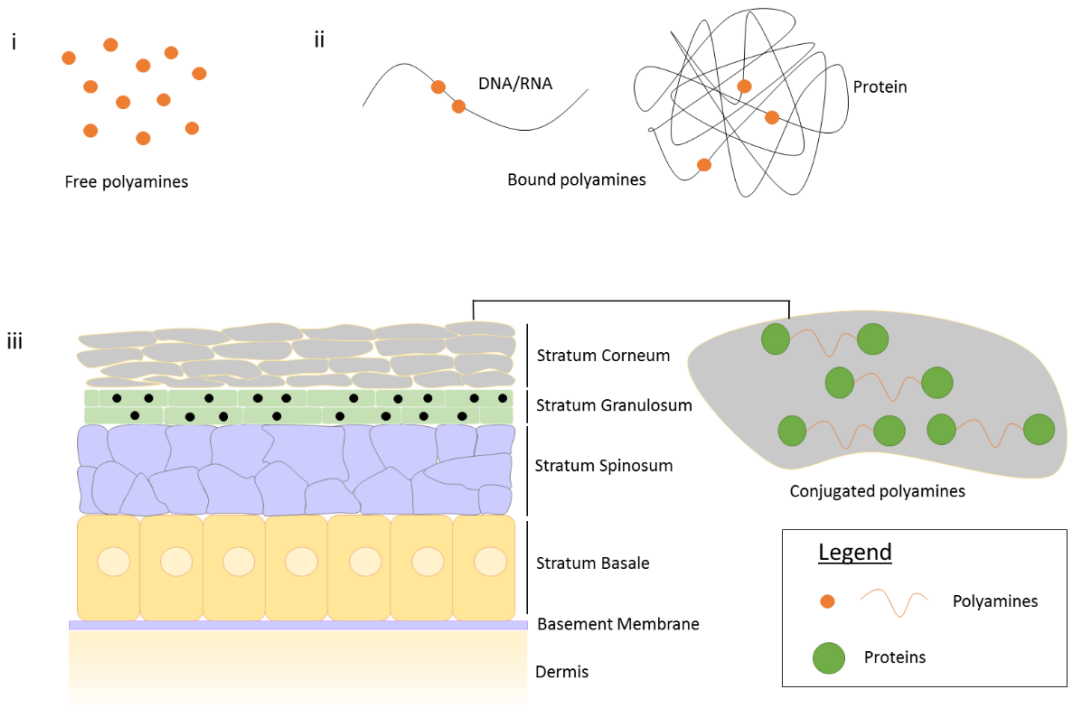

Figure 60: Different forms of polyamines present in mammalian cell. Polyamines (orange) exist as either (i) free, (ii) bound or (iii) conjugated forms within the cell. While most polyamines are bound to nucleic acids or proteins, the possibility of polyamine cross-links to proteins has been reported in the literature to be present at levels equivalent to lysine cross-links in the stratum corneum.

HPLC measures free and bound polyamines but not the protein conjugated polyamines. Hence the shift in polyamine levels that we observe during keratinocyte differentiation is attributed to a decrease in free/bound Put and an increase in free/bound Spm. The Spd/Spm antibodies were raised against polyamine conjugated protein but it is unknown if the antibodies detect the free and bound polyamines in addition to the protein-conjugated polyamines. The absence of Spd/Spm staining in the nucleus suggests that the antibodies could potentially be detecting only the conjugated forms of polyamines but not the free or bound forms.

The individual roles of Spd and Spm has been explored in the literature. The relative levels of Spd and Spm differ markedly between different cell types (Tabor and Tabor 1984) and both polyamines may have different targets and hence different cellular functions (Tabor and Tabor 1976). Spd for instance is known to have an essential role as the precursor of hypusine, which is a post-translational modification of the elongation factor eIF5A. This modification is

necessary for eIF5A to function in protein synthesis (Park 2006, Park and Nishimura 2009). Thus, if hypusine synthesis is inhibited, then cells would cease to grow. Evidence in the literature also suggest a role for Spd to cross-link to proteins in the cornified epidermal envelopes (Martinet, Beninati et al. 1990). However, the role for Spm in this aspect is not entirely clear. Spm may serve as a storage reservoir for maintaining appropriate levels of free Spd though polyamine catabolism, which is mediated by SMOx, APAO and SAT1. Spm and to a lesser extent Spd, also play a role as an antioxidant and has free radical scavenging properties, to protect the cells against lipid peroxidation (Matkovics, Kecskemeti et al. 1993, Pegg 2014).

Both Spd and Spm can interact with nucleic acids and they may have a role in polyamine-mediated ribosomal frameshifting which is required to decode the antizyme (AZ) mRNA (Matsufuji, Matsufuji et al. 1995). Spd and Spm can also have specific interactions with and have different affinities for various types of ion channels such as the glutamate receptors, inwardly-rectifying potassium channels and voltage-dependent Ca^{2+} channels (Williams 1997). Thus, the correct ratio of Spd:Spm is required for appropriate physiological activity and an increase in Spd may not be able to compensate for the loss of Spm.

It is not clear which polyamine, Spd or Spm is more important for the differentiation phenotype. Both polyamines may be essential for keratinocyte differentiation and it is possible that spermine synthase is more efficient than spermidine synthase thus, Spd is instantaneously converted to Spm during keratinocyte differentiation. The addition of Spd alone won't rescue the phenotype in AMD1 knockdown or EGBG-treated keratinocytes since Spd cannot be converted to Spm in the absence of AMD1. The addition of Spm alone may rescue the phenotype, because Spm can still be back-converted to Spd by polyamine catabolic enzymes if

Spd is also required for keratinocyte differentiation. For this reason, I have always added both Spd/Spm to all experimental cultures.

4.6 Rescue of AMD1 knockdown and inhibition with Spd/Spm during keratinocyte differentiation

With an AMD1 inhibition experiment using EGBG, the activity of AMD1 is completely blocked as opposed to AMD1 knockdown keratinocytes where the protein level of AMD1 is reduced, likely causing a decrease in total AMD1 cellular activity. Cells may respond in different ways to a block in AMD1 activity and a decrease in its activity. It is well known that polyamine levels are modulated tightly by a combination of synthesis, catabolism and transport and these processes may be differentially affected in the knockdown verses the inhibition. Variations in the levels of Spd and Spm in AMD1 knockdown and AMD1 inhibited keratinocytes can be attributed to several potential factors. It is possible that spermine synthase is more efficient that spermidine synthase hence Spd may be almost immediately converted to Spm. While AMD1 activity is manipulated, polyamine catabolic enzymes such as SAT1 and SMOx are still active and thus higher order polyamines can also be catabolized back to Spd and Put. Spd has been shown to be a substrate for protein cross-linking while the role of Spm in cross-linking is not clear (Martinet, Beninati et al. 1990). Additionally, Spd is utilized as a substrate for the modification of lysine on eIF5A to hypusine, which is crucial for cell growth and protein translation (Park 2006, Park and Nishimura 2009). The interplay of all these events may be varied under AMD1 inhibition and AMD1 knockdown conditions, thereby accounting for the variability in Spd and Spm levels.

4.7 Expression of other polyamine regulators during AMD1 knockdown/inhibition

The activity of ODC1 was not determined in AMD1 knockdown keratinocytes. However, with reduced AMD1 activity as a result of decreased AMD1 protein expression, Put levels would increase. High levels of Put will inhibit the synthesis of new polyamines by decreasing the translation of ODC1 which is mediated by an uORF and a GC-rich sequence located at the 5'

UTR of *ODC1* mRNA (Shantz, Hu et al. 1996, Ivanov, Loughran et al. 2008, Miller-Fleming and Olin-Sandoval 2015). However, this mechanism is not well understood. High Put levels would also promote the binding of antizyme (AZ) to ODC1 monomers. This would inhibit ODC1 dimerization and target it for degradation (Heller, Fong et al. 1976, Li, Stebbins et al. 1996, Erales and Coffino 2014). Thus, with an AMD1 knockdown or inhibition, the activity of ODC1 would decrease to prevent further accumulation of Put.

The low Spd to Spm ratio in addition to low levels of Put in D6 keratinocytes compared to D0 undifferentiated keratinocytes suggest that polyamine catabolism is reduced. Hence, the expression of polyamine catabolic enzyme SAT1, APAO and SMOx is expected to decrease.

4.8 Polyamine supplementation in Microarray Experiments

Cell toxicity assays were performed using Put, Spd and Spm to determine a tolerable working concentration for these compounds in my experiment. Put has a role in cell proliferation (Takigawa, Inoue et al. 1977, Farriol, Segovia-Silvestre et al. 2001). This was demonstrated using either ODC1-K5 or ODC1-K6 Tg overexpression mice which displayed increased susceptibility to tumour formation in the presence of UV treatment or when exposed to carcinogen (O'Brien, Simsiman et al. 1975, Chen, Megosh et al. 2000, Ahmad, Gilliam et al. 2001). Thus, if Put was added to D0 undifferentiated keratinocytes, it would likely increase proliferation.

For the microarray experiment, all polyamines whether Put, Spd or Spm were added at D3 of keratinocyte differentiation when AMD1 was already high and where keratinocyte proliferation was low to negligible as the cells are confluent. A cell count performed at D3 and D6 of differentiation using shScrambled keratinocytes suggests that the cell numbers are not significantly different between the two time points. This suggests that the effects that I observe with Put addition, is on keratinocyte differentiation and not proliferation. Since AMD1 protein is already high by D3 of differentiation, the addition of Put at this time point would be a substrate to produce Spd/Spm. This is also reflected by the heat map which shows a similar

gene expression profile for Put and Spd/Spm supplementation at D3 of keratinocyte differentiation (**Figure 46A**).

4.9 Identification of AMD1-sensitve genes during keratinocyte differentiation

From my microarray gene analysis, I identified AP1 transcription factor *JUNB*, as a downstream target of *AMD1* (Eckert, Adhikary et al. 2013). AP1 transcription factors comprise of a family of Jun and Fos proteins that are capable of forming homo- or heterodimer complexes. These complexes then interact with AP1 factor, DNA binding site thereby influencing gene expression. AP1 transcription factors are known to regulate competing cellular processes such as proliferation and differentiation, and their role in mouse keratinocyte differentiation was explored with TAM-67, a truncated form of c-jun (Han, Rorke et al. 2012). For instance, the binding of TAM-67 to an AP1-5 binding site of an *Ivl* promoter reduced its protein expression during keratinocyte differentiation. Thus, it is possible that up-regulation of AMD1 during keratinocyte differentiation, and a shift in the ratios of polyamines as a consequence may enhance the binding of JUNB to AP1 binding sites on several differentiation genes.

Other key drivers of keratinocyte differentiation that were downstream of AMD1 were, ZNF750, KLF4 and NOTCH1. ZNF750 is an established marker of keratinocyte differentiation, which is particularly enriched in the SG. Knockdown of *ZNF750* is known to affect genes of the EDC and mutations in ZNF750 have been associated with phenotypes reminiscent of psoriasis (Cohen, Birnbaum et al. 2012). ZNF750 has also been identified as a downstream target of p63, a master regulator of epidermal differentiation and it controls the expression of *KLF4* transcription factor by binding to multiple regions within its transcriptional start site (TSS) (Koster and Roop 2004, Sen, Boxer et al. 2012). Here, I have shown that AMD1 is an upstream regulator of both ZNF750 and KLF4, but independent of p63. Recently, Sun et al., proposed a ZNF750-TINCR-CALML5-SFN network in promoting epidermal differentiation,

as shown in **Figure 59** (Sun, Boxer et al. 2015). AMD1 could be potentially upstream of this regulatory network.

I observed an up-regulation of AQP3 and down-regulation of NOTCH1 during keratinocyte differentiation. The role of NOTCH1 and AQP3 during keratinocyte differentiation still remains controversial. A previous study using mouse epidermal keratinocytes, reported a role for phospholipase-D2 (PD2)-AQP3 signaling in mediating keratinocyte differentiation (Bollag, Xie et al. 2007). Another study reported comparable levels of differentiation markers between control and AQP3-knockdown neonatal human keratinocytes (Hara-Chikuma, Takahashi et al. 2009). A study by Guo et al., demonstrated *AQP3* to be a transcriptional target of NOTCH1. Thus, NOTCH1 activation during keratinocyte differentiation was reported to down-regulate AQP3 expression (Guo, Chen et al. 2013). Additionally, mice with a *Notch1-/-* gene deletion in the skin displayed higher expression of late differentiation markers FLG and LOR while intermediate differentiation markers K1 and IVL were not significantly affected (Rangarajan, Talora et al. 2001). My study shows that AQP3 and NOTCH1 are downstream targets of AMD1 during keratinocyte differentiation, but their roles in differentiation are still not well understood.

I have identified CPEB4 as a downstream target of AMD1 that was enriched in the SG and this requires further verification by co-staining with a granular layer marker, IVL. At higher magnification, I saw CPEB4 staining as a single foci in the periphery of the nuclei, in the majority of the cells in the basal and suprabasal layers of the epidermis. It is possible that CPEB4 localises to the centrosome and this can be further verified by co-localization studies with a centrosomal marker, pericentrin.

CPEB4 is an RNA binding protein that has been demonstrated to play several roles in neuronal development and tumour progression. CPEB4 is known to be expressed in neuronal tissues such as the brain and the spinal cord (Shin, Salameh et al. 2016). It contains an unstructured and low complexity domain (LCD) with unknown function. While CPEB4-null mice developed normally, mice expressing only the LCD of CPEB4 were neonatal lethal with impaired mobility

and neuronal developmental defects (Shin, Salameh et al. 2016). CPEB4 LCD-expressing mice had altered ribosomal RNA biogenesis and high levels of stress response genes such as DRR1, an actin bundling protein that impedes neurite outgrowth (Shin, Salameh et al. 2016). Since DRR1 is commonly responsible for several neurodegenerative disorders, this study revealed the potential role of LCD mediated neurodevelopmental defect.

Other studies have demonstrated CPEB4 to be associated with tumour progression (Tsai, Chang et al. 2016, Hu, Zhang et al. 2017, Zhijun, Dapeng et al. 2017). The role of CPEB4 was accessed in hepatocellular carcinoma (HCC) and the protein levels of CPEB4 were found to be higher in early-stage HCC compared to late-stage HCC patients (Tsai, Chang et al. 2016). CPEB4 expression was found to be higher in glioma tissues as compared to their corresponding non-neoplastic brain tissues (Zhijun, Dapeng et al. 2017). Here, the expression of CPEB4 correlated with the grade of clinical gliomas, making it an oncogenic promoter in glioblastomas (Zhijun, Dapeng et al. 2017). Hence, the altered expression of CPEB4 in different cancers suggest its complicated role in tumorigenesis.

No evidence in the literature have shown CPEB4 expression in the skin nor its role in keratinocyte differentiation, thus making it a novel candidate of research. We observed that the expression of CPEB4 resembled Ndel1 and Lis1, which are centrosomal proteins. These centrosomal proteins present in the proliferative epidermal cells re-localize to the desmosomes during keratinocyte differentiation **(Figure 61)**. It was reported that in desmoplakin (DP) KO mice, Lis1 expression was lost in the suprabasal cells **(Figure 62)**. This lead to microtubule organization defects and severe loss of desmosome stability, reduced attachment of keratin filaments and elevated desmosomal protein turnover at the cell cortex (Sumigray, Chen et al. 2011). As a consequence, epidermal barrier activity was impaired which lead to lethality in these mice shortly after birth (Sumigray, Chen et al. 2011). This study demonstrates that

desmosomal-associated components are important for controlling cortical microtubule organization and an unknown role for centrosomal proteins in epidermis function.

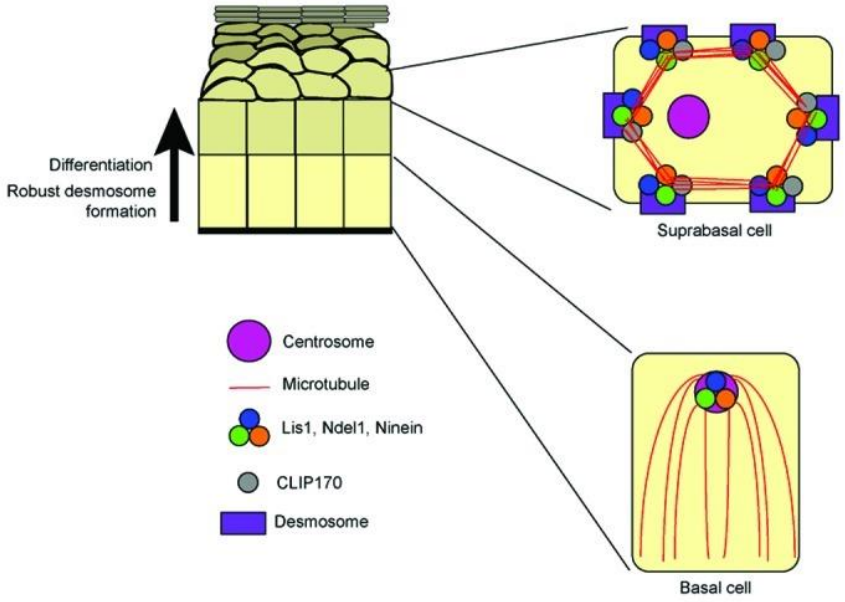

Figure 61: Centrosomal proteins and microtubule organization in the epidermis. In the basal keratinocytes, the centrosome is apically localized with a radial organization of microtubules around it. Proteins such as Lis1, Ndel1 and ninein are localized at the centrosome. In differentiated suprabasal keratinocytes, Lis1, Ndel1 and ninein are lost from the centrosome and are recruited to the desmosomes by desmoplakin and are reorganized with microtubules around the cell cortex. Adapted from: (Sumigray and Lechler 2011).

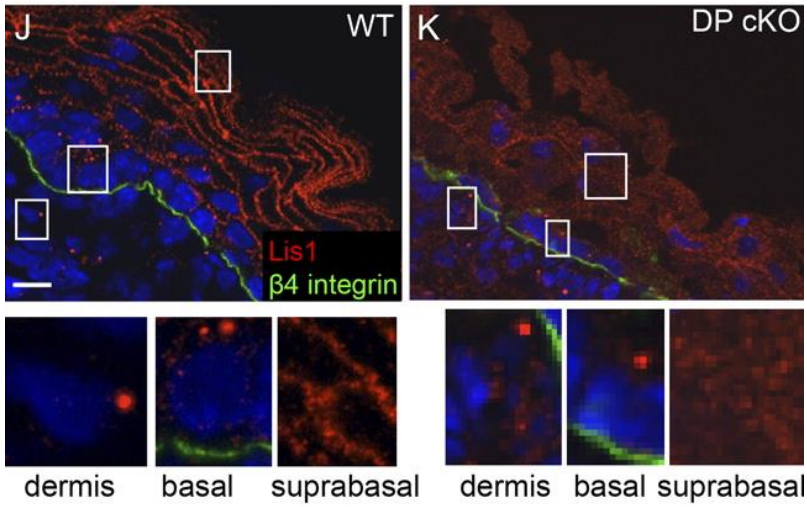

Figure 62: Lis1 expression in wild-type (Wt) and desmoplakin (DP) conditional knockout e17.5 mice skin. Lis1 protein expression was stained in red and the basement membrane was denoted by β4 integrin staining in green. Boxed regions are magnified below to indicate centrosomal staining in the dermis and the basal keratinocyte but cortical staining in the suprabasal cells. In DP conditional KO mice, the cortical expression of Lis1 was lost in the suprabasal cells. Adapted from (Sumigray, Chen et al. 2011).

Since CPEB4 stains the centrosome in the basal layer keratinocytes and the SG in the differentiated keratinocytes, I postulate that CPEB4 may have a similar role to Lis1 in associating with the desmosomes through a linker protein desmoplakin to promote cortical microtubule reorganization and desmosome stability during keratinocyte differentiation (Sumigray, Chen et al. 2011, Sumigray and Lechler 2011). The expression of CPEB4 could be mediated by AMD1 and the shift in the ratios of polyamines from Put to Spd/Spm.

Future work to explore the role of CPEB4 during keratinocyte differentiation would involve adopting a similar approach used to study the function of AMD1. We would knockdown and overexpress CPEB4 to determine if it is required for keratinocyte differentiation in monolayer cultures. The requirement of CPEB4 to form a fully stratified epidermis would be determined by establishing organotypic skin equivalents using shCPEB4 knockdown keratinocytes in comparison to shScrambled controls. Desmoplakin expression would be compared between shScrambled and shCPEB4-derived organotypics. Likewise, we would determine the cortical expression of CPEB4 in desmoplakin knockdown monolayer keratinocytes and organotypic skin equivalents. We postulate that the over-expression of CPEB4 in AMD1 inhibited keratinocytes may partially rescue the perturbed differentiation phenotype. Since, CPEB4 is a novel target of keratinocyte differentiation, it may work in combination with other well-established key transcription factors such as ZNF750, KLF4 or NOTCH1 but is likely not to be the only factor that drives keratinocyte differentiation.

It has been demonstrated that CPEB1, an RNA binding protein, is located in the centrosomes of rat astrocytes and remains associated with *cyclin B1* mRNA (Kim, Oh et al. 2011). In response to a growth stimuli, CPEB1 gets phosphorylated and activated, which then polyadenylates *cyclin B1* mRNA. This increases its protein production, hence allowing cell cycle to progress (Kim, Oh et al. 2011). Since, CPEB4 and CPEB1 are proteins of the same family, we would examine the role of CPEB4 in regulating RNA by looking at translational changes in shScrambled and shCPEB4 knockdown keratinocytes during differentiation.

4.10 Potential role for AMD1 in regulating downstream genes during keratinocyte differentiation

AMD1 is a rate limiting enzyme in the polyamine biosynthesis pathway which decarboxylates adenosyl methionine to decarboxylated adenosyl methionine thereby providing the amino propyl donor groups for the formation of Spd and Spm. An up-regulation of AMD1 protein and a subsequent shift in polyamine ratios from high Put, low Spm to low Put, high Spm was required for keratinocyte differentiation. The changes in polyamine levels could play a crucial role in modulating gene expression at the level of transcription, RNA stability, RNA translation and protein function (Bachrach 2005, Lightfoot and Hall 2014). As discussed above, it is possible that the Spd/Spm antibodies are binding only the conjugated polyamines which would explain their enrichment in the cytoplasm. It has been shown that polyamines are present in the nucleus and the cytoplasm where they can influence gene expression (Igarashi and Kashiwagi 2010, Igarashi and Kashiwagi 2011, Kashiwagi, Terui et al. 2018). I propose that the increase in Spm during keratinocyte differentiation may have regulatory roles in promoting the expression of genes that are essential to drive keratinocyte differentiation. Polyamines, unlike other divalent cations such as Ca^{2+} or Mg^{2+}, have distinct regulatory roles in modulating the function of nucleic acids and proteins (Igarashi and Kashiwagi 2010, Lightfoot and Hall 2014). The three polyamines have specificity in their binding and are able to influence the function of DNA, RNA and proteins by binding to different targets. I propose that polyamines can bind to specific regions of DNA and either influence its transcription or bind to specific regions of the RNA and increase its stability during keratinocyte differentiation. In this context, Spm could be influencing the stability or the transcription of some of the key transcription factors, signaling molecules or RNA binding proteins that are essential for keratinocyte differentiation. These key drivers may in turn regulate a cascade of genes downstream, eventually influencing the expression of genes encompassing the epidermal differentiation complex (EDC). Though polyamines are cationic, the interaction between polyamines and DNA is weaker compared to RNA (Igarashi and Kashiwagi 2000, Igarashi and Kashiwagi 2010). Evidence in the literature

suggest some possibilities of the regulatory role mediated by polyamines in modulating gene expression and signal transduction.

For instance, low concentrations of polyamines can bind to and influence the conversion of B-DNA to Z-DNA (Behe and Felsenfeld 1981). The binding of estrogen receptor at an upstream region of estrogen response gene is favoured at a region near the Z-DNA compared to B-DNA (Thomas, Gallo et al. 1995). The Z-DNA conformation in rat nucleolin (Ncl) gene is preferred as it in a metabolically active state, which inhibits promoter activity of Ncl gene (Rothenburg, Koch-Nolte et al. 2001). In another finding, Z-DNA conformation at the upstream region of human colony-stimulating factor 1 (CSF1) gene enhances its promoter activity (Liu, Liu et al. 2001). Other reports have stated that polyamine depletion induces Smad proteins, which are transcription activators that are associated with a significant increase in target gene transcription (Liu, Santora et al. 2003). It has also been reported that polyamines can enhance the transcription of human polyamine-modulated factor-1, a transcriptional cofactor associated with the transcription factor Nrf-2; the interaction of both with the polyamine responsive element on the promoter region can enhance the transcription of several genes such as the gene encoding SAT1 (Wang, Devereux et al. 1999). It has also been demonstrated that polyamines can promote the transcription of E-cadherin by facilitating the binding of c-Myc to an E-Pal box located proximally to the E-cadherin promoter (Liu, Guo et al. 2009). These evidence suggest that polyamines can either positively or negatively influence transcription in a cell and tissue specific manner. However, the exact sequences which polyamines bind to are difficult to deduce and further studies are needed to confirm these findings.

Since the only known role for AMD1 is to decarboxylate AdoMet to dcAdoMet, the gene expression changes that we observe with AMD1 knockdown or inhibition studies would be specific and hence will not be affected in other systems (Grillo 1985, Bale and Ealick 2010). The result of changes in polyamine levels in other cells and tissues will be dependent on the RNAs and proteins expressed in that tissue at the time. For example, our group has previously

shown that AMD1 is highly expressed in ESCs and is down-regulated in NPCs (Zhang, Zhao et al. 2012, Zhao, Goh et al. 2012). High levels of AMD1 or the supplementation of Spm inhibits ESC differentiation to NPCs (Zhang, Zhao et al. 2012). It was shown that AMD1 promotes self-renewal at least in part through the promotion of high levels of Myc, a known self-renewal regulator (Zhang, Zhao et al. 2012). As such, changes in polyamine ratios and levels will have a cell type specific effect on cells, dependent on which mRNAs and proteins are expressed.

4.11 Polyamines in epigenetic regulation

Both DNA methylation and polyamine biosynthesis are dependent on a common substrate, AdoMet. The cellular levels of AdoMet are usually higher than dcAdoMet (Heby, Persson et al. 1988). DNA methylation is catalysed by methyl transferases, which involves the addition of a methyl group to cytosine to form 5-methyl-cytosine (m5C) (Razin and Shemer 1995, Li, Guo et al. 2015). Changes in the DNA methylation status of genes directly impacts expression levels. For example during embryonic development, methylation of CpG islands in DNA regulates gene expression by preventing the binding of transcription factors or altering the chromatin structure (Razin and Shemer 1995). While dcAdoMet also contains a methyl group, it does not act as a methyl donor, and instead can inhibit methyl transferase activity (Cox 1979, Soda, Kano et al. 2013). Hence, fluctuations in the ratios of AdoMet to dcAdoMet could influence the availability of the methyl donor AdoMet and thus affect cellular methylation. DNA methylation is a major form of gene expression control so this has the potential to influence cellular behaviour dramatically. Under normal circumstances, AMD1 expression is low to ensure that AdoMet levels are sufficient for methyl transferase reactions. However, during keratinocyte differentiation, an increase in AMD1 will result in an increased conversion of AdoMet to dcAdoMet thereby reducing the availability of the AdoMet substrate for DNA methylation. As a consequence, global methylation may be reduced. In order to determine if global methylation is affected during keratinocyte differentiation, the expression of histone

methylation marks such as H3K4me3 or H3K27me3 could be examined by immunoblotting (Sen, Webster et al. 2008).

There is substantial evidence in the literature illustrating epigenetic regulation of genes during epidermal differentiation. The presence of DNA methyltransferase 3A (DNMT3A) and DNMT3B in basal layer keratinocytes facilitates DNA methylation which is essential for skin stem cell differentiation (Sen, Reuter et al. 2010, Nandakumar, Vaid et al. 2011). Conditional ablation of DNMT1 in mice demonstrated epidermal thickening and aberrant differentiation (Sen, Reuter et al. 2010). Promoters of several late differentiation genes are marked by H3K27me3 (Ezhkova, Pasolli et al. 2009). Enhancer of zeste homolog 2 (Ezh2), a histone-lysine N-methyltransferase enzyme is down-regulated in the suprabasal keratinocytes of mice. It was demonstrated that Ezh2-mediated repression of epidermal differentiation genes prevent the binding of AP1 transcription factors (Ezhkova, Pasolli et al. 2009). Human keratinocytes expressing a histone H3K27-demethylase JMJD3, differentiate prematurely, whereas loss of JMJD3 leads to arrested differentiation (Sen, Webster et al. 2008).

Likewise, acetylation also plays an important role in mediating keratinocyte differentiation. PCAF is an acetyltransferase that acetylates retinoblastoma protein (Rb) so that it is retained in the nuclei during keratinocyte differentiation (Pickard, Wong et al. 2010). However, either a knockdown of PCAF or an exogenous overexpression of deacetylase SIRT1 mis-localises Rb to the cytoplasm, thereby affecting keratinocyte differentiation (Pickard, Wong et al. 2010). Blander et al., also demonstrated that SIRT1 activation or inhibition influenced the promotion or reduction of keratinocyte differentiation makers in normal human keratinocytes (Blander, Bhimavarapu et al. 2009). Polyamines can bind to DNA and are known to modulate chromatin structure by influencing acetylation. For instance, the skin from K6/ODC1 Tg mice and skin tumours of ODC1/Ras double Tg mice displayed higher HAT activities compared to normal littermates (Hobbs, Paul et al. 2002, Wei, Hobbs et al. 2007). HAT activity was significantly reduced with DFMO treatment confirming that it was dependent on the levels of polyamines.

ODC1 overexpression also promoted histone acetylation in several epidermal and fibroblast cells while DFMO treatment abrogated this increase (Hobbs and Gilmour 2000, Wei, Hobbs et al. 2007). Acetylation of Lys373 and Lys320 in p53 was linked to an elevated level of polyamines in ODC1 overexpressing tissues, but further research on this is needed (Wei, Hobbs et al. 2007). Spd is also linked to increasing lifespan in yeast by reducing acetylation (**Figure 23**) (Minois 2014). Polyamine deficiency in Jurkat and HT-29 cells altered global DNA methylation status and this was rescued when Spm was supplemented exogenously to augment DNA methyltransferase activity (Soda, Kano et al. 2013). Since polyamines are involved in modulating acetylation and methylation, it would be interesting to determine whether there is any crosstalk between epigenetic gene regulation and transcription factors regulated by AMD1 in maintaining the balance between proliferation and differentiation.

4.12 Role of polyamines in a proliferation to differentiation switch

While we only attempted to understand the regulation of AMD1 during keratinocyte differentiation, it would be interesting to determine whether AMD1 functions via a proliferation to differentiation switch, ensuring a tight balance in epidermal homeostasis. To understand this molecular switch, we could examine the role of AMD1 in earlier time points of differentiation. We could determine when the polyamine levels shift and when the earliest differentiation phenotype is detected in the knockdown cells.

4.13 Polyamines and their regulators during aging

We compared the expression of AMD1 between young and aged skin sections. However, due to the limited availability of donor skin excised during surgery, we only managed to receive foreskin from juveniles and abdominal skin sections from adults. My data shows that AMD1 staining is stronger in the adult skin compared to the juvenile skin. Younger human skin is thicker and has a higher proliferative potential compared to aged skin (Engelke, Jensen et al.

1997, Gilhar, Ullmann et al. 2004). My data showing high levels of Put in D0 undifferentiated keratinocytes, suggests that proliferative keratinocytes in the basal layer have higher levels of Put. With juvenile skin being more proliferative and less differentiated compared to adult skin, it is possible that the decreased AMD1 levels in juvenile skin contribute to this.

Spd/Spm levels have been shown to be lower in aged skin compared to juvenile skin (Nishimura, Shiina et al. 2006). Based on this notion, it is rather surprising that higher AMD1 expression was observed in the adult epidermis compared to the juveniles. While a decrease in polyamine levels has been reported with age, it was measured based on the whole epidermis and not in reference to any particular layer of the epidermis. It was also a measurement based on free and unconjugated polyamines excluding potential cross-linked polyamines. Older donor skin has less abundant stem cells, thus are less proliferative than adult skin (Engelke, Jensen et al. 1997, Michel M. 1997). As aged skin is more differentiated compared to adult skin, it is possible that more polyamines are cross-linked to proteins in the suprabasal layers resulting in a decrease in unconjugated polyamines.

When Spd/Spm levels are high during keratinocyte differentiation, cells are likely to increase polyamine catabolism, through the back conversion of Spm to Spd by catabolic enzyme SMOx or from Spm to Spd and Put by SAT1 and APAO, so as to maintain the polyamines levels within the physiological range of the cell (Thomas and Thomas 2003). As a consequence, H_2O_2 is released as a by-product. It is not known whether H_2O_2 generated as a result of polyamine catabolism has a role to play in keratinocyte differentiation. However, evidence in the literature suggest that H_2O_2 generated by DUOX1, acts as a signalling molecule to drive keratinocyte differentiation (Choi, Park et al. 2014).

Given the significant number of genes I show are downstream of AMD1, I think it is unlikely that they will all be absent in juvenile skin, where AMD1 protein levels are low. While the protein expression of AMD1 is different between adult and juvenile skin sections, it does not

necessarily imply that the Put:Spd:Spm ratio is affected. It is possible that aged skin has a higher rate of polyamine synthesis and catabolism, known as polyamine flux, as compared to juvenile skin (Casero and Pegg 2009). To verify this, skin sections need to be assessed for polyamine catabolic enzymes SAT1 and SMOx. It is possible that aged skin has heighted polyamine catabolism induced by the high AMD1 levels. It is also important to note that AMD1 protein levels do not necessarily correlate with its enzymatic activity. As such, it is possible that juvenile skin sections may have a lower expression of AMD1 protein that is highly active while the adult skin has a high expression of AMD1 protein that is less active. Given the tight regulation of polyamine levels that are known to exist, further studies are needed to understand this.

In the future, we plan to perform polyamine measurements to compare the polyamine levels between three independent neonate and adult human primary keratinocytes at D0 undifferentiated and D6 differentiated states. Expression of AMD1 would be determined by immunoblotting to further confirm our immunofluorescence staining. We further plan to determine the expression of AMD1 in non-lesional and lesional skin sections from psoriatic patients. Psoriasis is a chronic accelerated epidermopoiesis associated with several metabolic abnormalities (Proctor, Fletcher et al. 1975). It has been reported that psoriatic lesional skin has twice as much of all polyamines as opposed to non-lesional skin (Bohlen, Grove et al. 1978, Broshtilova, Lozanov et al. 2013). Stuttgen et al., reported that the skin of psoriasis patients had lower levels of Spd and Spm; however the authors failed to elaborate whether observations were taken from lesional or non-lesional skin (Stuttgen 1968, Proctor, Fletcher et al. 1975). Other reports have demonstrated high ODC1 activity and as a consequence higher levels of Put in psoriatic lesions compared to non-lesional regions (Lowe, Breeding et al. 1982). Moreover, there were higher levels of Spd/Spm in psoriatic skin lesions compared to non-lesional skin (Lowe, Breeding et al. 1982). Broshtilova et al., also reported highest Spm levels in psoriatic lesions compared to non-lesional skin from psoriasis patients suggesting a likely role of AMD1

in the pathogenesis of psoriasis (Broshtilova, Lozanov et al. 2013). Based on our earlier observation of equal ODC1 protein expression during keratinocyte differentiation, we would speculate that ODC1 protein would show mild staining pattern in all layers of the non-lesional epidermis. However, we would potentially observe a higher intensity of ODC1 staining in all layers of the epidermis from psoriasis lesions because ODC1 activity and Put levels are elevated in psoriasis. We predict an atypical staining pattern for AMD1, with possibly lower levels in the differentiated layers and increased levels in the proliferative layers.

4.14 Potential role for polyamine transporters during keratinocyte differentiation

While little is known about polyamine transporters during keratinocyte differentiation, we have shown that the expression of polyamine transporter, SLC12A8 is high in undifferentiated keratinocytes, but gradually decreases upon differentiation. Hewett et al., have recently linked a single nucleotide polymorphism (SNP) at the 3' UTR of SLC12A8 gene to psoriasis (Hewett, Samuelsson et al. 2002). However, the role of this mutation in the pathogenesis of psoriasis is not clearly understood (Hewett, Samuelsson et al. 2002). It is possible that a decrease in SLC12A8 might be essential for the import/export of certain polyamines required to drive keratinocyte differentiation. A SNP in SLC12A8, may disrupt this flow of import/export, leading to an accumulation of intracellular polyamines in psoriasis. Additional studies are needed to determine the function of this transporter in the formation of a normal skin barrier and its potential role in psoriasis

ATP13A3 and Caveolin-1 have been reported as potential biomarkers for pancreatic cancers (Madan, Patel et al. 2016). ATP13A3 was highly abundant in pancreatic cancer cell line L3.6pl, which has a higher polyamine import activity (Madan, Patel et al. 2016). With a peak in ATP13A3 expression at D2 of keratinocyte differentiation, we can infer that polyamine import might play an additional role in driving the shift in polyamine ratios from Put to Spd/Spm, especially when ODC1 protein levels are unaffected during keratinocyte differentiation. The

expression of ATP13A3 slowly declines with late differentiation possibly to ensure that the polyamine levels do not exceed beyond the physiological range of the keratinocytes. Whether SLC12A8 or ATP13A3 transporter is selective for a particular polyamine still remains elusive.

Caveolin-1 is a structural component of caveolae. Phosphorylation of Caveolin-1 on Try14 by Src, loosens its interaction with the oligomeric caveolar coat thereby increasing caveolae-mediated endocytosis and polyamine uptake (del Pozo, Balasubramanian et al. 2005, Zimnicka, Husain et al. 2016). Total caveolin-1 expression remains unchanged in N/TERT-1 keratinocytes throughout the course of differentiation. Hence, it is necessary to determine the phosphorylation status of Caveolin-1 using phospho-caveolin-1 antibodies to confirm the role of caveolae-mediated polyamine uptake during keratinocyte differentiation.

4.15 Identification of Spd/Spm conjugated proteins

In mammalian cells, two different types of polyamine mediated post-translational modification of proteins have been characterized (Piacentini, Farrace et al. 1990). The first mechanism involves the modification of Spd to hypusine while the other involves the covalent linkage of the amide group of polyamines to the ɤ-carboxy group of the glutamyl residues of proteins (Piacentini, Farrace et al. 1990, Park 2006). The latter mechanism is catalysed by TGMs which are a group of Ca^{2+}-dependent enzymes that are highly abundant in differentiating keratinocytes. These epidermal TGMs catalyse the formation of ε-(ɤ-glutamyl)lysine cross-links between proteins in the late cornified envelope. There is evidence in the literature which suggests the presence of Spd cross-links in levels similar to ε-(ɤ-glytamyl)lysine cross links in the stratum cornuem. Since, Spd has a more extended chemical structure compared to lysine, it allows bis(ɤ-glutamyl)Spd cross links between two proteins at a distance apart, which are not suitable for cross-linking by ε-(ɤ-glytamyl)lysine bonds (Martinet, Beninati et al. 1990). Thus, a decrease in Spd levels during keratinocyte differentiation by HPLC measurement may reflect a concomitant increase in Spd cross-linking of proteins that may be being detected by immunofluorescence staining with the Spd/Spm antibody. It has been reported that hypusine

biosynthesis is reduced in keratinocytes induced to differentiate with high Ca^{2+} (Piacentini, Martinet et al. 1988). It is possible that Spm may also be involved in protein conjugation but previously not reported to be detected due to an efficient APAO which may catalyse the breakdown of ɤ-glutamylSpd conjugates (Martinet, Beninati et al. 1990). The unidentified ~15kDa protein band that is up-regulated at D6 of keratinocyte differentiation suggest a possibility of Spd/Spm protein conjugation during keratinocyte differentiation.

I have shown that eIF5A or its isoform, eIF5A2 are not regulated during keratinocyte differentiation. This suggests that the unidentified ~15 kDa protein could be a novel target of polyamine-cross linking during terminal differentiation. During cornified envelope formation, several proteins are gradually deposited including SPRR such as cornifin-B (SPRR1B). Cornifin-B runs at approximately 15 kDa by immunoblotting and acts as a substrate for TGMs (Tarcsa, Candi et al. 1998). It was reported that the presence of glutamine (Gln) residues in cornifin-B allows it to function as an amine acceptor in cross-linked reactions catalysed by TGMs (Austin, Fujimoto et al. 1996). Since Spd and Spm contain amine groups, it is possible that they can be directly cross-linked at Gln residues on cornifin-B in epidermal cell envelopes. While high levels of free Spd and Spm are reported in psoriasis patients, an increase in cornifin proteins is also evidenced in psoriatic lesions, which have characteristic abnormal squamous differentiation (Fujimoto, Nakanishi et al. 1997).

In order to determine the ~15 kDa protein, D0 undifferentiated and D6 differentiated keratinocytes would be pelleted to extract cellular proteins. These proteins would be trypsinized to fragment them into peptides. Immunoprecipitation will be performed using the digested lysates followed by LC-MS to identify the peptides that have a Spd/Spm conjugation. The peptide sequence will then be matched against the protein ID database to determine the unidentified ~15 kDa protein. Subsequently, antibodies will be purchased against this protein to further validate by immunoblotting. LC-MS will also allow the identification of the specific amino acids containing the Spd/Spm conjugation, and the importance of this site for Spd/Spm conjugation can be determined by mutating this amino acid.

CHAPTER 5

CONCLUSION & FUTURE IMPLICATIONS

Our identification of AMD1 as an essential regulator of epidermal differentiation highlights the importance of polyamine regulation in epidermal homeostasis. While AMD1 regulation and polyamine levels have been linked to cancer and proliferation, their significance is less appreciated during epidermal differentiation. Here, we demonstrate that *AMD1* is translationally up-regulated during keratinocyte differentiation and high AMD1 protein is required for the shift in polyamine ratios from Put to Spd/Spm, which is necessary to drive keratinocyte differentiation. A failure to regulate this polyamine switch impedes keratinocyte differentiation and stratification. Since, it is known that AMD1 protein expression is translationally down-regulated during ESC differentiation by miRNAs, it would be interesting to determine which other cis-acting elements that are important in increasing AMD1 protein expression would also be essential for keratinocyte differentiation. Polyamines are known to be up-regulated in psoriatic lesions and it would be motivating to explore the regulation of AMD1 during psoriasis and to determine what role it may play in disrupting the polyamine distribution in lesional skin. This could pave ways to develop more effective strategies to treat psoriasis by targeting multiple aspects of polyamine metabolism.

By performing gene expression analysis, we have unravelled AMD1 as an upstream regulator of several key transcription factors of keratinocyte differentiation, through which it determines the expression of majority of the genes in the EDC. Among several novel targets of keratinocyte differentiation that are AMD1-dependent, we have verified the expression of CPEB4, an RNA binding protein, to be both present in the granular layer of the epidermis and potentially localized in the centrosomes of basal and suprabasal keratinocytes. Future studies would be directed at determining the role of CPEB4 in epidermal function. This would demonstrate a yet unidentified role for polyamines and their regulators in governing centrosomal to non-centrosomal microtubule

organization of keratinocytes during differentiation. Moreover, polyamine-mediated conjugation of proteins is a less explored field of research and it is now promising to know that AMD1 may regulate Spd/Spm cross-links to either known or novel targets of keratinocyte differentiation. Further understanding the role of AMD1 in keratinocyte differentiation will greatly broaden our knowledge of the various regulatory pathways it operates on to direct the differentiation of keratinocytes.

REFERENCES

Abeloff, M. D., M. Slavik, G. D. Luk, S. B. Baylin, M. Zeltzman and A. Sjoerdsma (1986). "Phase II trials of alpha-difluoromethylornithine, an inhibitor of polyamine synthesis, in advanced small cell lung cancer and colon cancer." Cancer Treat. Rep. **70**: 843-845.

Abeloff, M. D., M. Slavik, G. D. Luk, C. A. Griffin, J. Hermann and O. Blanc (1984). "Phase I trial and pharmacokinetic studies of alpha-difluoromethylornithine-an inhibitor of polyamine biosynthesis." J. Clin. Oncol. **2**: 124-130.

Abernethy, J. L., R. L. Hill and L. A. Goldsmith (1977). "epsilon-(gamma-Glutamyl)lysine cross-links in human stratum corneum." J Biol Chem **252**(6): 1837-1839.

Ahmad, N., A. C. Gilliam, S. K. Katiyar, T. G. O'Brien and H. Mukhtar (2001). "A definitive role of ornithine decarboxylase in photocarcinogenesis." Am J Pathol **159**(3): 885-892.

Akiyama, M. (2011). "Updated molecular genetics and pathogenesis of ichthiyoses." Nagoya J Med Sci **73**: 1063-1072.

Alam, H., L. Sehgal, S. T. Kundu, S. N. Dalal and M. M. Vaidya (2011). "Novel function of keratins 5 and 14 in proliferation and differentiation of stratified epithelial cells." Mol Biol Cell **22**(21): 4068-4078.

Austin, S. J., W. Fujimoto, K. W. Marvin, T. M. Vollberg, L. Lorand and A. M. Jetten (1996). "Cloning and regulation of cornifin beta, a new member of the cornifin/spr family. Suppression by retinoic acid receptor-selective retinoids." J Biol Chem **271**(7): 3737-3742.

Bachrach, U. (2005). "Naturally occurring polyamines: interaction with macromolecules." Curr. Protein Pept. Sci. **6**(559-566): 559.

Bale, S. and S. E. Ealick (2010). "Structural biology of S-adenosylmethionine decarboxylase." Amino Acids **38**(2): 451-460.

Bale, S., M. M. Lopez, G. I. Makhatadze, Q. Fang, A. E. Pegg and S. E. Ealick (2008). "Structural basis for putrescine activation of human S-adenosylmethionine decarboxylase." Biochemistry **47**(50): 13404-13417.

Banks-Schlegel, S. and H. Green (1981). "Involucrin synthesis and tissue assembly by keratinocytes in natural and cultured human epithelia." J Cell Biol **90**(3): 732-737.

Baroni, A., E. Buommino, V. D. Gregorio, E. Ruocco, V. Ruocco and R. Wolf (2012). "Structure and function of the epidermis related to barrier properties." Clinics in Dermatology **30**(2): 257-262.
Bassiri, H., A. Benavides, M. Haber, S. K. Gilmour, M. D. Norris and M. D. Hogarty (2015).

"Translational development of difluoromethylornithine (DFMO) for the treatment of neuroblastoma." Transl Pediatr **4**(3): 226-238.

Becerra-Solano, L. E., J. Butler, G. Castaneda-Cisneros, D. E. McCloskey, X. Wang, A. E. Pegg, C. E. Schwartz, J. Sanchez-Corona and J. E. Garcia-Ortiz (2009). "A missense mutation, p.V132G, in the

X-linked spermine synthase gene (SMS) causes Snyder-Robinson syndrome." Am J Med Genet A **149A**(3): 328-335.

Behe, M. and G. Felsenfeld (1981). "Effects of methylation on a synthetic polynucleotide: the B--Z transition in poly(dG-m5dC).poly(dG-m5dC)." Proc Natl Acad Sci U S A **78**(3): 1619-1623.

Bernerd, F., T. Magnaldo and M. Darmon (1992). "Delayed onset of epidermal differentiation in psoriasis." J. Invest. Dermatol. **98**: 902-910.

Bhawan, J., C. Bansal, K. Whren and U. Schwertschlag (2004). "K16 expression in uninvolved psoriatic skin: a possible marker of pre-clinical psoriasis." J. Cutan. Pathol. **31**: 471-476.

Bikle, D. D., Z. Xie and C. L. Tu (2012). "Calcium regulation of keratinocyte differentiation." Expert Rev Endocrinol Metab. **7**(4): 461-472.

Bjelaković, G., I. Stojanović, S. T. Jevtović, D. Pavlović, G. Kocić, S. Rossi, C. Tabolacci, J. Nikolić, D. Sokolović and L. J. Bjelakovic (2010). "Metabolic correlations of glucocorticoids and polyamines in inflammation and apoptosis." Amino Acids **39**: 29-43.

Blander, G., A. Bhimavarapu, T. Mammone, D. Maes, K. Elliston, C. Reich, M. S. Matsui, L. Guarente and J. J. Loureiro (2009). "SIRT1 promotes differentiation of normal human keratinocytes." J Invest Dermatol. **129**(1): 41-49.

Blanpain, C. and E. Fuchs (2009). "Epidermal homeostasis: a balancing act of stem cells in the skin." Nat. Rev. Mol. Cell Biol. **10**: 207-217.

Boer, M., E. Duchnik, R. Maleszka and M. Marchlewicz (2016). "Structural and biophysical characteristics of human skin in maintaining proper epidermal barrier function." Postepy Dermatol Alergol **33**(1): 1-5.

Bohlen, P., J. Grove, M. F. Beya, J. Koch-Weser, M. H. Henry and E. Grosshans (1978). "Skin polyamine levels in psoriasis: the effect of dithranol therapy." Eur J Clin Invest. **8**(4): 215-218.

Bollag, W. B., D. Xie, X. Zheng and X. Zhong (2007). "A potential role for the phospholipase D2-aquaporin-3 signaling module in early keratinocyte differentiation: production of a phosphatidylglycerol signaling lipid." J Invest Dermatol. **127**: 2823-2831.

Bowcock, A. M., W. Shannon, F. Du, J. Duncan, K. Cao, K. Aftergut, J. Catier, M. A. Fernandez-Vina and A. Menter (2001). "Insights into psoriasis and other inflammatory diseases from large-scale gene expression studies." Hum Mol Genet **10**(17): 1793-1805.

Breitkreutz, D., I. Koxholt, K. Thiemann and R. Nischt (2013). "Skin basement membrane: the foundation of epidermal integrity--BM functions and diverse roles of bridging molecules nidogen and perlecan." Biomed Res Int **2013**: 179784.

Broshtilova, V., V. Lozanov and L. Miteva (2012). "Comparative analysis of polyamine metabolism in benign and neoplastic keratinocytic proliferations." Acta Dermatovenerol Alp Pannonica Adriat. **21**(1): 3-5.

Broshtilova, V., V. Lozanov and L. Miteva (2013). "Polyamine metabolism changes in psoriasis." Indian J Dermatol. **58**(4): 306-309.

Broshtilova, V., V. Lozanov and L. Miteva (2013). "Polyamine metabolism changes in psoriasis." Indian J Dermatol. **58**(4): 306-309.

Burns, M. R., G. F. Graminski, R. S. Weeks, Y. Chen and T. G. O'Brien (2009). "Lipophilic lysine-spermine conjugates are potent polyamine transport inhibitors for use in combination with a polyamine biosynthesis inhibitor." J Med Chem **52**(7): 1983-1993.

Candi, E., R. Schmidt and G. Melino (2005). "The cornified envelope: a model of cell death in the skin." Nat Rev Mol Cell Biol **6**(4): 328-340.

Casero, R. A. and L. J. Marton (2007). "Targeting polyamine metabolism and function in cancer and other hyperproliferative diseases." Nature Reviews Drug Discovery **6**: 373-390.

Casero, R. A. and A. E. Pegg (2009). "Polyamine catabolism and disease." Biochem J **421**(3): 323-338.

Casero, R. A. J. and L. J. Marton (2007). "Targeting polyamine metabolism and function in cancer and other hyperproliferative diseases." Nat. Rev. Drug Discov. **6**: 373-390.

Cason, A. L., Y. Ikeguchi, C. Skinner, T. C. Wood, K. R. Holden, H. A. Lubs, F. Martinez, R. J. Simensen, R. E. Stevenson, A. E. Pegg and C. E. Schwartz (2003). "X-linked spermine synthase gene (SMS) defect: the first polyamine deficiency syndrome." Eur J Hum Genet **11**(12): 937-944.

Chassé, H., S. Boulben, V. Costache, P. Cormier and J. Morales (2017). "Analysis of translation using polysome profiling." Nucleic Acids Res. **45**(3): e15.

Chen, Y., L. C. Megosh, S. K. Gilmour, J. A. Sawicki and T. G. O'Brien (2000). "K6/ODC transgenic mice as a sensitive model for carcinogen identification." Toxicol Lett **116**(1-2): 27-35.

Chen, Y., R. S. Weeks, M. R. Burns, D. W. Boorman, A. Klein-Szanto and T. G. O'Brien (2006). "Combination therapy with 2-difluoromethylornithine and a polyamine transport inhibitor against murine squamous cell carcinoma." Int J Cancer **118**(9): 2344-2349.

Choi, H., J. Y. Park, H. J. Kim, M. Noh, T. Ueyama, Y. Bae, T. R. Lee and D. W. Shin (2014). "Hydrogen peroxide generated by DUOX1 regulates the expression levels of specific differentiation markers in normal human keratinocytes." J Dermatol Sci. **74**(1): 56-63.

Cipolla, B., F. Guille, J. P. Moulinoux, V. Quemener, F. Staerman, L. Corbel and B. Lobel (1993). "Polyamines and prostatic carcinoma: clinical and therapeutic implications." Eur Urol **24**(1): 124-131.

Cipolla, B., F. Guilli and J. P. Moulinoux (2003). "Polyamine-reduced diet in metastatic hormone-refractory prostate cancer (HRPC) patients. ." Biochem. Soc. Trans. **31**: 384-387.

Clement, P. M., H. E. Johansson, E. C. Wolff and M. H. Park (2006). "Differential expression of eIF5A-1 and eIF5A-2 in human cancer cells." FEBS J **273**(6): 1102-1114.

Cohen, I., R. Y. Birnbaum, K. Leibson, R. Taube, S. Sivan and O. S. Birk (2012). "ZNF750 is expressed in differentiated keratinocytes and regulates epidermal late differentiation genes." PLoS One **7**(8): e42628.

Cohen, I., R. Y. Birnbaum, K. Leibson, R. Taube, S. Sivan and O. S. Birk (2012). "ZNF750 is expressed in differentiated keratinocytes and regulates epidermal late differentiation genes." PLoS One **7**(8): e42628.

Coleman, C. S., A. E. Pegg, L. C. Megosh, Y. Guo, J. A. Sawicki and T. G. O'Brien (2002). "Targeted expression of spermidine/spermine N1-acetyltransferase increases susceptibility to chemically-induced skin carcinogenesis." Carcinogenesis. **23**: 359-364.

Cox, R. (1979). "Polyamines inhibit DNA methylation in vitro." Biochem Biophys Res Commun **86**(3): 594-598.

Daigle, N. D., G. A. Carpentier, R. Frenette-Cotton, M. G. Simard, M. H. Lefoll, M. Noel, L. Caron, J. Noel and P. Isenring (2009). "Molecular characterization of a human cation-Cl- cotransporter (SLC12A8A, CCC9A) that promotes polyamine and amino acid transport." J Cell Physiol **220**(3): 680-689.

Davis, R. L. (2013). "Spermidine cures flies of senior moments." Nat Neurosci **16**(10): 1363-1364.
Dayoub, R., W. E. Thasler, A. K. Bosserhoff, T. Singer, K. W. Jauch, H. J. Schlitt and T. S. Weiss (2006). "Regulation of polyamine synthesis in human hepatocytes by hepatotrophic factor augmenter of liver regeneration." Biochem Biophys Res Commun **345**(1): 181-187.

del Pozo, M. A., N. Balasubramanian, N. B. Alderson, W. B. Kiosses, A. Grande-Garcia, R. G. Anderson and M. A. Schwartz (2005). "Phospho-caveolin-1 mediates integrin-regulated membrane domain internalization." Nat Cell Biol **7**(9): 901-908.

Deyrieux, A. F. and V. G. Wilson (2007). "In vitro culture conditions to study keratinocyte differentiation using the HaCaT cell line." Cytotechnology. **54**(2): 77-83.

Dickson, M. A., W. C. Hahn, Y. Ino, V. Ronfard, J. Y. Wu, R. A. Weinberg, D. N. Louis, F. P. Li and J. G. Rheinwald (2000). "Human keratinocytes that express hTERT and also bypass a p16(INK4a)-enforced mechanism that limits life span become immortal yet retain normal growth and differentiation characteristics." Mol Cell Biol **20**(4): 1436-1447.

Dyachuk, V., C. Bierkamp and A. Merdes (2016). "Non-centrosomal Microtubule Organization in Differentiated Cells." The Microtubule Cytoskeleton **189**: 27-41.

Eaaswarkhanth, M., D. Xu, C. Flanagan, M. Rzhetskaya, M. G. Hayes, R. Blekhman, N. G. Jablonski and O. Gokcumen (2016). "Atopic Dermatitis Susceptibility Variants in Filaggrin Hitchhike Hornerin Selective Sweep." Genome Biol. Evol. **8**(10): 3240–3255.

Eberlin, L. S. (2014). "DESI-MS imaging of lipids and metabolites from biological samples." Methods Mol Biol **1198**: 299-311.

Eckert, R. L., G. Adhikary, C. A. Young, R. Jans, J. F. Crish, W. Xu and E. A. Rorke (2013). "AP1 transcription factors in epidermal differentiation and skin cancer." J Skin Cancer **2013**: 537028.

Eckert, R. L., M. T. Sturniolo, A. M. Broome, M. Ruse and E. A. Rorke (2005). "Transglutaminase function in epidermis." J Invest Dermatol **124**(3): 481-492.

Eckhart, L., S. Lippens, E. Tschachler and W. Declercq (2013). "Cell death by cornification." Biochim Biophys Acta **1833**(12): 3471-3480.

Eichner, R., T. T. Sun and U. Aebi (1986). "The role of keratin subfamilies and keratin pairs in the formation of human epidermal intermediate filaments." J Cell Biol **102**(5): 1767-1777.

Eisenberg T., K. H., Schauer A., Büttner S., Ruckenstuhl C., Carmona-Gutierrez D., Ring J., Schroeder S., Magnes C., Antonacci L., Fussi H., Deszcz L., Hartl R., Schraml E., Criollo A., Megalou E., Weiskopf D., Laun P., Heeren G., Breitenbach M., Grubeck-Loebenstein B., Fahrenkrog B., Fröhlich K. U., Sinner F., Tavernarakis N., Minois N., Kroemer G. & Madeo F. (2009). "Induction of autophagy by spermidine promotes longevity." Nat Cell Biol **11**: 1305-1314.

El, B. P., G. Milano, P. Verrando, N. Renée and J. P. Ortonne (1983). "Polyamine levels in normal human skin. A comparative study of pure epidermis, pure dermis, and suction blister fluid." Arch Dermatol Res. **275**(4): 218-221.

Elias, P., S. Ahn, B. Brown, D. Crumrine and K. R. Feingold (2002). "Origin of the epidermal calcium gradient: regulation by barrier status and role of active vs passive mechanisms." J Invest Dermatol. **119**(6): 1269-1274.

Engelke, M., J. M. Jensen, S. Ekanayake-Mudiyanselage and E. Proksch (1997). "Effects of xerosis and ageing on epidermal proliferation and differentiation." Br J Dermatol **137**(2): 219-225.

Erales, J. and P. Coffino (2014). "Ubiquitin-independent proteasomal degradation." Biochim Biophys Acta **1843**(1): 216-221.

Ezhkova, E., H. A. Pasolli, J. S. Parker, N. Stokes, I. H. Su, G. Hannon, A. Tarakhovsky and E. Fuchs (2009). "Ezh2 orchestrates gene expression for the stepwise differentiation of tissue-specific stem cells." Cell **136**(6): 1122-1135.

Farriol, M., T. Segovia-Silvestre, J. M. Castellanos, Y. Venereo and X. Orta (2001). "Role of putrescine in cell proliferation in a colon carcinoma cell line." Nutrition **17**(11-12): 934-938.

Feith, D. J., D. K. Bol and J. M. Carboni (2005). "Induction of ornithine decarboxylase activity is a necessary for MEK-induced skin tumorigenesis." Cancer Res. **65**: 572-578.

Feith, D. J., S. Origanti, P. L. Shoop, S. Sass-Kuhn and L. M. Shantz (2006). "Tumor suppressor activity of ODC antizyme in MEK-driven skin tumorigenesis." Carcinogenesis. **27**(5): 1090-1098.

Feith, D. J., S. Origanti, P. L. Shoop, S. Sass-Kuhn and L. M. Shantz (2006). "Tumour suppressor activity of ODC1 antizyme in MEK-driven skin tumorigenesis." Carcinogenesis. **27**(5): 1090-1098.

Feith, D. J., L. M. Shantz, P. L. Shoop, K. A. Keefer, C. Prakashagowda and A. E. Pegg (2007). "Mouse skin chemical carcinogenesis is inhibited by antizyme in promotion-sensitive and promotion-resistant genetic backgrounds." Mol Carcinog. **46**(6): 453-465.

Frydman, B., R. B. Frydman, C. De los Santos, D. A. Garrido, S. H. Goldemberg and I. D. Algranati (1984). "Putrescine distribution in Escherichia coli studied in vivo by 13C nuclear magnetic resonance." Biochim Biophys Acta **805**(4): 337-344.

Fuchs, E. (1995). "Keratins and the skin." Annu Rev Cell Dev Biol **11**: 123-153.

Fuchs, E. and S. Raghavan (2002). "Getting under the skin of epidermal morphogenesis." Nat Rev Genet **3**(3): 199-209.

Fujimoto, W., G. Nakanishi, J. Arata and A. M. Jetten (1997). "Differential expression of human cornifin alpha and beta in squamous differentiating epithelial tissues and several skin lesions." J Invest Dermatol **108**(2): 200-204.

Gamble, L. D., M. D. Hogarty, X. Liu, D. S. Ziegler, G. Marshall, M. D. Norris and M. Haber (2012). "Polyamine pathway inhibition as a novel therapeutic approach to treating neuroblastoma." Front Oncol **2**: 162.

Gangatirkar, P., S. Paquet-Fifield, A. Li, R. Rossi and P. Kaur (2007). "Establishment of 3D organotypic cultures using human neonatal epidermal cells." Nat Protoc **2**(1): 178-186.

Gangatirkar, P., S. Paquet-Fifield, A. Li, R. Rossi and P. Kaur (2007). "Establishment of 3D organotypic cultures using human neonatal epidermal cells." Nature Publishing Group **2**(1): 178-186.

Garrod, D. and M. Chidgey (2008). "Desmosome structure, composition and function." Biochim Biophys Acta **1778**(3): 572-587.

Gerner, E. W. and F. L. J. Meyskens (2004). "Polyamines and cancer: old molecules, new understanding." Nat. Rev. Cancer **4**: 781-792.

Gilhar, A., Y. Ullmann, R. Karry, R. Shalaginov, B. Assy, S. Serafimovich and R. S. Kalish (2004). "Aging of human epidermis: reversal of aging changes correlates with reversal of keratinocyte fas expression and apoptosis." J Gerontol A Biol Sci Med Sci **59**(5): 411-415.

Gilmour, S. K. (2007). "Polyamines and Nonmelanoma Skin Cancer." Toxicol Appl Pharmacol. **224**(3): 249-256.

Gimelli, G., S. Giglio, O. Zuffardi, L. Alhonen, S. Suppola, R. Cusano, C. Lo Nigro, R. Gatti, R. Ravazzolo and M. Seri (2002). "Gene dosage of the spermidine/spermine N(1)-acetyltransferase (SSAT) gene with putrescine accumulation in a patient with a Xp21.1p22.12 duplication and keratosis follicularis spinulosa decalvans (KFSD)." Hum Genet. **111**(3): 235-241.

Gottlieb-Abraham, E., D. E. Shvartsman, J. C. Donaldson, M. Ehrlich, O. Gutman, G. S. Martin and Y. I. Henis (2013). "Src-mediated caveolin-1 phosphorylation affects the targeting of active Src to specific membrane sites." Mol Biol Cell **24**(24): 3881-3895.

Grillo, M. A. (1985). "Metabolism and function of polyamines." Int J Biochem **17**(9): 943-948.

Guo, L., H. Chen, T. Li, Q. Zhou and Y. Sui (2013). "An Aquaporin 3-Notch1 Axis in Keratinocyte Differentiation and Inflammation." PLoS One **8**(11): e80179.

Gupta, V. K., L. Scheunemann, T. Eisenberg, S. Mertel, A. Bhukel, T. S. Koemans, J. M. Kramer, K. S. Liu, S. Schroeder, H. G. Stunnenberg, F. Sinner, C. Magnes, T. R. Pieber, S. Dipt, A. Fiala, A. Schenck, M. Schwaerzel, F. Madeo and S. J. Sigrist (2013). "Restoring polyamines protects from age-induced memory impairment in an autophagy-dependent manner." Nat Neurosci **16**(10): 1453-1460.

Han, B., E. A. Rorke, G. Adhikary, Y. C. Chew, W. Xu and R. L. Eckert (2012). "Suppression of AP1 transcription factor function in keratinocyte suppresses differentiation." PLoS One **7**(5): e36941.

Hara-Chikuma, M., K. Takahashi, S. Chikuma, A. S. Verkman and Y. Miyachi (2009). "The expression of differentiation markers in aquaporin-3 deficient epidermis." Arch Dermatol Res **301**(3): 245-252.

Hayes, C. S., M. R. Burns and S. K. Gilmour (2014). "Polyamine blockade promotes antitumor immunity." Oncoimmunology **3**(1): e27360.

Hayes, C. S., A. C. Shicora, M. P. Keough, A. E. Snook, M. R. Burns and S. K. Gilmour (2014). "Polyamine-blocking therapy reverses immunosuppression in the tumor microenvironment." Cancer Immunol Res **2**(3): 274-285.

Heby, O., L. Persson and S. S. Smith (1988). "Polyamines, DNA methylation and cell differentiation." Adv Exp Med Biol **250**: 291-299.

Helariutta, Y., P. Elomaa, M. Kotilainen, P. Seppanen and T. H. Teeri (1993). "Cloning of cDNA coding for dihydroflavonol-4-reductase (DFR) and characterization of dfr expression in the corollas of Gerbera hybrida var. Regina (Compositae)." Plant Mol Biol **22**(2): 183-193.

Heller, J. S., W. F. Fong and E. S. Canellakis (1976). "Induction of a protein inhibitor to ornithine decarboxylase by the end products of its reaction." Proc Natl Acad Sci U S A **73**(6): 1858-1862.

Herman, M. L., S. Farasat, P. J. Steinbach, M. H. Wei, O. Toure, P. Fleckman, P. Blake, S. J. Bale and J. R. Toro (2009). "Transglutaminase-1 gene mutations in autosomal recessive congenital ichthyosis: summary of mutations (including 23 novel) and modeling of TGase-1." Hum Mutat **30**(4): 537-547.

Hewett, D., L. Samuelsson, J. Polding, F. Enlund, D. Smart, K. Cantone, C. G. See, S. Chadha, A. Inerot, C. Enerback, D. Montgomery, C. Christodolou, P. Robinson, P. Matthews, M. Plumpton, J. Wahlstrom, G. Swanbeck, T. Martinsson, A. Roses, J. Riley and I. Purvis (2002). "Identification of a psoriasis susceptibility candidate gene by linkage disequilibrium mapping with a localized single nucleotide polymorphism map." Genomics **79**(3): 305-314.

Hill, J. R. and D. R. Morris (1993). "Cell-specific translational regulation of S-adenosylmethionine decarboxylase mRNA. Dependence on translation and coding capacity of the cis-acting upstream open reading frame." J Biol Chem **268**(1): 726-731.

Hiramatsu, Y., K. Eguchi and K. Sekiba (1985). "Alterations in polyamine levels in amniotic fluid, plasma and urine during normal pregnancy." Acta Med Okayama. **39**(5): 339-346.

Hobbs, C. A. and S. K. Gilmour (2000). "High levels of intracellular polyamines promote histone acetyltransferase activity resulting in chromatin hyperacetylation." J Cell Biochem **77**: 345-360.

Hobbs, C. A., B. A. Paul and S. K. Gilmour (2002). "Deregulation of polyamine biosynthesis alters intrinsic histone acetyltransferase and deacetylase activities in murine skin and tumors." Cancer Res. **62**: 67-74.

Hogarty, M. D., M. D. Norris, K. Davis, X. Liu, N. F. Evageliou, C. S. Hayes, B. Pawel, R. Guo, H. Zhao, E. Sekyere, J. Keating, W. Thomas, N. C. Cheng, J. Murray, J. Smith, R. Sutton, N. Venn, W. B. London, A. Buxton, S. K. Gilmour, G. M. Marshall and M. Haber (2008). "ODC1 is a critical determinant of MYCN oncogenesis and a therapeutic target in neuroblastoma." Cancer Res **68**(23): 9735-9745.

Holland, D. B., E. J. Wood, W. J. Cunliffe and D. M. Turner (1989). "Keratin gene expression during the resolution of psoriatic plaues: effect of dithranol, PUVA, etretinate and hydrixyurea regimens." Br. J. Dermatol. **120**: 9-19.

Horn, Y., P. J. Schechter and L. J. Marton (1987). "Phase I-II clinical trial with alpha-difluoromethylornithine-an inhibitor of polyamine biosynthesis." Eur. J. Cancer Clin. Oncol. **23**: 1103-1107.

Hu, J., L. Zhang, Q. Chen, J. Lin, S. Wang, R. Liu, W. Zhang, K. Miao and T. Shou (2017). "Knockdown of CPEB4 expression suppresses cell migration and invasion via Akt pathway in non-small cell lung cancer." Cell Biol Int.

Huang da, W., B. T. Sherman and R. A. Lempicki (2009). "Bioinformatics enrichment tools: paths toward the comprehensive functional analysis of large gene lists." Nucleic Acids Res **37**(1): 1-13.

Huang da, W., B. T. Sherman and R. A. Lempicki (2009). "Systematic and integrative analysis of large gene lists using DAVID bioinformatics resources." Nat Protoc **4**(1): 44-57.

Hyvönen, M. T., T. Koponen, J. Weisell, M. Pietilä, A. R. Khomutov, J. Vepsäläinen, L. Alhonen and T. A. Keinänen (2013). "Spermidine promotes adipogenesis of 3T3-L1 cells by preventing interaction of ANP32 with HuR and PP2A." Biochem J **453**: 467-474.

Igarashi, K. and K. Kashiwagi (2000). "Polyamines: mysterious modulators of cellular functions." Biochem. Biophys. Res. Commun. **271**: 559-564.

Igarashi, K. and K. Kashiwagi (2006). "Polyamine Modulon in Escherichia coli: genes involved in the stimulation of cell growth by polyamines." J Biochem **139**(1): 11-16.

Igarashi, K. and K. Kashiwagi (2010). "Modulation of cellular function by polyamines." Int J Biochem Cell Biol **42**(1): 39-51.

Igarashi, K. and K. Kashiwagi (2010). "Modulation of cellular function by polyamines." The International Journal of Biochemistry & Cell Biology **42**: 39-51.

Igarashi, K. and K. Kashiwagi (2011). "Characterization of genes for polyamine modulon." Methods Mol Biol **720**: 51-65.

Igarashi, K. and K. Kashiwagi (2015). "Modulation of protein synthesis by polyamines." IUBMB Life **67**(3): 160-169.

Igarashi, K., K. Kashiwagi, H. Hamasaki, A. Miura, T. Kakegawa, S. Hirose and S. Matsuzaki (1986). "Formation of a compensatory polyamine by Escherichia coli polyamine-requiring mutants during growth in the absence of polyamines." J Bacteriol **166**(1): 128-134.

Ivanov, I. P. and J. F. Atkins (2007). "Ribosomal frameshifting in decoding antizyme mRNAs from yeast and protists to humans: close to 300 cases reveal remarkable diversity despite underlying conservation." Nucleic Acids Res **35**(6): 1842-1858.

Ivanov, I. P., G. Loughran and J. F. Atkins (2008). "uORFs with unusual translational start codons autoregulate expression of eukaryotic ornithine decarboxylase homologs." Proc Natl Acad Sci U S A **105**(29): 10079-10084.

Jansen, M., C. H. de Moor, J. S. Sussenbach and J. L. van den Brande (1995). "Translational control of gene expression." Pediatr Res **37**(6): 681-686.

Jensen, J. M., R. Fölster-Holst, A. Baranowsky, M. Schunck, S. Winoto-Morbach, C. Neumann, S. Schütze and E. Proksch (2004). "Impaired sphingomyelinase activity and epidermal differentiation in atopic dermatitis." J. Invest. Dermatol. **122**(6): 1423-1431.

Kalinin, A., L. N. Marekov and P. M. Steinert (2001). "Assembly of the epidermal cornified cell envelope." Journal of Cell Science **114**: 3069-3070.

Kapyaho, K., J. Lauharanta and J. Janne (1982). "Combined topical use of difluoromethyl ornithine and methylglyoxal bis(guanylhydrazone) in UV-irradiated mouse skin." Br. J. Dermatol. **107**: 415-422.

Kapyaho, K., K. Linnamma and J. Janne (1982). "Effect of epidermal polyamine depletion on the accumulation of methylglycoxyl bis(guanylhydrazone) in mouse skin." J Invest Dermatol. **78**: 391-394.

Kashiwagi, K., Y. Terui and K. Igarashi (2018). "Modulation of Protein Synthesis by Polyamines in Mammalian Cells." Methods Mol Biol **1694**: 325-336.

Kawasaki, H., A. Kubo and T. Sasaki (2011). "Loss-of-function mutations withing the filaggrin gene and atopic dermatitis." Curr. Probl. Dermatol. **41**: 35-46.

Kim, K. C., W. J. Oh, K. H. Ko, C. Y. Shin and D. G. Wells (2011). "Cyclin B1 expression regulated by cytoplasmic polyadenylation element binding protein in astrocytes." J Neurosci **31**(34): 12118-12128.

Kondo, T. and V. J. Hearing (2011). "Update on the regulation of mammalian melanocyte function and skin pigmentation." Expert Rev Dermatol **6**(1): 97-108.

Koomoa, D. L., L. P. Yco, T. Borsics, C. J. Wallick and A. S. Bachmann (2008). "Ornithine decarboxylase inhibition by alpha-difluoromethylornithine activates opposing signaling pathways via phosphorylation of both Akt/protein kinase B and p27Kip1 in neuroblastoma." Cancer Res **68**(23): 9825-9831.

Korhonen, V. P., K. Niiranen, M. Halmekyto, M. Pietila and P. Diegelman (2001). "Spermine deficiency resulting from targeted disruption of thr spermine synthase gene in embryonic stem cells leads to enhanced sensitivity to antiproliferative drugs." Mol. Pharmacol. **59**: 231-238.

Koster, M. I. and D. R. Roop (2004). "The role of p63 in development and differentiation of the epidermis." J Dermatol Sci **34**(1): 3-9.

Kousa, M., K. Kapyaho, J. Lauharanta, K. Linnamaa, J. Janne and K. Mustakallio (1982). "Methylglycoxyl bys(guanylhydrazone) and α-difluoromethylornithine-induced polyamine deprivation in psoriatic lesions." Acta Derm Venereol (Stock) **62**: 221-224.

Kubo, A., M. Kajimura and M. Suematsu (2012). "Matrix-Assisted Laser Desorption/Ionization (MALDI) Imaging Mass Spectrometry (IMS): A Challenge for Reliable Quantitative Analyses." Mass Spectrom (Tokyo). **1**(1): A0004.

Kuechle, M. K., C. D. Thulin, R. B. Presland and B. A. Dale (1999). "Profilaggrin requires both linker and filaggrin peptide sequences to form granules: implications for profilaggrin processing in vivo." J Invest Dermatol **112**(6): 843-852.

Kurian, L., R. Palanimurugan, D. Godderz and R. J. Dohmen (2011). "Polyamine sensing by nascent ornithine decarboxylase antizyme stimulates decoding of its mRNA." Nature **477**(7365): 490-494.
Kypriotou, M., M. Huber and D. Hohl (2012). "The human epidermal differentiation complex: cornified envelope precursors, S100 proteins and the 'fused genes' family." Exp Dermatol **21**(9): 643-649.

Lam, K., L. Zhang, M. Bewick and R. M. Lafrenie (2005). "HSG cells differentiated by culture on extracellular matrix involves induction of S-adenosylmethione decarboxylase and ornithine decarboxylase." J Cell Physiol **203**(2): 353-361.

Lan, L., C. S. Hayes, L. Laury-Kleintop and S. K. Gilmour (2005). "Suprabasal induction of ornithine decarboxylase in adult mouse skin is sufficient to activate keratinocytes." J. Invest. Dermatol. **124**: 602-614.

Lan, L., C. S. Trempus and S. K. Gilmour (2000). "Inhibition of ornithine decarboxylase (ODC) decreases tumour vascularization and reverses spontaneous tumours in ODC/Ras transgenic mice." Cancer Res. **60**: 5696-5703.

Larqué, E., M. Sabater-Molina and S. Zamora (2007). "Biological significance of dietary polyamines." Nutrition. **23**(1): 87-95.

Law, G. L., A. Raney, C. Heusner and D. R. Morris (2001). "Polyamine regulation of ribosome pausing at the upstream open reading frame of S-adenosylmethionine decarboxylase." J Biol Chem **276**(41): 38036-38043.

Lechler, T. and E. Fuchs (2005). "Asymmetric cell divisions promote stratification and differentiation of mammalian skin." Nature Publishing Group **437**: 275-280.

Lechler, T. and E. Fuchs (2007). "Desmoplakin: an unexpected regulator of microtubule organization in the epidermis." J. Cell Biol. **176**: 147-154.

Lee, S. H., S. K. Jeong and S. K. Ahn (2006). "An update of the defensive barrier function of skin." Yonsei Med J **47**(3): 293-306.

Lee, Y. S., S. H. Yuspa and A. A. Dlugosz (1998). "Differentiation of cultured human epidermal keratinocytes at high cell densities is mediated by endogenous activation of the protein kinase C signaling pathway." J Invest Dermatol. **111**(5): 762-766.

Leveue, J., F. Foucher, J. Y. Bansard, R. Havouis, J. Y. Grall and J. P. Moulinous (2000). "Polyamine profiles in tumour, normal tissue of the homologous breast, blood and urine of breast cancer suffers." Breast Cancer Res. Treat. **60**: 99-105.

Li, C., S. Guo, M. Zhang, J. Gao and Y. Guo (2015). "DNA methylation and histone modification patterns during the late embryonic and early postnatal development of chickens." Poult Sci **94**(4): 706-721.

Li, L., T. Tennenbaum and S. H. Yuspa (1996). "Suspension-induced murine keratinocyte differentiation is mediated by calcium." J Invest Dermatol. **106**(2): 254-260.

Li, X., B. Stebbins, L. Hoffman, G. Pratt, M. Rechsteiner and P. Coffino (1996). "The N terminus of antizyme promotes degradation of heterologous proteins." J Biol Chem **271**(8): 4441-4446.

Lightfoot, H. L. and J. Hall (2014). "Endogenous polyamine function--the RNA perspective." Nucleic Acids Res **42**(18): 11275-11290.

Lightfoot, H. L. and J. Hall (2014). "Endogenous polyamine function-the RNA perspective." Nucleic Acids Res. **42**(18): 11275-11290.

Liu, L., X. Guo, J. N. Rao, T. Zou, L. Xiao, T. Yu, J. A. Timmons, D. J. Turner and J. Y. Wang (2009). "Polyamines regulate E-cadherin transcription through c-Myc modulating intestinal epithelial barrier function." Am J Physiol Cell Physiol **296**(4): C801-810.

Liu, L., R. Santora, J. N. Rao, X. Guo, T. Zou, H. M. Zhang, D. J. Turner and J. Y. Wang (2003). "Activation of TGF-beta-Smad signaling pathway following polyamine depletion in intestinal epithelial cells." Am J Physiol Gastrointest Liver Physiol **285**(5): G1056-1067.

Liu, R., H. Liu, X. Chen, M. Kirby, P. O. Brown and K. Zhao (2001). "Regulation of CSF1 promoter by the SWI/SNF-like BAF complex." Cell **106**(3): 309-318.

Lonsdale-Eccles, J. D., D. C. Teller and B. A. Dale (1982). "Characterization of a phosphorylated form of the intermediate filament-aggregating protein filaggrin." Biochemistry **21**(23): 5940-5948.
Lowe, N. J., J. Breeding and D. Russell (1982). "Cutaneous polyamines in psoriasis." Br J Dermatol **107**(1): 21-25.

Luk, G. D., C. I. Civin, R. M. Weissman and S. B. Baylin (1982). "Ornithine decarboxylase: essential in proliferation but not differentiation of human promyelocytic leukemia cells." Science **216**: 75-77.

Luk, G. D., G. Goodwin, A. F. Gazdar and S. B. Baylin (1982). "Growth inhibitory effects of DL-alpha-difluoromethylornithine in the spectrum of human lung carcinoma cells in culture." Cancer Res. **42**: 3070-3073.

Mackintosh, C. A. and A. E. Pegg (2000). "Effect of spermine synthase deficiency on polyamine biosynthesis and content in mice and embryonic fibroblasts and the sensitivity of fibroblasts to 1,3-bis(2-chloroethyl)-N-nitrosourea. ." Biochem. J. **351**: 439-447.

Madan, M., A. Patel, K. Skruber, D. Geerts, D. A. Altomare and O. P. Iv (2016). "ATP13A3 and caveolin-1 as potential biomarkers for difluoromethylornithine-based therapies in pancreatic cancers." Am J Cancer Res **6**(6): 1231-1252.

Madeo, F., T. Eisenberg, S. Büttner, C. Ruckenstuhl and G. Kroemer (2010). "Spermidine: A novel autophagy inducer and longevity elixir." Autophagy **6**(1): 160-162.

Madeo, F., A. Zimmermann, M. C. Maiuri and G. Kroemer (2015). "Essential role for autophagy in life span extension." J Clin Invest **125**(1): 85-93.

Maris, J. M., C. Guo, P. S. White, M. D. Hogarty, P. M. Thompson, D. O. Stram, R. Gerbing, K. K. Matthay, R. C. Seeger and G. M. Brodeur (2001). "Allelic deletion at chromosome bands 11q14-23 is common in neuroblastoma." Med Pediatr Oncol **36**(1): 24-27.

Martinet, N., S. Beninati, T. P. Nigra and J. E. Folk (1990). "N1N8-bis(gamma-glutamyl)spermidine cross-linking in epidermal-cell envelopes. Comparison of cross-link levels in normal and psoriatic cell envelopes." Biochem J **271**(2): 305-308.

Mathews, M. B. and J. W. Hershey (2015). "The translation factor eIF5A and human cancer." Biochim Biophys Acta **1849**(7): 836-844.

Matkovics, B., V. Kecskemeti, S. I. Varga, Z. Novak and Z. Kertesz (1993). "Antioxidant properties of di- and polyamines." Comp Biochem Physiol B **104**(3): 475-479.

Matsufuji, S., T. Matsufuji, Y. Miyazaki, Y. Murakami, J. F. Atkins, R. F. Gesteland and S. Hayashi (1995). "Autoregulatory frameshifting in decoding mammalian ornithine decarboxylase antizyme." Cell **80**(1): 51-60.

McCullough, J. L., G. D. Weinstein, M. G. Rosenblum and J. J. Jenkins (1983). "Percutaneous Penetration of Methylglyoxal Bis(guanylhydrazone): Effects on Hairless Mouse Epidermis In Vivo." The Journal of Investigative Dermatology **81**(5): 388-392.

Megosh, L. C., S. K. Gilmour, D. Rosson, A. P. Soler, M. Blessing, J. A. Sawicki and T. G. O'Brien (1995). "Increased frequency of spontaneous skin tumours in transgenic mice which overexpress ornithnie decarboxylase." Cancer Res. **55**: 4205-4209.

Mehic, D., L. Bakiri, M. Ghannadan, E. F. Wagner and E. Tschachler (2005). "Fos and Jun Proteins Are Specifically Expressed During Differentiation of Human Keratinocytes." Journal of Investigative Dermatology **124**(1): 212-220.

Metcalf, B. W., P. Bey, C. Danzin, M. J. Jung, P. Casara and J. P. Vevert (1978). "Catalytic irreversible inhibition of mammalian ornithine decarboxylase (E.C4.1.1.17) by substrate and product analogues." J. Am. Chem. Soc. **100**: 2551-2553.

Meyskens, F. L., E. M. Kingsley, T. Glattke, L. Loescher and A. Booth (1986). "A phase II study of alpha-difluoromethylornithine (DFMO) for the treatment of metastatic melanoma." Invest. New Drugs. **4**: 257-262.

Michel M., L. H. N., Auger F. A., Germain L. (1997). "From newborn to adult: phenotypic and functional properties of skin equivalent and human skin as a function of donor age." J Cell Physiol. **171**(2): 179-189.

Miller-Fleming, L. and V. Olin-Sandoval (2015). "Remaining Mysteries of Molecular Biology: The Role of Polyamines in the Cell." J. Mol. Biol. **427**: 3389-3406.

Miller, A. M. and S. P. Schoenberger (2015). "Notch signaling maintains T cell memories." Nat Med **21**(1): 16-18.

Miner, J. H. and P. D. Yurchenco (2004). "Laminin functions in tissue morphogenesis." Annu Rev Cell Dev Biol **20**: 255-284.

Minois, N. (2014). "Molecular Basis of the 'Anti-Aging' Effect of Spermidine and Other Natural Polyamines – A Mini-Review " Gerontology **60**: 319-326.

Minois, N., D. Carmona-Gutierrez and F. Madeo (2011). "Polyamines in aging and disease." Aging (Albany NY) **3**(8): 716-732.

Minois, N., D. Carmona-Gutierrez and F. Madeo (2011). "Polyamines in aging and disease." Aging (Albany NY). **3**(8): 716-732.

Mokkapati, S., A. Baranowsky, N. Mirancea, N. Smyth, D. Breitkreutz and R. Nischt (2008). "Basement membranes in skin are differently affected by lack of nidogen 1 and 2." J Invest Dermatol **128**(9): 2259-2267.

Moll, R., M. Divo and L. Langbein (2008). "The human keratins: biology and pathology." Histochem Cell Biol **129**(6): 705-733.

Murakami, Y., S. Matsufuji, T. Kameji, S. Hayashi, K. Igarashi, T. Tamura, K. Tanaka and A. Ichihara (1992). "Ornithine decarboxylase is degraded by the 26S proteasome without ubiquitination." Nature. **360**: 597-599.

Muroyama, A. and T. Lechler (2017). "Microtubule organization, dynamics and functions in differentiated cells." Development **144**: 3012-3021.

Murray-Stewart, T. R., P. M. Woster and R. A. Casero (2016). "Targeting polyamine metabolism for cancer therapy and prevention." Biochemical Journal **473**: 2937-2953.

Murray-Stewart, T. R., P. M. Woster and R. A. Casero, Jr. (2016). "Targeting polyamine metabolism for cancer therapy and prevention." Biochem J **473**(19): 2937-2953.

Nandakumar, V., M. Vaid, T. O. Tollefsbol and S. K. Katiyar (2011). "Aberrant DNA hypermethylation patterns lead to transcriptional silencing of tumor suppressor genes in UVB-exposed skin and UVB-induced skin tumors of mice." Carcinogenesis **32**(4): 597-604.

Nicotera, P. and G. Melino (2007). "Caspase-14 and epidermis maturation." Nat Cell Biol **9**(6): 621-622.

Nishifuji, K. and J. S. Yoon (2013). "The stratum corneum: the rampart of the mammalian body." Vet Dermatol. **24**(1): 60-72.

Nishimura, K., N. Araki, Y. Ohnishi and S. Kozaki (2001). " Effects of dietary polyamine deficiency on Trypanosoma gambiense infection in rats. ." Exp. Parasitol. **97**: 95-101.

Nishimura, K., K. Murozumi, A. Shirahata, M. H. Park, K. Kashiwagi and K. Igarashi (2005). "Independent roles of eIF5A and polyamines in cell proliferation." Biochem J **385**(Pt 3): 779-785.

Nishimura, K., F. Nakatsu, K. Kashiwagi, H. Ohno, T. Saito and K. Igarashi (2002). "Essential role of S-adenosylmethionine decarboxylase in mouse embryonic development." Genes Cells **7**(1): 41-47.
Nishimura, K., R. Shiina, K. Kashiwagi and K. Igarashi (2006). "Decrease in polyamines with aging and their ingestion from food and drink." J. Biochem. **139**: 81-90.

Nishimura, K., R. Shiina, K. Kashiwagi and K. Igarashi (2006). "Decrease in polyamines with aging and their ingestion from food and drink." J Biochem **139**(1): 81-90.

Nowotarski, S. L., D. J. Feith and L. M. Shantz (2015). "Skin Carcinogenesis Studies Using Mouse Models with Altered Polyamines." Cancer Growth Metastasis. **8**(Suppl 1): 17–27.

Nowotarski, S. L., D. J. Feith and L. M. Shantz (2015). "Skin Carcinogenesis Studies Using Mouse Models with Altered Polyamines." Cancer Growth Metastasis **8**(Suppl 1): 17-27.

Nowotarski, S. L. and L. M. Shantz (2010). "Cytoplasmic accumulation of the RNA-binding protein HuR stabilizes the ornithine decarboxylase transcript in a murine nonmelanoma skin cancer model." J Biol Chem **285**(41): 31885-31894.

Nowotarski, S. L. and L. M. Shantz (2017). "The ODC 3'-Untranslated Region and 5'-Untranslated Region Contain cis-Regulatory Elements: Implications for Carcinogenesis." Med Sci (Basel) **6**(1).
Nowotarski, S. L., P. M. Woster and R. A. Casero (2013). "Polyamines and cancer: Implications for chemoprevention and chemotherapy." Expert Rev Mol Med. **15**: e3.

Nowotarski, S. L., P. M. Woster and R. A. Casero, Jr. (2013). "Polyamines and cancer: implications for chemotherapy and chemoprevention." Expert Rev Mol Med **15**: e3.

O'Brien, T. G., L. C. Megosh, G. Gilliard and A. Peralta Soler (1997). "Ornithine decarboxylase overexpression is a sufficient condition for tumour promotion in mouse skin." Cancer Res. **57**: 2630-2637.

O'Brien, T. G., R. C. Simsiman and R. K. Boutwell (1975). "Induction of the polyamine-biosynthetic enzymes in mouse epidermis and their specificity for tumour promotion." Cancer Res. **35**: 2426-2433.

Origanti, S., S. L. Nowotarski, T. D. Carr, S. Sass-Kuhn, L. Xiao, J. Y. Wang and L. M. Shantz (2012). "Ornithine decarboxylase mRNA is stabilized in an mTORC1-dependent manner in Ras-transformed cells." Biochem J **442**(1): 199-207.

Ota, T., S. Takekoshi, T. Takagi, K. Kitatani, K. Toriumi, T. Kojima, M. Kato, N. Ikoma, T. Mabuchi and A. Ozawa (2014). "Notch Signaling May Be Involved in the Abnormal Differentiation of Epidermal Keratinocytes in Psoriasis." Acta Histochem Cytochem. **47**(4): 175-183.

Palanimurugan, R., H. Scheel, K. Hofmann and R. J. Dohmen (2004). "Polyamines regulate their synthesis by inducing expression and blocking degradation of ODC antizyme." EMBO J. **23**(24): 4857-4867.

Palmer, C. N., A. D. Irvine and A. Terron-Kwiatkowski (2006). "Common loss-of-function variants of the epidermal barrier protein filaggrin are a major predisposing factor for atopic dermatitis." Nat. Genet. **38**: 441-446.

Pardoll, D. M. (2012). "The blockade of immune checkpoints in cancer immunotherapy." Nat Rev Cancer. **12**(4): 252-264.

Park, M. H. (2006). "The post-translational synthesis of a polyamine-derived amino acid, hypusine, in the eukaryotic translation initiation factor 5A (eIF5A)." J Biochem **139**(2): 161-169.

Park, M. H. and K. Igarashi (2013). "Polyamines and their metabolites as diagnostic markers of human diseases." Biomol Ther. **21**(1): 1-9.

Park, M. H. and K. Nishimura (2009). "Functional significance of eIF5A and its hypusine modification in eukaryotes." Amino Acids **38**(2): 491-500.

Pegg, A. E. (1988). "Polyamine metabolism and its importance in neoplastic growth as a target for chemotherapy." Cancer Res. **48**: 759-774.

Pegg, A. E. (2006). "Regulation of Ornithine Decarboxylase." The Journal of Biological Chemistry **281**: 14529-14532.

Pegg, A. E. (2009). "Mammalian polyamine metabolism and function." IUBMB Life **61**(9): 880-894.

Pegg, A. E. (2009). "Mammalian Polyamine Metabolism and Function." IUBMB Life **61**(9): 880-894.

Pegg, A. E. (2014). "The Function of Spermine." International Union of Biochemistry and Molecular Biology **66**(1): 8-18.

Pegg, A. E. (2016). "Function of Polyamines in Mammals." J. Biol. Chem. **291**(29): 14904-14912.
Pendeville, H., N. Carpino, J. C. Marine, Y. Takahashi, M. Muller and J. A. Martial (2001). "The ornithine decarboxylase gene is essential for cell survival during early murine development." Mol. Cell Biol. **21**: 6549-6558.

Peralta Soler, A., G. Gilliard, L. C. Megosh, K. George and T. G. O'Brien (1998). "Polyamines regulate expression of the neoplastic phenotype in mouse skin." Cancer Res. **58**: 1654-1659.

Piacentini, M., M. G. Farrace, M. Imparato, L. Piredda and F. Autuori (1990). "Polyamine-dependent post-translational modification of proteins in differentiating mouse epidermal cells." J Invest Dermatol **94**(5): 694-699.

Piacentini, M., M. G. Farrace, M. Imparato, L. Piredda and F. Autuori (1990). "Polyamine-dependent post-translational modification of proteins in differentiating mouse epidermal cells." J Invest Dermatol. **94**(5): 694-699.

Piacentini, M., N. Martinet, S. Beninati and J. E. Folk (1988). "Free and protein-conjugated polyamines in mouse epidermal cells. Effect of high calcium and retinoic acid." J Biol Chem **263**(8): 3790-3794.

Piacentini, M., N. Martinet, S. Beninati and J. E. Folk (1988). "Free and protein-conjugated polyamines in mouse epidermal cells. Effect of high calcium and retinoic acid." J Biol Chem. **263**(8): 3790-3794.

Pickard, A., P. P. Wong and D. J. McCance (2010). "Acetylation of Rb by PCAF is required for nuclear localization and keratinocyte differentiation." J Cell Sci. **123**(Pt 21): 3718-3726.

Pietilä, M., J. J. Parkkinen, L. Alhonen and J. Jänne (2001). "Relation of skin polyamines to the hairless phenotype in transgenic mice overexpressing spermidine/spermine N-acetyltransferase." J Invest Dermatol. **116**(5): 801-805.

Pietilä, M., E. Pirinen, S. Keskitalo, S. Juutinen, S. Pasonen-Seppänen, T. Keinänen, L. Alhonen and J. Jänne (2005). "Disturbed keratinocyte differentiation in transgenic mice and organotypic keratinocyte cultures as a result of spermidine/spermine N-acetyltransferase overexpression." J Invest Dermatol. **124**(3): 596-601.

Pleshkewych, A., D. L. Kramer, E. Kelly and C. W. Porter (1980). "Independence of drug action on mitochondria and polyamines in L1210 leukemia cells treated with methylglyoxal-bis(guanylhydrazone)." Cancer Res **40**(12): 4533-4540.

Pless, M., K. Belhadj, H. D. Menssen, W. Kern, B. Coiffier, J. Wolf, R. Herrmann, E. Thiel, D. Bootle, I. Sklenar, C. Muller, L. Choi, C. Porter and R. Capdeville (2004). "Clinical efficacy, tolerability, and safety of SAM486A, a novel polyamine biosynthesis inhibitor, in patients with relapsed or refractory non-Hodgkin's lymphoma: results from a phase II multicenter study." Clin Cancer Res **10**(4): 1299-1305.

Porter, C. W. and R. J. Bergeron (1983). "Spermidine reuirement for cell proliferation in eukaryotic cells: structural specificity and quantitation." Science **219**: 1083-1085.

Presland, R. B., D. Boggess, S. P. Lewis, C. Hull, P. Fleckman and J. P. Sundberg (2000). "Loss of normal profilaggrin and filaggrin in flaky tail (ft/ft) mice: an animal model for the filaggrin-deficient skin disease ichthyosis vulgaris." J Invest Dermatol **115**(6): 1072-1081.

Presland, R. B., P. V. Haydock, P. Fleckman, W. Nirunsuksiri and B. A. Dale (1992). "Characterization of the human epidermal profilaggrin gene. Genomic organization and identification of an S-100-like calcium binding domain at the amino terminus." J Biol Chem **267**(33): 23772-23781.

Proctor, M. S., H. V. Fletcher, J. B. Shukla and O. M. Rennert (1975). "Elevated Spermidine and Spermine Levels in the Blood of psoriasis patients." Journal of investigative dermatology **65**(4): 409-411.

Pucciarelli, S., B. Moreschini, D. Micozzi, G. S. De Fronzo, F. M. Carpi, V. Polzonetti, S. Vincenzetti, F. Mignini and V. Napolioni (2012). "Spermidine and spermine are enriched in whole blood of nona/centenarians." Rejuvenation Res **15**(6): 590-595.

Raney, A., G. L. Law, G. J. Mize and D. R. Morris (2002). "Regulated translation termination at the upstream open reading frame in s-adenosylmethionine decarboxylase mRNA." J Biol Chem. **277**(8): 5988-5994.

Rangarajan, A., C. Talora, R. Okuyama, M. Nicolas, C. Mammucari, H. Oh, J. C. Aster, S. Krishna, D. Metzger, P. Chambon, L. Miele, A. M., F. Radtke and G. P. Dotto (2001). "Notch signaling is a direct determinant of keratinocyte growth arrest and entry into differentiation." EMBO J. **20**(12): 3427-3436.

Razin, A. and R. Shemer (1995). "DNA methylation in early development." Hum Mol Genet **4 Spec No**: 1751-1755.

Regenass, U., G. Caravatti, H. Mett, J. Stanek, P. Schneider, M. Muller, A. Matter, P. Vertino and C. W. Porter (1992). "New S-adenosylmethionine decarboxylase inhibitors with potent antitumor activity." Cancer Res **52**(17): 4712-4718.

Regenass, U., H. Mett, J. Stanek, M. Mueller, D. Kramer and C. W. Porter (1994). "CGP 48664, a new S-adenosylmethionine decarboxylase inhibitor with broad spectrum antiproliferative and antitumor activity." Cancer Res **54**(12): 3210-3217.

Reijnders, C. M., A. van Lier, S. Roffel, D. Kramer, R. J. Scheper and S. Gibbs (2015). "Development of a Full-Thickness Human Skin Equivalent In Vitro Model Derived from TERT-Immortalized Keratinocytes and Fibroblasts." Tissue Eng Part A **21**(17-18): 2448-2459.

Rieder, C. L., S. Faruki and A. Khodjakov (2001). "The centrosome in vertebrates: more than a microtubule-organizing center." Trends Cell Biol. **11**(10): 413-419.

Rizzo, J. M., A. Oyelakin, S. Min, K. Smalley, J. Bard, W. Luo, J. Nyquist, E. Guttman-Yassky, T. Yoshida, A. D. Benedetto, L. A. Beck, S. Sinha and R.-A. Romano (2016). "ΔNp63 regulates IL-33 and IL-31 signaling in atopic dermatitis." Cell Death and Differentiation **23**: 1073-1085.

Roberson, E. D. and A. M. Bowcock (2010). "Psoriasis genetics: breaking the barrier." Trends Genet **26**(9): 415-423.

Rothenburg, S., F. Koch-Nolte, A. Rich and F. Haag (2001). "A polymorphic dinucleotide repeat in the rat nucleolin gene forms Z-DNA and inhibits promoter activity." Proc Natl Acad Sci U S A **98**(16): 8985-8990.

Rothnagel, J. A. and G. E. Rogers (1984). "Transglutaminase-mediated cross-linking in mammalian epidermis." Mol Cell Biochem **58**(1-2): 113-119.

Roy, U. K., N. S. Rial, K. L. Kachel and E. W. Gerner (2008). "Activated K-RAS increases polyamine uptake in human colon cancer cells through modulation of caveolar endocytosis." Mol Carcinog **47**(7): 538-553.

Russell, D. H. and T. A. McVicker (1972). "Polyamine biogenesis in the rat mammary gland during pregnancy and lactation." Biochem J. **130**(1): 71-76.

Samal, K., P. Zhao, A. Kendzicky, L. P. Yco, H. McClung, E. Gerner, M. Burns, A. S. Bachmann and G. Sholler (2013). "AMXT-1501, a novel polyamine transport inhibitor, synergizes with DFMO in inhibiting neuroblastoma cell proliferation by targeting both ornithine decarboxylase and polyamine transport." Int J Cancer **133**(6): 1323-1333.

Sanchez, A. D. and J. L. Feldman (2016). "Microtubule-organizing centers: from the centrosome to non-centrosomal sites." Current Opinion in Cell Biology **44**: 93-101.

Sandilands, A., C. Sutherland, A. D. Irvine and W. H. I. McLean (2009). "Filaggrin in the frontline: role in skin barrier function and disease." J Cell Sci. **122**(9): 1285-1294.

Seidenfeld, J. (1985). "Effects of difluoromethylornithine on proliferation, polyamine content and plating efficiency of cultured human carcinoma cells." Cancer Chemother. Pharmacol. **15**: 196-202.

Sen, G. L., L. D. Boxer, D. E. Webster, R. T. Bussat, K. Qu, B. J. Zarnegar, D. Johnston, Z. Siprashvili and P. A. Khavari (2012). "ZNF750 is a p63 target gene that induces KLF4 to drive terminal epidermal differentiation." Dev Cell **22**(3): 669-677.

Sen, G. L., L. D. Boxer, D. E. Webster, R. T. Bussat, K. Qu, B. J. Zarnegar, D. Johnston, Z. Siprashvili and P. A. Khavari (2012). "ZNF750 is a p63 Target Gene that Induces KLF4 to Drive Terminal Epidermal Differentiation." Dev Cell. **22**(3): 669-677.

Sen, G. L., J. A. Reuter, D. E. Webster, L. Zhu and P. A. Khavari (2010). "DNMT1 maintains progenitor function in self-renewing somatic tissue." Nature **463**(7280): 563-567.

Sen, G. L., D. E. Webster, D. I. Barragan, H. Y. Chang and P. A. Khavari (2008). "Control of differentiation in a self-renewing mammalian tissue by the histone demethylase JMJD3." Genes Dev **22**(14): 1865-1870.

Seneschal, J., R. A. Clark, A. Gehad, C. M. Baecher-Allan and T. S. Kupper (2012). "Human epidermal Langerhans cells maintain immune homeostasis in skin by activating skin resident regulatory T cells." Immunity **36**(5): 873-884.

Seppanen, P., H. Ruohola and J. Janne (1984). "Ethylglyoxal bis(guanylhydrazone) as an inhibitor of polyamine biosynthesis in L1210 leukemia cells." Biochim Biophys Acta **803**(4): 331-337.

Serafini-Fracassini, D., S. Del Duca, F. Monti, F. Poli, G. Sacchetti, A. M. Bregoli, S. Biondi and M. Della Mea (2002). "Transglutaminase activity during senescence and programmed cell death in the corolla of tobacco (Nicotiana tabacum) flowers." Cell Death Differ **9**(3): 309-321.

Shantz, L. M., Y. Guo, J. A. Sawicki, A. E. Pegg and T. G. O'Brien (2002). "Overexpression of a dominant-negative ornithine decarboxylase in mouse skin: effect on enzyme activity and papilloma formation." Carcinogenesis **23**(4): 657-664.

Shantz, L. M., R. H. Hu and A. E. Pegg (1996). "Regulation of ornithine decarboxylase in a transformed cell line that overexpresses translation initiation factor eIF-4E." Cancer Res **56**(14): 3265-3269.

Shantz, L. M. and A. E. Pegg (1999). "Translational regulation of ornithine decarboxylase and other enzymes of the polyamine pathway." Int J Biochem Cell Biol **31**(1): 107-122.

Shi, C., T. K. Cooper, D. E. McCloskey, A. B. Glick, L. M. Shantz and D. J. Feith (2012). "S-adenosylmethionine decarboxylase overexpression inhibits mouse skin tumor promotion." Carcinogenesis. **33**(7): 1310-1318.

Shin, J., J. S. Salameh and J. D. Richter (2016). "Impaired neurodevelopment by the low complexity domain of CPEB4 reveals a convergent pathway with neurodegeneration." Sci Rep **6**: 29395.

Siu, L. L., E. K. Rowinsky, L. A. Hammond, G. R. Weiss, M. Hidalgo, G. M. Clark, J. Moczygemba, L. Choi, R. Linnartz, N. C. Barbet, I. T. Sklenar, R. Capdeville, G. Gan, C. W. Porter, D. D. Von Hoff and S. G. Eckhardt (2002). "A phase I and pharmacokinetic study of SAM486A, a novel polyamine biosynthesis inhibitor, administered on a daily-times-five every-three-week schedule in patients with Advanced solid malignancies." Clin Cancer Res **8**(7): 2157-2166.

Smith, M. K., C. S. Trempus and S. K. Gilmour (1998). "Co-operation between follicular ornithine decarboxylase and v-Ha-ras induces spontaneous papillomas and malignant conversion in transgenic skin." Carcinogenesis. **19**: 1409-1415.

Smits, J. P. H., H. Niehues, G. Rikken, I. van Vlijmen-Willems, G. van de Zande, P. Zeeuwen, J. Schalkwijk and E. H. van den Bogaard (2017). "Immortalized N/TERT keratinocytes as an alternative cell source in 3D human epidermal models." Sci Rep **7**(1): 11838.

Soda, K. (2009). " Anti-aging effect of polyamine (No. 1)." New Food Industry **51**: 55-64.

Soda, K., Y. Kano, F. Chiba, K. Koizumi and Y. Miyaki (2013). "Increased polyamine intake inhibits age-associated alteration in global DNA methylation and 1,2-dimethylhydrazine-induced tumorigenesis." PLoS One **8**(5): e64357.

Sriram, G., P. L. Bigliardi and M. Bigliardi-Qi (2015). "Fibroblast heterogeneity and its implications for engineering organotypic skin models in vitro." Eur J Cell Biol **94**(11): 483-512.

Stevens, L. (1969). "The binding of spermine to the ribosomes and ribosomal ribonucleic acid from Bacillus stearothermophilus." Biochem J **113**(1): 117-121.

Stoler, A., R. Kopan, M. Duvic and E. Fuchs (1998). "Use of monospecific antisera and cRNA probes to localize the major changes in keratin expression during normal and abnormal epidermal differentiation." J. Cell Biol. **107**: 427-446.

Stuttgen, G. (1968). "Basic low molecular weight amines content of the skin." Fette Seifen Anstrichmittel **70**: 667-669.

Sumigray, K. D., H. Chen and T. Lechler (2011). "Lis1 is essential for cortical microtubule organization and desmosome stability in the epidermis." J Cell Biol **194**(4): 631-642.

Sumigray, K. D., H. Chen and T. Lechler (2011). "Lis1 is essential for cortical microtubule organization and desmosome stability in the epidermis." J. Cell Biol. **194**: 631-642.

Sumigray, K. D., H. P. Foote and T. Lechler (2012). "Noncentrosomal microtubules and type II myosins potentiate epidermal cell adhesion and barrier formation." J. Cell Biol. **199**: 513-525.

Sumigray, K. D. and T. Lechler (2011). "Control of cortical microtubule organization and desmosome stability by centrosomal proteins." Bioarchitecture **1**(5): 221-224.

Sun, B. K., L. D. Boxer, J. D. Ransohoff, Z. Siprashvili, K. Qu, V. Lopez-Pajares, S. T. Hollmig and P. A. Khavari (2015). "CALML5 is a ZNF750- and TINCR-induced protein that binds stratifin to regulate epidermal differentiation." Genes Dev **29**(21): 2225-2230.

Sun, T. T. and H. Green (1976). "Differentiation of the epidermal keratinocyte in cell culture: formation of the cornified envelope." Cell **9**(4 Pt 1): 511-521.

Swensson, O. and R. A. Eady (1996). "Morphology of the keratin filament network in palm and sole skin: evidence for site-dependent features based on stereological analysis." Arch Dermatol Res **288**(2): 55-62.

Tabor, C. W. and H. Tabor (1976). "1,4-Diaminobutane (putrescine), spermidine, and spermine." Annu Rev Biochem **45**: 285-306.

Tabor, C. W. and H. Tabor (1984). "Polyamines." Ann. Rev. Biochem. **53**: 749-790.

Takigawa, M., H. Inoue, E. Gohda, A. Asada, Y. Takeda and Y. Mori (1977). "The role of putrescine in cell proliferation of the skin of mice induced by ethylphenylpropriolate." Exp Mol Pathol **27**(2): 183-196.

Takigawa, M., A. K. Verma, R. C. Simsiman and R. K. Boutwell (1982). "Polyamine biosynthesis and skin tumor promotion: inhibition of 12-O-tetradecanoylphorbol-13-acetate-promoted mouse skin tumor formation by the irreversible inhibitor of ornithine decarboxylase alpha-difluoromethylornithine." Biochem Biophys Res Commun. **105**(3): 969-976.

Tang, X., A. L. Kim, D. J. Feith, A. E. Pegg, J. Russo, H. Zhang, M. Aszterbaum, L. Kopelovich, E. H. Epstein, D. R. Bickers and M. Athar (2004). "Ornithine decarboxylase is a target for chemoprevention of basal and squamous cell carcinomas in Ptch1+/- mice." J Clin Invest. **113**(6): 867-875.

Tarcsa, E., E. Candi, T. Kartasova, W. W. Idler, L. N. Marekov and P. M. Steinert (1998). "Structural and transglutaminase substrate properties of the small proline-rich 2 family of cornified cell envelope proteins." J Biol Chem **273**(36): 23297-23303.

Thewes, M., R. Stadler, B. Korge and D. Mischke (1991). "Normal psoriatic epidermis expression of hyperproliferation-associated keratins." Arch. Dermatol. Res. **283**: 465-471.

Thomas, T., M. A. Gallo, C. M. Klinge and T. J. Thomas (1995). "Polyamine-mediated conformational pertubations in DNA alter the binding of estrogen receptor to poly(dG-m5dC).poly(dG-m5dC) and a plasmid containing the estrogen response element." J. Steroid Biochem. Mol. Biol. **54**: 89-99.

Thomas, T., M. A. Gallo, C. M. Klinge and T. J. Thomas (1995). "Polyamine-mediated conformational perturbations in DNA alter the binding of estrogen receptor to poly(dG-m5dC).poly(dG-m5dC) and a plasmid containing the estrogen response element." J Steroid Biochem Mol Biol **54**(3-4): 89-99.

Thomas, T. and T. J. Thomas (2003). "Polyamine metabolism and cancer." J Cell Mol Med **7**(2): 113-126.

Thomas, T. and T. J. Thomas (2003). "Polyamine metabolism and cancer." J. Cell Mol. Med. **7**: 113-126.

Tiwari, A., C. A. Copeland, B. Han, C. A. Hanson, K. Raghunathan and A. K. Kenworthy (2016). "Caveolin-1 is an aggresome-inducing protein." Sci Rep **6**: 38681.

Tomitori, H., K. Kashiwagi and K. Igarashi (2012). "Structure and function of polyamine-amino acid antiporters CadB and PotE in Escherichia coli." Amino Acids **42**(2-3): 733-740.

Tsai, L. Y., Y. W. Chang, M. C. Lee, Y. C. Chang, P. I. Hwang, Y. S. Huang and C. F. Cheng (2016). "Biphasic and Stage-Associated Expression of CPEB4 in Hepatocellular Carcinoma." PLoS One **11**(5): e0155025.

Uemura, T. and E. W. Gerner (2011). "Polyamine transport systems in mammalian cells and tissues." Methods Mol Biol **720**: 339-348.

Uemura, T., K. Kashiwagi and K. Igarashi (2007). "Polyamine uptake by DUR3 and SAM3 in Saccharomyces cerevisiae." J Biol Chem **282**(10): 7733-7741.

Uemura, T., D. E. Stringer, K. A. Blohm-Mangone and E. W. Gerner (2010). "Polyamine transport is mediated by both endocytic and solute carrier transport mechanisms in the gastrointestinal tract." Am J Physiol Gastrointest Liver Physiol **299**(2): G517-522.

Uemura, T., H. F. Yerushalmi, G. Tsaprailis, D. E. Stringer, K. E. Pastorian, L. Hawel, 3rd, C. V. Byus and E. W. Gerner (2008). "Identification and characterization of a diamine exporter in colon epithelial cells." J Biol Chem **283**(39): 26428-26435.

Vasilopoulos, Y., M. J. Cork and R. Murphy (2004). "Genetic association between an AACC insertion in the 3'UTR of the stratum corneum chymotryptic enzyme gene and atopic dermatitis patients." J Invest Dermatol. **123**: 62-66.

Vaughan, M. B., R. D. Ramirez, C. M. Andrews, W. E. Wright and J. W. Shay (2009). "H-ras expression in immortalized keratinocytes produces an invasive epithelium in cultured skin equivalents." PLoS One **4**(11): e7908.

Vivo, M., N. de Vera, R. Cortes, G. Mengod, L. Camon and E. Martinez (2001). "Polyamines in the basal ganglia of human brain. Influence of aging and degenerative movement disorders." Neurosci Lett **304**(1-2): 107-111.

Vörsmann, H., F. Groeber, H. Walles, S. Busch, S. Beissert, H. Walczak and D. Kulms (2013). "Development of a human three-dimensional organotypic skin-melanoma spheroid model for in vitro drug testing." Cell Death & Disease **4**: e719.

Vuohelainen, S., E. Pirinen, M. Cerrada-Gimenez, T. A. Keinänen, M. Uimari, A. R. Khomutov, J. Jänne and L. Alhonen (2010). "Spermidine is indispensable in differentiation of 3T3-L1 fibroblasts to adipocytes." J Cell Mol Med **14**: 1683–1692.

Wallace, H. M. (2009). "The polyamines: past, present and future." Essays Biochem. **46**: 1-9.

Wallick, C. J., I. Gamper, M. Thorne, D. J. Feith, K. Y. Takasaki, S. M. Wilson, J. A. Seki, A. E. Pegg, C. V. Byus and A. S. Bachmann (2005). "Key role for p27Kip1, retinoblastoma protein Rb, and MYCN in polyamine inhibitor-induced G1 cell cycle arrest in MYCN-amplified human neuroblastoma cells." Oncogene **24**(36): 5606-5618.

Wang, P., S. M. Henning and D. Heber (2010). "Limitations of MTT and MTS-Based Assays for Measurement of Antiproliferative Activity of Green Tea Polyphenols." PLoS One **5**(4): e10202.

Wang, Y., W. Devereux, T. M. Stewart and R. A. Casero, Jr. (1999). "Cloning and characterization of human polyamine-modulated factor-1, a transcriptional cofactor that regulates the transcription of the spermidine/spermine N(1)-acetyltransferase gene." J Biol Chem **274**(31): 22095-22101.

Wei, G., C. A. Hobbs, K. DeFeo, C. S. Hayes and S. K. Gilmour (2007). "Polyamine-Mediated Regulation of Protein Acetylation in Murine Skin and Tumors." Molecular Carcinogenesis **46**: 611-617.

Welsh, P. A., S. Sass-Kuhn, C. Prakashagowda, D. McCloskey and D. Feith (2012). "Spermine synthase overexpression in vivo does not increase susceptibility to DMBA/TPA skin carcinogenesis or Min-Apc intestinal tumorigenesis." Cancer Biol Ther. **13**(6): 358-368.

Wickett, R. R. and M. O. Visscher (2006). "Structure and function of the epidermal barrier." American Journal of Infection Control **34**(10): S98-S110.

Wikramanayake, T. C., O. Stojadinovic and M. Tomic-Canic (2014). "Epidermal Differentiation in Barrier Maintenance and Wound Healing." Adv Wound Care (New Rochelle) **3**(3): 272-280.

Williams-Ashman, H. G. and Z. N. Canellakis (1979). "Polyamines in mammalian biology and medicine." Perspect Biol Med **22**(3): 421-453.

Williams-Ashman, H. G. and A. Schenone (1972). "Methyl glyoxal bis(guanylhydrazone) as a potent inhibitor of mammalian and yeast S-adenosylmethionine decarboxylases." Biochem Biophys Res Commun **46**(1): 288-295.

Williams, K. (1997). "Modulation and block of ion channels: a new biology of polyamines." Cell Signal **9**(1): 1-13.

Wu, H. Y., S. F. Chen, J. Y. Hsieh, F. Chou, Y. H. Wang, W. T. Lin, P. Y. Lee, Y. J. Yu, L. Y. Lin, T. S. Lin, C. L. Lin, G. Y. Liu, S. R. Tzeng, H. C. Hung and N. L. Chan (2015). "Structural basis of antizyme-mediated regulation of polyamine homeostasis." Proc Natl Acad Sci U S A **112**(36): 11229-11234.

Xie, Z., P. A. Singleton, L. Y. W. Bourguignon and B. D. D. (2005). "Calcium-induced Human Keratinocyte Differentiation Requires src- and fyn-mediated Phosphatidylinositol 3-Kinase–dependent Activation of Phospholipase C-γ1." Mol Biol Cell. **16**(7): 3236–3246.

Yordanova, M. M., G. Loughran, A. V. Zhdanov, M. Mariotti, S. J. Kiniry, P. B. F. O'Connor, D. E. Andreev, I. Tzani, P. Saffert, A. M. Michel, V. N. Gladyshev, D. B. Papkovsky, J. F. Atkins and P. V. Baranov (2018). "AMD1 mRNA employs ribosome stalling as a mechanism for molecular memory formation." Nature **553**(7688): 356-360.

Zabala-Letona, A., A. Arruabarrena-Aristorena, N. Martin-Martin, S. Fernandez-Ruiz, J. D. Sutherland, M. Clasquin, J. Tomas-Cortazar, J. Jimenez, I. Torres, P. Quang, P. Ximenez-Embun, R. Bago, A. Ugalde-Olano, A. Loizaga-Iriarte, I. Lacasa-Viscasillas, M. Unda, V. Torrano, D. Cabrera, S. M. van Liempd, Y. Cendon, E. Castro, S. Murray, A. Revandkar, A. Alimonti, Y. Zhang, A. Barnett, G. Lein, D. Pirman, A. R. Cortazar, L. Arreal, L. Prudkin, I. Astobiza, L. Valcarcel-Jimenez, P. Zuniga-Garcia, I. Fernandez-Dominguez, M. Piva, A. Caro-Maldonado, P. Sanchez-Mosquera, M. Castillo-Martin, V. Serra, N. Beraza, A. Gentilella, G. Thomas, M. Azkargorta, F. Elortza, R. Farras, D. Olmos, A. Efeyan, J. Anguita, J. Munoz, J. M. Falcon-Perez, R. Barrio, T. Macarulla, J. M. Mato, M. L. Martinez-Chantar, C. Cordon-Cardo, A. M. Aransay, K. Marks, J. Baselga, J. Tabernero, P. Nuciforo, B. D. Manning, K. Marjon and A. Carracedo (2017). "mTORC1-dependent AMD1 regulation sustains polyamine metabolism in prostate cancer." Nature **547**(7661): 109-113.

Zhang, D., T. Zhao, H. S. Ang, P. Chong, R. Saiki, K. Igarashi, H. Yang and L. A. Vardy (2012). "AMD1 is essential for ESC self-renewal and is translationally down-regulated on differentiation to neural precursor cells." Genes Dev. **26**(5): 461-473.

Zhao, T., K. J. Goh, H. H. Ng and L. A. Vardy (2012). "A role for polyamine regulators in ESC self-renewal." Cell Cycle **11**(24): 4517-4523.

Zhijun, L., W. Dapeng, J. Hong, W. Guicong, Y. Bingjian and L. Honglin (2017). "Overexpression of CPEB4 in glioma indicates a poor prognosis by promoting cell migration and invasion." Tumour Biol **39**(4): 1010428317694538.

Zimnicka, A. M., Y. S. Husain, A. N. Shajahan, M. Sverdlov, O. Chaga, Z. Chen, P. T. Toth, J. Klomp, A. V. Karginov, C. Tiruppathi, A. B. Malik and R. D. Minshall (2016). "Src-dependent phosphorylation of caveolin-1 Tyr-14 promotes swelling and release of caveolae." Mol Biol Cell **27**(13): 2090-2106.

Zwighaft, Z., R. Aviram, M. Shalev, L. Rousso-Noori, J. Kraut-Cohen, M. Golik, A. Brandis, H. Reinke, A. Aharoni, C. Kahana and G. Asher (2015). "Circadian Clock Control by Polyamine Levels through a Mechanism that Declines with Age." Cell Metab. **22**(5): 874-885.

APPENDIX

QUALIFYING EXAMINATION REPORT

(as attached from next page)

NANYANG TECHNOLOGICAL UNIVERSITY

Institute of Medical Biology

NANYANG TECHNOLOGICAL UNIVERSITY

SCHOOL OF BIOLOGICAL SCIENCE

Unravelling the 'ribosomal code' during epidermal stress

Ph.D. Qualifying Examination Report

Candidate: ANISA BANU BTE ABDUL RAHIM

Supervisor: DR. LEAH VARDY, A*STAR (IMB)

Co-supervisor: PROF. TAN SUET MIEN, NTU (SBS)

2015

Table of Contents

Table of Figures

1. Abstract

Control of mRNA translation is essential for the function and differentiation of many different cell types. This regulation is predominantly exerted by target specific microRNAs (miRNAs) and RNA binding proteins, which control the spatial and temporal expression of many proteins. Recently, the core of the ribosome itself has been shown to regulate the translation of specific mRNAs during embryonic development and this control is mediated by ribosomal proteins (RPs). The eukaryotic ribosome is composed of 4 RNA molecules and over 80 different RPs. There is considerable heterogeneity in RP composition of the ribosome in different cells types and under various environmental conditions. We are interested in understanding the role of RP heterogeneity in the skin during wound healing and osmotic stress. Polysome profiling of normal and osmotically stressed keratinocytes revealed that translation was repressed in keratinocytes subjected to osmotic stress while the polysome profiles of normal and wounded keratinocytes were comparable. iTRAQ™ labelling and subsequent mass spectrometry analysis of pooled translational fractions from normal and stressed keratinocytes showed that the majority of RPs remain unchanged under stress. We did, however identify a number of RPs and non-RPs that were either up or down-regulated upon keratinocyte stress. Here, we will discuss these results, drawbacks as well as additional studies aimed at characterizing the role of RPs/non-RPs in keratinocytes subjected to stress.

2. Introduction

2.1 The Eukaryotic Ribosome, Ribosome biogenesis and Ribosomal proteins

Ribosomes are functional molecular machines that play a pivotal role of catalysing protein synthesis [1-3]. In eukaryotes, the mature 80S ribosome comprises the small 40S and the large 60S subunits, which are made up of four ribosomal RNA (rRNA) molecules and over 80 ribosomal proteins (RPs) [4]. Ribosome synthesis is an energetically demanding process that accounts for more than 50% of cellular energy and is tightly coupled to the proliferative potential of a cell [2]. This process is accelerated in actively dividing cells such as cancer cells and perturbed during cellular stress or nutritional starvation [5]. It is precisely orchestrated by all three RNA polymerases and over 200 *trans*-acting factors associated with the ribosome. The 18S, 5.8S and 28S are three of the four rRNAs that are co-transcribed as a single transcript by RNA polymerase I (Pol I) in the nucleolus **(Figure 1)** [6]. The fourth rRNA, 5S, is transcribed independently by RNA Pol III in the nucleus. The pre-ribosomal RNA undergoes extensive modifications such as methylation and pseudouridylation before it is cleaved to form the mature rRNA [7]. The 18S rRNA together with 33 RPS are assembled to form the 40S subunit while the 28S, 5.8S and 5S rRNA together with the 47 RPL are assembled to form the large 60S subunit [6]. The individual 40S and 60S subunits are exported to the cytoplasm where they undergo maturation before decoding the cellular genome.

In addition to the role of RPs in regulating the assembly and function of the ribosome, many have extra-ribosomal functions [3, 8]. For example under nucleolar stress, RPL7 and RPL11 are implicated in the p53-mediated surveillance pathway where they sequester MDM2 from p53 to induce cell cycle arrest or apoptosis [3].

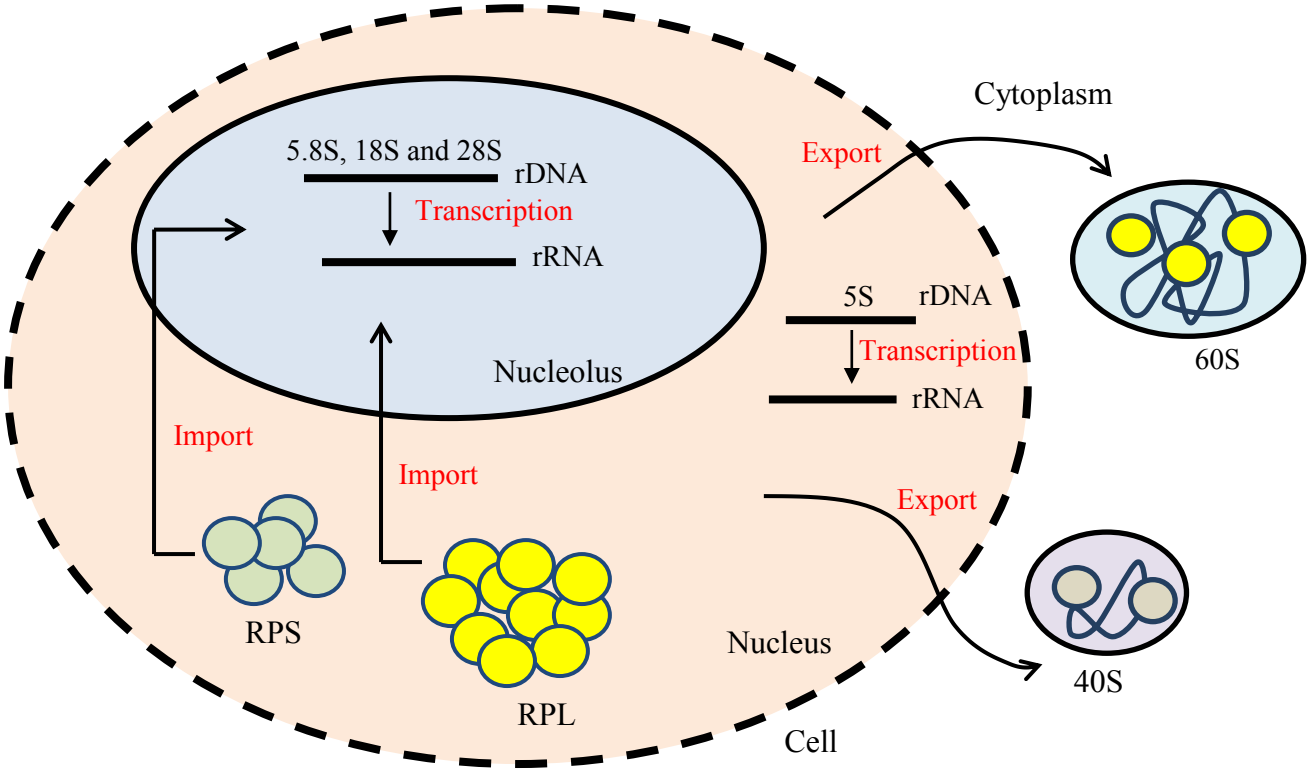

Figure 1: Eukaryotic ribosome biogenesis. The process of ribosome biogenesis comprises of rRNA processing in the nucleolus, the synthesis and import of RPs to the nucleolus and their assembly onto the pre-RNA and the subsequent transport of ribosomal subunits to the cytoplasm for maturation.

2.2 Translation and Translational Control

Gene expression is predominantly regulated at the level of transcription, RNA stability, translation, protein stability and its function. Although dramatic changes in transcription alter the RNA content of a cell, the process of translational control eventually determines the protein repertoire of a cell [9]. The basic mechanism of translation is well conserved throughout all forms of life due to the universality of the genetic code. However, eukaryotic protein translation involves a higher degree of regulation compared to prokaryotes and thus, requires a greater number of interacting factors and higher complexity of the ribosome. Protein translation is an extremely rapid and accurate process [2]. This speed is essential for organisms to respond to changing environmental conditions by regulating gene expression [10]. Protein translation is divided into three stages: initiation, elongation and termination. Translation is attenuated predominantly during initiation phase. For instance, the cap

recognition mediated by eIF4F-complex and ternary complex formation involving eIF2 are two key targets for controlling mRNA translation [11, 12]. Translational control of gene expression is predominantly exerted by target specific microRNAs (miRNAs) or RNA binding proteins that regulate the spatial and temporal expression of proteins [7, 13]. Recently, the ribosome itself has been shown to regulate gene expression, adding another layer of complexity to the cell's gene regulation.

2.3 Ribosomal protein expression and 'Specialized ribosomes'

For decades, ribosomes have been considered as unchanging homogenous entities responsible for protein synthesis. However, this notion has been challenged recently due to the accumulating evidence of cell and tissue specific expression of RPs. In *Arabidopsis thaliana* for instance, RPS5A is ubiquitously expressed in dividing cells while its paralog, RPS5B is restricted to cells undergoing differentiation **(Figure 2A)** [7]. Similarly, in *Drosophila melanogaster*, RPL22 is ubiquitously expressed on polysomes while RPL22L displays testis-specific polysomal expression **(Figure 2B)** [7]. While in human, RPS4Y1 is ubiquitously expressed, RPS4Y2 displays testis and prostate specificity **(Figure 2C)** [7].

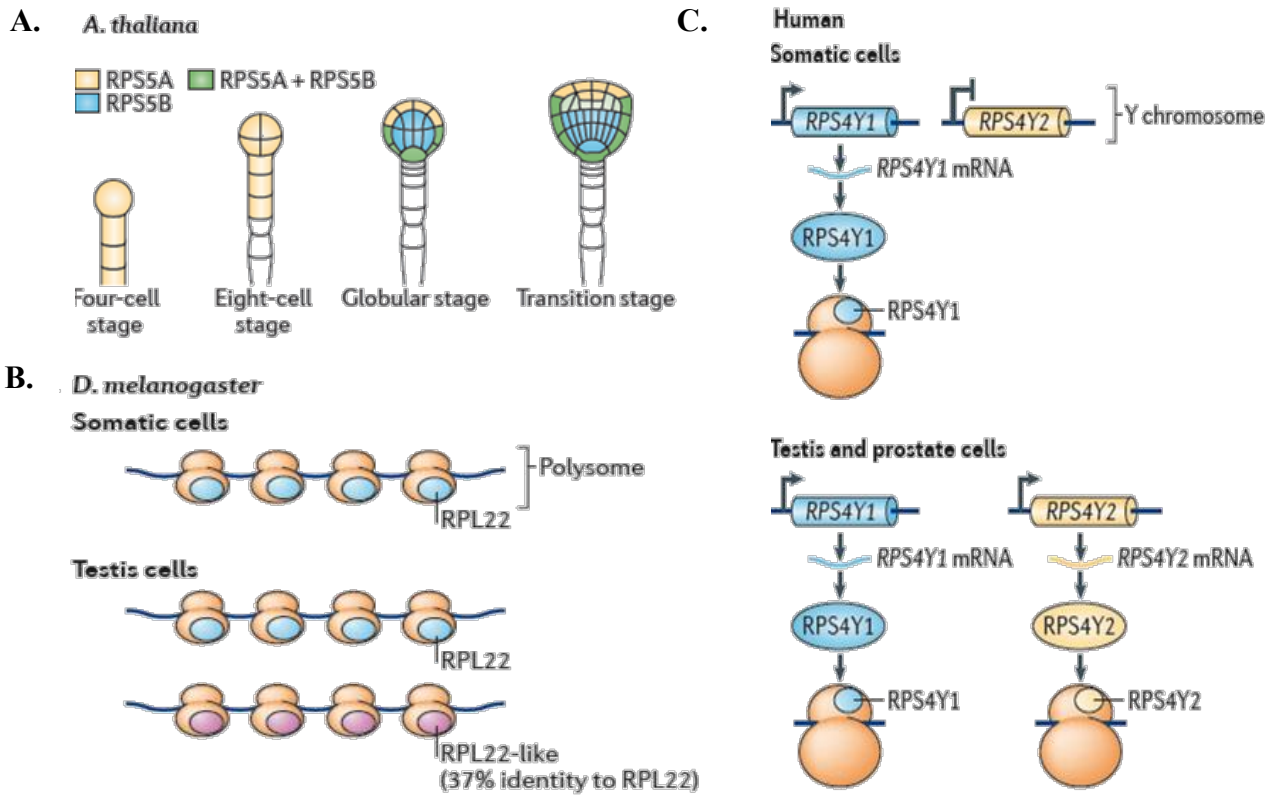

Figure 2: Heterogeneous ribosomes across different species. **A.** RPS5A displays high expression in dividing cells while RPS5B is expressed during cell differentiation in *Arabidopsis thaliana*. **B.** RPL22 is expressed on the polysomes of somatic cells while RPL22L is expressed on the polysomes of testis cells in *Drosophila melanogaster.* **C.** RPS4Y1 is expressed in human somatic cells while RPS4Y2 is restricted to the testis and prostate cells (Excerpted from *Nature Reviews*, 2012. **13**: p. 355-369).

In S. *cerevisiae*, ribosomal protein paralogs regulate the translation of *ASH1* mRNA. While the presence of RPL12a inhibits the translation of *ASH1* mRNA, its paralog RPL12b is selectively recruited onto ribosomes instead of RPL12a during yeast cell division [14]. RPL12b regulates *ASH1* mRNA translation and localization to the growing bud tip of the daughter cell, which is essential to prevent mating type switch [15]. This led to the idea of the 'ribosomal code', which refers to the functional specialization of 'heterogeneous' ribosomes toward a particular subset of mRNAs [15-17]. Additional evidence of RP mutations and its association with translational impairment of certain mRNAs is also mounting. For instance, RPL38 was demonstrated to be a ribosomal protein of the eukaryotic ribosome that is highly

enriched in the somites and neural tube of developing mouse embryos. The ablation of RPL38 in mice lead to the reduced translation of a particular subset of *Hox* mRNAs which was responsible for the establishment of the mammalian body plan [17, 18] **(Figure 3A)**. In a study published by our group recently, a microarray analysis was performed to delineate the gene expression pattern of 89 RPs across 22 different tissues [9]. Although most RP genes were homogenously expressed across different tissues, a particular subset of RP genes was identified that displayed heterogeneous expression across these tissues. These RP genes were RP paralogs that are known to be recently evolved **(Figure 3B)** [9]. These evidence suggest a crucial role of RPs in the translational control of a subset of mRNAs in different tissues.

A.

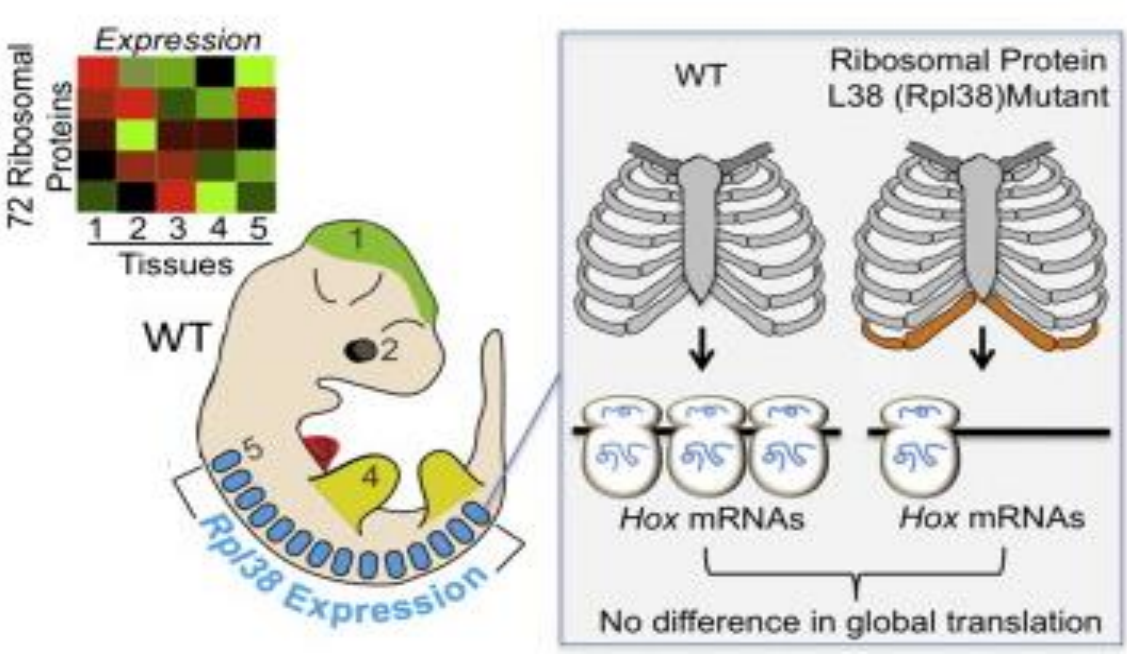

B.

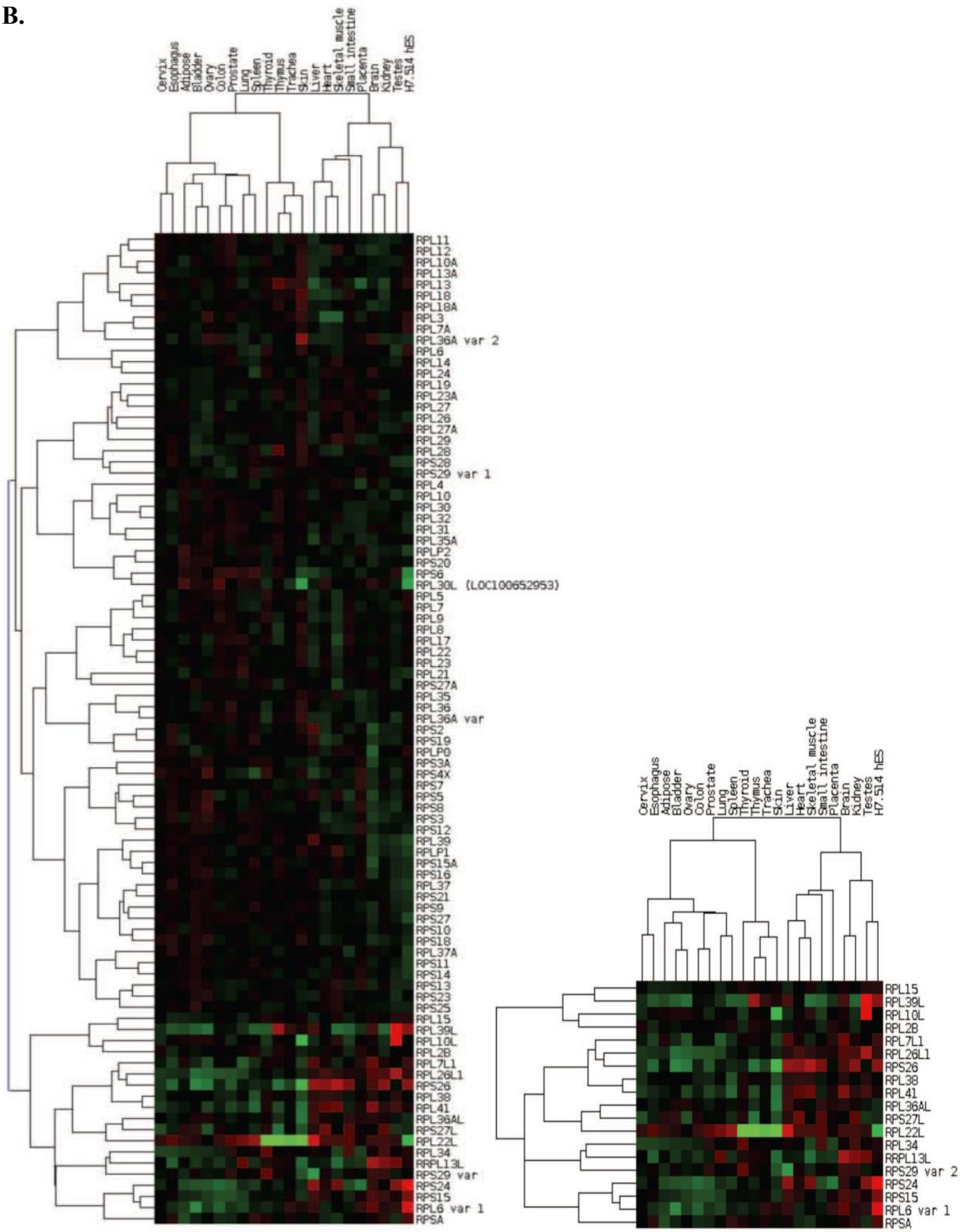

Figure 3: 'Specialized ribosomes'. A. RPL38 mutation impedes the translation of a particular subset of *Hox* mRNAs and thus leads to skeletal patterning defects in Ts/+ mice. (Excerpted from *Nature Reviews Molecular Cell Biology* (2011) **11**, 344-345). **B.** Heat map showing the hierarchical clustering of 89 RPs across 22 human tissues where a cluster of 19 RPs displayed heterogeneous expression among these tissues (Excerpted from *RNA Biology* (2014) **11**(1): p. 33-41).

2.4. Trans-acting factors on ribosomes

Apart from RPs, proteomic studies in *S. cerevisiae* have revealed 77 ribosome-associated proteins in polysomal fractions suggesting a role of *trans*-acting factors in modulating ribosome activity [19]. Cells lacking these factors displayed reduced rate and fidelity of protein translation as well as ribosome biogenesis. The ribosomal associated protein, Reaper, binds specifically to the 40S subunit of the ribosome in *D. melanogaster,* where it prevents cap-mediated translation initiation [19]. Knockdown of glycogen synthase 1 (GYS1) in HeLa cells, resulted in decreased polysomes and reduced translation of a particular subset of mRNAs [20]. These evidence persuade the possibility of distinct ribosomal composition in mediating translation, thereby adding another layer of complexity to the translational machinery.

2.5 Ribosomal protein deficiencies, development defects and diseases

Haploinsufficiency in one of several RPs results in minute phenotype in *D. melanogaster*, which is characterized by developmental defects and impaired fertility. Similarly, haploinsufficiency in RPS6, RPS19 and RPS20 in mice triggers p53 stabilization, eventually leading to melanocyte proliferation and increased pigmentation on footpads, tails and epidermis [21]. In humans, mutations in RPs cause disorders known as ribosomopathies [22]. Diamond-Blackfan Anaemia (DBA) is one such ribosomopathy that is caused by mutations in several ribosomal proteins, predominantly RPS19, which leads to bone marrow failure [23, 24]. Reduced levels of RPS19 perturbed the translation of certain mRNAs that correlated with the disease phenotype. Increased translation or aberrant expression of certain RPs is often associated with cancers. RPL19 is up-regulated in prostate cancers while the increased expression of certain RPs such as RPL39L is associated with more advanced hepatocellular carcinomas (HCC) [9, 25].

2.6 The epidermis

The skin is the largest organ of the body and is comprised of the dermis and epidermis **(Figure 4A)**. The epidermis, which is the outermost layer of the skin, is a dynamic tissue that builds a physical barrier to protect the body from harsh external agents, prevents dehydration and provides the first line of defense against physical, chemical and biological stresses. The epidermis is made up of a basal layer that is comprised of predominantly proliferative keratinocytes that are marked by keratin 14 (K14) **(Figure 4B)**. To maintain the integrity of the epidermis, keratinocytes undergo a complex process of differentiation. This involves structural and morphological changes in keratinocytes to give rise to spinous and granular layers that express keratin 10 (K10) and involucrin (IVL) as early and later markers of differentiation respectively **(Figure 4B)**. These layers eventually differentiate to form the stratum corneum composed of corneocytes that are completely devoid of nuclei. Filaggrin (FLG), a keratin filament associated protein essential for the formation of the skin barrier, is a marker of terminal differentiation **(Figure 4B)**. Several skin disorders are attributed to a defective skin barrier. For instance, atopic dermatitis (AD) is a skin disease which is characterized by dry itchy skin and is caused by filaggrin mutations [26]. Epidermolysis bullosa simplex (EBS), a disorder caused by epidermal basal keratin 5 (K5) and keratin 14 (K14) mutation is associated with excessive blistering and skin fragility [27]. Thus, understanding the role of translational control in regulating effective barrier formation becomes crucial.

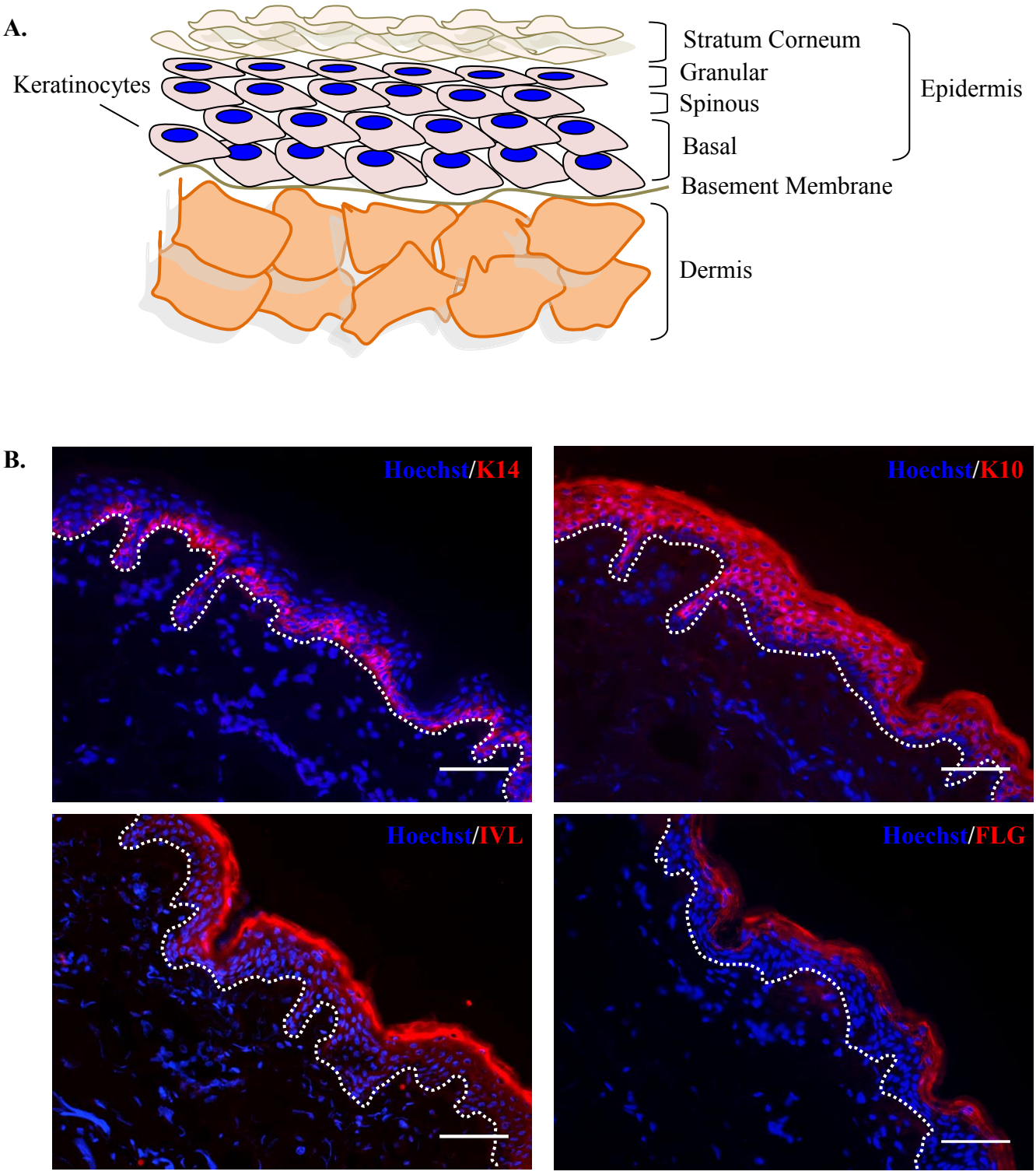

Figure 4: The Human Skin. A. The human skin comprises of the dermis and the epidermis. The epidermis is made up of 4 layers: basal, spinous, granular and stratum corneum. **B.** Keratin 14 (K14) is a maker of the basal layer of cells while keratin 10 (K10) and involucrin (IVL) are early and later markers of differentiation. The stratum corneum is indicated by filaggrin (FLG) which is a marker for terminal differentiation. White dotted lines indicate the basement membrane separating the dermis from the epidermis. Scale bar = 50μm.

2.7 Epidermal stress

The epidermis is constantly and variably subjected to harsh physical, chemical and environmental insults. The barrier function of the skin is usually compromised under the circumstance of a physical stress such as wounding or an osmotic stress such as dehydration [28]. A wound healing response is initiated as a consequence of a disrupted skin barrier function, which demands a series of tightly controlled events that occur in four phases: (i) hemostasis, (ii) inflammation, (iii) migration and proliferation of keratinocytes followed by (iv) keratinocyte maturation [29]. During hemostasis, fibrin clot formation occurs to seal the wound gap followed by the accumulation of neutrophils and macrophages at the wound bed to engulf bacteria and pathogens [30]. Migration of keratinocytes at the leading edge of the wound occurs at 24h post injury, accompanied by the proliferation and granulation of keratinocytes to close the wound [29].

Osmotic stress or dehydration is characterized by rapid loss of water from the surface of the epidermis. Hyper-osmosis leads to reduced flexibility and increased dryness of the skin. Extensive water loss over prolonged duration from the epidermis increases the susceptibility to infections and irritation of the skin. [31, 32].

2.8 Hypothesis and Aims

Hypothesis: Alteration in ribosome associated RPs or non-RPs occurs during epidermal stresses such as wounding and dehydration. This change in composition of the ribosome would result in 'heterogeneous ribosomes', which may be essential for the translation of a specific subset of mRNAs that are required for an effective stress response.

Aims: To validate our hypothesis, I will model wound healing in N/TERT-1 keratinocyte monolayer cultures using established scratch assays [33]. Osmotic stress will be modelled in

a 2D monolayer culture system using a high concentration of sorbitol, a sugar alcohol [32]. Sorbitol has been previously demonstrated to create a hyperosmotic stress condition within a short duration in treated keratinocytes [34]. This method has been used to mimics dehydration in cell cultures.

The rate of translation is usually determined by the number of ribosomes bound to an mRNA transcript. A heavily translating mRNA is bound by several ribosomes and is thus referred to as poly-ribosomes or polysomes. Polysome profiling is a technique that involves the velocity separation of translational complexes in linear sucrose gradients, allowing the distinct separation of non-translating and actively translating ribosomes [35]. To determine the role of RP heterogeneity or the recruitment of non-RPs during wounding and dehydration, activated and migratory keratinocytes post-wounding or osmotically stressed keratinocytes will be subjected to polysome profiling with their respective untreated controls. Actively translating ribosomes will be purified under both stress conditions, and subsequent iTRAQ™ labelling and mass spectrometry analysis will be performed to identify RP/non-RP differences under normal and stress conditions. RP/non-RP candidates that are significantly up/down regulated on polysomes during stress conditions will be shortlisted and validated by immunoblotting. Functional studies, such as shRNA knock-down will be performed on validated candidates to determine the role of these candidates during stress.

3. Material and Methods

3.1 Cell Culture and Reagents

N/TERT-1 keratinocytes were maintained in keratinocyte serum-free medium (KSFM) (Gibco®-BRL, Invitrogen, Merelbeke, Belgium) supplemented with 25µg/mL of bovine pituitary extract (BPE), 0.2ng/mL epidermal growth factor (EGF), 1% penicillin/streptomycin (P/S) and 0.09mM calcium chloride ($CaCl_2$) in a 37°C, 5% CO_2 incubator. Cells were grown to approximately 70% confluence before passaging and fresh medium was changed every other day. To achieve full confluence, cells were transited to DFK-2 medium prepared using a (1:1) mix of KSFM:DFK-1 medium. DFK-1 medium is a (1:1) mixture of Dulbecco's Modified Eagle Medium (DMEM) (HyClone™, Thermo Scientific, USA):F12 GlutaMAX™ medium (Gibco®-BRL, Invitrogen, Merelbeke, Belgium) containing 25µg/mL BPE, 0.2ng/mL EGF, 1% P/S and 1% L-glutamine.

3.2 Wound healing Assay

N/TERT-1 keratinocytes were seeded at a density of 0.8 million cells per 110cm^2 rectangular dishes (Nunc, Therno Scientific, Waltham, Massachusetts, USA) in KSFM supplemented with 25µg/mL BPE, 0.2ng/mL EGF, 1% P/S and 0.09mM $CaCl_2$. Cells were grown to approximately 70% confluence for 3 days and fresh KSFM was replaced on the third day. On the fourth day, KSFM was replaced with DFK-2 medium and cells were allowed to grow to full confluence for another 3 days. Wounds were made in the monolayer culture using a cell comb (Merck Millipore, Germany) or approximately 1cm apart from each other in the vertical direction using blue pipette tips. Cells were harvested at 2, 4, 6 or 24h post-scratch for protein extraction or ribosome purification with a no scratch control.

3.3 Sorbitol Stress Treatment

N/TERT-1 keratinocytes were seeded at a density of 0.5 million cells per 150mm tissue culture dishes (Corning) in KSFM supplemented with 25µg/mL of BPE, 0.2ng/mL EGF, 1% P/S and 0.09mM $CaCl_2$ and grown to approximately 50% confluence for 2 days. Forty-eight hours prior to treatment, cells were starved with growth factor deprived KSFM supplemented with 1% P/S and 0.09mM $CaCl_2$. Keratinocytes were incubated with growth factor deprived medium (control) or with the same medium made hypertonic with 200mM sorbitol (Sigma-Aldrich, Bornem, Belgium). Cells were harvested at 1, 2, 4, 6, 8 and 12h after addition of sorbitol for protein extraction and ribosome purification with an untreated control.

3.4 Polysome Profiling

N/TERT-1 keratinocytes were treated with 100µg/mL of cycloheximide (Sigma-Aldrich, Bornem, Belgium) for 10 mins in a 37°C, 5% CO_2 incubator. Cells were washed with warm phosphate buffered saline (PBS) containing 100µg/mL of cycloheximide and incubated with 0.25% trypsin/EDTA (Gibco®-BRL, Invitrogen, Merelbeke, Belgium) containing 100µg/mL of cycloheximide in a 37°C, 5% CO_2 incubator for 7 mins. Trypsin was neutralized with ice-cold DMEM (Thermo Scientific, HyClone™) containing 10% Fetal bovine serum (FBS), 1% P/S and 100µg/mL of cycloheximide and cells were transferred to pre-chilled falcon tubes. Cells were pelleted at 1,500 rpm for 5 mins at 4°C and washed twice with ice-cold PBS containing 100µg/mL of cycloheximide. 2X re-suspension buffer (RSB) was prepared by using 20mM Tris-HCL (pH 7.4), 1.2 M potassium chloride (KCL) and 30mM magnesium chloride ($MgCl_2$). Cell pellet was re-suspended in 150µl of fresh 1X RSB prepared by adding 150µl of 2X RSB, 22.5µl of 20U/µl SuperaseIn (Ambion Austin, TX), 0.6µl of cycloheximide, 12µl of 25X protease inhibitor (PI) (Roche, USA) topped up to 300µl of RNase free water. 200µl of cell lysates were transferred to fresh pre-chilled eppendorf tubes

and an equal volume of fresh 1X Lysis buffer (LB) containing 500µl of 2X RSB, 1% Triton-X, 2% Tween-20, 1% sodium deoxycholate topped up to 100µl of water, was added. Cell lysates were incubated on ice for 10 mins, with occasional shaking of tube every 2 mins. Cell lysates were spun at 13,200 rpm for 10 mins at 4°C to pellet nuclei. Supernatant was transferred to fresh pre-chilled eppendorf tubes. Equal OD units of cell extracts were layered onto 10-50% linear sucrose gradients containing either 5g (10%) or 25g (50%) of sucrose in 75mM KCL, 1.5mM $MgCl_2$ and 10mM Tris-HCL (pH 7.4) topped up to 50mL of RNase free water and centrifuged for 1h and 5 mins at 36,000 rpm at 8°C in a Beckman SW-60 Ti rotor. Five fractions were collected using a Piston Gradient fractionator (Biocomp Instruments, Inc. New Brunswick, Canada) while monitoring the optical density at 254 nm. Fraction 6 at the bottom of the gradient was collected manually. Fractions 3-5 were pooled together as the actively translating fractions and protein precipitation was performed.

3.5 TCA/Acetone Protein Precipitation

100% Trichloroacetic acid (TCA) (Sigma-Aldrich, Bornem, Belgium) was added to pooled actively translating fractions such that the final concentration of TCA was 20%. Samples were vortexted to mix and incubated on ice for 30 mins. Samples were spun at 4°C at 13,200 rpm for 30 mins. Supernatant was discarded and protein was pelleted with 300µl of ice-cold 100% acetone (Sigma-Aldrich, Bornem, Belgium). Pellet was centrifuged at 4°C at 13,200 rpm for 15 mins. Supernatant was removed and protein pellet was air-dried for 5 mins. Pellet was re-suspended in 100µl of TUTS buffer containing 25mM Tetraethylammonium bromide (TEAB), 2% Triton-X, 8M Urea, 0.1% Sodium dodecyl sulfate (SDS) and 1 tablet of protease inhibitor (Roche, USA) made to 50mL with PBS. Protein concentration was determined using BCA protein assay reagent (Pierce Chemical Company, IL) according to manufacturers' protocol. 1µg of protein was loaded onto SDS/PAGE gels and silver staining (Invitrogen,

Carlsbad, CA, USA) was performed according to manufacturers' protocol. Silver stained gel image was captured using Gel documentation XR^+ system (Bio-Rad, USA) at appropriate exposure.

3.6 In-gel digestion, iTRAQ labelling and mass spectrometry

To 45µg of protein sample, 40µl of 10% SDS, 25µl of 40% Acrylamide (29:1 C), 2.5µl of 10% ammonium peroxodisulfate (APS) and 0.25µl of Tetramethylethylenediamine (TEMED) was added and topped up to 100µl of water to polymerize into a gel for 30 mins at room temperature (RT). The gel was fixed with 50% methanol, 12% acetic acid for 30 mins at RT. Gels were cut into smaller pieces using a clean blade. Finely-cut gels were transferred to a 1.5mL Eppendorf tube and washed with 500µl of 50mM NH_4HCO_3/50% (v/v) acetonitrile. Gel pieces were vortexed, let to stand for 5 mins and the solution was discarded. Washing was performed thrice and the gel pieces were dehydrated by adding 500µl of acetonitrile. Solvent was removed and reduction was performed by incubating gel pieces with 400µl of 5mM Tris(2-carboxyethyl)phosphine (TCEP) in 100mM NH_4HCO_3 at 57°C for 1h. TCEP solution was removed after incubation, and 500µl of acetonitrile was added to each tube, vortexed and removed. Alkylation was performed by adding 120µl of 10mM methyl methanethiosulfonate (MMTS) solution in 100mM NH_4HCO_3 and incubated at RT for 1hr with occasional vortexing. Supernatant was removed and gel pieces were incubated with 500µl of 50mM TEAB for 5 mins at RT. Supernatant was removed and gel pieces were dehydrated with 500µl of acetonitrile for 5 mins. Supernatant was removed again and 500µl of 50mM TEAB was added to gel pieces for 5 mins. Supernatant was removed and 100µl of acetonitrile was added to dehydrate gel pieces for 5mins. Solvent was discarded and gel pieces were dried in a vacuum centrifuge for 5 mins. Digestion was performed using 12.5 ng/µl of trypsin (Promega, Madison, WI, USA) in 500mM TEAB for 30 mins at 4°C. Excess trypsin solution was removed and 40µl of 500mM TEAB was added to the gel pieces and

incubated overnight in an oven at 37°C. The following day, gel pieces were cooled to RT and centrifuged at 6000 rpm for 10 mins. Supernatant was saved. Gel pieces were treated with 200µl of 50mM TEAB, mixed and let to stand for 10 mins followed by centrifugation at 6000 rpm for 10 mins. Supernatant was saved. Gel pieces were treated with 200µl of 5% formic acid in 50% aqueous acetonitrile, mixed and let to stand for 10 mins prior to centrifugation at 6000 rpm for 10 mins. Supernatant was saved and gel pieces were treated with 100% acetonitrile, mixed and let to stand for 10 mins prior to centrifugation at 6000 rpm for 10 mins. Supernatant was saved and pooled together with those collected previously and dried in a vacuum centrifuge overnight. The following day, desalting of samples was carried out using Sepak C-18 (Waters) columns according to manufacturers' protocol, dried using speed vacuum and reconstituted with 0.5M TEAB. Each vial of iTRAQ reagent (AB SCIEX) (113, 114, 115, 116, 117, 118, 119 and 121) was dissolved in 50µl of isopropanol. The content of each reagent was transferred to one sample tube, mixed and incubated for 2h at RT. The pH of contents were maintained between 7.5-8.5 for optimum labelling efficiency. Equal amount of labelled samples were pooled and strong cation exchange (SCX) (AB SCIEX) was performed according to manufactures' protocol to remove excess labels. Eluted samples were desalted using Sepak C-18 columns and reconstituted with 100µl of 5% acetonitrile and 0.05% formic acid for 1D LC-MS/MS analysis. 2µg of peptides were concentrated and analyzed by reverse phase liquid chromatography (RP-LC) on 1000 nano UPLC system (Thermo, Germany). Reverse phase separation was performed using a 200µm X 0.5mm precolumn and subsequently eluted onto a 75 µm X 150 mm analytical column packed with ChromXP C18-CL-3µm 120Å phase (Eksigent, Dublin, CA) in a 90 min linear gradient of 12-30% mobile phase A (0.2% HCOOH in water) and mobile phase B (98% ACN/0.1% HCOOH). Acquisitions were performed with the following settings: Survey scan acquired in 5600 Triple TOF analyzer (QqTOF, AB SCIEX) with a flow rate of 300 nl/min and m/z

range 400-1800 was followed by selection of the most intense peptide ions for MS/MS analyses. Raw MS/MS spectra were processed using ProteinPilot Software 4.2 (AB SCIEX). Peak lists were search against Human Uniprot database using Mascot (Matrix Science) search engine with the following parameters: Fixed modification: Carbamidomethyl cysteine. Variable modifications: Oxidation on methionine, Acetylated N-terminal protein, deamidation (NQ), iTRAQ 8plex (Peptide Labeled), 3 missed cleavages, MS accuracy 30 ppm, MS/MS accuracy 0.06 Da. Identification cut-off was based on False discovery Rate 1%. Unique peptides were used for protein ratio quantification with a minimum ratio count of 1. Dataset obtained for each sample was auto-bias corrected for unequal mixing.

3.7 In-solution digestion, TMT labelling and mass spectrometry

For 24h wounded keratinocytes, polysomal fractions 3-5 were pooled and re-suspended in 8M Urea/Tris (pH 8.5) at a ratio of (1:1). Sucrose was removed from samples using centrifugal concentrators (3000 or 5000 MWCO) (Merck Millipore) and rinsed with 4mL of 8M urea/Tris (pH 8.5) followed by 3mL of 100mM (TEAB) (pH 8.5). 20mM of TCEP was added to samples and incubated at 25°C for 20 mins. Following this, 55mM of Chloro Acetamid (CAA) was added to samples and incubated at RT for 30 mins in the dark. Samples were diluted in 100mM TEAB to a total volume of 5mL and digested with 25µg of Lys-C for 1.5h at RT in a thermomixer. Samples were diluted with 100mM of TEAB to a total volume of 8mL and digested with 25µg of trypsin overnight at RT in a thermomixer. Desalting of samples was carried out using Sepak C-18 columns equilibrated with 5 mL of 100% acetonitrile followed by 5mL of 0.5% acetic acid and residual fluid sharply expelled with air twice using a 5mL syringe. The column was connected to a new 5mL syringe and pressed slowly to bind the samples to the column, twice. The column was washed once with 5mL of 0.5% acetic acid and the residual fluid was expelled sharply. The column was then connected

to a new 5mL syringe and 600µl of 80% acetonitrile in 0.5% acetic acid was added to the syringe. The fluid was eluted slowly into a low-binding eppendorf tube. The step was repeated twice and residual fluid was expelled with air.

Samples were then solubilized with 25µl of 50mM TEAB (pH 8.5). Isobaric mass tandem tag (TMT) labels were solubilized in 41µl of acetonitrile and 10µl of the each independent label (126, 127, 128, 129, 130 and 131) was added to each protein sample and incubated for 1h at RT. The reaction was quenched with 50µl of 1M Tris (pH 7.4) and let to stand for 5 mins. For each sample, a 15mL tube was prepared and 1mL of 0.5% acetic acid was added to each tube. All samples were pooled into one tube and 200µl of 10% TFA was added followed by 4mL of 0.5% acetic acid. Desalting of samples were performed using Sepak C-18 columns as previously described and residual fluid was eluted in a clean eppendorf tube. Excess TMT labels were removed on SCX (STRATA-X) column according to manufactures' protocol. Peptides were concentrated and analyzed by reverse phase liquid chromatography (RP-LC) on 1000 nano UPLC system (Thermo, Germany). Reverse phase separation was performed using an id75µm/50 cm long EASYspray column in a 160 min gradient of solvent A (0.1% HCOOH in water) and solvent B (99.9% MeCN/0.1% HCOOH). Acquisitions were performed with the following settings: Survey scan acquired in Orbitrap analyzer with a resolution 60,000 and m/z range 300-1500 was followed by selection of the most intense peptide ions for HCD MS/MS in orbitrap. Raw MS/MS spectra were processed using Proteome Discoverer software version 1.4 (Thermo). Peak lists were search against Human Uniprot database using Mascot (Matrix Science) search engine with the following parameters: Fixed modification: Carbamidomethyl cysteine, Variable modifications: Oxidation on methionine, Acetylated N-terminal protein, deamidation (NQ), TMT labelling, 3 missed cleavages, MS accuracy 30 ppm, MS/MS accuracy 0.06 Da. Identification cut-off was based on False discovery Rate of 1%. Unique peptides were used for protein ratio

quantification with a minimum ratio count 1. Dataset obtained for each sample was normalized to its respective median.

3.8 Western Blot Analysis

Protein for immunoblotting was extracted using 100µl of RIPA buffer containing 150mM sodium chloride (NaCl), 1% Triton-X, 0.5% sodium deoxycholate, 0.1% SDS, 50mM Tris-HCL (pH 7.4), 1% NP-40, 1X protease and phosphatase inhibitor, 1X EDTA and 1X PMSF. Protein concentration was quantified using the BCA Protein Assay Reagent (Pierce Chemical Company, IL). 20µg of protein from total cell lysates or 5µg of polysomal protein were resolved in a 4-12% Bis-Tris gel (Novex, Invitrogen) by gel electrophoresis at 90V for 2.45 h followed by a semi-dry electro-transfer using 2X Transfer buffer (10mL of 20X Transfer buffer and 10mL methanol top up to 100mL dH_2O) onto nitrocellulose membrane (Hybond-C Super, Amersham, Rosendaal, the Netherlands) for total or PVDF membranes (H-ybond, GE healthcare) for polysomal protein. Membrane was blocked using Tris-buffered saline – containing 0.1% Tween 20 (TBS-T) supplemented with 5% non-fat dry milk for at least 1h at RT. Membrane was incubated overnight with primary antibodies in blocking buffer at 4°C. Primary antibodies, rabbit Anti-ERK1/2 (1:1000, cell signalling technology), rabbit Anti-phospho-ERK1/2, (1:1000, cell signalling technology), rabbit Anti-p38 (1:1000, cell signalling technology), rabbit Anti-phospho-p38 (1:1000, cell signalling technology), mouse Anti-paxillin (1:1000, BD Transduction Lab), rabbit Anti-phospho-paxillin (1:500, Invitrogen), rabbit Anti-EBP-1 (1:1000, abcam), rabbit Anti-RPLP0 (1:500, abcam), rabbit Anti-RPS6 (1;1000, cell signalling technology), rabbit Anti-RPL4 (1:1000, abcam), rabbit Anti-RPL18 (1:1000, Atlas antibodies), mouse Anti-RPL29 (1:1000, abcam), rabbit Anti-BiCD2 (1:250, Atlas antibodies) and mouse Anti-β-actin (1:5000, abcam) were used. Membranes were washed four times with TBS-T for 15 mins each, and incubated for 2h at

room temperature with either peroxidase conjugated Goat Anti-mouse or Donkey Anti-rabbit secondary antibodies in blocking buffer at 1:5000 dilution. Membranes were washed four times with TBS-T for 15 mins each and autoradiographed using enhanced chemiluminescence as directed by manufacturers' protocol (Pierce Chemical Company, IL). Protein band intensities were determined by Kodak ID 3.5 imaging software. To probe for house-keeping genes, membranes were stripped using 25mL of stripping buffer containing 62.5 mM Tris (pH 7.4), 2% SDS and 180µl of β-mercaptoethanol, freshly added. For validation of protein expression levels of iTRAQ candidates, respective technical replicates were used for immunoblotting.

3.9 Immunofluorescence staining

Human scalp skin sections obtained from NUH were immediately embedded with OCT (Tissue-Tek®). Tissue was sectioned at 7μm, mounted onto microscopic glass slides and stored at -80°C till further use. Tissue sections were thawed to RT for 30 mins prior to blocking with 10% goat serum in PBS (Leica, Wetzlar, Germany) for 30 mins. Blocking buffer was removed and tissue sections were incubated with primary antibody mouse Anti-K14 (LH001) (Neat, made in-house), mouse Anti-K10 (LH10) (Neat, made in-house), mouse Anti-INV (1:500, Leica, Wetzlar, Germany) and mouse mouse Anti-FLG (1:500, abcam) in blocking buffer for 2h. Sections were rinsed thrice with 1X PBS for 5 mins each and incubated with Alexa 594 Goat Anti-mouse secondary antibody (Invitrogen) at 1:500 dilution in blocking buffer for 30 mins. Sections were rinsed thrice for 5 mins each and incubated with Hoechst at 1:2000 dilution in 1X PBS for 10 mins. After which, sections were rinsed with 1X PBS thrice for 5 mins each. Sections were mounted using Hydromount mounting agent (National Diagnostics, Atlanta, GA, USA) containing 2.5% DABCO.

3.10 Statistical Analysis

Coefficient of variation (CV) was calculated by dividing the standard deviation between the ratios (experimental/control) of three independent biological replicates to its mean. Two tailed, Student's *t*-test was performed to determine ratios with statistically significant *p*-values of <0.05 (*), <0.01 (**) and <0.001 (***) and a cut-off of more than 1.5 fold after normalization were considered as differentially abundant.

4. Results

4.1 Wounding activates p38 MAPK in N/TERT-1 keratinocytes

In order to model wound healing, I used confluent monolayer keratinocyte cultures and performed bi-directional scratches using a cell comb to mimic wound–induced keratinocyte migration. To determine the activation of stress response in these keratinocytes, I investigated the levels of p38 phosphorylation at 2, 4 and 6 hours post-wounding **(Figure 5A)**. p38 is a key player in the MAP kinase (MAPK) stress signalling pathway that coordinates a cascade of gene responses under physical and environmental stresses [31]. Phase contrast images captured prior and post wounding displayed a decrease in wound width over the course of 6 hours post-wounding, suggesting an increase in cell migration upon scratch **(Figure 5B)**. p38 MAPK showed a strong phosphorylation at all time points suggesting that wounding induced a stress response in these keratinocytes **(Figure 5C)**. Here, I have chosen 6h post-wounding as a time-point for subsequent polysome profiling experiment.

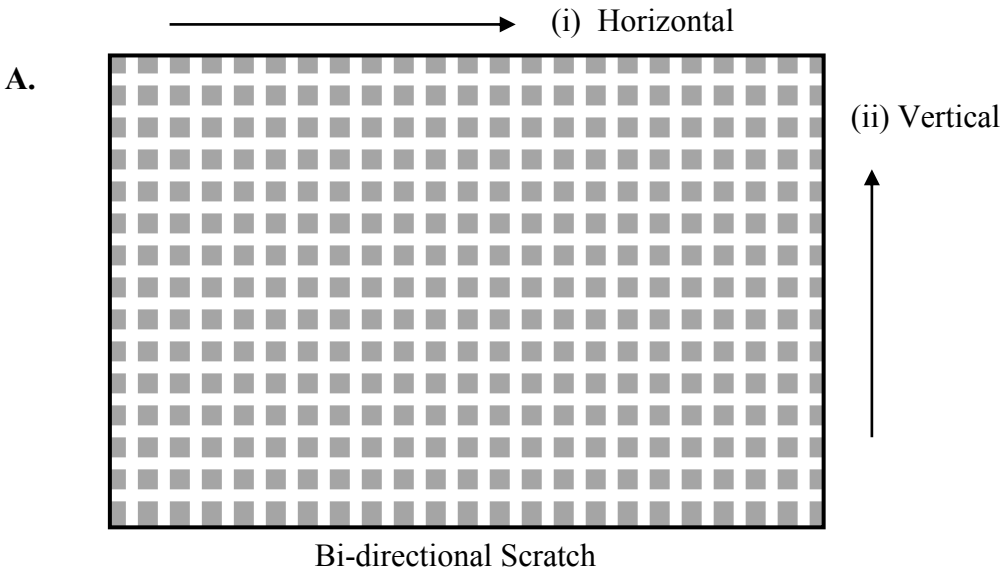

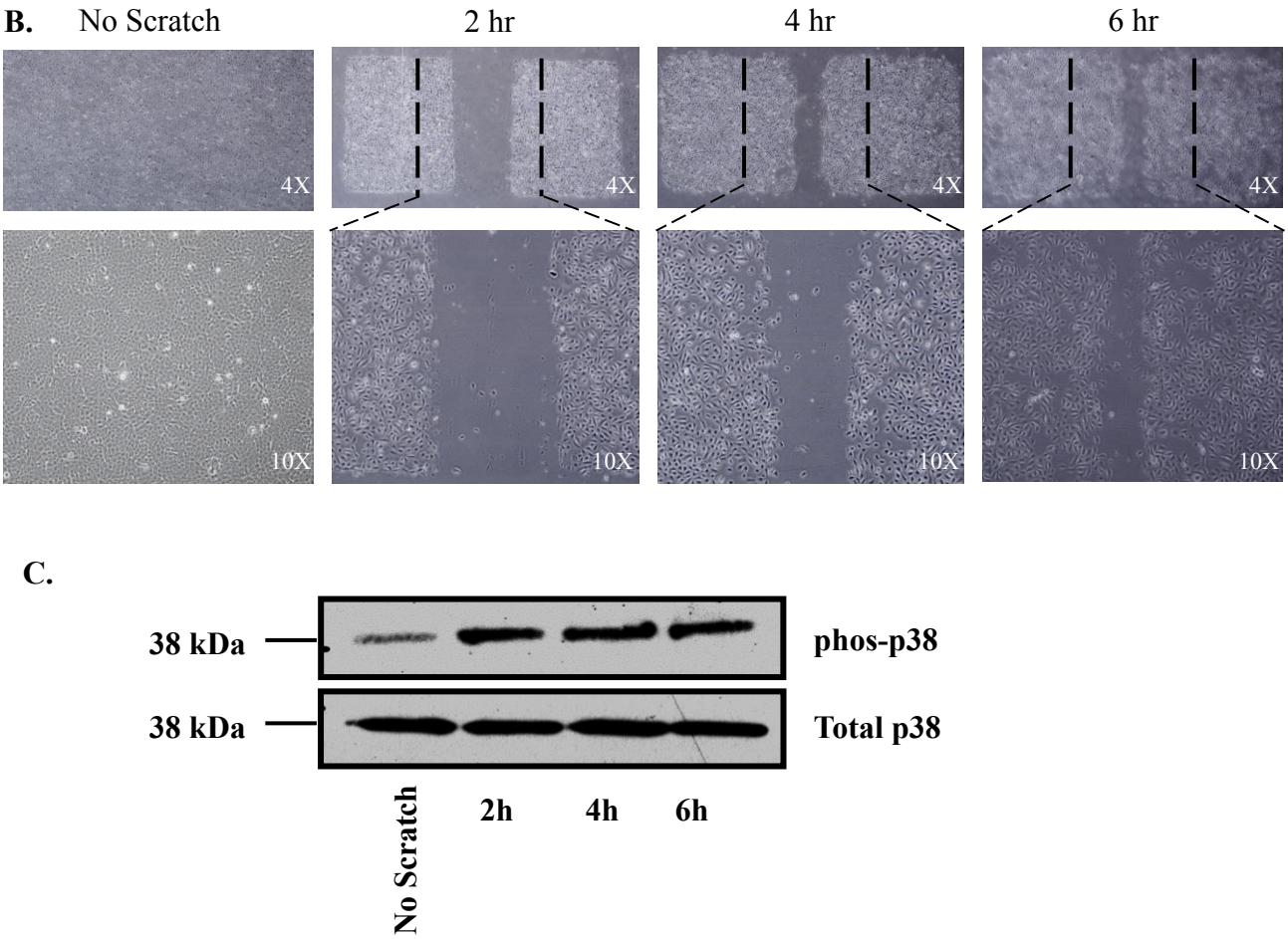

Figure 5: p38 MAPK activation upon wounding. **A.** An illustration of the bi-directional wounding made in a confluent monolayer culture of N/TERT-1 keratinocytes. **B.** Phase contrast (PH) images showing time-dependent wound closure of N/TERT-1 keratinocytes in a confluent monolayer culture. **C.** Immunoblotting of p38 phosphorylation as an indication of stress activation over a time course of 6 hours post-wounding.

4.2 Osmotic stress induces phosphorylation of ERK1/2 MAPK in N/TERT-1 keratinocytes

In order to mimic a drying osmotic condition in 2D cultures, I used sorbitol an alcohol sugar to induce an efflux of water molecules from keratinocytes. A sorbitol concentration of 200mM was used to induce osmotic stress over a time course of 12 hours and protein lysates were extracted to determine the phosphorylation of ERK1/2 as an indicator of an activated stress response **(Figure 6A)**. Since MAPK p38 phosphorylation is transient with 200mM of sorbitol and occurs between 5-30 mins of treatment, the activation of ERK1/2 was determined in this case [31]. Phosphorylation of both ERK1/2 was observed as early as 4 hours post-sorbitol stress and thus was chosen as a time-point to extract actively translating ribosomes **(Figure 6B)**.

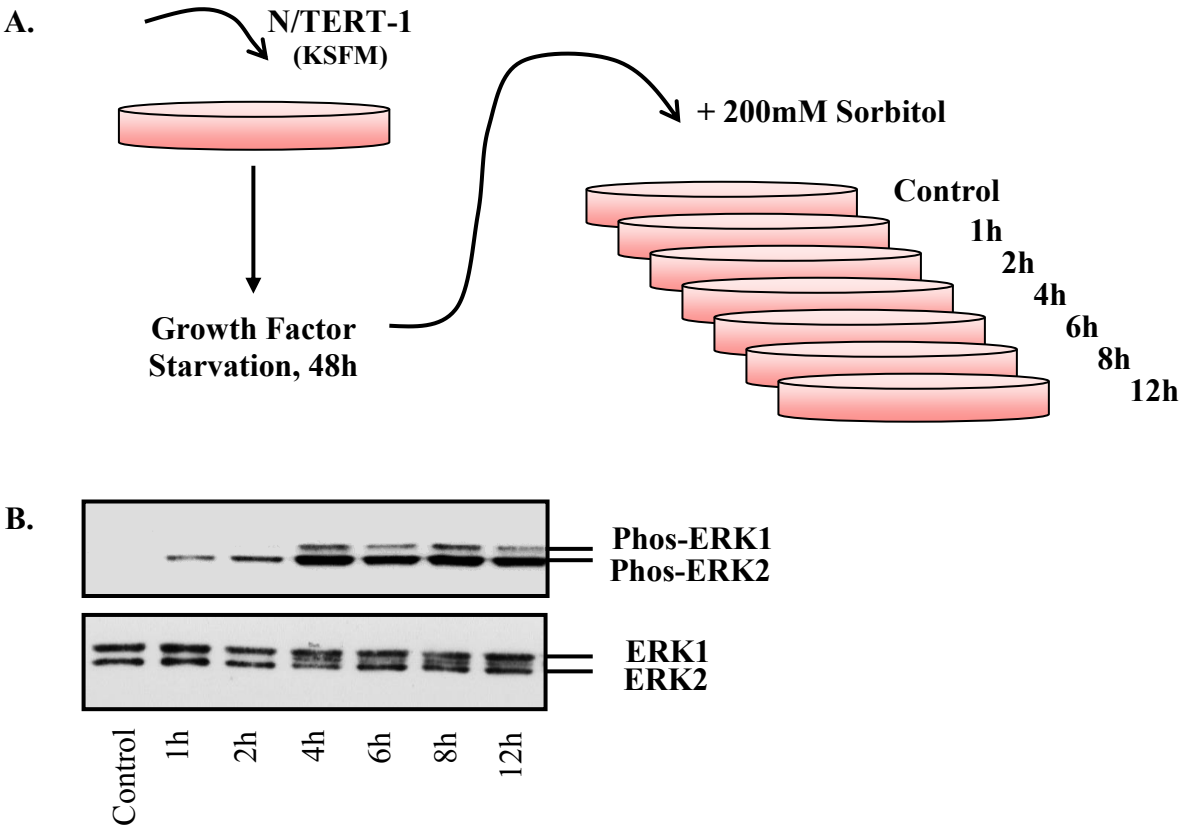

Figure 6: ERK1/2 phosphorylation induced upon osmotic stress. **A.** Experimental workflow of osmotic stress on N/TERT-1 keratinocytes using 200mM sorbitol over a time course of 12 hours. B. Immunoblotting of ERK1/2 phosphorylation as an indication of stress activation over a time course of 12 hours of 200mM sorbitol treatment.

4.3 Actively translating ribosomes were identified from non-wounded and 6h post-wounded keratinocytes

Since I hypothesize that alteration in RP/non-RP composition might be required for translation of a subset of mRNAs under stress, I needed to purify actively translating ribosomes which are bound to mRNAs. To do this, non-wounded and 6h post-wounded keratinocytes were subjected to polysome profiling. Phosphorylation of p38 was checked by immunoblotting to confirm the activation of stress response 6 hours post-wounding prior to polysome fractionation **(Figure 7A)**. Equal O.D. units of cytoplasmic extract from un-wounded and 6h post-wounded keratinocytes were layered onto continuous 10-50% sucrose gradients prepared by a sucrose gradient maker and subjected to high velocity centrifugation **(Figure 7B)**. Fractions 3-5 represented actively translating ribosomes also known as polysomes, which were of higher density and therefore sedimented at the bottom of the gradient **(Figure 7B)**. These were distinguished from the non-translating monosomes which remained at the top of the sucrose gradients in Fractions 1 and 2. The translational profiles of non-wounded and 6 hours post-wounded keratinocytes were comparable suggesting that there was no global translational repression 6 hours post-wounding **(Figure 7C)**. However, this does not imply that there are no changes in ribosome composition upon wounding. Thus, fractions 3-5 were pooled and protein was purified by TCA/Acetone protein precipitation for subsequent mass spectrometry analysis.

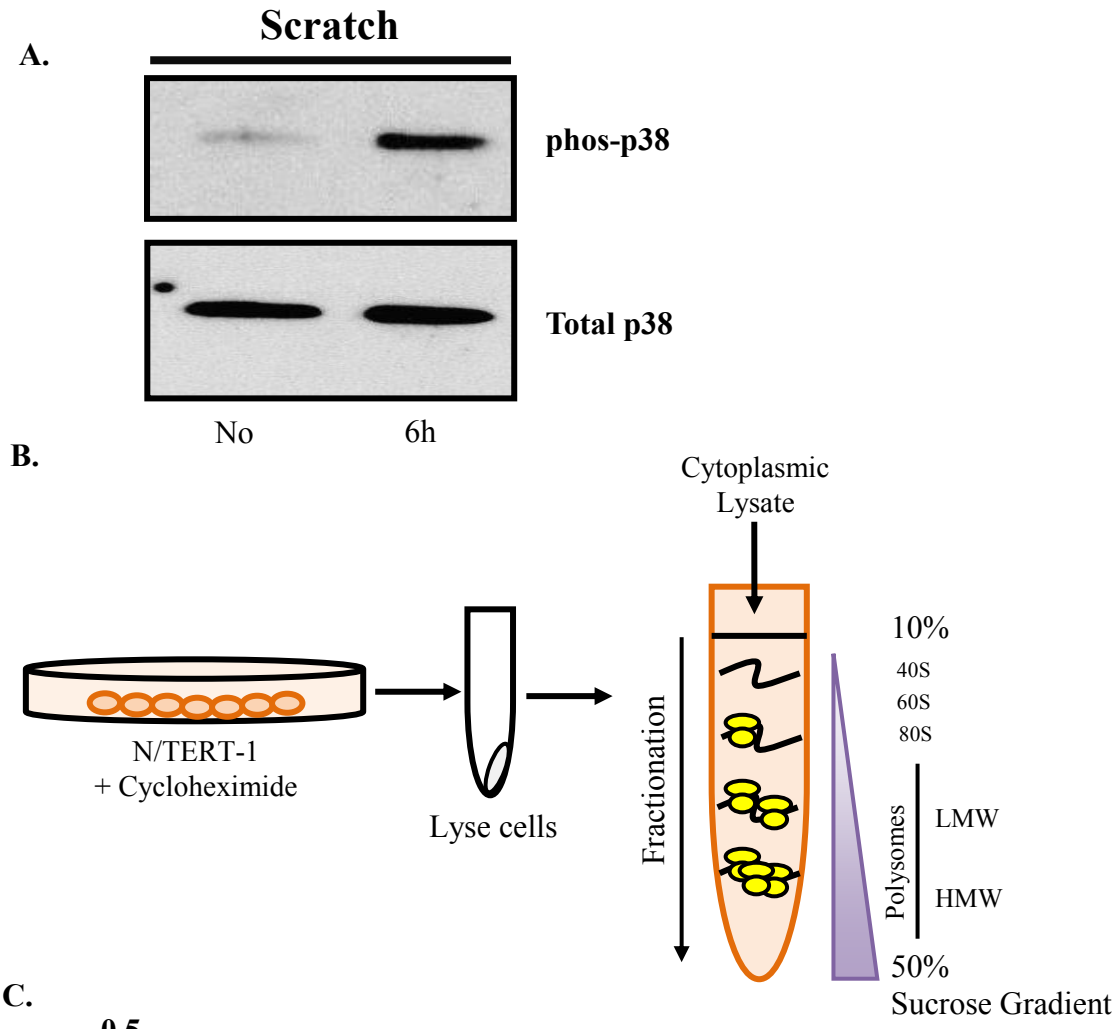
A.
Scratch
phos-p38
Total p38
No
6h
B.
Cytoplasmic
Lysate
N/TERT-1
+ Cycloheximide
Lyse cells
Fractionation
10%
40S
60S
80S
Polysomes
LMW
HMW
50%
Sucrose Gradient
C.
No scratch 0h
Scratch 6h
60/80S
40S
Polysome
O.D. 254nm
0.5
0.45
0.4
0.35
0.3
0.25
0.2
0.15
0.1
0.05
0
1
2
3
4
5
Fraction

Figure 7: Identification of actively translating ribosomes in wounded and non-wounded keratinocytes. A. Immunoblotting of p38 phosphorylation for non-wounded and 6h post-wounded N/TERT-1 keratinocytes. **B.** Schematic representation of polysome profiling experiment shows the treatment of keratinocytes with cycloheximide, followed by cell lysis and subsequent velocity separation of translation complexes in linear sucrose gradients. **C.** Polysome profiles of 6h post-wounded and non-wounded N/TERT-1 keratinocytes. Actively translating ribosome fractions are highlighted in yellow.

4.4 Actively translating ribosomes were identified from untreated control and 200mM, 4h sorbitol treated keratinocytes

Similar to wounding, sorbitol control and 200mM, 4h sorbitol treated keratinocytes were subjected to polysome profiling in order to purify actively translating ribosomes. The phosphorylation of ERK1/2 was determined by immunoblotting to confirm the activation of stress response 4h after 200mM sorbitol treatment prior to polysome fractionation **(Figure 8A)**. The polysome profile of 200mM, 4h sorbitol stressed keratinocytes revealed that there was a decrease in polysome peaks and an increase in monosome peaks compared to the profile of untreated control keratinocytes, suggesting that there was a global translational repression upon osmotic stress **(Figure 8B)**. Fractions 3-5 which contain the actively translating ribosomes, were pooled. Protein was purified by TCA/Acetone protein precipitation for subsequent mass spectrometry analysis.

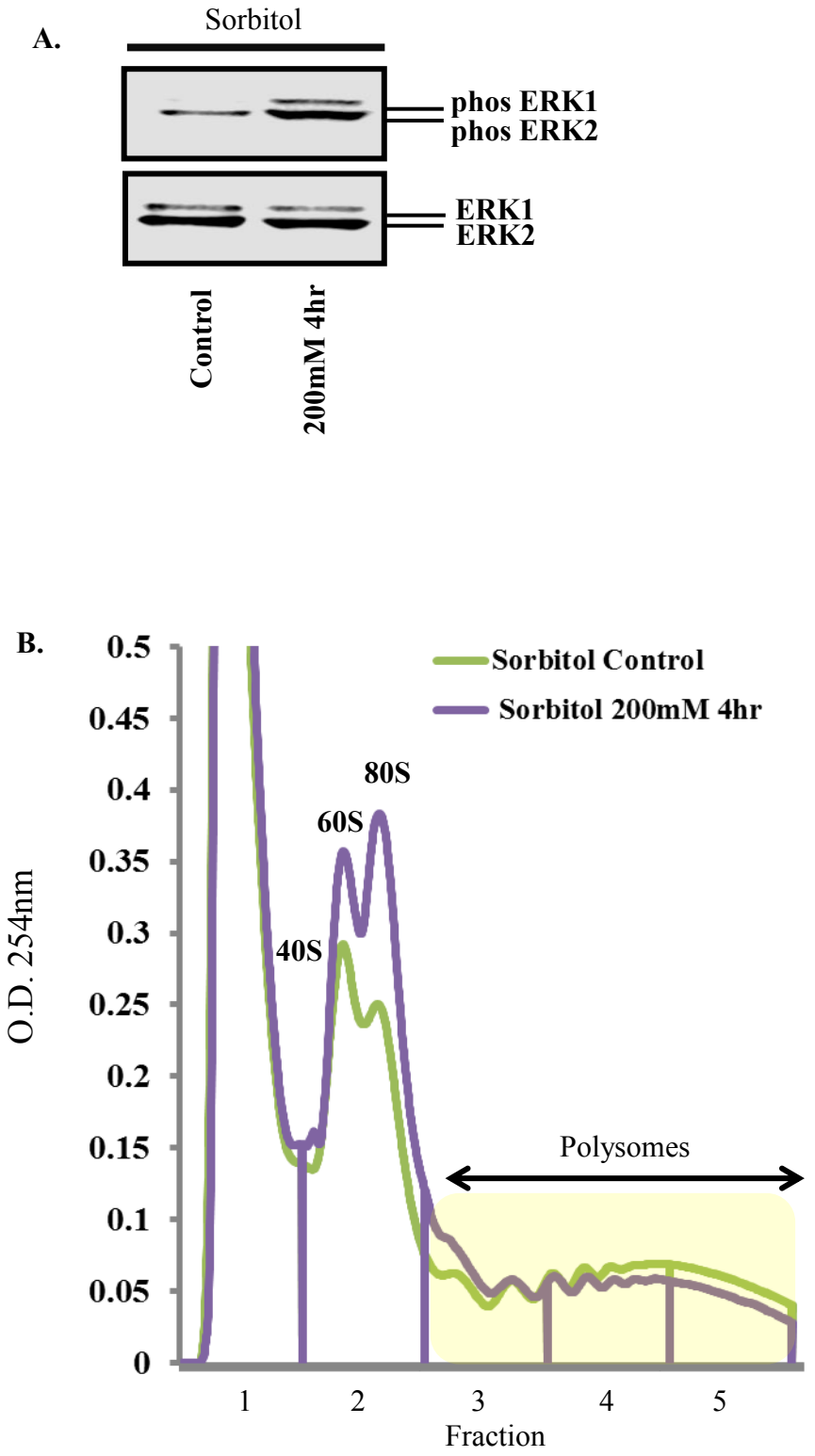

Figure 8: Identification of actively translating ribosomes in control and sorbitol stressed keratinocytes. A. Immunoblotting of ERK1/2 phosphorylation for 4h of 200mM sorbitol treated and untreated N/TERT-1 keratinocytes. **B.** Polysome profiles of 4h, 200mM sorbitol treated and un-treated N/TERT-1 keratinocytes. Actively translating ribosome fractions are highlighted in yellow.

4.5 Changes in RP and non-RP candidates in response to wounding and osmotic stress

Two biological replicates of polysome profiling was performed for wounding and sorbitol stress. The actively translating ribosomes in fractions 3-5 of wounded and sorbitol stressed keratinocytes with their respective controls, were pooled and subjected to TCA/Acetone protein purification to precipitate proteins. These proteins were quantified using BCA protein estimation kit and 1μg of protein was loaded onto an SDS/PAGE gel. Silver staining was performed to check for equal loading **(Figure 9A)**. Approximately 45μg of protein was subjected to in-gel tryptic digestion to generate a peptide pool. Peptides from each sample were labelled independently with an iTRAQ label and an equal amount of labelled peptides were pooled and subjected to LC-MS/MS analysis **(Figure 9B)**. A total of 116 proteins were detected by LC-MS/MS analysis out of which 95 of them were of 95% confidence. Under osmotic stress, 7 RPs and 3 non-RPs were either up or down-regulated while 29 RPs and 56 non-RPs remained unchanged. Within these candidates, RPL29 ($p<0.05$) showed a 1.5 fold up-regulation while RPL4 ($p<0.001$) and RPS21 ($p<0.001$) showed more than 1.5 fold down-regulation upon osmotic stress. On wounding by scratch assay, 9 RPs and 12 non-RPs were either up or down-regulated while 27 RPs and 47 non-RPs remained unchanged **(Figure 9C)**. Among these candidates, EBP-1 ($p<0.05$) showed a 1.8 fold up-regulation while RPS29 ($p<0.01$), RPL18 ($p<0.05$), RPS21 ($p<0.05$) and Bicaudal D2 homolog (BiCD2) ($p<0.05$) displayed more than 1.5 fold down-regulation 6h post-wounding **(Figure 9D)**.

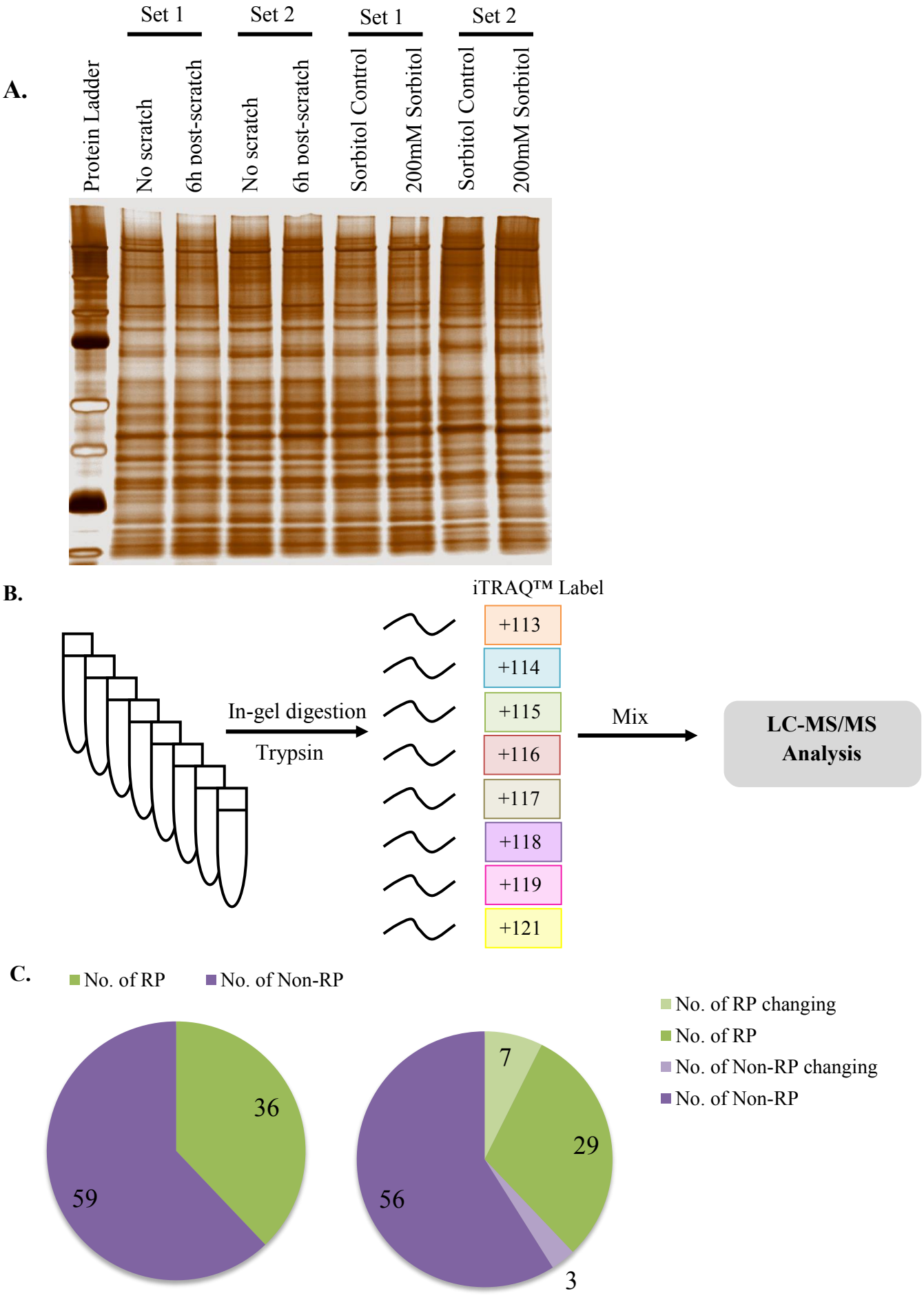
A.
Set 1
Set 2
Set 1
Set 2
Protein Ladder
No scratch
6h post-scratch
No scratch
6h post-scratch
Sorbitol Control
200mM Sorbitol
Sorbitol Control
200mM Sorbitol
B.
iTRAQ™ Label
+113
+114
+115
+116
+117
+118
+119
+121
In-gel digestion
Trypsin
Mix
LC-MS/MS Analysis
C.
No. of RP
No. of Non-RP
36
59
No. of RP changing
No. of RP
No. of Non-RP changing
No. of Non-RP
7
29
3
56

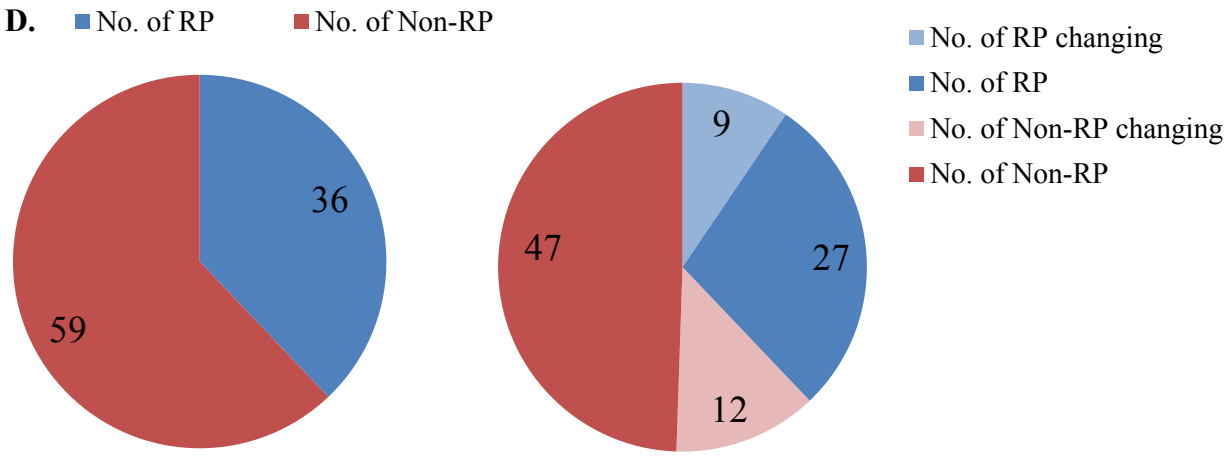

Figure 9: Changes in RP and non-RP candidates in response to wounding and osmotic stress. **A.** Silver staining gel image of 1µg of protein to check for equal loading. **B.** Schematic workflow of in-gel tryptic digestion of proteins followed by iTRAQ labelling of peptides and LC-MS/MS analysis of peptide pool. **C.** Pie chart depicting proteins with 95% confidence detected from LC-MS/MS analysis upon sorbitol stress. 7 RPs and 3 non-RPs were changing in response to sorbitol treatment. **D.** Pie chart depicting proteins with 95% confidence detected from LC-MS/MS analysis upon wounding. 9 RPs and 12 non-RPs were changing in response to wounding.

4.6 Validation of selected candidates from sorbitol stress

RP candidates that were significantly up/down regulated by 1.5 fold or more upon osmotic stress were RPL29, RPL4 and RPS21. Among these candidates, RPL29 and RPL4 were validated by immunoblotting to determine the reproducibility of the mass spectrometry dataset **(Figure 10A)**. A marginal increase in RPL29 protein abundance was observed after 4h of 200mM sorbitol treatment in both biological replicates **(Figure 10B and 10D)**. Similarly, a marginal decrease in RPL4 protein abundance was determined in both biological replicates under osmotic stress **(Figure 10C and 10D)**. RPS21 is a small molecular weight protein that migrates at approximately 9 kDa on SDS/PAGE gel. It was not successfully resolved and thus requires further optimization.

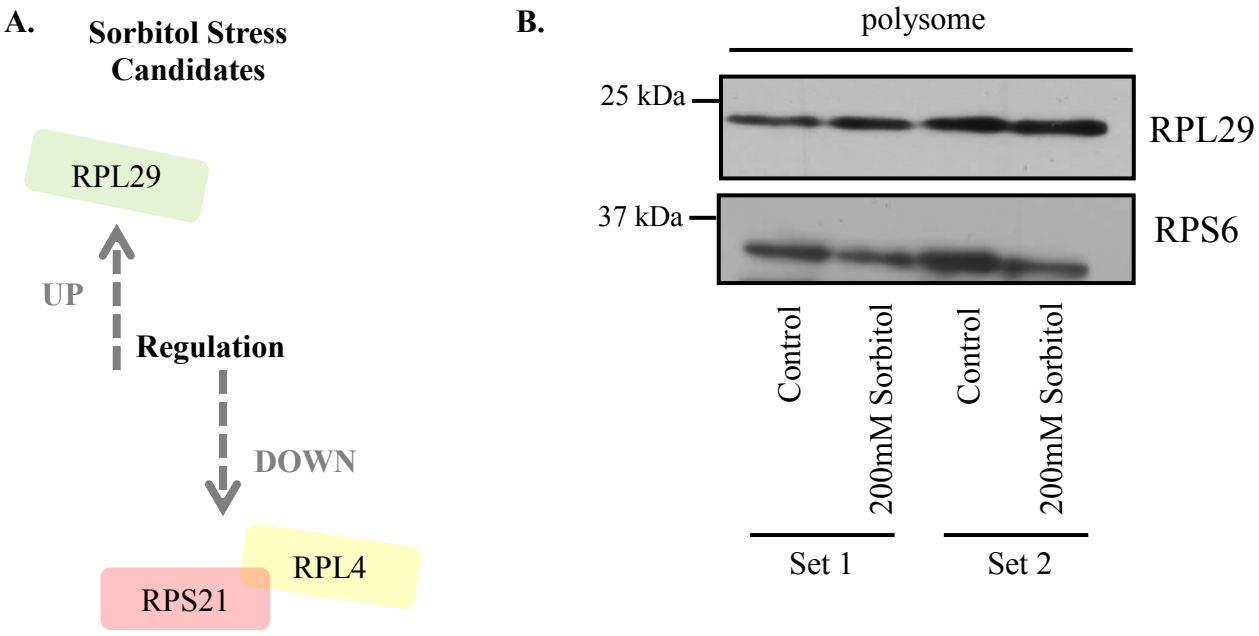

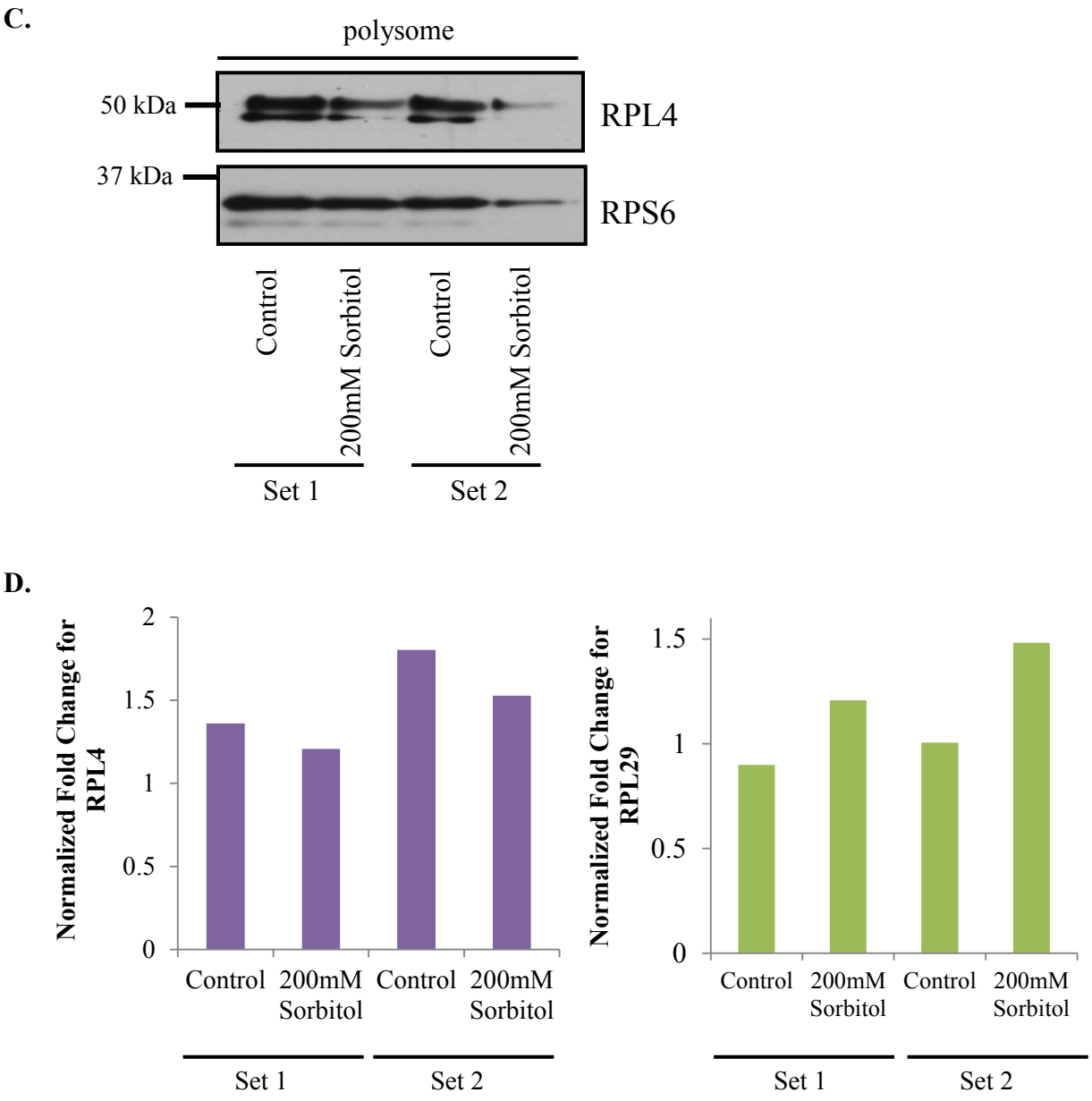

Figure 10: Validation of sorbitol stress candidates. A. Selected RP candidates that were up/down-regulated upon sorbitol stress. **B.** Immunoblotting showing RPL29 abundance in untreated and 200mM, 4h sorbitol treated keratinocytes. **C.** Immunoblotting showing RPL4 abundance in untreated and 200mM, 4h sorbitol treated keratinocytes. **D.** Normalized fold change of RPL4 and RPL29 band intensities to RPS6 loading control. Top band was used for quantification for RPL4.

4.7 EBP-1 and BiCD2 are two non-RP candidates that were up-regulated in polysomal fractions upon wounding

RPL18 as well as EBP-1 and BiCD2 which were two non-RP candidates, selected from 6h post-wounded keratinocytes to be validated by immunoblotting **(Figure 11A).** EBP-1 showed an increase in protein abundance in polysomal fractions for both technical replicates of the mass spectrometry dataset **(Figure 11B)**. A third biological replicate of polysome profiling for non-wounded and 6h post-wounded keratinocytes was performed. The up-regulation of EBP-1 on polysomal fractions was reproducible in the third replicate **(Figure 11B)**. The protein expression of BiCD2 determined by immunoblotting displayed a decrease in protein abundance in polysomal fractions for both technical replicates of the mass spectrometry dataset, where RPS6 was used as a loading control **(Figure 11C)**. As for RPL18, no decrease in protein abundance was observed in both technical replicates of the mass spectrometry dataset **(Figure 11D)**.

A.

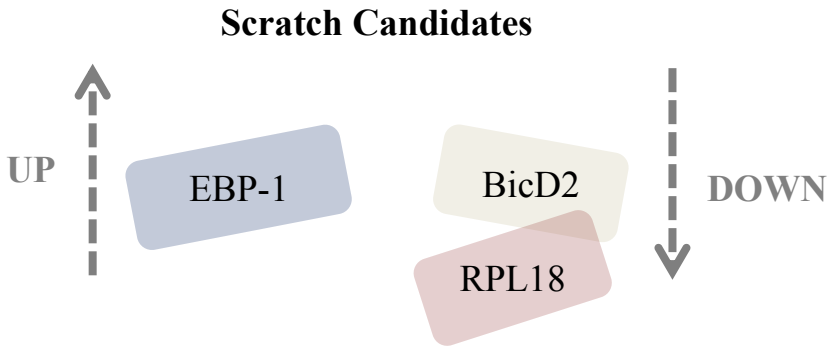
Scratch Candidates
UP
EBP-1
BicD2
RPL18
DOWN

B.

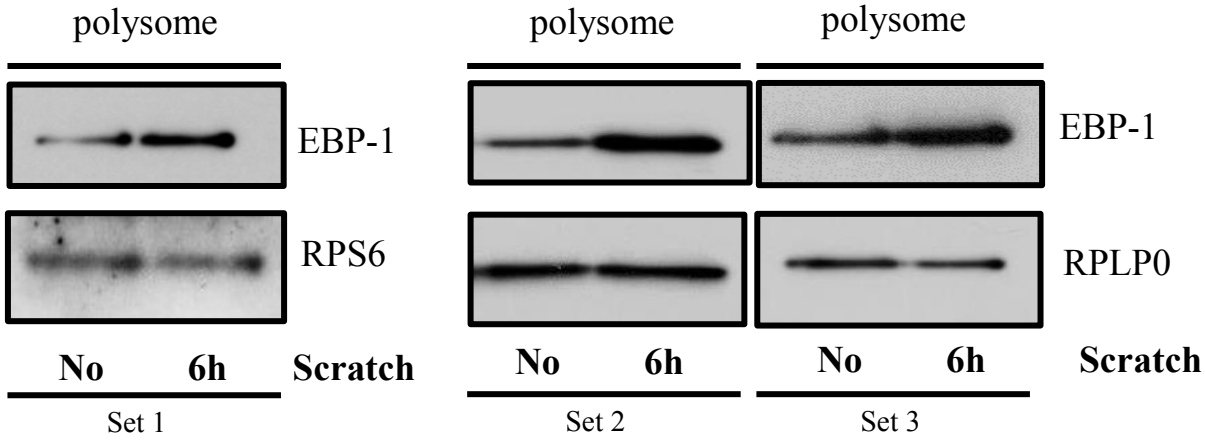
polysome
polysome
polysome
EBP-1
EBP-1
RPS6
RPLP0
No
6h
Scratch
No
6h
No
6h
Scratch
Set 1
Set 2
Set 3

C.

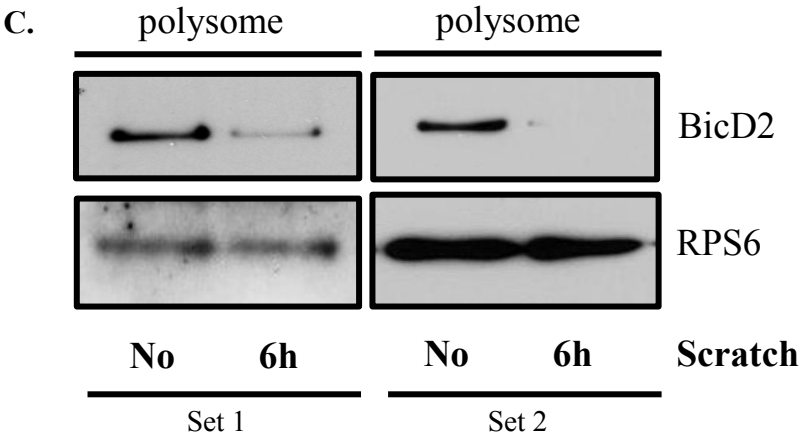
polysome
polysome
BicD2
RPS6
No
6h
No
6h
Scratch
Set 1
Set 2

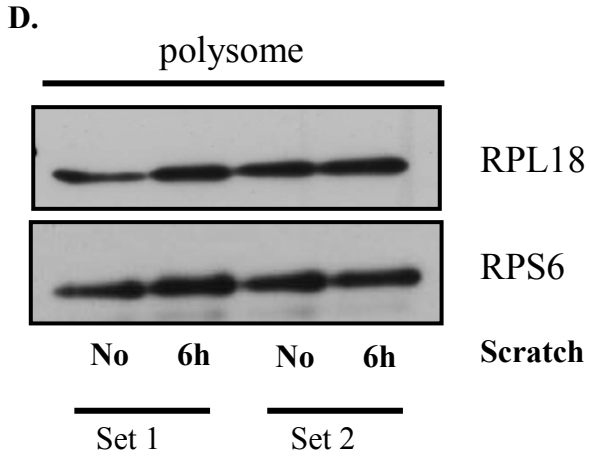

Figure 11: Validation of candidates from scratch assay. A. Selected RP and non-RP candidates that were up/down-regulated at 6h post-scratch. **B.** Immunoblotting showing EBP-1 abundance in non-scratch and 6h post-scratch keratinocytes in three biological replicates. Either RPLP0 or RPS6 was used as a loading control. **C.** Immunoblotting showing BiCD2 abundance in non-scratch and 6h post-scratch keratinocytes in two biological replicates. **D.** Immunoblotting showing RPL18 abundance in non-scratch and 6h post-scratch keratinocytes in two biological replicates.

4.8 Expression pattern of EBP-1 in monosomal and polysomal fractions

To determine the recruitment of EBP-1 onto the translational machinery upon scratch, we accessed the enrichment of EBP-1 in the monosomal fractions as compared to the polysomal fractions under non-scratch and 6h post-scratch keratinocytes by immunoblotting. EBP-1 is encoded by the PA2G4 gene and is a 394 amino acid protein. EBP-1 exists as two isoforms. The larger isoform migrates at approximately 48 kDa while the smaller isoform migrates at 42 kDa on SDS/PAGE gels. Here, we identified both p42 and p48 isoforms in non-scratch and 6h post-scratch keratinocytes **(Figure 12A and 12B)**. While p42 isoform was only identified in the monosomal fractions 1 and 2, p48 isoform was highly enriched in the polysomal fractions 3-5 of 6h post-scratch keratinocytes compared to the non-scratch controls. An unidentified band migrating at approximately 50 kDa was also observed in the monosomal fractions 1 and 2 of both 6h post-scratch and control keratinocytes.

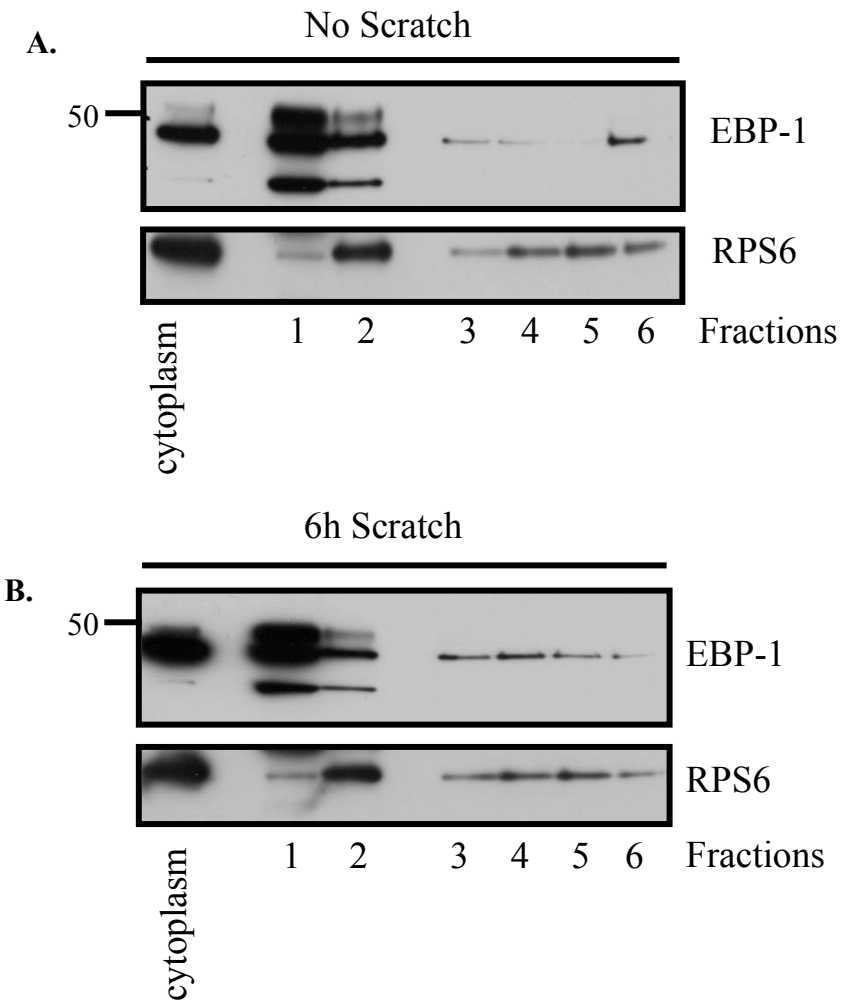

Figure 12: Expression of EBP-1 in monosome and polysome fractions. Immunoblotting showing EBP-1 abundance in cytoplasmic, monosomal (1 and 2), polysomal (3, 4 and 5) and bottom (6) fractions **A.** no scratch and **B.** 6h post-scratch keratinocytes. RPS6 was used as a loading control.

4.9 Optimization of mass spectrometry with 200mM, 6h sorbitol stressed keratinocytes

The preliminary round of mass spectrometry resolved only 95 proteins that were of 95% confidence in the actively translating polysome fractions under both wounding and sorbitol stress conditions. The quantity of proteins detected was drastically lower compared to that reported in the literature which ranged from approximately 575 to 991 proteins [36]. The validation of several candidates selected from the mass spectrometry dataset was not reproducible by immunoblotting. However, this could be partially attributed to the unequal loading of samples. Nonetheless, the sample preparation for LC-MS/MS analysis was optimized with (i) in-solution digestion of proteins instead of in-gel digestion; and (ii) by performing Lys-C/Trypsin digestion instead of trypsin alone. The optimized protocol was performed using 6h of 200mM sorbitol treated keratinocytes with untreated controls. The phosphorylation of ERK1/2 was determined prior to polysome profiling to ensure the activation of stress response upon 6h of sorbitol treatment **(Figure 13A)**. Polysome profiling was performed to identify actively translating ribosome fractions in untreated and 200mM, 6h sorbitol treated keratinocytes, as previously described **(Figure 13B)**. Protein was purified from fractions 3-5 representing actively translating ribosomes using Amicon protein centrifugal concentrators. Protein was prepared according to the optimized protocol; TMT labelling was performed and subjected to LC-MS/MS analysis. Notably, our approach revealed a total of 926 proteins with this round of mass spectrometry, which comprised of 78 RPs and 849 non-RPs **(Figure 13C)**. Within these RPs, 31 RPS and 47 RPL were detected **(Figure 13C)**. In this dataset, 63 proteins were significantly ($P<0.05$) changing in response to 6h of 200mM sorbitol stress. However, none of these proteins showed a significant 1.5 fold up-regulation or 0.75 fold down-regulation upon stress treatment.

A.

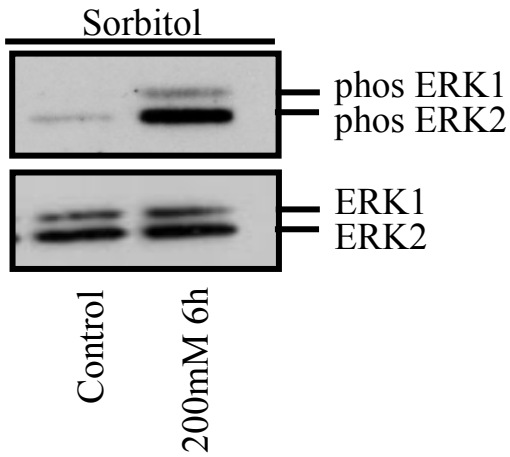
Sorbitol
phos ERK1
phos ERK2
ERK1
ERK2
Control
200mM 6h

B.

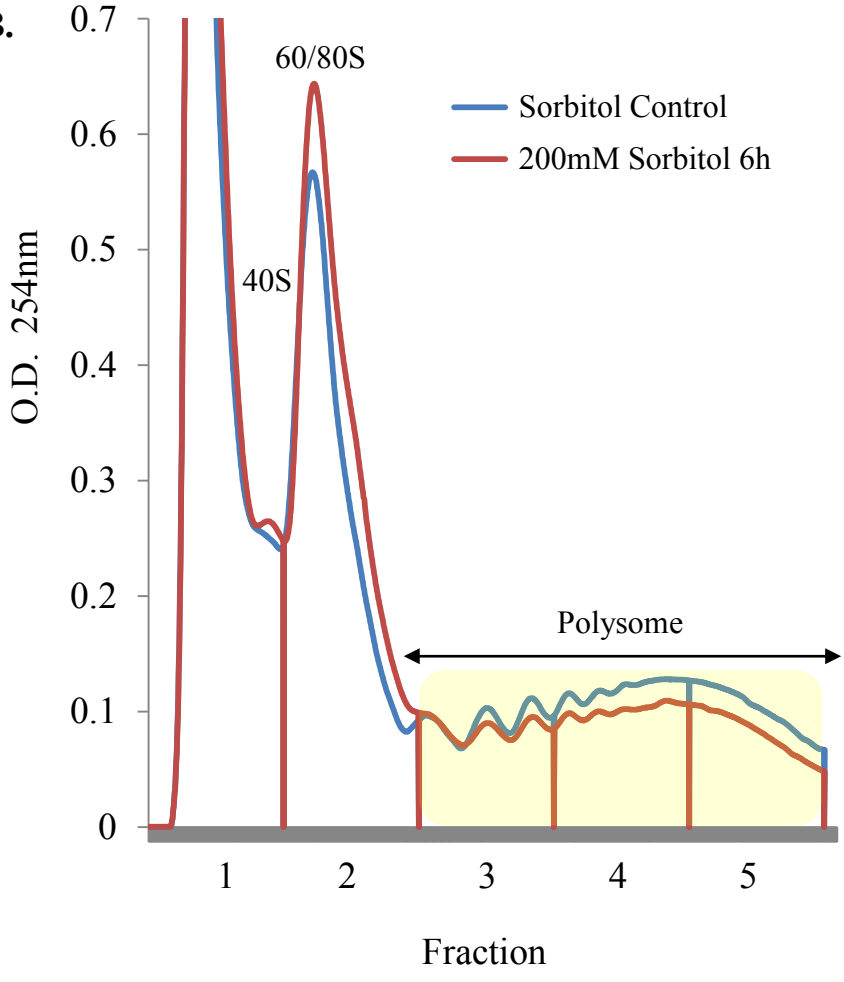
0.7
0.6
0.5
0.4
0.3
0.2
0.1
0
O.D. 254nm
60/80S
40S
Sorbitol Control
200mM Sorbitol 6h
Polysome
1
2
3
4
5
Fraction

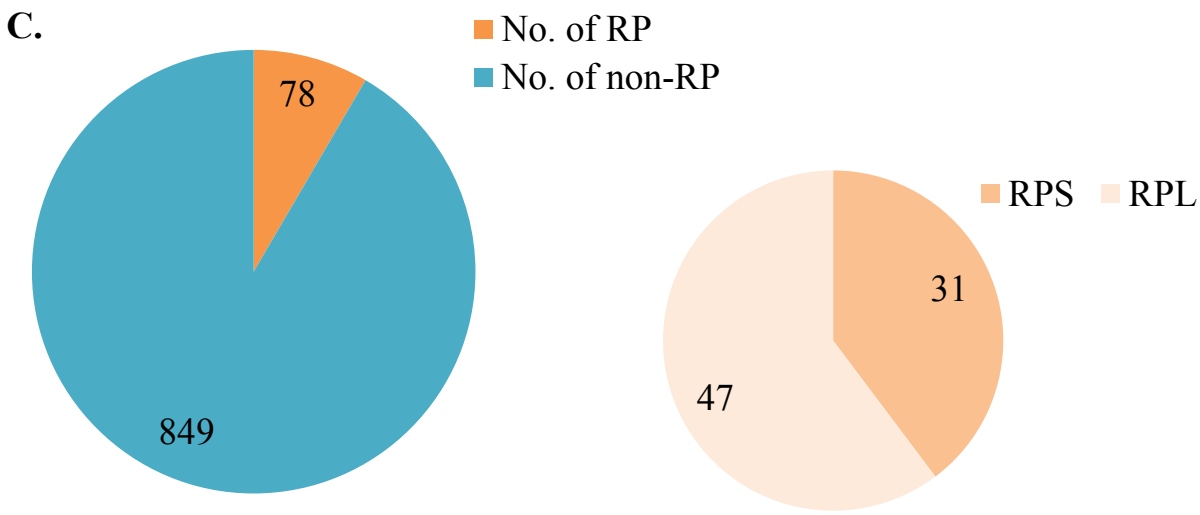

Figure 13: Optimization of mass spectrometry using 6h, 200mM sorbitol stressed keratinocytes. **A.** Immunoblotting of ERK1/2 phosphorylation for 6h of 200mM sorbitol treated and untreated N/TERT-1 keratinocytes. **B.** Polysome profiles of 6h, 200mM sorbitol treated and untreated N/TERT-1 keratinocytes. **C.** Pie chart depicting 926 proteins with 95% confidence detected from LC-MS/MS analysis upon 6h sorbitol stress, which composed of 78 RPs and 849 non-RPs. Among the RPs detected, 31 proteins were RPS while 47 proteins were RPL.

4.10 Optimization of stress duration for wounded keratinocytes

The overall quantity of proteins detected in the second round of mass spectrometry suggested that the optimization was successful. In order to fulfil the cut-off of a significant 1.5 fold up/down-regulation of candidates upon stress treatment, we next focused on extending the duration of stress. We hypothesize that ribosomal protein changes may take a considerable amount of time as new ribosomes are synthesized. Therefore, we decided to extend the stress duration to 24 hours **(Figure 14A)**. The phosphorylation of paxillin was determined at 24h post-scratch with a non-scratched control as an indication of keratinocyte migration. Paxillin is a focal adhesion associated signalling molecule that mediates motility and cell spreading [37]. Here, we optimized and performed polysome profiling on 24h post-wounded keratinocytes with non-wounded controls **(Figure 14B)**. The polysome profiles revealed an increase in polysomal peaks and a decrease in monosomal peaks in 24h-wounded keratinocytes compared to non-wounded keratinocyte controls suggesting there was increased

translation 24h post-wounding. Similar to previous experiments, the actively translating ribosome fractions 3-5 were pooled and subjected to protein extraction using centrifugal concentrators. Concentrated protein was subjected to optimized LC-MS/MS analysis. This experimental workflow is currently in progress.

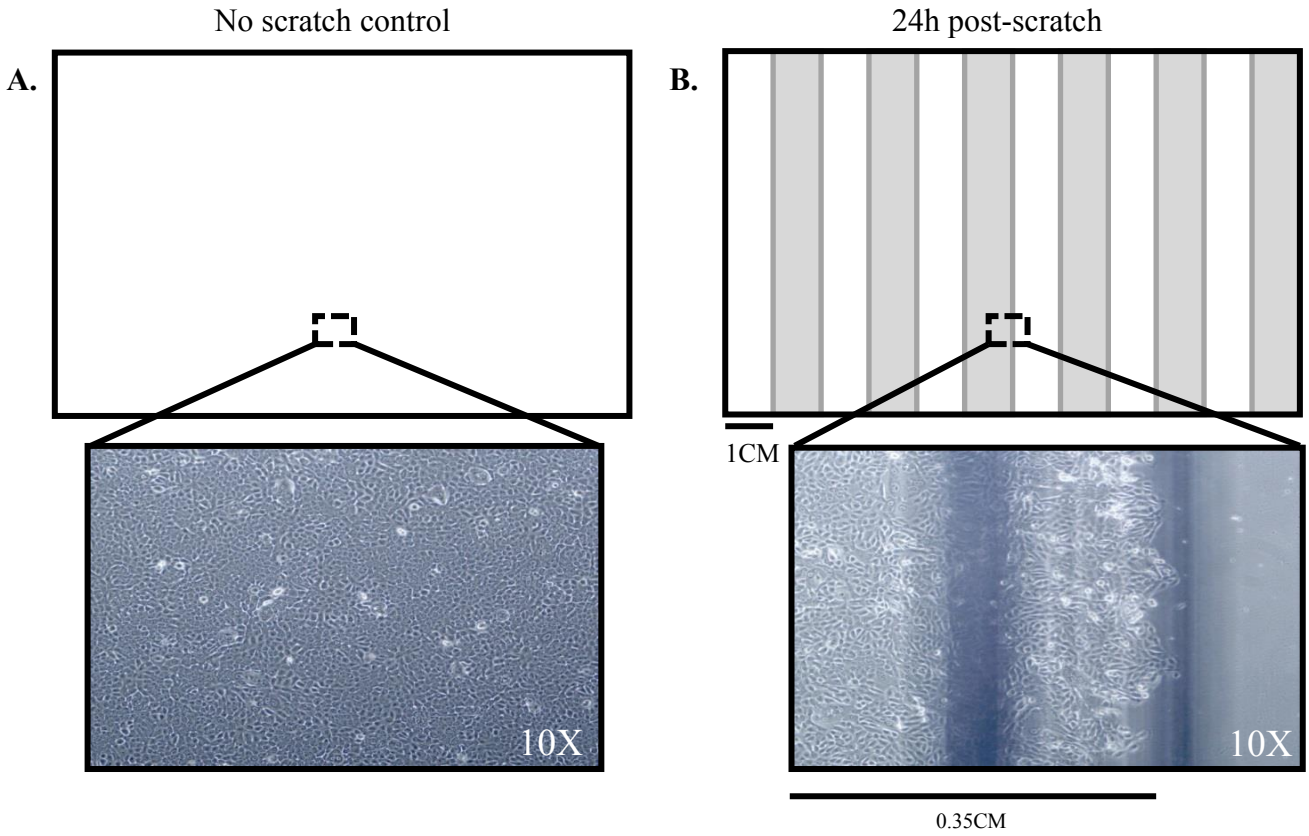

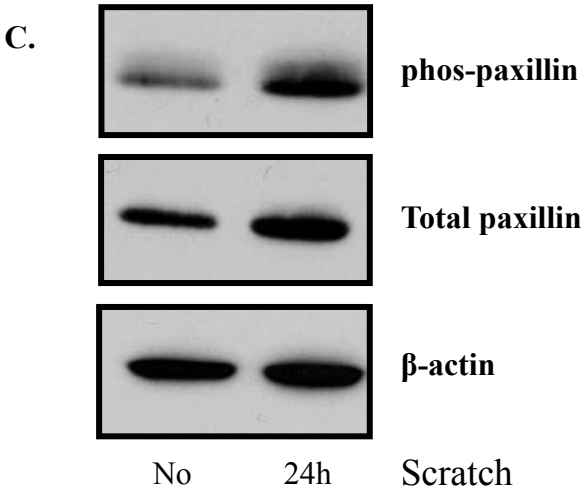

D.

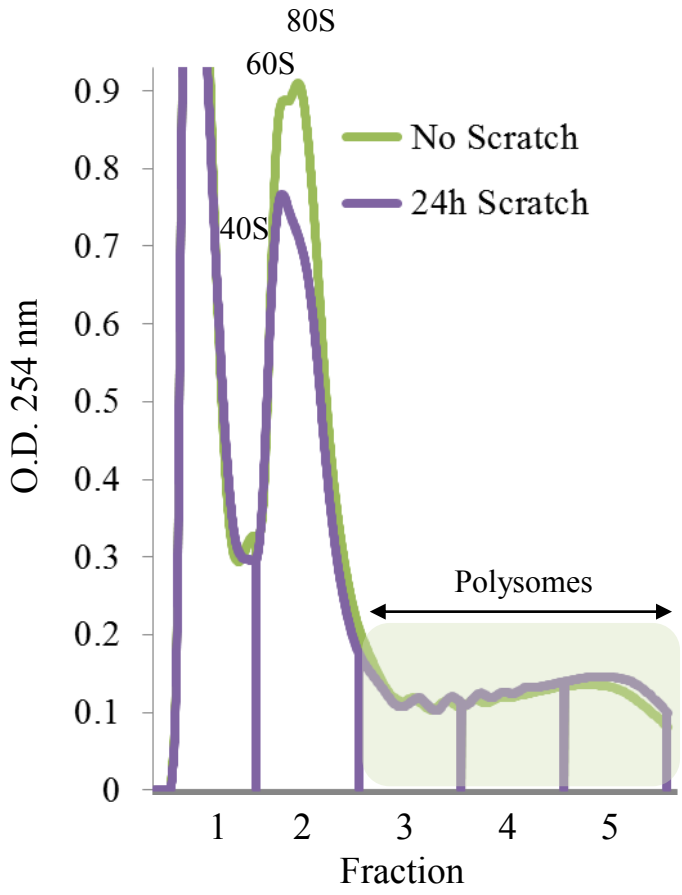

Figure 14: Optimization of stress duration in wounded keratinocytes using multiple vertical scratch assay. A. In non-scratch culture dishes, N/TERT-1 keratinocytes were grown to full confluence. **B.** Confluent keratinocytes were wounded, by making multiple vertical scratches 1 cm apart from each other. **C.** Immunoblotting of total and phosphorylated paxillin for non-wounded and 24h post-wounded N-TERT-1 keratinocytes as an indication of keratinocyte migration. β-actin was used as a loading control. **D.** Polysome profiles of 24h post-wounded and non-wounded N/TERT-1 keratinocytes.

5. Discussion

Over the past decade, a growing body of research has been conducted to elucidate the role of heterogeneous ribosomes in regulating translation; particularly though the alteration of RP composition. However, the role of 'specialized' ribosomes in the epidermis, particularly under stress, has yet to be elucidated. Here, I present my preliminary efforts to unravel the role of a 'ribosomal code' in the epidermis under wounding and osmotic stress conditions. I used either a confluent monolayer culture of keratinocytes and performed scratch assays to model wounding or high molarity sorbitol to recapitulate osmotic stress.

I hypothesized that under epidermal stress conditions, RP changes would occur during ribosome biogenesis when (i) newly synthesized RPs or (ii) existing RPs are assembled onto each individual 40S and 60S subunits, or during (iii) ribosome maturation. This switch in RPs or the recruitment of non-RPs would then re-define a new composition of translation machinery that eventually regulates the translation of specific mRNA required under stress conditions. To validate our hypothesis, we first optimized the wounding and osmotic stress conditions in N/TERT-1 keratinocytes and showed the phosphorylation of either p38 or ERK-1/2, which are key players in the MAPK stress signalling pathway. While JNK is a classical stress-regulated kinase which is upregulated upon osmotic stress, I did not observe any upregulation of JNK phosphorylation with sorbitol treatment. It is possible that the concentration of sorbitol used in my experiment was not high enough to detect JNK phosphorylation. In a previous report, JNK phosphorylation was observed with 400mM of sorbitol as early as 15 mins of treatment. However, only a mild upregulation of JNK phosphorylation was observed with 200mM of sorbitol for 1h of treatment [38]. Hence, I used ERK phosphorylation as an indicator for stress response, since it has been previously demonstrated to increase with sorbitol treatment [39]. Heat shock proteins could also be determined as markers for sorbitol stress induction. Since the keratinocytes were starved of

growth factors for 48h prior to sorbitol treatment, the increase in ERK phosphorylation observed was a consequence of osmotic stress induction.

Subsequently, polysome profiling, protein purification, iTRAQ labelling and preliminary mass spectrometry analysis was performed to determine the riboproteome under these stress conditions. The preliminary mass spectrometry analysis revealed 95 proteins in polysomal fractions of wounded and osmotically stressed keratinocytes. This dataset was of low confidence primarily due to the marginal number of proteins detected and the inefficiency of candidate validation by immunoblotting. Next, I delved into the optimization of sample preparation before LC-MS/MS analysis and predicted two potential ways to improve the protocol.

It is possible that in-gel digestion with trypsin alone might have resulted in the reduced yield of proteins detected. The optimal efficiency of in-gel tryptic cleavage is affected by size and surface area of the gel which then influences the permeation of the enzyme **(Figure 15)**. Smaller-sized gel pieces exhibiting a larger surface area eases enzyme permeability, thereby resulting in enhanced protein digestion [40]. The process of excessive pipetting to collect peptide elution might have resulted in additional sample loss. In the case of in-solution digestion, these pitfalls were overcome and the efficiency of proteolytic cleavage was enhanced leading to a greater resolution of proteins.

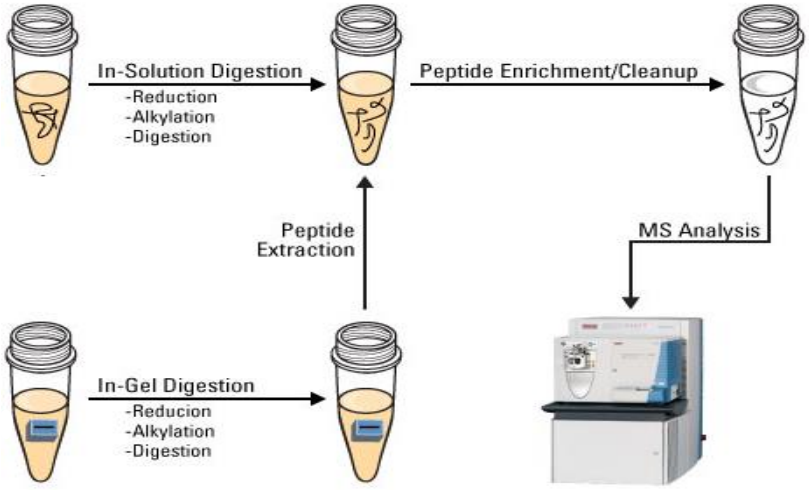

Figure 15: Comparison between in-solution and in-gel digestion prior to peptide enrichment and MS analysis (Excerpted from http://www.creative-proteomics.com/Services/Digestion-in-gel-or-in-solution.htm).

Trypsin favours cleavage at the carboxyl terminal of arginine (R) residues compared to lysine (K) residues. In a typical tryptic digestion, 80-90% of mis-cleavages occur at lysine residues **(Figure 16)**. Thus, the addition of Lys-C prior to trypsin, maximizes digestion at lysine residues and thus, improves the overall proteolytic efficiency. Since RPs are rich in lysine and arginine residues, the use of a combination of Lys-C/Trypsin has improved the number of RPs detected and has increased the overall identification of proteins in the second mass spectrometry dataset.

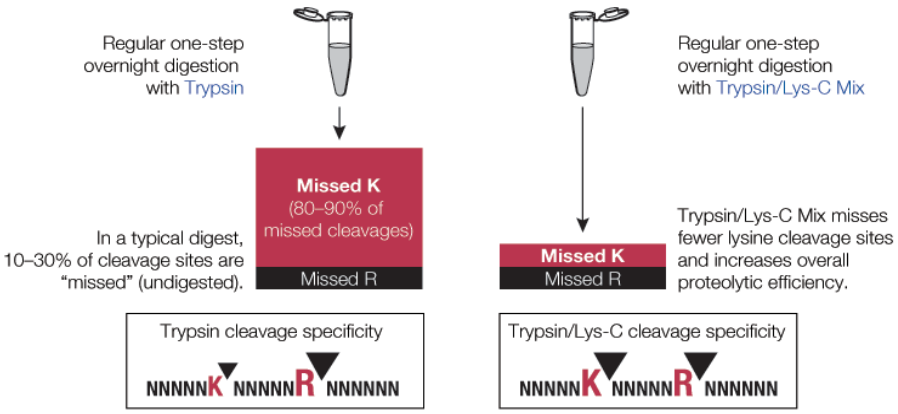

Figure 16: Comparison between one-step trypsin digestion and complementary Lys-C/Trypsin digestion (Excerpted from http://www.promega.com/products/mass-spectrometry/proteases-and-surfactants/trypsin_lys_c_mix_mass_spec_grade/).

Despite the increase in detected proteins, none were up/down-regulated by 1.5 fold or above on treatment. This might be because 6h post-scratch or 4h of sorbitol treatment could be an insufficient duration of stress for RP alterations to occur on the ribosome. Thus, I focused on optimizing the duration of stress conditions. Although the rate of RP recruitment onto the ribosome remains elusive, the half-life of ribosomal proteins in the rat liver ribosome is reported to be 5 days [41]. Thus, I hypothesized that an extension of stress duration might increase the likelihood of RP switches being detected. I first considered the extension of 24h post-scratch duration, however this would not be feasible with cell comb scratch assay system. These pre-made cell combs have a smaller width of approximately 0.2 mm that would close within 8h post-scratch. Wound width was increased by inducing scratch using a blue tip, 1cm apart from each other in a confluent N/TERT-1 monolayer culture. Keratinocytes were harvested for polysome extraction 24h post-wounding. An increase in global translation was observed at 24h as compared to 6h post scratch. I postulate that there would be evidence of RPs significantly changing at the 24h time-point, and the analysis of this dataset is in progress.

By 24 h post-scratch, there would be two population of cells; the migrating cells at the leading edge of the wound as well as the proliferative cells behind the wound edge. The longer 24h scratch duration was chosen over 6h, based on the notion that RPs would require sufficient amount of time to switch in order to be detected. However, it is important to segregate the two population of cells as the RP changes observed in migratory keratinocytes may be distinctly different from the RP changes observed in proliferative keratinocytes. Thus, the sorting of migratory keratinocytes from proliferative keratinocytes is necessary to allow for accurate interpretation of data. A Boyden chamber assay is also a good method to distinguish the migratory keratinocytes from the proliferative keratinocytes [42]; however, it is more expensive. The major drawback for Boyden chamber assays in my experiment, is the

ability to harvest sufficient migratory cells to perform subsequent polysome profiling studies in order to detect significant RP changes in migratory cells. Thus, the 24h cell wounding method seems the most feasible to generate a large pool of keratinocytes in order to purify actively translating ribosomes. The sorting of migrating from proliferative keratinocytes would be challenging as cell sorting might pose an additional stress response on these keratinocytes. Alternatively, cell proliferation could be negated by serum starvation or by the addition of mitomycin C, which arrests cell mitosis irreversibly by DNA crosslinking [42-44], prior to scratch. It is important to note that, mitomycin C treatment may also influence potential RP changes.

Nonetheless, any candidates that are selected from the 24h wounding study would be validated using organotypic cultures. To do this, I would generate stable lentiviral cell lines for the candidate of interest in parallel with a non-silencing positive control using N/TERT-1 keratinocytes. I would then derive three-dimensional *ex vivo* de-epidermised dermis (DED) human skin equivalents (HSEs) using these cells lines, as previously described [45]. Partial thickness excisional wounds would be created on these DED-HSEs, excising through the epidermis. The rate of wound closure would be evaluated to determine the role of this candidate in wound healing.

Though I am optimizing the scratch conditions, EBP-1 was one potential candidate that was significantly up-regulated on the polysomes by 1.8-fold 6h post-scratch. EBP-1 is a human epidermal growth factor receptor binding protein that is known to transduce growth regulatory signals [46, 47]. It has three ATG start codons and exits as two isoforms, p48 and p42 based on two alternative translation start sites [48]. The larger p48 isoform displays both nucleolar and cytoplasmic localization while the p42 isoform is cytoplasmic [49, 50]. p48 isoform is known to suppress apoptosis and promote PC12 cell proliferation while p42 isoform promotes PC12 cell differentiation [48]. EBP-1 is highly expressed in proliferating

and differentiated C2C12 myoblasts [49]. EBP-1 up-regulation is known to regulate Schwann cell differentiation and migration during sciatic nerve injury [51]. However, no studies have demonstrated a role of EBP-1 during keratinocyte migration. Our future direction would be to address how EBP1 binding to the translation machinery influences keratinocyte migration.

6. Future Work

In the event that 24h post-scratch conditions prove to reveal some RP/non-RP candidates that are significantly up/down-regulated on the polysomes by a cut-off of 1.5 fold, we would pursue functional studies to characterize their role during keratinocyte migration. For instance, if EBP-1 is up-regulated in both 6h and 24h post-scratch conditions, we would perform knock-down studies on EBP-1 to determine if it impedes keratinocyte migration by measuring wound width. The extent of migration upon EBP-1 knockdown would be validated by immunoblotting and immunofluorescence using keratinocyte migration markers such as F-actin, paxillin and focal adhesion kinase (FAK). Studies will be extended to primary keratinocytes as well as 3D organotypic cultures. In organotypic cultures, keratinocytes will be seeded onto de-epidermalized dermis (DED) and allowed to grow to full confluence for approximately 7 days. Subsequently, the confluent monolayer of keratinocytes will be elevated at an air-liquid interface to allow differentiation and stratification, thereby recapitulating the actual epidermis [52]. EBP-1 is known to regulate differentiation in several cell types such as PC12 cells and C2C12 myoblasts. Therefore, a doxycycline inducible keratinocyte cell line will be used to knockdown EBP-1 when the keratinocytes have undergone differentiation and stratification.

It is likely that proteins that bind the translating ribosome in a regulated manner on stress influence mRNA translation. In order to determine which mRNAs are specifically regulated by the presence of EBP-1 on polysomes, I will perform polysome profiling experiments on

keratinocyte cell lines that have EPB-1 knocked down by an shRNA together with an shRNA control in wounded and non-wounded conditions. RNA will be extracted from actively translating polysomal fractions under these conditions and subjected to either ribosome profiling, microarray analysis or RNA-sequencing to determine the mRNAs that are regulated by EBP-1. Alternatively, EBP-1 could be subjected to immunoprecipitation whereby a monoclonal antibody specific to EBP-1 could be immobilized onto an insoluble support such as magnetic beads and incubated with polysomal cell extracts containing EBP-1. The binding of the target protein, EBP-1, to the monoclonal specific antibody followed by elution and microarray analysis would unveil mRNAs that are specifically bound by EBP-1 polysomes. mRNAs that are either known to regulate keratinocyte migration or novel target mRNAs would be selected and validated by immunoblotting. Mechanistic studies would then be performed to determine how EBP-1 regulates the translation of target mRNAs. A similar approach would be used in the studies with regards to osmotic stress.

The rationale of this study was to prove the concept of a 'ribosomal code' during epidermal stress. In the circumstance that 24h post-wounding is insufficient to induce changes in RP/non-RP candidates on the polysome, I would be performing an alternative stress treatment on the keratinocytes, which is UV-B radiation. UV stress has been previously described to induce RP changes in plants [53]. UV radiation causes DNA damage and is known to influence ribosome biogenesis and assembly [54]. Thus, it is highly possible that significant RP changes will also be observed in keratinocytes treated with UV. UV radiation will induce a homogenous stress response across the entire cell culture dish. Hence, all stressed cells could be harvested for subsequent polysome profiling studies, which is a major drawback for scratch assay.

If there are no changes in polysome associated RP/non-RPs in my wounding and UV stress assays it suggests that changes in the translating ribosome may not be important for these

stress responses. If this is the case we will explore the role of RP heterogeneity in keratinocytes during differentiation. We have previously determined the gene expression pattern of a panel of 89 RPs during N/TERT-1 keratinocyte differentiation. Preliminary qRT-PCR data suggest that most RP genes were homogeneously expressed while a few candidates were significantly up/down-regulated during keratinocyte differentiation. Some of these candidates validated positively in organotypic skin cultures as well as by immunohistological staining of human scalp skin sections. Additionally, differentiation of keratinocytes is induced over a time course of 6 days, which might be long enough to detect changes on polysome during stress. This aspect will be pursued if none of the above stress conditions reveal significant changes in RP/non-RP composition on polysomes.

If I fail to detect any changes in proteins associated with the ribosome under the conditions stated above, it suggests that my hypothesis is incorrect and that changes in ribosomal protein heterogeneity may not be required for the keratinocyte responses discussed. Alternatively our method may not be sensitive enough to detect small but potentially important changes in proteins. If this happens, I will address the role of translational control during keratinocyte stress response. Several evidence have been reported in the literature on the role of translational control mediated by miRNAs and RNA binding proteins during cellular stress response [55, 56]. For instance, VICKZ is an RNA binding protein which mediates cell motility and migration [57]. In addition to β-actin mRNA, VICKZ proteins regulate targets such as cofilin and actin depolymerisation proteins which mediate lamellipodia formation and cell migration [57, 58]. Thus, I will determine the mRNAs that are translationally regulated under normal and stressed conditions in keratinocytes. Novel candidate genes translationally up/down-regulated during epidermal stress would be of interest for subsequent validation. Validated candidates will be pursued with mechanistic studies to determine the mode of translational regulation by either miRNAs, RNA binding proteins or RPs. This will be

followed by studies to determine how this regulatory mechanism is functionally useful to mediate the stress response.

7. Conclusion

In conclusion, I have started to address the question of whether changes in ribosomal proteins or ribosome associated proteins are important for stress response in keratinocytes. I have optimized the sample preparation for mass spectrometry of polysomal protein samples by performing in-solution digestion using Lys-C/Tyrpsin mix to yield greater protein coverage. I have optimized longer stress duration of 24h for wounding to provide sufficient time for new ribosome assembly and RP changes to occur and this work is currently under progress. In the event that no changes in polysomal RPs/non-RPs are observed, I will examine the potential of RP switches occurring during UV-B stress on keratinocytes. The aim of my study is to identify novel RP or non-RP candidates that are specifically recruited onto polysomes during stress, which could potentially regulate the translation of a specific subset of mRNAs to mediate a stress response. This will provide important implications to understand the underlying mechanisms of the role RPs/non-RPs in translationally regulating genes that are involved in epidermal stress response or promoting wound healing.

8. References

1. Thomson, E., Ferreira-Cerca, S., and Hurt, E., *Eukaryotic ribosome biogenesis at a glance.* Journal of Cell Science, 2013. **126**: p. 4815-4821.
2. Frank, J., *The ribosome - a macromolecular machine par excellence.* Chem. Biol, 2000. **7**: p. R133-R141.
3. Kim, T.-H., Leslie, P., and Zhang, Y., *Ribosomal proteins as unrevealed caretakers for cellular stress and genomic instability.* Oncotarget, 2014. **5**(4): p. 860-871.
4. Adam, B.-S., et al., *The Structure of the Eukaryotic Ribosome at 3.0 Å Resolution.* Science, 2011. **334**: p. 1524-1529.
5. Kressler, D., Hurt, E. and Baβler, J., *Driving ribosome assembly.* Biochimica et Biophysica Acta, 2010: p. 673–683.
6. Panse, V., G. and Johnson, A., W., *Maturation of Eukaryotic Ribosomes: Acquisition of Functionality.* Trends Biochem Sci, 2010. **35**(5): p. 260-266.
7. Xue, S., and Barna, M., *Specialized ribosomes: a new frontier in gene regulation and organismal biology.* Nature Reviews, 2012. **13**: p. 355-369.
8. Caldarola, S., Stefano, M., C., D., Amaldi, F. and Loreni F., *Synthesis and function of ribosomal proteins - fading models and new perspectives.* FEBS Journal, 2009. **276**: p. 3199-3210.
9. Wong, Q.W., Li, J., Ng, S. R., Lim, S. G., Yang, H., Vardy, L. A., *RPL39L is an example of a recently evolved ribosomal protein paralog that shows highly specific tissue expression patterns and is upregulated in ESCs and HCC tumors.* RNA Biology, 2014. **11**(1): p. 33-41.
10. Liu, B., and Qian, S.B., *Translational reprogramming in cellular stress response.* WIREs RNA, 2013.
11. Gebauer, F.a.H., M., W., *Molecular Mechanisms of Translational Control.* Nature Reviews, 2004. **5**: p. 827-835.
12. Kong, J., and Lasko, P., *Translational control in cellular and developmental processes.* Nature Reviews, 2012. **13**: p. 383-394.
13. Beilharz, T., H., and Preiss., T., *Translational profiling: The genome-wide measure of the nascent proteome.* Briefings in Functional Genomics and Proteomics, 2004. **3**(2): p. 103-111.
14. Komili, S., Farny, N., G., Roth, F., P. and Silver, P., A., *Functional specificity among ribosomal proteins regulates gene expression.* Cell, 2007. **131**(3): p. 557-571.
15. Just, W., *Specialization from synthesis: How ribosome diversity can customize protein function.* FEBS Letters, 2013. **587**(8): p. 1189-1197.
16. Schuldt, A., *Gene expression: Personalized ribosomes.* Nature Reviews Molecular Cell Biology, 2011. **12**: p. 344-345.
17. Topisirovic, I.a.S., N., *Translational Control by Eukaryotic Ribosome.* Cell, 2011. **145**: p. 333-334.

18. Kondrashov, N., Pusic, A., Stumpf, C., R., Shimizu, K., Hsieh, A., C., Xue, S., Ishijima, J., Shiroishi, T. and Barna, M., *Ribosome-mediated specificity in Hox mRNA translation and vertebrate tissue patterning.* Cell 2011. **145**(3): p. 383-397.
19. Fleischer, T.C., Weaver, C. M., McAfee, K. J., Jennings, J. L. and Link, A., J., *Systematic identification and functional screens of uncharacterized proteins associated with eukaryotic ribosomal complexes.* Genes Development 2006. **20**: p. 1294-1307.
20. Fuchs, G., Diges, C., Kohlstaedt, L., A., Wehner, K., A. and Sarnow, P., *Proteomic Analysis of Ribosomes: Translational Control of mRNA populations by Glycogen Synthase GYS1.* Journal of Molecular Biology, 2011. **410**(1): p. 118-130.
21. McGowan, K., A., Li, J., Z., Park, C., Y., Beaudry, V., Tabor, H., K., Sabnis, A., J., *Ribosomal mutations cause p53-mediated dark skin and pleiotropic effects.* Nat Genet. , 2008. **40**(8): p. 963–970.
22. MaCann, K.L., and Baserga, S. J., *Mysterious Ribosomopathies.* Science, 2013. **341**: p. 849-850.
23. Horos, R., IJspeert, H., Pospisilova, D., Sendtner, R. et al., *Ribosomal deficiencies in Diamond-Blackfan anemia impair translation of transcripts essential for differentiation of murine and human erythroblasts.* Blood, 2012. **119**(1): p. 262-272.
24. Nakhoul, H., Ke, J., Zhou, X., Liao, W., Zheng, S., X. and Lu., H., *Ribosomopathies: Mechanisms of Disease.* Clinical Medicine Insights: Blood Disorders, 2014. **7**: p. 7-16.
25. Ruggero, D., and Pandolfi, P. P., *Does the ribosome translate cancer?* Nature Reviews, 2003. **3**: p. 179-192.
26. Rogers, A., J., Celedón, J., C., Lasky-Su, J., A., Weiss, S., T. and Raby, B., A., *Filaggrin mutations confer susceptibility to atopic dermatitis but not to asthma.* J Allergy Clin Immunol. , 2007. **120**(6): p. 1332-1337.
27. Bolling, M., C., Lemmink, H., H., Jansen, G., H. and Jonkman, M., F., *Mutations in KRT5 and KRT14 cause epidermolysis bullosa simplex in 75% of the patients.* The British Journal of Dermatology, 2011. **164**(3): p. 637-644.
28. Hanel, K., H., Cornelissen, C., Luscher, B. and Baron, J., M., *Cytokines and the Skin Barrier.* Int. J. Mol. Sci, 2013. **14**: p. 6720-6745.
29. Kirfel, G.a.H., V., *Migration of epidermal keratinocytes: mechanisms, regulation, and biological significance.* Protoplasma, 2004. **223**: p. 67-78.
30. Haase, I., Evans, R., Pofahl, R. and Watt, F., M., *Regulation of keratinocyte shape, migration and wound epithelialization by IGF-1- and EGF-dependent signalling pathways.* Journal of Cell Science, 2003. **116**: p. 3227-3238.
31. Garmyn, M., Mannone, T., Pupe, A., Gan, D., et al., *Human keratinocytes Respond to Osmotice Stress by p38 Map Kinase Regulated Induction of HSP70 and HSP27.* The Journal of Investigative Dermatology, 2001. **117**(5): p. 1290-1295.
32. Mammone, T., Ingrassia, M., and Goyarts, E., *Osmotic stress induces terminal differentiation in cultured normal human epidermal keratinocytes.* In Vitro Cell.Dev.Biol.-Animal, 2008. **44**: p. 135-139.

33. Chun-Chi Liang1, A.Y.P.J.-L.G., *In vitro scratch assay: a convenient and inexpensive method for analysis of cell migration in vitro.* Nature Protocols, 2007. **2**: p. 329-333.
34. Mammone, T., M. Ingrassia, and E. Goyarts, *Osmotic stress induces terminal differentiation in cultured normal human epidermal keratinocytes.* In Vitro Cell Dev Biol Anim, 2008. **44**(5-6): p. 135-9.
35. Ingolia, N., T., *Ribosome profiling: new views of translation, from single codons to genome scale.* Nature Reviews Genetics, 2014. **5**: p. 205-213.
36. Reschke, M., Clohessy, J., G., Seitzer, N., Goldstein, D., P., Susanne, B., et al., *Characterization and analysis of the composition and dynamices of the mammalian riboproteome.* Cell Rep., 2013. **4**(6): p. 1-23.
37. Schaller, M., D., *Paxillin: a focal adhesion-associated adaptor protein.* Oncogene, 2001. **20**(44): p. 6459-6472.
38. Lee, S.H., et al., *Osmotic stress inhibits proteasome by p38 MAPK-dependent phosphorylation.* J Biol Chem, 2010. **285**(53): p. 41280-9.
39. Fischer, O.M., et al., *Oxidative and osmotic stress signaling in tumor cells is mediated by ADAM proteases and heparin-binding epidermal growth factor.* Mol Cell Biol, 2004. **24**(12): p. 5172-83.
40. Shevchenko, A., Tomas, H., Havli, J., Olsen, J., V. and Mann, M., *In-gel digestion for mass spectrometric characterization of proteins and proteomes.* Nature Protocols, 2007. **1**: p. 2856-2860.
41. Dice, J., F. and Schimke, T.,, *Turnover and Exchange of RIbosomal Proteins from Rat Liver.* The Journal of Biological Chemistry, 1972. **247**(1): p. 99-111.
42. Nyegaard, S., B. Christensen, and J.T. Rasmussen, *An optimized method for accurate quantification of cell migration using human small intestine cells.* Metab Eng Commun, 2016. **3**: p. 76-83.
43. Iyer, V.N. and W. Szybalski, *Mitomycins and Porfiromycin: Chemical Mechanism of Activation and Cross-Linking of DNA.* Science, 1964. **145**(3627): p. 55-8.
44. Tomasz, M., *Mitomycin C: small, fast and deadly (but very selective).* Chem Biol, 1995. **2**(9): p. 575-9.
45. Xie, Y., et al., *Development of a three-dimensional human skin equivalent wound model for investigating novel wound healing therapies.* Tissue Eng Part C Methods, 2010. **16**(5): p. 1111-23.
46. Squatrito, M., Mancino, M., Donzelli, M., Areces, L., B. and Draetta, G., F., *EBP1 is a nucleolar growth-regulating protien that is part of pre-ribosomal ribonucleoprotien complexes.* Oncogene, 2004. **23**(4454-4465): p. 4454.
47. Judah, D., Chang, W., Y., Dagnino, L., *EBP1 is a novel E2F Target Gene Regulated by Transforming Growth Factor-B.* Plos One, 2010. **5**(11).
48. Liu, Z., Ahn, J-Y., Liu, X. and Ye., K., *Ebp1 isoforms distinctively regulate cell survival and differentiation.* PNAS, 2006. **103**(29): p. 10917-10922.

49. Figeac, N., Serralbo, O., Marcelle, C., Zammit, P., S., *ErbB3 binding protein-1 (EBP1) controls proliferation and myogenic differentiation of muscle stem cells.* Developmetal Biology, 2014. **386**: p. 135-151.
50. Zhang, Y., Linn, D., Liu, Z., Melamed, J., Tavora, F., Young, C., Y., Burger, A., M. and Hamburger, A., W., *EBP1, an ErbB3-binding protein, is decreased in prostate cancer and implicated in hormone resistance.* Molecular Cancer Therapeutics, 2008. **7**(10): p. 3176-3186.
51. Liu, Y., Liu, Y., Cao, J., Zhu, X., Nie, X., Yao, L., Chen, M., Cheng, X., Wang, Y., *Upregulated expression of ebp1 contributes to schwann cell differentiation and migration after sciatic nerve crush.* Journal of Molecular Neuroscience, 2014. **54**(4): p. 602-613.
52. Oh, J., W., Hsi, T-C., Juarez, G., C., F., Ramos, R., and Plikus, M., V., *Organotypic Skin Culture.* Journal of Investigative Dermatology, 2013. **133**: p. e14. doi:10.1038/jid.2013.387.
53. Falcone Ferreyra, M.L., et al., *Plant L10 ribosomal proteins have different roles during development and translation under ultraviolet-B stress.* Plant Physiol, 2010. **153**(4): p. 1878-94.
54. Boulon, S., Westman, B., J., Hutten, S., Boisvert, F-M. and Lamond, A., I., *The Nucleolus under stress.* Molecular Cell Bilogy, 2010. **40**(2): p. 216-227.
55. Spriggs, K., A., Bushell, M. and Willis, A., E., *Translational Regulation of Gene Expression during Conditions of Cell Stress.* Molecular Cell Review, 210. **40**: p. 228-237.
56. Carpenter, S., Ricci, E. P., Mercier, B. C., Moore, M. J., and Fitzgerald, K. A., *Post-transcriptional regulation of gene expression in innate immunity.* Nature Reviews, 2014. **14**: p. 361-376.
57. Oberman, F., Rand, K., Maizels, Y. et al., *VICKZ proteins mediate cell migration via their RNA binding activity.* RNA Biology, 2007. **13**(9): p. 1558–1569.
58. Ghosh, M., Song, X., Mouneimne, G., Sidani, M., Lawrence, D.S. and Condeelis, J.S., *Cofilin promotes actin polymerization and defines the direction of cell motility. .* Science, 2004. **304**: p. 743-746.